



Dublin City University
Ollscoil Chathair Bhaile Atha Cliath
Dublin 9, Ireland

**NOVEL AMPEROMETRIC ENZYME
BIOSENSORS
OF
ENVIRONMENTAL INTEREST**

by

Stephen A. Kane B.Sc.

Thesis Submitted for the Degree of Doctor of Philosophy

Supervisor: Prof. Malcolm R. Smyth

Dublin City University

July 1998

DECLARATION

I hereby certify that this material, which I now submit for assessment on the programme of study leading to the award of Doctor of Philosophy (Ph.D.) is entirely my own work and has not been taken from the work of others save and to the extent that such work has been cited and acknowledged within the text of my own work.

Signed: 
Stephen Kane

ID No: 95970673

Date: 31/07/98

For my Family

Acknowledgements

I wish to thank my supervisor Prof. Malcolm R. Smyth for his guidance, support, advice, patience and insight over the last three years. I am indebted to him for providing me with the opportunity to carry out research in his group and also for allowing me to study in New Mexico State University.

Thanks to Prof. Joseph Wang at New Mexico State University for allowing me to work in his group and also to Dr. Kim Rogers and the United States Environmental Protection Agency for his scientific advice and also for awarding me a fellowship to study in the USA.

An immense word of thanks to Paraic and Mary for their advice and help. Also to Fergus and Jane for all their help and support. A very special thanks to Eoin for everything.

A big word of thanks to all the staff and postgrads in the Chemistry Dept. at DCU. Especially to Brendan, for all the heated arguments. Joey, for the business cards. Caroline for all the laughs. Conchi for all her hard work and help. Thanks also to Shane, Fran, Carol, Aogan, Brendan, Gaele, Dermot, Yvonne, Bernie, Dave, Jim and Frank. Thanks to Frances for all your support. I am also extremely grateful to Dr. Emmanuel I. Iwuoha for all the help and assistance with the final projects of this thesis.

Not forgetting of course 'The Hacienda Mafia' and my singing buddies, the band, Robert and his family, Mark, Tracey, Dr. Lara, Carol, Kurt, Jack, Valberes and his family, Wendy and everyone in Las Cruces for all the entertainment and parties.

Finally I would like to thank my family and also my adopted family for all the help.

TABLE OF CONTENTS

	Page
Declaration	ii
Dedication	iii
Acknowledgements	iv
Table of Contents	v
Abstract	x

Chapter 1.	Performance and Characteristics of Amperometric Biosensors for Environmental Monitoring of Enzyme Inhibitors and Phenols	1
1.1.	Biosensors - An Introduction	2
1.2.	Enzyme Catalysis	2
1.3.	Electrochemical Enzyme Biosensors - Theoretical Aspects	3
1.4.	Electrochemical Signal Transduction and Working Electrodes	8
1.4.1.	Glassy Carbon	8
1.4.2.	Carbon Paste	9
1.4.3.	Platinum	10
1.5.	Electron Transfer - The Mediation Process	11
1.6.	Enzyme Immobilisation Methods	13
1.6.1.	Adsorption	13
1.6.2.	Covalent Bonding	14
1.6.3.	Entrapment	14
1.6.4.	Encapsulation	17
1.6.5.	Crosslinking	17
1.7.	Properties of Tyrosinase Enzyme	17
1.8.	Biosensors and Enzyme Inhibition	19
1.9.	Types of Enzyme Inhibition	20
1.9.1.	Reversible Inhibition	21
1.9.1.1.	Competitive Inhibition	21
1.9.1.2.	Non-competitive Inhibition	23
1.9.1.3.	Uncompetitive Inhibition	25
1.9.2.	Irreversible Inhibition	25
1.10.	Disposable Biosensors and Screen Printed Technology	27

1.11.	Tissue and Cell-based Biosensors for Environmental Monitoring	30
1.12.	Binder Modified Tyrosinase Biosensors for the Monitoring of Phenols	32
1.12.1.	Standard Methods of Analysis for Phenolic Compounds	32
1.12.2.	Biosensing and Phenol Analysis	33
1.12.3.	Binder Modified Biosensors and Phenol Analysis	36
1.13.	References	38
Chapter 2	Enzyme Inhibition-based Biosensors	44
2.1.	Mushroom Tissue-based Biosensor for Inhibitor Monitoring	45
2.1.1.	Introduction	45
2.1.2.	Experimental	47
2.1.2.1.	Reagents	47
2.1.2.2.	Instrumentation	47
2.1.2.3.	Electrode Preparation	47
2.1.2.4.	Procedures	48
2.1.3.	Results and Discussion	50
2.1.3.1.	Investigation of Mushroom Tissue Loading and Activity Distribution	50
2.1.3.2.	Batch Response Characteristics of the Mushroom Tissue Biosensor	53
2.1.3.3.	Flow Injection Analysis Response Profile	56
2.1.3.4.	Detection Limits and Stability Considerations	58
2.1.4.	Conclusion	59
2.2.	Screen Printed Tyrosinase containing Electrodes for the Biosensing of Inhibitors	60
2.2.1.	Introduction	60
2.2.2.	Experimental	62
2.2.2.1.	Reagents	62
2.2.2.2.	Instrumentation	62
2.2.2.3.	Screen Printing Fabrication	62
2.2.2.4.	Procedures	63
2.2.3.	Results and Discussion	64
2.2.3.1.	Investigation of Tyrosinase Enzyme Loading	64
2.2.3.2.	Inhibitor Screening	67
2.2.3.3.	Detection Limits, Reproducibility and Stability Properties	70
2.2.4.	Conclusion	72
2.3.	Elucidation of Tyrosinase Inhibition and Inhibitor Type	73
2.3.1.	Introduction	73
2.3.2.	Experimental	73
2.3.2.1.	Reagents	74
2.3.2.2.	Instrumental	74

2.3.2.3.	Electrode Preparation	74
2.3.2.4.	Procedures	74
2.3.3.	Results and Discussion	76
2.3.3.1.	Theoretical Treatism on Inhibition by Sodium Diethyldithiocarbamate	76
2.3.3.2.	Experimental Elucidation of Inhibitor Type	82
2.3.4.	Conclusions	87
2.4.	References	88
Chapter 3	Hydrocarbon Pasting Liquids for Improved Tyrosinase-based Carbon Paste Phenol Biosensors	91
3.1.	Introduction	92
3.2.	Experimental	94
3.2.1.	Reagents	94
3.2.2.	Instrumentation and Procedures	94
3.2.3.	Electrode Preparation	95
3.3.	Results and Discussion	96
3.3.1.	Characterisation and Performance of the Hydrocarbon Pasting Liquid Modified Biosensors	96
3.3.2.	Sensitivity, Reproducibility and Limit of Detection	100
3.3.3.	Applicability to Chromatographic Analysis of Phenols	104
3.4.	Conclusion	106
3.5.	References	107
Chapter 4	Sol-Gel based Sensor & Biosensor Applications	109
4.1.	Sol-Gels	110
4.1.1.	An Introduction to Sol-Gels	110
4.1.2.	Sol-Gel Processing	112
4.1.2.1.	Structural Evolution	115
4.1.3.	Sol-Gel Film Formation - Spin Coating	115
4.1.4.	Universal Sol-Gel Application.	117
4.1.4.1.	Thin Films and Coatings	118
4.1.4.1.1.	Optical Coatings	118
4.1.4.1.2.	Protective Films	118
4.1.4.2.	Monoliths	119
4.1.4.3.	Powders, Grains, Spheres & Fibres	119
4.1.4.4.	Composites	119
4.1.4.5.	Porous Gels & Membranes	120
4.1.5.	Biosensor Applications of Sol-Gel Systems	120
4.1.5.1.	Optical Methods	120
4.1.5.1.1.	Dissolved Oxygen Biosensor	120
4.1.5.1.2.	Nitric Oxide Biosensor	121
4.1.5.1.3.	Glucose Biosensor	121
4.1.5.2.	Electrochemical Methods	121

4.1.6.	Experimental Overview	122
4.2.	Sol-Gel Composite Electrode as an Amperometric Detector for Liquid Chromatography of Catecholamines	123
4.2.1.	Introduction	123
4.2.2.	Experimental	126
4.2.2.1.	Reagents	126
4.2.2.2.	High Performance Liquid Chromatography	126
4.2.2.3.	Electrode Preparation	127
4.2.2.4.	Procedures	128
4.2.3.	Results and Discussion	129
4.2.3.1.	Mechanism of Catecholamine Oxidation	129
4.2.3.2.	Choice of Sol-Gel Porosities	130
4.2.3.3.	Hydrodynamic Voltammetry	131
4.2.3.4.	Operational Characteristics and Performance of the LCEC	134
4.2.3.5.	Detection Limits and Reproducibility	136
4.2.4.	Conclusion	139
4.3.	Development of a Sol-Gel based Amperometric Biosensor for the Analysis of Phenolics	140
4.3.1.	Introduction	140
4.3.2.	Experimental	144
4.3.2.1.	Reagents	144
4.3.2.2.	Instrumentation	144
4.3.2.3.	Sol-Gel and Electrode Preparation	145
4.3.2.4.	Procedures	146
4.3.3.	Results and Discussion	147
4.3.3.1.	Electrochemical Behaviour of the Biosensor	147
4.3.3.2.	Biosensor Catalytic Response	149
4.3.3.3.	Steady State Amperometry	153
4.3.3.4.	Temperature Optimisation	154
4.3.3.5.	Screening of Phenols	155
4.3.3.6.	Organic Phase Analysis	160
4.3.3.7.	Storage and Stability	161
4.3.4.	Conclusion	162
4.4.	References	163
Chapter 5	Electrochemical Reactivities of Cytochrome P450_{cam} Immobilised in a Methyltriethoxysilane Sol-Gel and its Environmental Application	170
5.1.	Introduction	171
5.2.	Experimental	174
5.2.1.	Reagents	174
5.2.2.	Instrumentation	174

5.2.3.	Sol-gel and Electrode Preparation	175
5.2.3.1.	Sol-gel Preparation	175
5.2.3.2.	GCE-[P450 _{cam} + DDAB + Sol-gel] Biosensor Preparation	175
5.2.4.	Procedures	176
5.2.5.	Steady State Amperometry	176
5.3.	Results and Discussion	177
5.3.1.	Properties of Cytochrome P450 _{cam}	177
5.3.2.	Electrode Characterisation	179
5.3.3.	Cyclic Voltammetry of the GCE-[P450 _{cam} /DDAB/SG] Biosensor	180
5.3.4.	Electrochemical Catalysis of the GCE-[P450 _{cam} /DDAB/SG] Biosensor	183
5.3.5.	Temperature Optimisation	186
5.3.6.	Organic Phase Studies	188
5.3.7.	Steady State Amperometry	190
5.3.8.	Electrode Lifetime	193
5.4.	Conclusion	194
5.5.	References	195
Chapter 6	Summary, Future Trends and Conclusion	198
6.1.	Summary and Future Trends	199
6.2.	Conclusion	201
Publications and Presentations		202

Abstract

Novel Amperometric Enzyme Biosensors of Environmental Interest

The performance and characteristics of amperometric enzyme-based biosensors for environmental monitoring are described in detail in Chapter 1. The concept of enzyme inhibition is also outlined including detailed theoretical evaluation of inhibitor type.

The inhibition of one or more enzymes in a metabolic pathway can have detrimental effects *in vivo*. Inhibitors range from food constituents, pesticides, halide, azide and cyanide compounds, drug and related therapeutic agents, respiratory poisons, oxides and peroxides. In Chapter 2 the use of screen printing is described as a disposable tyrosinase based biosensor for the monitoring of selected inhibitors. The characterisation and attractive performance of single use inhibitor biosensor strips is presented. Exploitation of mushroom tissue electrodes for the convenient monitoring of tyrosinase inhibitors is also outlined, including detailed elucidation of inhibitor type using native tyrosinase enzyme.

Tyrosinase as a polyphenol oxidase is also an ideal candidate for the biosensing of phenolic compounds. The use of several hydrocarbon pasting liquids for improved tyrosinase-based carbon paste phenol biosensors is demonstrated in Chapter 3.

Much interest has evolved in recent years on the use of sol-gel glasses in sensor manufacturing. Chapter 4 addresses this area with a sol-gel carbon composite electrode as an amperometric detector for catecholamines in liquid chromatography. An example of a sol-gel amperometric biosensor for the analysis of phenolics is also described.

The most recent advancement in amperometric biosensing models, has been the proposed use of cytochrome P450 enzyme for environmental monitoring. Cytochrome P450s are haemthiolate monooxygenase enzymes that result in the hydroxylation of a wide range of substances. This novel biosensing technique is presented in Chapter 5 in relation to the encapsulation of the P450 enzyme along with membrane vesicles, within a methyltriethoxysilane gel. The behaviour of this biosensor for the analysis of polyaromatic hydrocarbons is evaluated.

The thesis concludes in Chapter 6 with a critical assessment of the work performed there-in, along with suggestions for future work.

Chapter 1

Performance and Characteristics of Amperometric Biosensors for Environmental Monitoring of Enzyme Inhibitors and Phenols

1.1. Biosensors - An Introduction

Biosensors have often been described as the marriage of a biological component e.g. an enzyme or antibody with a transduction system allowing measurement and amplification of the signal. In enzyme-based biosensors the redox protein forms the heart of the system. Many transduction systems have been used in the construction of biosensors including optical, piezoelectronic, potentiometric and amperometric transducers. These transducers have many practical applications in biosensors for both environmental and pharmaceutical monitoring. Some applications would include a wide range of uses in research and development; process monitoring and control; quality control and the monitoring of the work environment. For example, the market for blood glucose monitoring is worth more than \$800 million world-wide, hence emphasising the valuable position enzyme biosensors hold in the marketplace [1].

Although an ideal biosensor should be sensitive, selective, stable, accurate, precise, simple, inexpensive, have a rapid response, be ideally rugged and reagentless, in reality these requirements are seldom achieved. It is important to emphasise that biosensors are a potentially powerful tool for biochemical monitoring. However, the realisation of their potential requires a close appreciation of the materials required for their interfacing needs. An integrated approach that combines engineering with chemistry in both academic and industrial circles is vital if such devices are to have practical uses.

Many institutes are now recognising these demands, with many academic establishments working closely with industrial circles to overcome these obstacles for the successful development of enzyme-based biosensors. Ideally what is required are systems which can operate without mediators. The more simple the reaction, the less complications involved comprising leaching of mediators and so on. The ability of such biosensors for qualitative and quantitative monitoring must also be realised, if such devices are to find their niche in routine analysis.

1.2. Enzyme Catalysis

Two important aspects of enzymatic catalysis are molecular recognition and rate acceleration [2]. The function of catalytic groups at the active site of enzymes is to

induce electron density changes in the substrate, thus facilitating bond cleavage and formation. It is therefore not surprising that these catalytic groups can also catalyse different reactions, but only those which involve a similar direction of electron flow to that of the 'natural environment'.

The first step in enzyme catalysed reactions is the bringing together of the substrate and the enzyme. This binding process brings the reacting groups on the enzyme and substrate into close proximity. Such favourable interaction between enzyme and substrate is usually referred to as the 'binding energy'. Despite the unique 3-D structure of enzymes, the free energy of folding amounts to only 15-60 KJ mol⁻¹ as there is a large unfavourable energy change accompanying protein folding because of the decrease in surface area exposed to water. This emphasises the large unfavourable entropic contribution upon folding as a result of the loss of internal rotations. Their dimensional size alone is the minimum required to obtain a unique 3-D structure. The large binding energies between enzymes and substrates is a result of the close packing of atoms within the protein which constitutes as much as 75 % of the enzyme interior.

The number of interactions between substrate and enzyme can be quite large [3]. For example, there are eight amino acid residues in citrate synthase which form hydrogen bonds to citrate and another eight which form similar bonds to coenzyme A. However, these residues range from number 46 to number 421. Most of the 437 amino acid residues of citrate synthase are therefore required to bring the enzyme into the required geometrical conformation. Most enzymes are in the molecular weight range 30,000-50,000 [4]. The surface to volume ratio for most enzymes is constant, and as the radius increases there is proportionately less surface area. The common size of enzymes represents the minimal required for multiple interactions within the cell. The regulatory control of enzyme action also requires extensive binding sites, and hence the large size of an enzyme molecule.

1.3. Electrochemical Enzyme Biosensors - Theoretical Aspects

The general mechanism on which an amperometric enzyme-based biosensor is based depends on the interaction between the analyte present in the sample, and the enzyme

immobilised on the surface of the electrode; the consequent formation of an electroactive species generates an electrical signal or variation of a pre-existing one [5]. This signal is therefore proportional to the activity of the chemical species to be determined. Electrochemical biosensors should be developed so as to maximise their sensitivity towards the specific chemical species to be detected and to minimise the time constant for the response.

The most general rational correlation amongst any biological, physiological or pharmacological effect e.g. due to an interaction between a chemical species and its receptor, indicated as Θ , the consequent generation of an electrical signal, and the activities of the chemical species involved in the interaction, can be described on the basis of the following considerations [5]. The effect Θ , which is the interaction between the analyte and the enzyme, its maximum effect Θ_{\max} , the concentration of free agonist C_F , the concentration of occupied active sites on the receptor macromolecule, C_{ZF} , the total concentration of active sites, C_{Ztot} , and the equilibrium constant, K , of the interaction between F and Z, are connected by the following equations:

$$K = (C_F C_Z) / C_{ZF} \quad (1.1)$$

The effect of interaction, Θ , between the chemical species and the enzyme, is a parameter correlated with the fraction of active sites on the enzyme through a constant, k . More precisely, Θ and Θ_{\max} are respectively proportional to the concentration of occupied active sites on the receptor macromolecule, i.e. the enzyme,

$$\Theta = k C_{ZF} \quad (1.2)$$

and to the total concentration of active sites on the enzyme, C_{Ztot}

$$\Theta_{\max} = k C_{Ztot} \quad (1.3)$$

It must be stressed that k is just a proportionality constant and it is not a velocity constant. This means that, since k is not dependent on the time, the effect takes place

at the same time as the interaction between F and Z. The possibility of obtaining prompt and continuous signals by means of electrochemical biosensors is closely correlated with the value of an energy of interactions or sort of 'chemical affinity', ΔG^* , that is generally relatively low.

ΔG^* is therefore proportional to the electrical energy present under the specified conditions of temperature, pressure and the activity of the considered chemical species, and is converted into an electrical signal, according to the general equation:

$$\Delta G^* = -nF\Delta\Psi \quad (1.4)$$

where n is the electrochemical valency of the reaction, or the number of Faraday, F , per equivalent of reaction and $\Delta\Psi$, is the electrical potential difference. ΔG^* is conventionally taken as negative, and hence $\Delta\Psi$ as positive, if the reactants are written on the left and the products on the right hand side of the chemical equation.

The relationship between $\Delta\Psi$ and Θ , given by an electrochemical enzyme-based biosensor is therefore self evident. Both these entities are in fact proportional to the concentrations of the chemical species involved in the interaction. With such electrochemical enzyme based biosensors, the reactions involve an incredible number of molecules and take place at a very high rate. It is a worthwhile feature that the validity of relationship (1.4) extends from the electrical signals of biosensors, and can be used to explain electrical signals associated to transport phenomena at the level of nerve fibers or to other facilitated transport processes. It can thus be written that:

$$\Theta/\Theta_{\max} = (C_{ZF}/C_{Z\text{tot}}) = [C_F/(K + C_F)] \quad (1.5)$$

or by rearranging

$$1/\Theta = 1/\Theta_{\max} + [(K/\Theta_{\max})(1/C_F)] \quad (1.6)$$

These are schematically represented by Figures 1.1 and 1.2 respectively. It clearly appears that by replacing the effect of the interactions with the velocities of an enzymatic reaction i.e., by replacing the K with K_M , and the substrate concentration C_F with S , the concentration of substrate, equation (1.5) becomes the reciprocal of the Michaelis-Menten equation, also known as the Lineweaver-Burk relationship:

$$1/V = 1/V_{\max} + [(K_M/V_{\max})(1/S)] \quad (1.7)$$

It has therefore been demonstrated that the mechanism of action of an electrochemical enzyme-based biosensor, deduced in equation (1.5) and (1.6), stems from the Michaelis-Menten equation, which is well known in the study of enzyme kinetics.

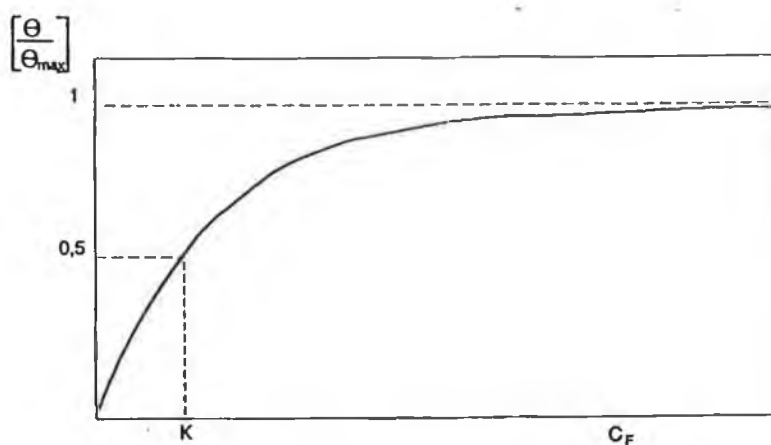


Figure 1.1. Relationship between Θ/Θ_{\max} and C_F

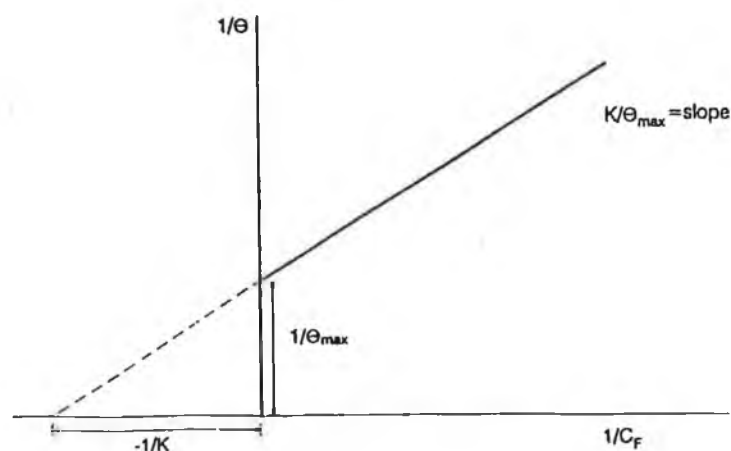


Figure 1.2. Relationship between $1/\Theta$ and $1/C_F$

Figures 1.1 and 1.2 also resemble the well known variation of reaction velocity with substrate concentration, and the Lineweaver-Burk plot for evaluation of critical constants, in Michaelis-Menten kinetics. The only difference in the representation here is that one depicts the relationship between the effect of interaction and the concentration of the free substrate.

It is clear from Figure 1.1, that the interaction between enzyme and substrate plateaus at a certain concentration of substrate. At this point the enzyme becomes saturated and represents the maximum electrical signal, $\Delta\Psi$, obtainable from the system. Figure 1.2 allows other constants to be evaluated and recorded for such a system. Figure 1.3 summarises the mechanistic performance of an electrochemical enzyme-based biosensor.

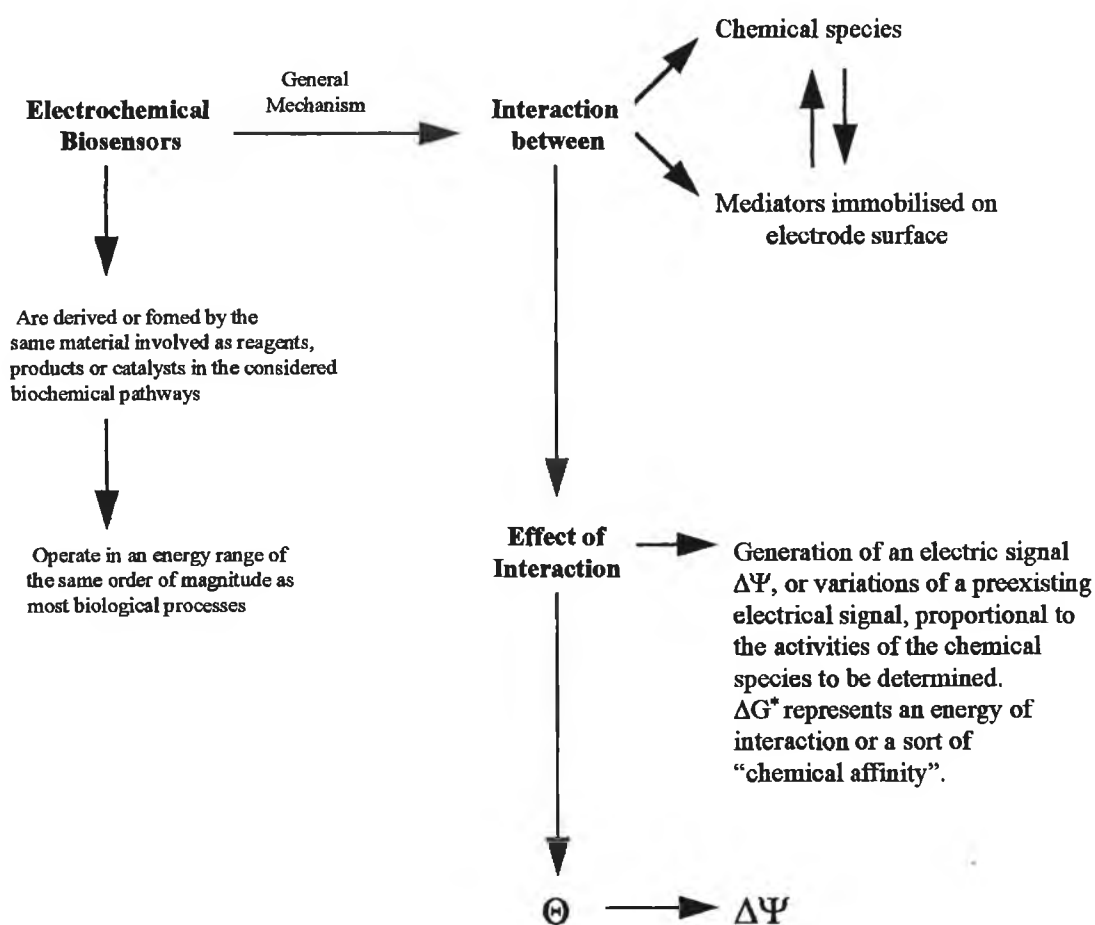


Figure 1.3. Summary of electrochemical enzyme-based biosensor mechanism.

The validity of equations (1.5-1.6) are, however, limited to the following cases:

(a) the effect Θ must be proportional to the number of receptorial sites occupied by the substrate; (b) each molecule of substrate must stoichiometrically interact with each receptorial site; and (c) the number of molecules of substrate must be much greater than the number of receptorial sites, i.e. only a small fraction of the number of total molecules can interact with the receptor sites.

1.4. Electrochemical Signal Transduction and Working Electrodes

In order to convert these biochemical reactions into an electronic signal that can be easily manipulated, a transducer is required. In electrochemical signal transduction, the transducer is a working electrode and can take many forms, some of which include glassy carbon, carbon paste and platinum electrodes respectively.

1.4.1. Glassy Carbon

Glassy carbon is widely used in electrochemistry for the analysis of electroactive substances and as a support for surface modified electrodes. The electrochemical properties of this material can be improved by surface treatment. At present, electrochemical pre-treatment through oxidation and reduction of the electrode surface is a widely used method to improve the activity and performance of glassy carbon electrodes for catalysis and in applications as electrochemical detectors of electroactive substances [6-9]. For example, immobilisation of horseradish peroxidase in a polyphenol film at an electrochemically activated glassy carbon electrode showed excellent biocatalytic activity and stability. The enzyme electrode exhibited linear responses to H_2O_2 in a concentration range of 5×10^{-8} to $1 \times 10^{-5} \text{M}$ and its response time was less than 5 s. At a moderate operating potential of 0 V vs. SCE, the direct responses of H_2O_2 and other electroactive interferents such as ascorbate and urate, on the activated glassy carbon electrode were minimal. The interference of ascorbate and urate was further reduced by the insulating polyphenol film [10]. The long term stability of the enzyme electrode was investigated by measuring the response to $2 \times 10^{-5} \text{M}$ H_2O_2 in phosphate buffer and there was no apparent loss of sensitivity after 2 months of storage. A detection limit of $2 \times 10^{-8} \text{M}$ was obtained.

Bianco and Aghroud [11] have used glassy carbon electrodes modified with cation exchangers to study the electrochemical behaviour of herbicides and plant growth regulators from the quaternary ammonium family e.g. mepiquat, chlormequat and difenzoquat. The kinetics and stability of incorporation into the cation exchange layer were evaluated, providing valuable information for future environmental applications.

In a similar way, Deng and Dong [12] modified a glassy carbon electrode with a cobalt(II)tetraphenylporphyrin (CoTPP) and co-immobilised acetylcholinesterase in the layer. With the present widespread concern about human health and environmental conditions, more and more researchers are showing great interest in the enzyme acetylcholinesterase because of its important role in the metabolism of neurotransmitters and its blockage by some inhibitors. The use of cobalt(II)tetraphenylporphyrin in the biosensor protocol has the ability of reducing the overvoltage by 300 - 400 mV for the electroanalysis of thiocholine, and also has showed high electrocatalytic activity. The biosensor composite yielded a limit of detection of $0.8 \mu\text{mol l}^{-1}$ thiocholine, with a relative standard deviation less than 2% and a storage stability of 3 months.

1.4.2. Carbon Paste

As one of the most important composite electrodes, the carbon paste electrode (CPE) was invented by Adams in 1958 [13]. It is consisted of mixing electrically conducting graphite powder and an organic pasting liquid which is immiscible with contacting aqueous solution [14]. These electrodes have been used extensively in the construction of biosensors, due to their high versatility in immobilising their matrix co-factors, activators and a large spectrum of additives that improve the electrochemical and/ or biochemical reaction, and consequently the analytical performance of carbon paste-based biosensors [15].

During the past 15 years, carbon paste electrodes have received great attention and have been extensively used in the fields of electroanalysis and biosensors [16]. The broad application of carbon paste electrodes is based mainly on its attractive advantages such as low cost, a wide potential window, ease of preparation and renewal and

convenient modification. Although modification of carbon paste electrodes began in 1964 [17], real chemical modification of such electrodes was only first attempted by Check and Nelson [18] in 1978, who introduced complexing functional groups to the electrode surface. The resultant electrode was used in the preconcentration of silver. Another modification was reported by Yao and Musha [19], by dissolving a modifier in the organic pasting liquid for electroanalysis. However, the real break-through regarding widespread use of carbon paste electrodes was achieved by Ravichandran and Baldwin [20] who directly mixed a modifier with carbon paste in 1981.

Since then, the number of publications dealing with modified carbon paste electrodes has exhibited an exponential increase. Since 1988, the main development in this field has involved doping carbon paste with a variety of biological materials such as enzymes, plant tissues and whole microbial cells, resulting in functionalised electrodes for the determination of phenols, lactate, glucose and a whole variety of other substances [16]. The application of carbon paste electrodes has been extended to almost all fields of electroanalysis. The effects of paste composition and surface pre-treatment on reaction kinetics and capacitance have been evaluated [21,22]. The surface properties of carbon paste electrodes have been studied by scanning tunnelling [23], electron and electrochemical scanning microscopy [24,25], as well as by electrogenerated chemiluminescence [26]. Kulys et al. [27] recently studied electrochemical properties and corresponding possible mechanisms of unmodified and modified carbon paste electrodes using chronoamperometry and cyclic voltammetry.

1.4.3. Platinum

Platinum has been a popular electrode material because of its inherent superior response characteristics. Nanjo and Guilbault [28] immobilised uricase on the surface of a platinum working electrode for the monitoring of uric acid in biological fluids. Other groups have modified platinum working electrodes with polyphenol films to eliminate interferences in clinical analysis [29]. The reduction in electrode poisoning in a biosensor for the monitoring of glucose has also been achieved by incorporating platinum electrode particles in a Nafion film dispersed on glassy carbon [30].

Moser et al. [31] have also developed advanced immobilisation techniques for glucose oxidase and lactate oxidase biosensors using highly purified platinum surfaces. These immobilisation techniques have involved the use of benzene tetracarboxylic acid anhydride (BTCAD), succinic anhydride and carbodiimide, and BTCAD with p-phenylenediamine. These immobilisation techniques have resulted in outstanding biosensor performance by virtue of their interfacial and surface chemistry properties. The long term stability of the glucose biosensors incubated at 4°C showed no decrease in sensor response even after one year. Immobilisation of the lactate oxidase resulted in no significant increase in enzyme stability compared to other techniques and may require further crosslinking of the immobilised enzyme layer in order to improve their long term stability.

1.5. Electron Transfer - The Mediation Process

Enzymes involved in the oxidation and reduction of biological molecules either contain a redox centre such as iron, copper, flavin, quinone at their active site or perform their biological role in conjunction with a redox active cofactor such as NAD(P)⁺. The difficulty in obtaining direct electrochemistry between an enzyme's redox centre and a naked electrode, together with the absence of an effective electrocatalytic surface for the efficient recycling of reduced cofactor, led to the first enzyme electrodes indirectly exploiting electrochemistry to monitor enzyme activity. The classic example is the glucose electrode sensor proposed by Clark and Lyons [32] and described by Updike and Hicks [33] based on the enzyme glucose oxidase and a polarographic oxygen electrode. Glucose oxidase is an FAD containing enzyme which catalyses the oxidation of glucose to gluconic acid. During the catalytic cycle, the flavin prosthetic group is first reduced by glucose and then reoxidised by molecular oxygen. The amount of glucose present in the solution is determined by following either the rate of oxygen consumption or the rate at which hydrogen peroxide is produced.



Although O_2 is the physiological electron acceptor for oxidases such as glucose oxidase, it can be replaced in the majority of cases by an electron transfer mediator. A mediator is a low molecular weight redox couple which shuttles electrons from the redox centre of the enzyme to the surface of the indicator electrode. During the catalytic cycle the mediator first reacts with the enzyme and then diffuses to the electrode surface where it undergoes rapid charge transfer.

The use of a mediator introduces a number of distinct advantages. Provided the mediator is unreactive with oxygen, it makes measurement virtually independent of pO_2 . Secondly, the working potential of the enzyme electrode is now determined by the formal potential (E^0) of the mediator couple. This can be particularly advantageous if the mediator has a low E^0 since it lessens the chance of interference. Finally, if the oxidation of reduced mediator does not involve protons it can make the enzyme electrode relatively pH insensitive.

Molecules such as quinones, organic ions, and inorganic ions such as ferricyanide and redox dyes have all been used with some degree of success. A practical mediator must react rapidly with the enzyme. It should exhibit reversible kinetics, and should be stable in both oxidised and reduced forms, should not react with O_2 and ideally be non-toxic. The overpotential for the regeneration of the oxidised mediator should be low and pH independent.

An extremely practical configuration in mediated biosensor construction is to have the mediator firmly anchored to the surface of the electrode or within the enzyme immobilised layer, in such a way that it is still electrochemically active and able to react with the enzyme. One of the most successful classes of mediator compounds that has been used in this way has been based on the use of ferrocene and its derivatives. Ferrocene is a transition metal π -arene complex which consists of an iron atom sandwiched between two cyclopentadienyl rings. It has a well behaved electrochemical redox couple ($E^0 / (mV) \text{ vs. SCE} = 165$) with variation in physical and chemical properties available through substitution in either of the two ring systems.

1.6. Enzyme Immobilisation Methods

Selection of support material and the method of immobilisation is made by evaluating the various characteristics and required features of the particular application against the properties of the particular support and immobilisation method. A number of practical considerations are required before embarking on an experimental design to ensure that the final immobilised enzyme will operate at optimum effectiveness.

In solution, soluble enzyme molecules behave as any other solute in that they are readily dispersed in the solution and have complete freedom of movement. However, once the enzyme is immobilised on the support surface, this freedom of rotation is somewhat hindered by the particular method used. The physical and chemical properties of the support material are important, and factors such as available surface area, degree of porosity, inertness towards the enzyme material, availability of functional groups for modification, and regeneration and re-use of the electrode surface all have an important part to play in the immobilisation process chosen. The stability of the electrode and resistance to microbial attack, effect of pH, temperature, and organic solvents are also important considerations. The most popular immobilisation methods are adsorption, covalent binding, entrapment, encapsulation and crosslinking.

1.6.1. Adsorption

This is the simplest method of immobilisation and involves reversible interactions between the enzyme and the support material. The forces involved are electrostatic in nature, such as van der Waals forces, ionic and hydrogen bonding interactions, although hydrophobic bonding can also be significant. These forces are very weak, but sufficiently large in number to enable reasonable binding.

Existing surface chemistry between the enzyme and the support material is utilised so that no chemical modification is required and little denaturation of the enzyme is caused. The procedure consists of placing the biological component on the support material, under suitable conditions, for a certain period of time. This is a simple, cheap and efficient method of immobilisation and is reversible allowing regeneration of the support material. However, the most significant disadvantage is leakage of the enzyme

from the support. Desorption can occur under many circumstances, and environmental changes in pH, temperature, and ionic strength will promote desorption. However, this latter factor can be turned to advantage if regeneration of the support is built into the operational regime, to allow rapid expulsion of the exhausted enzyme and replacement with fresh biocatalytic layer.

1.6.2. Covalent Binding

This immobilisation method involves the formation of a covalent bond between the enzyme and the support material. The bond is normally formed between functional groups present on the surface of the support and functional groups belonging to amino acid residues on the surface of the enzyme. A number of amino acid functional groups are suitable for participation in covalent bond formation. Those that are most often involved are the amino group (NH₂) of lysine or arginine, the carboxyl group (CO₂H) of aspartic acid or glutamic acid, the hydroxyl group (OH) of serine or threonine, and the sulfhydryl group (SH) of cysteine.

Functional groups on the support material are first activated by a specific reagent, and then the enzyme is added in a coupling reaction to form a covalent bond with the support material. Normally the activation reaction is designed to make the functional groups on the support strongly electrophilic (electron deficient). In the coupling reaction, these groups will react with strong nucleophiles (electron donating), such as the amino (NH₂) functional groups of certain amino acids on the surface of the enzyme, to form a covalent bond. Chemical modification increases the range of immobilisation methods that can be used for a given support material. Derivatisation can also be used to modify charges on the surface of a support material to improve binding of the biocatalyst.

1.6.3. Entrapment

Entrapment differs from adsorption and covalent binding in that the enzyme molecules are free in solution, but restricted to movement by the lattice structure of a gel. The porosity of the gel lattice is controlled to ensure that the structure is tight enough to prevent leakage of enzyme, and yet at the same time allow free movement of substrate

and product. Entrapment can be achieved by mixing an enzyme with a polyionic polymer material and then crosslinking the polymer with multivalent cations in an ion-exchange reaction to form a lattice structure that traps the enzyme (ionotropic gelation). Temperature change is a simple method of gelation by phase transition using a 1-4% solution of agarose or gelatin. However, the gels formed are soft and unstable. A significant development in this area has been the introduction of κ -carrageenan polymers that can form gels by ionotropic gelation and by temperature-induced phase transition, which has introduced a greater degree of flexibility in gelation systems for immobilisation.

Alternatively, it is possible to mix the enzyme with chemical monomers that are then polymerised to form a crosslinked polymeric network, trapping the enzyme in the interstitial spaces of the lattice. The latter method is more widely used, and a number of acrylic monomers are available for the formation of hydrophilic copolymers. The pore size of the gel and its mechanical properties are determined by the relative amounts of monomer and crosslinking agent. It is therefore possible to vary these concentrations to influence the lattice structure.

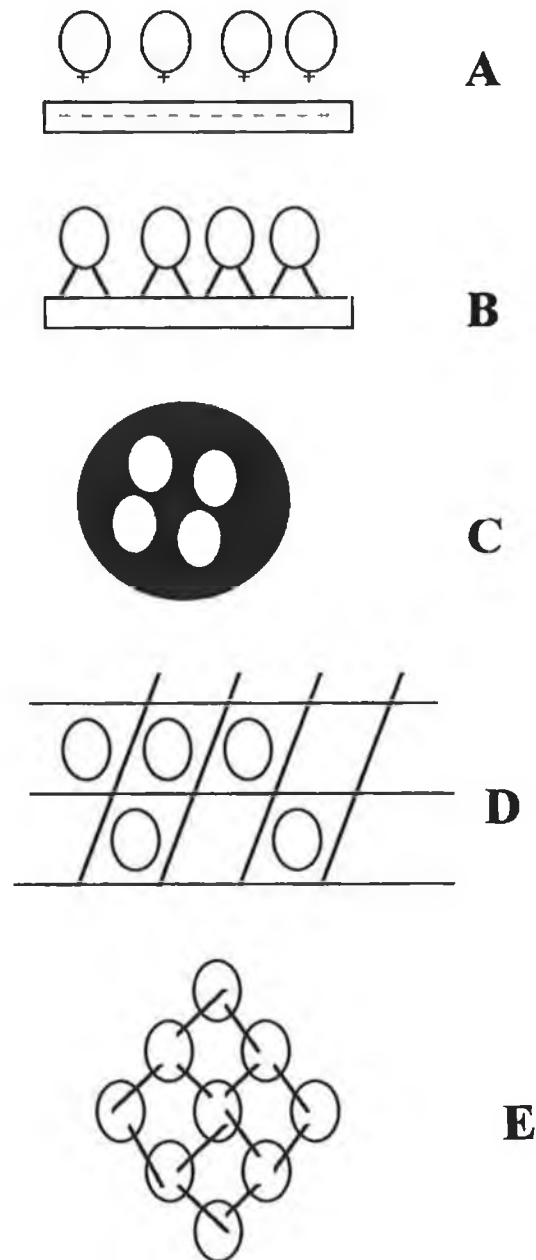


Figure 1.4. Immobilisation methods. A. Adsorption. B. Covalent Bonding. C. Encapsulation. D. Entrapment. E. Crosslinking.

1.6.4. Encapsulation

Encapsulation involves enveloping the biological entity within various forms of semi-permeable membranes. It is similar to entrapment in that the enzymes are free in solution but restricted in space. Large proteins cannot pass out of or into the membrane, but small substrates and products can pass freely across it. Many materials have been used to construct microcapsules varying from 10-100 μm in diameter; for example nylon and cellulose nitrate have proven popular.

1.6.5. Crosslinking

This involves joining enzymes to each other to form a large three dimensional complex structure, and can be achieved by chemical or physical methods. Chemical methods of crosslinking normally involve covalent bond formation between the cells by means of a bi- or multifunctional reagent, such as glutaraldehyde or toluene diisocyanate. Both bovine serum albumin and gelatin have been used to provide additional protein molecules as spacers to minimise the close proximity problems that can be caused by crosslinking a single enzyme. Crosslinking is rarely used as the only means of immobilisation because the absence of mechanical properties and poor stability are severe limitations. Crosslinking is most often used to enhance other methods of immobilisation.

1.7. Properties of Tyrosinase Enzyme

Enzymes are catalysts, which have the ability to lower the energy of reaction, hence increasing considerably the fraction of molecules with sufficient energy to react and form the product. It therefore increases the rate of the reaction without itself being consumed in that reaction. This process occurs at the active site of the enzyme, as mentioned previously in Section 1.2.

As one is aware, enzymes are non-selective, in that many compounds are capable of undergoing substrate catalysis. This is best exemplified by tyrosinase and its reaction to phenol compounds. The enzyme is a polyphenol oxidase and oxidises phenols to quinone products, which can then be manipulated electroanalytically by a chemical

reduction at a working electrode surface, thus giving rise to an electrical signal.

Tyrosinase is a bifunctional, copper-containing oxidase having both catecholase and cresolase activity [34]. Most research work on tyrosinase has been performed using mushroom as the source. The enzyme is a tetramer containing four atoms of copper per molecule [35], and two binding sites for aromatic compounds including phenolic substrates. There is also a distinctively different binding site for oxygen, the copper site. Its kinetic properties have been widely studied and reported [36-39].

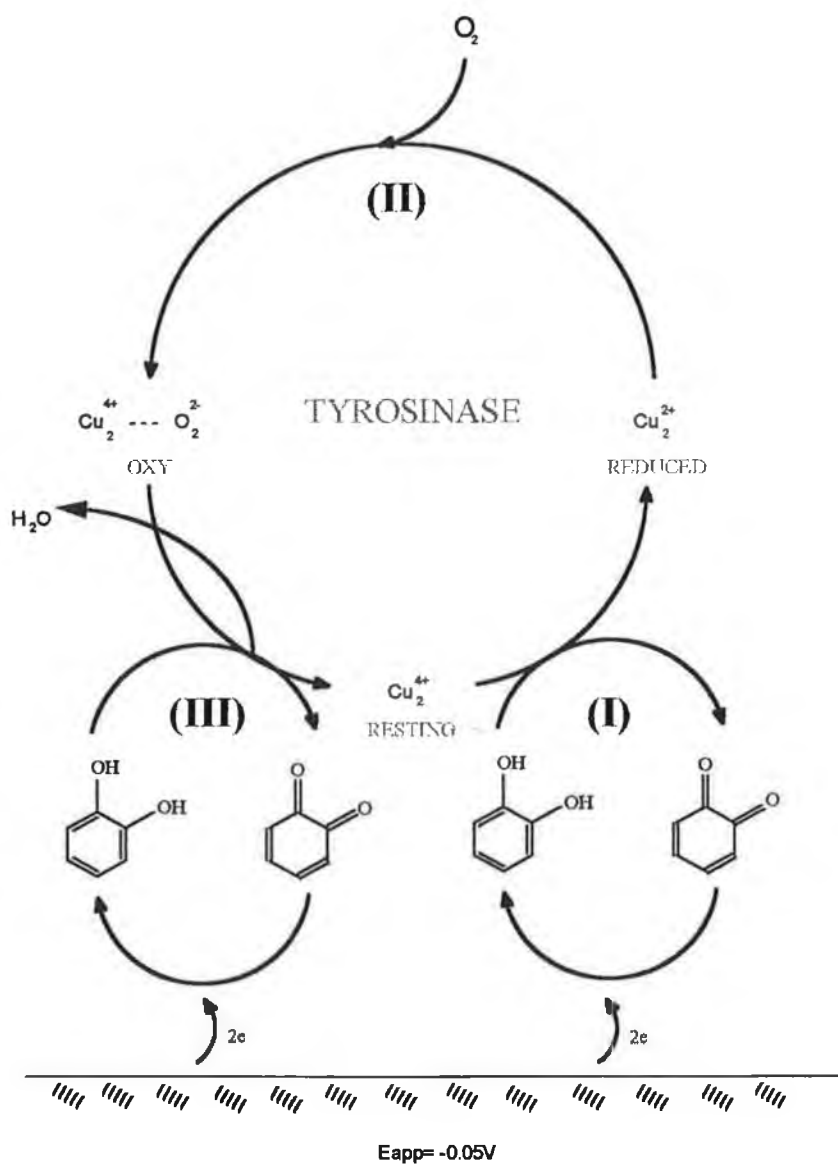


Figure 1.5. Mechanism of tyrosinase electrocatalysis.

The catalytic cycle of tyrosinase with catechol and subsequent electrochemical reduction of o-quinones occurring at the solution electrode interface are shown in Figure 1.5. Within one enzyme turnover, two catechol molecules participate with the production of o-quinone products. This step may be followed by an electrochemical reduction of the o-quinone to form catechol.

Tyrosinase plays a very important role in animal metabolism [40]. It is the only enzyme involved in the synthesis of melanins in pigment producing cells called melanocytes. It catalyses first the hydroxylation of tyrosine to 3,4-dihydroxyphenylalanine, more commonly known as Dopa. Dopa, which also acts as a cofactor for this reaction, is the substrate for a subsequent oxidation to dopaquinone, also catalysed by tyrosinase. In individuals, pigmentation is thus determined by the relative amounts of red and black melanins in skin, of which tyrosinase plays a vital role.

1.8. Biosensors and Enzyme Inhibition

Enzyme inhibition studies are of utmost importance in analytical chemistry. The inhibition of one or more enzymes in a metabolic pathway can have detrimental effects *in vivo*. Inhibitors range from food constituents [41-43], pesticides [44-46], halide [47], azide [48], and cyanide compounds [49], drug and related therapeutic agents [50-61], respiratory poisons [62], oxides and peroxides [63,64]. This list is by no means exhaustive, but highlights the necessity for analytical method development on inhibition work.

Many enzyme systems have been investigated for inhibition work. These have involved colorimetric assays using nitrate reductase [65,66] for benomyl cuparin; peroxidase [67] for mercury at the picogram level; malate dehydrogenase [68] for phenols; submitochondrial particles [69] for chlorophenols; glucose-6-phosphate dehydrogenase for chromium and cadmium; pyruvate kinase and hexokinase [70] for the monitoring of chromium, mercury and phenol inhibition respectively.

Amperometric methods have also been used, employing tyrosinase [71], acetylcholinesterase [72], cytochrome oxidase [73] and cyanobacteria [74] for the monitoring of inhibition by atrazine and cyanide, dichlorophenols, cyanide and diuron respectively. Inhibition of tyrosinase is associated with the interaction of a given compound with the copper active site of the enzyme [75]. Its role in electroanalytical chemistry as a screening agent for inhibitor compounds is extremely important. It is an extremely robust enzyme, with a very high catalytic activity, allowing relative substrate signals to be obtained very effectively with little noise. Its compatibility with graphite powder and sol gels allows various composite electrodes to be prepared. Its amazing resistance to high temperatures allows use of screen printed technology, which requires high temperatures in the curing stage, resulting in the availability of low cost, highly sensitive disposable biosensor strips for use in inhibition studies.

1.9. Types of Enzyme Inhibition

Although enzyme inhibition has been classified into reversible, competitive, uncompetitive, mixed and irreversible, non-competitive inhibition, one can more easily simplify inhibitor classification into two groups: poor inhibitors i.e., those which show an equilibrium constant similar to that for binding to aqueous copper complexes; and good inhibitors, which are substrate analogues, binding with an equilibrium constant higher by an order of magnitude relative to that for binding to aqueous copper complexes.

Thus, poor inhibitors usually give rise to reversible inhibition due to noncovalent binding of the inhibitor, giving rise to competitive and uncompetitive inhibition, whereas a good inhibitor gives rise to irreversible inhibition as a result of covalent binding and hence inactivation. Almost all irreversible enzyme inhibitors are toxic substances and are either natural or more commonly man made.

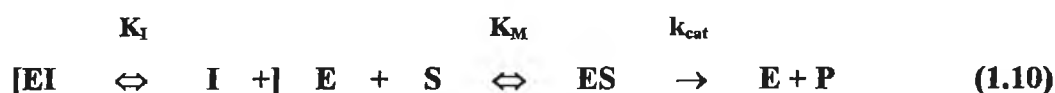
1.9.1. Reversible Inhibition

The various modes of reversible inhibition all involve the noncovalent binding of an inhibitor to the enzyme, but they differ in the mechanisms by which they decrease the enzyme's activity and in how they affect the kinetics of the reaction.

1.9.1.1. Competitive Inhibition

Suppose there exists a molecule that so closely resembles the substrate for an enzyme-catalysed reaction that the enzyme will accept it in its binding site. If this molecule can also be processed by the enzyme, it is merely a competing alternative substrate. However, if the molecule binds to the active site but cannot undergo the catalytic step. Such a molecule is called a competitive inhibitor.

For whatever fraction of time a competitive inhibitor molecule is occupying the active site, the enzyme is unavailable for catalysis. The overall effect is as if the enzyme cannot bind substrate as well when the inhibitor is present. Thus, one would expect that the enzyme would act as if its K_m , the Michaelis constant which is a measure of the strength of binding of the substrate to the enzyme (see Section 1.3 equation (1.7)), were increased by the presence of the inhibitor. Mathematically, this can be expressed as:



Here I stands for the inhibitory substance and K_I is a dissociation constant for inhibitor binding, defined as $K_I = ([E][I])/[EI]$. One can solve the rate equations, noting that

$$[E]_t = [E] + [ES] + [EI] \quad (1.11)$$

Total	Free	Enzyme	Enzyme
Enzyme	Enzyme	bound to	bound to
		Substrate	Inhibitor

where $[EI] = ([E][I])/K_I$, [I] being the concentration of free inhibitor. The result is

$$V = (V_{\max}[S])/([S] + K_M^{\text{app}}) \quad (1.12)$$

This resembles the Michaelis-Menten equation (see Section 1.3, equation (1.7)), except in this case K_M^{app} is the apparent Michaelis constant. Also, as mentioned, an increase in $[I]$ causes an increase in the K_M^{app} . Note that V_{\max} is unchanged, for as $[S]$ becomes very large, V approaches V_{\max} , just as in the absence of inhibition.

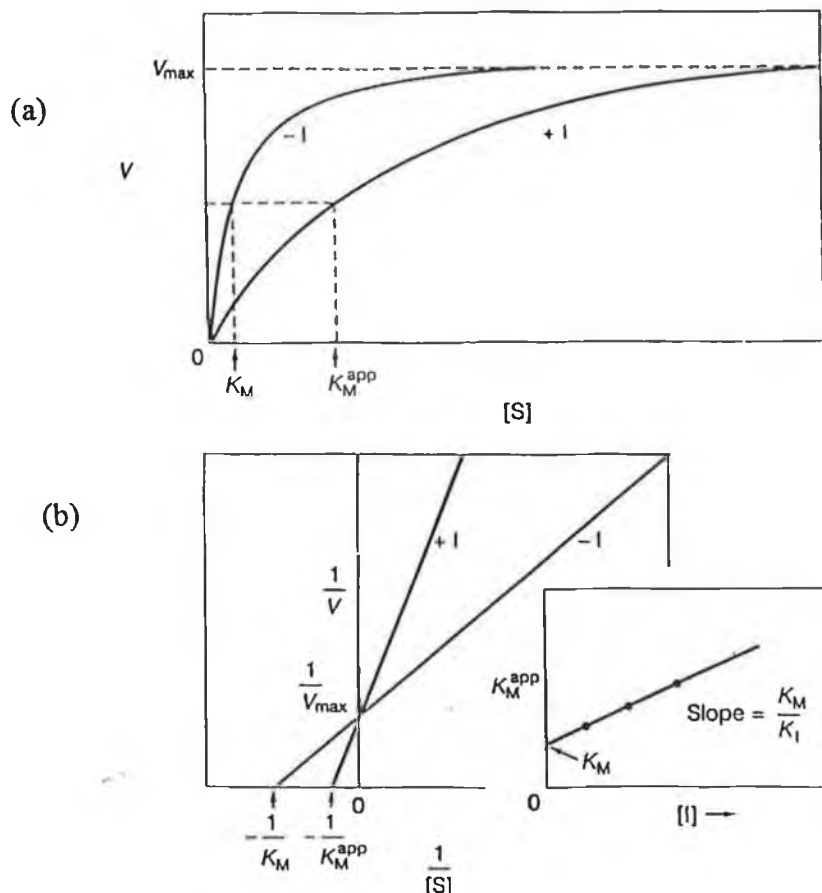
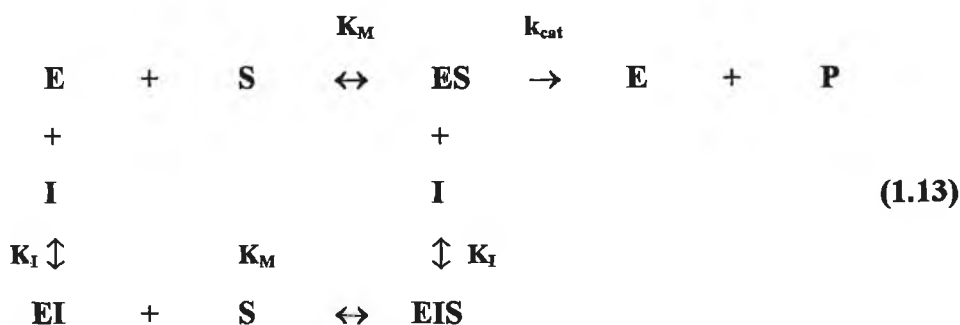


Figure 1.6. Effects of competitive inhibition on enzyme kinetics.

The effect of competitive inhibition on a graph of V versus $[S]$ is shown in Figure 1.6. Since the system at a given $[I]$, still obeys an equation of the Michaelis-Menten form, one must expect that Lineweaver-Burk plots and Eadie-Hofstee plots will still be linear graphs, with K_M but not V_{\max} changed by the presence of the inhibitor. As Figure 1.6(b) shows, this is exactly what happens. If one plots K_M^{app} versus $[I]$, we can determine both the true K_M and K_I as shown in the inset. The fact that the lines cross at the same V_{\max} proves that this is competitive inhibition.

1.9.1.2. Non-competitive Inhibition

This form of inhibition occurs when a molecule or ion can bind to a second site on an enzyme surface, not the active site, in such a way that it modifies k_{cat} . It might for example, distort the enzyme so that the catalytic process is not as efficient, as shown in Figure 1.7. Such a non-competitive inhibitor can be a molecule that does not interfere in any way with substrate binding but completely prevents the catalytic step. In this case, the inhibitor will bind equally well to both E and ES. One can therefore write:



Mathematical analysis yields

$$V = (k_{\text{cat}}^{\text{app}}[E]_t[S]) / ([S] + K_M) \quad (1.14)$$

The result is exactly what one would expect; the apparent K_M is uninfluenced by inhibitor, but the apparent k_{cat} decreases with increasing $[I]$. Therefore V_{max} is changed in this case (see Figure 1.7), for at high $[S]$ we find

$$V \rightarrow V_{\text{max}}^{\text{app}} = k_{\text{cat}}^{\text{app}}[E]_t = (k_{\text{cat}}[E]_t) / (1 + ([I]/K_I)) \quad (1.15)$$

The effect of non-competitive inhibition on a Lineweaver-Burk plot is shown in Figure 1.7.(b). Also, as shown in the insert, both k_{cat} and K_I may be determined by plotting $1/V_{\text{max}}^{\text{app}}$ versus $[I]$.

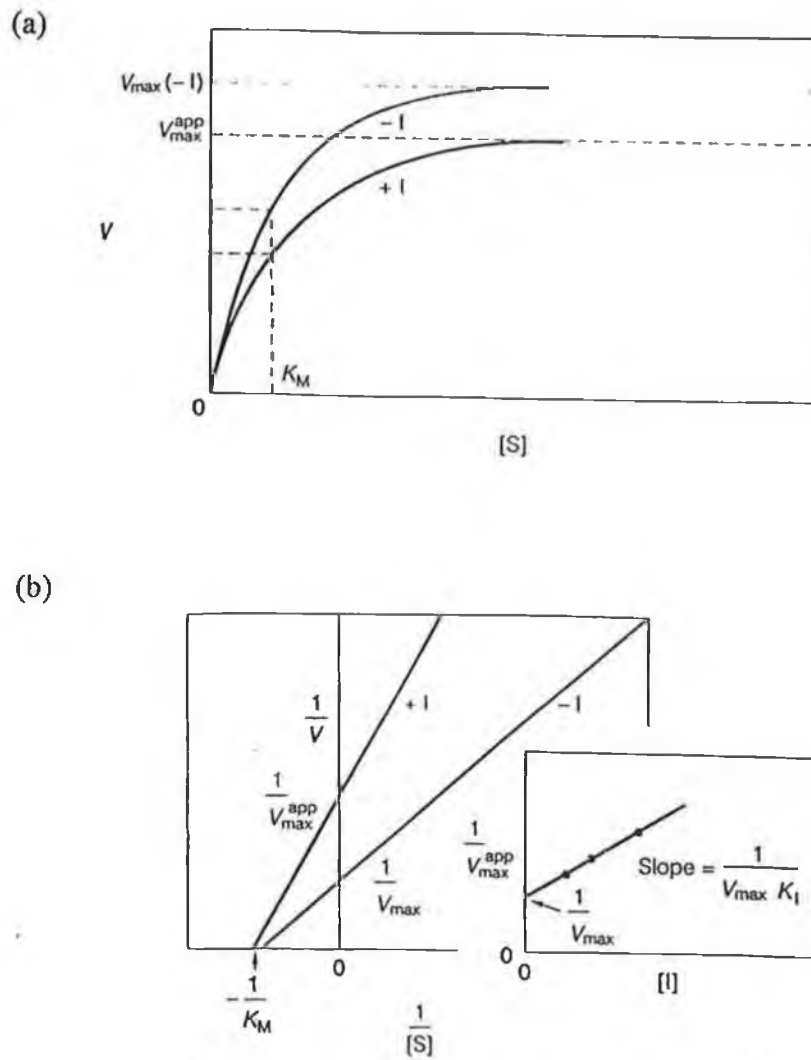
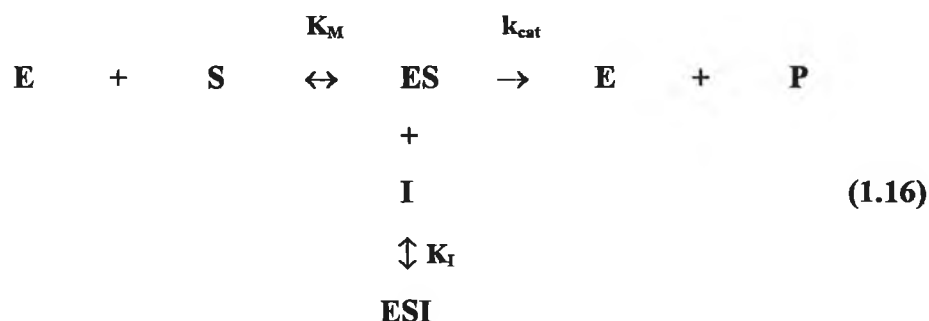


Figure 1.7. Effects of noncompetitive inhibition on enzyme kinetics. (a) Reaction velocity (V) versus $[S]$. K_M is not affected, but V_{max} is decreased because the enzyme is not as catalytically efficient in the presence of the inhibitor. (b) Lineweaver-Burk plots.

1.9.1.3. Uncompetitive Inhibition

There is a third class of reversible inhibition, in which the inhibitor binds only to the enzyme-substrate complex



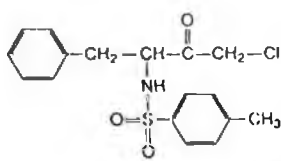
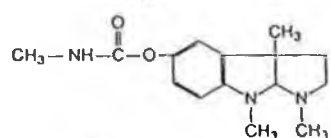
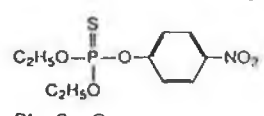
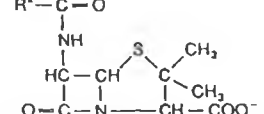
This binding blocks catalysis. When data for such an uncompetitive inhibition are plotted on a Lineweaver-Burk plot we find that both the apparent k_{cat} and K_M are changed by the addition of inhibitor. A series of parallel lines is obtained. The inhibitor therefore cannot bind to the enzyme in the absence of a substrate. Only when the enzyme substrate complex is formed, can the inhibitor bind. Since the inhibitor effectively 'siphons off' some of the enzyme substrate complex, K_M actually decreases in the presence of I. V_{max} decreases because the inhibited enzyme is less catalytically effective as in non-competitive inhibition.

1.9.2. Irreversible Inhibition

Some substances combine covalently with enzymes so as to inactivate them irreversibly. Almost all irreversible enzyme inhibitors are toxic substances. Some examples are shown in Table 1.1. In most cases, such substances react with some functional group in the active site to block the site from substrate or leave it catalytically inactive. A typical example of an irreversible competitive inhibitor is found in diisopropyl fluorophosphate (DFP). This compound reacts rapidly and irreversibly with serine hydroxyl groups to form the covalent adduct, as shown in Figure 1.8. Therefore, DFP acts as an irreversible inhibitor of enzymes that contain an essential serine in their active site. These include, amongst others, the serine proteases and the enzyme acetylcholinesterase. It is the inhibition of acetylcholinesterase that makes DFP such an exceedingly toxic substance to animals. The enzyme is essential for nerve conduction,

and its inhibition causes rapid paralysis of vital functions. Many insecticides and nerve gases are potent acetylcholinesterase inhibitors.

In other cases, irreversible inhibitors may be extremely selective because they resemble the substrate sufficiently to be strongly bound in the active site, facilitating covalent adduct formation. An example is tosyl-L-phenylalaninechloromethyl ketone (TPCK). TPCK is an excellent inhibitor for chymotrypsin, because the phenyl group fits nicely into the active site pocket, positioning the chlorine to react with the imidazole ring of the histidine amino acid number 57, HIS57. A larger number of such specific irreversible inhibitors have been synthesised to aid in the analysis of enzyme mechanisms and to control enzyme activity.

Name	Formula	Source	Mode of Action
Cyanide	CN^-	Bitter almonds	Reacts with enzyme metal ions (i.e., Fe, Zn, Cu)
Diisopropyl fluorophosphate (DFP)	$(\text{CH}_3)_2\text{CH-O-P(=O)(F)-O-CH}(\text{CH}_3)_2$	Synthetic	Inhibits enzymes with active site serine
Sarin	$(\text{CH}_3)_2\text{CH-O-P(=O)(F)-CH}_3$	Synthetic (nerve gas)	Like DFP
N-tosyl-L-phenylalaninechloromethyl ketone (TPCK)		Synthetic	Reacts with His 57 of chymotrypsin
Physostigmine		Calabar beans	Forms acyl derivative with acetylcholinesterase and other enzymes
Parathion		Synthetic (insecticide)	Acetylcholinesterase inhibition
Penicillin		From <i>Penicillium</i> fungus	Inhibits enzymes in bacterial cell wall synthesis

R⁺ = variable group; differs on different penicillins.

Table 1.1 Irreversible enzyme inhibitors.

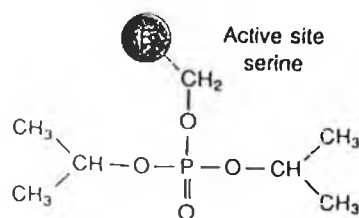


Figure 1.8. Adduct formed when DFP reacts with a serine group on a protein. The covalent bond renders the catalytically important serine ineffective in catalysis. The adduct also may block the site to substrate.

1.10. Disposable Biosensors & Screen Printing Technology

Despite the enormous number of publications concerning biosensors, very few of them are commercially available. One of the reasons is that there are still technical problems that retard their commercialisation, e.g. the reliability of biosensors is often well below that of the physical and chemical sensors [76]. Most of the commercialised biosensing devices are analyses based on enzyme membrane electrodes, and are developed for the determination of metabolites in body fluids by clinical laboratories. Due to the trends of decentralised testing in the doctor's office or by the patient, there is a need for simple to use analytical methods. This could be met by the development of test strips and disposable electrochemical biosensors.

Microfabrication of biosensors is possible through the thin film technology of photolithography and the thick film technology of screen printing. Although both technologies allow mass production of biosensors, the screen printing process is more popular. Such microfabrication allows the production of inexpensive biosensors, and since the screen printed strips are only 3 x 28 mm in size their applicability to hand held analysis can be realised. The screen printing process is relatively simple. It involves the use of a conducting ink; carbon based ones are commonly used due to electrochemical and economical considerations. The process then involves printing of different electrode

patterns (through a predesigned stencil) on the surface of ceramic or plastic substrates. The printed films are commonly baked at elevated temperatures to drive off the solvent and cure the patterned ink deposit. The process itself is outlined in Figure 1.9.

There are several companies offering inks differing in composition and electrical conductivity. The main materials required for the screen printing process are the ceramic plate substrate as mentioned. Solvents such as terpineol and ethylcellulose and varying additives depending on the application of the ink. These reagents are usually already incorporated into commercial inks upon manufacture, allowing a wide range to choose from depending on the application of concern.

The production of, for example, conducting line pastes, require a high conductivity, and therefore contain metal powders such as Au, Pt, Ag and Pd, whereas pastes for the production of dielectric layers may contain BaTiO₃ or silica. Choice of the thick film substrate is also important, and must meet certain requirements. They must be compatible with the ink and with the process at hand, and must be electrically non-conducting. Thus, the most common materials are ceramics. High purity, generally 96%, aluminium oxide, is the most widely used.

Disposable screen printed biosensors for the measurement of glucose have been developed by Wang and Chen [77]. This has involved the use of palladium-dispersed carbon inks with glucose oxidase polyphenol films grown electrochemically on the electrode strips after curing. The resulting strips yield favourable RSD's of 0.67%. The efficient electrocatalytic action of the Pd particles towards the oxidation of hydrogen peroxide together with the permselective properties of the polyphenol film led to a highly selective and sensitive response to the hydrogen peroxide product of the glucose oxidase catalysis of glucose.

Similar work has been performed on a disposable biosensor for cholesterol [78]. In this particular case a hydrogen peroxide cobalt phthalocyanine screen printed carbon electrode was prepared. This was then coated with a layer of cholesterol oxidase, covered with a film of cellulose acetate. However, the resultant probe remained stable for only a period of 5 days hence limiting its application.

Within the interests of enzyme inhibition, the use of screen printed electrodes seems a viable route. Cagnini et al. [79] have developed a disposable ruthenised screen printed choline biosensor for the monitoring of pesticides. The inhibitory effects of carbamate and organophosphate pesticides have been investigated. Pesticide levels as low as 1 nM have been detected. However, incubation times of 12 minutes were required and RSD's of 15% were common.

A more common practical solution to the latter sensor design is to use tyrosinase screen printed strips. The tyrosinase enzyme itself is highly robust and can withstand the high temperature curing steps of screen printing. The enzyme is incorporated into the ink and results in the formation of a thick film enzyme-ink strip. This procedure eliminates the problems involved with reproducibility of cast enzyme films on cured strips as depicted by Cagnini et al. [79]. Also, since the enzyme is trapped within the ink network, enzyme leaching is not a problem. Tyrosinase entrapment within the ink also eliminates time consuming casting procedures which are required by other enzyme systems .

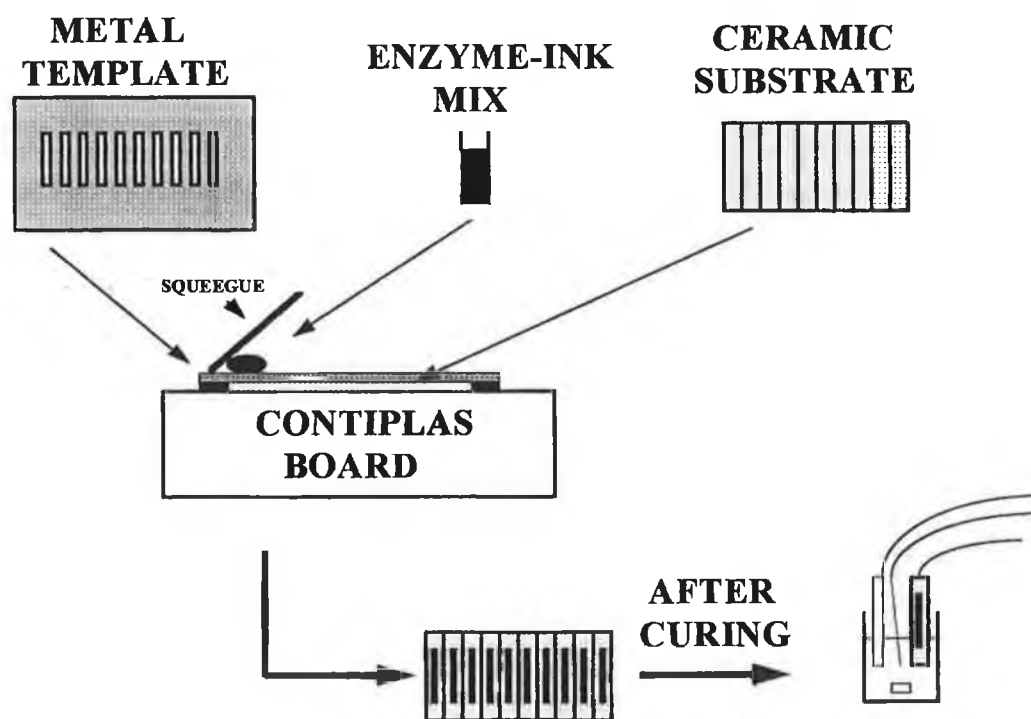


Figure 1.9. Schematic of the Screen Printing Process.

1.11. Tissue and Cell Based Biosensors for Environmental Monitoring

There has been increased interest over the years in the use of new biocatalytic materials in place of native enzymes i.e. pure isolated enzymes for the development of novel biosensors. Several biological materials such as bacterial cells, animal tissues and plant tissues have been proposed and used. The use of such materials offers some considerable advantages over conventional native enzyme-based biosensors. Whenever a whole tissue is used, all additional biological components such as enzyme cofactors which are responsible for the catalytic activity or at least stability of the enzyme of interest, are already included in the biocatalytic membrane. The tissue and cell components have usually higher catalytic activities, better stability, longer lifetimes and lower costs compared to their isolated enzyme counterparts.

Mazzei et al. [80] proposed the use of an acid phosphatase potato tissue biosensor for the determination of organophosphorous and carbamic acid pesticides. They compared the results obtained by the tissue biosensor to a biosensor constructed using native enzyme. However, the plant tissue based biosensor exhibited a longer shelf lifetime and better reliability. Detection limits as low as $0.5 \mu\text{g l}^{-1}$ were obtained, with RSD's of 3.0-3.4 %, along with a lifetime of 4 weeks.

The use of genetically engineered bacteria as biosensors for antimonite and arsenite was introduced by Scott et al. [81]. The bacteria used in this study, *Escherichia coli*, had been genetically engineered to produce the enzyme β -galactosidase in response to these ions. In the absence of antimonite or arsenite, a regulatory protein restricted the production of β -galactosidase. However, in the presence of these ions, β -galactosidase was produced, and the activity monitored electrochemically using p-aminophenyl β -D-galactopyranoside as substrate. RSD's of 1.1-1.7 % were obtained with detection limits as low as 1×10^{-7} M.

Several microbial cell based biosensors for the monitoring of cyanide have been reported [82-84]. Lee and Karube [82] developed a gas-phase biosensor using cyanide degrading bacteria, an oxygen electrode and a gas permeable PTFE membrane. The cyanide degrading bacteria, *Pseudomonas fluorescens*, consume oxygen upon degrading cyanide.

The change in oxygen concentration was then detected by the oxygen electrode. The performance of the biosensor was unaffected by the presence of other heavy metal ions, and a correlation coefficient of 0.995 was obtained for cyanide concentrations in the range 0.1 - 1mg/L, and yielded a lifetime of 1 month.

An alternative approach based on the inhibition of microbial cell respiration was exploited by Ikebukuro et al. [83]. The sensor consisted of a reactor flow system, with two oxygen electrodes and a reactor containing *Saccharomyces cerevisiae* immobilised on glass beads. This system offered better operating conditions compared to a similar study [84] using the same microbial cells immobilised in a cellulose membrane. A linear response of 0 - 15 μM was obtained, with a lower detection limit of 0.15 μM , and a lifetime of 9 days at ambient temperature.

A plant-tissue hybrid electrode was used for the determination of phosphate and fluoride by Schubert et al. [85]. This was based on the coupling of potato tissue and glucose oxidase with a Clark oxygen electrode. The relative standard deviation was 1.7% and 6.5%, with a lower detection limit of 2.5×10^{-5} M and 1×10^{-4} M for phosphate and fluoride respectively. Mazzei et al. [86] exploited the enzyme polyphenol oxidase in potato tissue for the monitoring of catechol, resulting in a linear range of 2.5×10^{-5} - 2.3×10^{-4} M for catechol and a lifetime of greater than 3 months. In a similar study, Ozsoz et al. [87] utilised mushroom tissue as a source of polyphenol oxidase for the determination of phenolic compounds.

Although plant tissue-based biosensors have their numerous advantages over conventional enzyme based ones, there are a number of uncertainties apparent. For example, incomplete knowledge about the freshness and the state of ripeness of the biocatalytic material is problematic, including the dependence of the biocatalytic activity of the plant materials on the growth conditions in which they were raised. It is therefore of prime importance to establish a well defined source of plant tissue materials in order to obtain reproducible sensor responses and lifetimes in addition to other analytical parameters. Navarantne and Rechnitz [88] have proposed the use of *in vitro* cultured plant tissues to overcome these problems. They have successfully cultured several plant

tissues with high activity and impressive analytical characteristics. For example, a cultured tobacco callus tissue for the analysis of hydrogen peroxide, yielded a lifetime of more than 5 months, fast response times of less than 2 s, a wide dynamic range of 5×10^{-6} - 1.1×10^{-4} M, with an RSD of less than 9.0 % and a detection limit of 7.5×10^{-7} M hydrogen peroxide.

1.12. Binder Modified Tyrosinase Biosensors for the Monitoring of Phenols

1.12.1. Standard Methods of Analysis for Phenolic Compounds

The concentration of phenolic compounds in natural waters vary to some degree, but on the whole they are usually present at the $\mu\text{g/L}$ level [89,90]. Concern for low level concentrations requires more than a total phenolic determination. Due to the varied effects of trace levels of phenolic compounds, it becomes necessary to evaluate them on an individual basis. This implies implementation of an isolation and identification scheme to perform the necessary analysis.

A suitable solvent must be used to extract the phenols from the environmental sample. Benzene, hexane, methylene chloride, chloroform and freon have been used for this purpose. Prior to positive identification, the phenolic compounds must then be successfully concentrated and isolated. Macroporous resins are usually used for this effort. XAD-2 resin, a copolymer of styrene-DVB, is quite popular. The phenols are adsorbed at an acidic pH and desorbed at a basic pH value. The desorption data is usually monitored using ultraviolet spectrophotometry. The last step in the analytical scheme involves the positive identification of the compounds. This is achieved through the use of gas liquid chromatography with flame ionisation detection, with a 3% OV1 column for separation. GC-MS has also been widely used for more in-depth studies.

Colorimetric methods are also commonly used for the analysis of phenolic compounds after extraction and isolation. These are based on the 4-aminoantipyrine colorimetric method that determines phenol, ortho- and meta-substituted phenols and under certain pH conditions, those para-substituted phenols where substitution is a carboxyl, halogen, methoxyl, or sulfonic acid group. However this method does not determine those para-

substituted compounds containing an alkyl, aryl, nitro, benzoyl, nitroso, or aldehyde group. A typical example of latter groups is para-cresol, which may be present in certain industrial wastewaters and in polluted surface waters. These methods are therefore limited in their applications, and rely on gas chromatography for total analytical determination.

Why attempt to use biosensors in comparison to these analytical techniques? There are many reasons, many of which will be mentioned in the following two sections. Firstly biosensors are more compact, and are applicable to field analysis, making the use of hand analysers viable. Technical expertise is less demanding and they are easy to use. This holds true when one compares the corresponding GC method, which requires a skilled operator for the numerous troubleshooting problems of which the method is notorious for.

The biosensing system for phenols using tyrosinase-based biosensors is essentially reagentless, and therefore cost effective. Results can be obtained within real time, due to fast response times. Signal decay is rapid allowing numerous samples up to 60 an hour to be analysed. The ideal of decentralised diagnostics is realised, i.e. very little sample preparation, hence allowing on-site testing and eliminating unnecessary manpower. Also with the growing interest in screen printing technology, vast numbers of good quality disposable tyrosinase strips could be produced, for rapid testing in routine analytical environmental monitoring.

1.12.2. Biosensing and Phenol Analysis

Amperometric detection of phenols is of growing importance in analytical environmental monitoring [91,92]. This is performed at usually a positive potential resulting in the oxidation of the compound and hence an analytically useful signal. However, the application of biosensors based on tyrosinase enzyme is of immense importance. In this particular case the phenol compound is converted into a quinone product by the enzyme, which is then reduced at a negative potential hence yielding a signal. This type of scenario is very attractive as it operates at a negative potential hence eliminating many natural interferences present in samples which undergo oxidation.

The environmental control of organic pollutants such as phenolic compounds in industrial waste effluents, has initiated the development of analytical techniques for fast, sensitive, and selective monitoring of hazardous compounds [93]. This is of particular interest for phenols, since they have been shown to be organic carcinogens and mutagens [94]. As mentioned, phenols can be determined amperometrically through direct electrochemical oxidation [94]. However, direct oxidation of phenols suffers from a number of drawbacks.

Due to the high overvoltage, a high anodic potential needs to be applied, opening up the detection system for interfering reactions. The high applied voltage is also followed by an increase in the background current and noise level. Moreover, direct electrochemical oxidation of phenols is coupled with fouling reactions due to the formation of nonconducting polyphenol films [95]. The utility of enzyme based amperometric biosensors to solve these obstacles for the determination of phenols has been experimentally demonstrated in a number of works, where enzymes such as tyrosinase [96-109], laccase [110,111] and peroxidase [112] have been successfully integrated with electrochemical transducers.

These biosensors operate in a potential window (around 0 V), where they are much less subjected to interfering reactions. Moreover, the sensitivity and detection limits achieved with biosensors are much improved compared to those obtained by direct oxidation. The latter is due to the amplification of the response current as a result of recycling of substrate at the surface of the bioelectrode.

Tyrosinase-modified electrodes have been used for the detection of monophenols and o-diphenols. Tyrosinase immobilisation procedures, electrode material, stability, and sensitivity have been extensively studied [96-109]. The sensitivity and the detection limits of some of those electrodes for the determination of catechol are shown in Table 1.2. As can be seen the highest sensitivity was observed with carbon paste electrodes doped with ruthenium and solid graphite chemically modified with tetracyanoquinodimethane. Ruthenium on carbon [96], Medula Blue in carbon paste [97] and chemical modification of solid graphite with tetracyanoquinodimethane [98] and

detergents in buffer solution [99] have been experimentally demonstrated to positively influence the sensitivity and the stability of tyrosinase-based biosensors.

The best detection limits were demonstrated with the tyrosinase electrochemically polymerised in polypyrrole or covalently cross-linked with glutaraldehyde on top of a solid graphite electrode. The detection limits for most of the tyrosinase modified electrodes still have to be improved in order to measure concentrations of phenolics in environmental waters lower than 5 nM. In some respects, the success of future developments of tyrosinase-modified electrodes depends on the mechanistic studies of their characteristics, an area of research which is urgently needed.

Electrode	Immobilisation Method	Analysis Mode	Sensitivity $A M^{-1} cm^{-2}$	Detection Limit nM
Glassy carbon	Polypyrrole tyrosinase layer	Steady state	1.5	2.0
Solid graphite	Covalently cross-linked tyrosinase carbodiimide-activated graphite	Flow injection	2.2	2.3
Carbon paste	Adsorbed tyrosinase	Steady state	1.8	10
Graphite/ epoxy	Enzyme mixed with composite	Flow injection	0.4	40
Graphite/ teflon	Enzyme mixed with composite	Flow injection	0.01	200
Solid graphite	Tyrosinase immobilised on chemically modified surface	Steady state	3.4	100-300
Carbon paste	5% Ru on carbon paste mixed enzyme and octadecylamine	Steady state	3.1	500
Carbon paste	Enzyme mixed with powder	Flow injection	0.8	900
Carbon paste	Carbon paste and eggplant tissue	Steady state	0.1	1000

Table 1.2. Comparison of the tyrosinase-modified electrodes for the detection of catechol in aqueous solution [103].

1.12.3. Binder Modified Biosensors and Phenol Analysis

As one is aware enzyme reactions have the ability to catalyse the oxidation/reduction of many substrates. Therefore, unlike an antibody, whose reactions are highly specific and selective, specificity with enzyme biosensors is not possible to achieve. However, one approach of improving the cognitive properties of an enzyme biosensor probe is to manipulate the physiochemical properties of either the surface, bulk or both. Although each phenol may display slightly different kinetic properties as a result of enzyme catalysis, it is still not enough information to characterise these compounds in a complex mixture. The tyrosinase biosensor operating in this mode only serves as a screening method for phenol compounds. A way of overcoming this is to have an array of tyrosinase electrodes with slightly modified surfaces and/or bulk.

In this model one could have an array of say 6 different electrode composites, operating via a computer controlled multichannel potentiostat. Each electrode would have different properties, and by virtue of the different equilibrium chemistry of the individual phenolic compounds, specific patterns due to partitioning effects of each phenolic compound at the different electrode surfaces will give rise to a specific recognition pattern. Ratios of times such as peak widths at half peak height, symmetry factors, such as the ratio of peak width of the region to the left of the maximum peak height divided by that shown by the region to the right. And also, the ratio of peak heights themselves can also yield valuable information.

The improvement in the performance of such biosensors is therefore highly desired to meet new challenges posed by clinical and environmental samples. One promising avenue to achieve such goals is to design surface micro-structures that meet specific detection needs [113,114]. Permselective coatings represent one direction by which modified electrodes can benefit flow analysis. This is accomplished by rejection from the surface of undesired interfering species while allowing the transport of the analyte. The size and charge exclusion discriminating properties of polymeric coatings such as cellulose acetate [115,116], perfluorinated [117,118] or polyester monomers [119] and poly(vinyl)pyridine [120] polymers have been exploited successfully for flow measurements.

An alternative route is to exploit the physiochemical properties of the various binders used in the construction of carbon composite electrodes. Although much research effort has been devoted by some research groups into the development of electrode surfaces derivatised with hydrophobic materials [121-124], work focusing on the entire bulk and surface of carbon paste electrodes is required. Such investigation would allow improvement in selectivity and enhanced sensitivity. The different responses of the various binder modified composites would suggest the possible use of this pattern recognition advantage in the construction of a biosensor array for the monitoring of phenols.

1.13. References

- [1] Harrowing, P.: *Analyst*, 121: (1996): 15N.
- [2] Page, M. I.; Williams, A.: *Enzyme Mechanisms*, (1987), R.Soc. Chem. Pub.
- [3] Remington, S.; Wiegand, G.; Huber, R.: *J. Mol. Biol.*, 158: (1982): 111.
- [4] Kiehn, E. D.; Holland, J. J.: *Nature*, 226: (1970): 544.
- [5] *Trends in Electrochemical Biosensors*. Costa & Miertus Eds.; (1992), World Scientific Pub.
- [6] Engstrom, R. C.: *Anal. Chem.*, 54: (1982): 2310.
- [7] Kepley, L. J.; Bard, A. J.: *Anal. Chem.*, 60: (1988): 1459.
- [8] Beilby, A. L.; Sasaki, T. A.; Stern, H. M.: *Anal. Chem.*, 67: (1995): 976.
- [9] Nagaoka, T.; Yoshino, T.: *Anal. Chem.*, 58: (1986): 1459.
- [10] Zhang, Z.; Lei, C.; Sun, W.; Liu, H.; Deng, J.: *J. Electroanal. Chem.*, 419: (1996): 85.
- [11] Bianco, P.; Aghroud, N.: *Electroanalysis*, 9: (1997): 602.
- [12] Deng, Q.; Dong, S.: *Analyst*, 121: (1996): 1123.
- [13] Adams, R. N.: *Anal. Chem.*, 30: (1958): 1576.
- [14] Olson, C.; Adams, R. N.: *Anal. Chim. Acta.*, 22: (1960): 582.
- [15] Beh, S. K.; Moody, G. J.; Thomas, J. D. R.: *Analyst*, 116: (1991): 459.
- [16] Gorton, L.: *Electroanalysis*, 7: (1995): 23.
- [17] Kuwana, T.; French, W. G.: *Anal. Chem.*, 36: (1964): 241.
- [18] Check, G. T.; Nelson, R. F.: *Anal. Lett.*, 11: (1978): 393.
- [19] Yao, T.; Musha, S.: *Anal. Chim. Acta.*, 110: (1979): 203.
- [20] Ravichandran, K.; Baldwin, R. P.: *J. Electroanal. Chem.*, 126: (1981): 293.
- [21] Ravichandran, K.; Baldwin, R. P.: *Anal. Chem.*, 56: (1984): 1744.
- [22] Albahadily, F. N.; Mottola, H. A.: *Anal. Chem.*, 59: (1987): 958.
- [23] Wang, J.; Martinez, T.; Yuniv, D. R.; McCormick, L.: *J. Electroanal. Chem.*, 286: (1990): 65.
- [24] Svancara, I.; Hvizdalova, K.; Vytras, K.; Kalcher, K.; Novotny, R.: *Electroanalysis*, 8: (1996): 61.
- [25] Wang, J.; Wu, L. H.; Li, R.: *J. Electroanal. Chem.*, 272: (1989): 285.
- [26] Engstrom, R. C.; Johnson, K. W.; Desjarlais, S.: *Anal. Chem.*, 59: (1987): 670.
- [27] Kulys, J.; Gorton, L.; Dominguez, E.; Emneus, J.; Jarskog, H.: *J. Electroanal.*

- Chem., 372: (1994): 49.
- [28] Nanjo, M.; Guillbault, G. G.: *Anal. Chem.*, 46: (1974): 1769.
- [29] Christie, I. M.; Vadgama, P.; Llyod, S.: *Anal. Chim. Acta.*, 274: (1993): 191.
- [30] Gunasingham, H.; Bengtan, C.: *Analyst*, 114: (1989): 695.
- [31] Moser, I.; Schalkhammer, T.; Mann-Buxbaum, E.; Hawa, G.; Rakohl, M.; Urban, G.; Pittner, F.: *Sensors and Actuators B*, 7: (1992): 356.
- [32] Clark, L. C.; Lyons, C.: *Ann. Acad. Sci.*, 102: (1962): 29.
- [33] Updike, S. J.; Hicks, G. P.: *Nature*, 214: (1967): 986.
- [34] Malmstrom, B.; Ryden, L.: *Biological Oxidations*, Singer, T., Ed., (1968), Interscience Pub.
- [35] Smith, J.; Krueger, R.: *J. Biol. Chem.*, 237: (1962): 1121.
- [36] Kertesz, D.; Brunori, M.; Zito, R.; Antonini, E.: *Biochim. Biophys. Acta*, 250: (1971): 306.
- [37] Kertesz, D.; Rotilio, G.; Brunori, M.; Zito, R.; Antonini, E.: *Biochim. Biophys. Res. Comm.*, 49: (1972): 1208.
- [38] Keyes, M.; Semersky, F.: *Biochem. Biophys.*, 148: (1972): 256.
- [39] Garcia-Carmona, F.; Calbenes, J.; Garcia-Canoras, F.: *Biochem. Intl.*, 14: (1987): 1003.
- [40] Matthews van Holde, *Biochemistry*, (1990), 1st Edn., Benjamin Cumin Pub.
- [41] Friedman, M.; Grosjean, O., K.; Zahnley, J.C.: *Food and Chemical Toxicology*, 24(9): (1986): 897-902.
- [42] Smit, M., H.; Rechnitz, G. A.: *Electroanalysis*, 5: (1993): 747.
- [43] Menon, S.; Fleck, R.W.; Yong, G.; Strothkamp, K.G.: *Arch. Biochem. Biophys.*, 280(1): (1990): 27.
- [44] El-Oshar, M. A.; Motoyama, N.; Hughes, P. B.; Dauterman, W. C.: *J. Econ. Ento.*, 78(6): (1985): 1203.
- [45] Koybayashi, Y.; Kayahara, H.; Tadasa, K.; Nakamura, T.; Tanaka, H.: *Bio. Biotechnol. & Biochem.*, 59(9): (1995): 1745.
- [46] Wang, J.; Dempsey, E.; Erememko, A.; Smyth, M. R.: *Anal. Chim. Acta.*, 279(2): (1993): 203.
- [47] Martinez, J. H.; Solano, F.; Penafiel, R.; Galinto, J. D.; Iborra, J. L.; Lozano, J. A.: *Biochem. Physio., B*, 83(3): (1986): 633.

- [48] Sugumaran, M.: *Biochem. Biophys. Res. Comm.*, 212(3): (1995): 834.
- [49] Boyer, R., F.; Mascotti, D., P.; Schori, B. E.: *Phytochem.*, (Oxford), 25(6): (1986): 1281.
- [50] Cabenes, J.; Garcia-Carmona. F.; Garcia-Canovas, F.; Iborra, J. L.: *Biochim. Biophys. Acta.*, 790(2): (1984): 101.
- [51] Andrawis, A.; Kahn, V.: *Biochem. J.*, 235(1): (1986): 91.
- [52] Iida, K.; Kase, K.; Shimomura, K.; Sado, S.; Kadota, S.; Namba, T.: *Planta Medica*, 61(5): (1995): 425.
- [53] Tyurina, Y.Y.; Tyurin, V. A.; Yalowich, J. C.; Quinn, P. J.; Claycamp, H.G.; Schor, N. F.; Pitt, B. R.; Kagan, V. E.: *Toxicol. App. Pharm.*, 131(2): (1995): 277.
- [54] Byfield-Naish, S.; Cooksey, C.J.; Riley, P. A.: *Biochem. Jour.*, 304(1): (1994): 155.
- [55] Funayama, M.; Arakawa, H, Yamamoto, R.; Nishino, T.; Shin, T.; Murao, S.: *Bio. Biotech. Biochem.*, 59(1): (1995): 143.
- [56] Matsuda, H.; Nakamura, S.; Kabo, M.: *Bio. Pharm. Bull.*, 17(10): (1994): 1417.
- [57] Cabanes, J.; Chazorra, S.; Garcia-Carmona.: *J. Pharm. Pharmacol.*, 46(12): (1994): 982.
- [58] Shirota, S.; Miyazaki, K.; Aiyama, R.; Ichioka, M.; Yokokura, T.: *Bio. Pharm. Bull.*, 17(2): (1994): 266.
- [59] Schallreuter, K. U.; Wood, J. W.: *Arch. Derm. Res.*, 282(3): (1990): 168.
- [60] Hider, R.C.; Lerch, K.: *Biochem. Jour.*, 257(1): (1989): 289.
- [61] Fukushima, M.; Kimura, S.; Shoyakugaku Z.: *Electroanalysis*, 43(2): (1989): 142.
- [62] Robinson, G.; Leech, D.; Smyth, M.R.: *Electroanalysis*, 7(10): (1995): 952.
- [63] Wood, J. M.; Schallreuter, K. U.: *Biochim. Biophys. Acta.*, 1074(3): (1991): 378.
- [64] Albisu, I.; King, R. D.; Kozlov, I. A.: *Jour. Agric. Food Chem.*, 37(3): (1989): 775.
- [65] Wiegand-Rosinus, M.; Obst, U.; Haberer, K.; Wild, A.: *Environ. Toxicol. Water Qual.*, 7: (1992): 313.
- [66] Worthington, C. (1988): *Worthington Manual: Enzyme Related Biochemicals*,

Worthington Biochemical Corp. Freehold Pub.

- [67] Shekhovtsova, T.N.; Chernetskaya, S. V.: *Anal. Lett.*, 27: (1994): 2883.
- [68] Henneke, C. M.; Wedding, R. T.: *Arch. Biochem. Bioelec.*, 168: (1975): 443.
- [69] Argese, E.; Bettiol, C.; Ghell, A.; Todeschini, R.; Miana, P.: *Environ. Toxicol. Chem.*, 14: (1995): 363.
- [70] Cowell, D. C.; Dowman, A. A.; Ashcroft, T.; Caffoor, I.: *Biosens. Bioelect.*, 10:(1995): 509.
- [71] McArdle, F.A.; Persuad, K. C.: *Analyst*, 118: (1993): 419.
- [72] Hartley, I. C.; Hart, J. P.: *Analyt. Proc.*, 31: (1994): 333.
- [73] Amine, A.; Alafandy, M.; Kauffmann, J-M.; Pekli, M. N.: *Anal. Chem.*, 67: (1995): 2822.
- [74] Preuss, M.; Hall, E. A.: *Anal. Chem.*, 67: (1995): 1940.
- [75] Wilcox, D. E.; Porras, A. G.; Hwang, Y. T.; Lerch, K.; Winkler, M., E.; Soloman, E., I.: *J. Amer. Chem. Soc.*, 107(13): (1985): 4015.
- [76] Schmidt, H., L.; Schumann, W.; Scheller, F., W.; Schubert, F.: *Sensors, A Comprehensive Survey, Vol. 3. Chemical Sensors Part II*, page 717. Eds., W. Gopel, T.A. Jones, M. Kleitz, I. Lundstrom, T. Seiyama. (VCH Weinheim) (1992).
- [77] Wang, J.; Chen, Q.: *Analyst*, 199(8): (1994): 1849.
- [78] Gilmartin, M., A., T.; Hart, J. P.: *Analyst*, 119(1): (1994): 2331.
- [79] Cagnini, A.; Palchetti, I.; Lioni, I.; Mascini, M.; Turner, A. P. F.: *Sens. Actuators, B*, B24(1-3): (1995): 85.
- [80] Mazzei, F.; Botre F.; Botre, C.: *Anal. Chim. Acta.*, 336: (1996): 67.
- [81] Scott, D. L.; Ramanathan, S.; Shi, W.; Rosen, B. P.; Daunert, S.: *Anal. Chem.*, 69: (1997): 16.
- [82] Lee, I. J.; Karube, I.: *Biosens. Bioelect.*, 11: (1996): 1147.
- [83] Ikebukuro, K.; Honda, M.; Nakanishi.: *Electroanalysis*, 8: (1996): 10.
- [84] Ikebukuro, K.; Miyata, A.; Cho, S. J.: *J. Biotech.*, 48: (1996): 73.
- [85] Schubert, F.; Renneberg, R.; Scheller, F. W.; Kirstein, L.: *Anal. Chem.*, 56: (1984): 1677.
- [86] Mazzei, F.; Lanzi, M.; Lorenti, G.; Botre, C.: *Anal. Chim. Acta.*, 255: (1991): 59.

- [87] Ozsoz, M.; Erdem, A.; Kilinc, E.; Gokgunnec, L.: *Electroanalysis*, 8: (1996): 147.
- [88] Navaratne, A.; Rechnitz, G. A.: *Anal. Chim. Acta.*, 257: (1992): 59.
- [89] Greenberg, A. E.; Trussell, R. R.; Clesceri, L. S.: *Standard Methods for the Examination of Water and Wastewater*, (1985), 16th Ed., APHA Pub.
- [90] Galen W. Ewing. *Environmental Analysis*, (1977). Academic Press Inc.
- [91] Stulik, K.; Pacakova, V.: (1987) *Electroanalytical Measurements in Flowing Liquids*. Ellis Horwood Pub.
- [92] Kissinger, P. T.: *Anal. Chem.*, 49: (1977): 447A.
- [93] Barcelo, D. *Environmental Analysis: Techniques, Applications and Quality Assurance*. (1993) Elsevier Pub.
- [94] Zimmermann, F.; Taylor-Mayer, R., Eds.: *Mutagenicity Testing in Environmental Pollution Control*: (1985) John Wiley and Sons Pub.
- [95] King, W. P.; Joseph, K. T.; Kissinger, P. T.: *J. Assoc. Off. Anal. Chem.*, 63: (1980): 137.
- [96] Wang, J.; Lu, F.; Lopez, D.: *Biosens. Bioelectron.*, 9: (1994): 9.
- [97] Kotte, H.; Grundig, B.; Vorlop, K. D.; Strehnitz, B.; Stottmeister, U.: *Anal. Chem.*, 67: (1995): 65.
- [98] Kulys, J.; Schmid, R. D.: *Anal. Lett.*, 23: (1990): 589.
- [99] Ortega, F.; Dominguez, E.; Burestedt, E.; Emnues, J.; Gorton, L.; Marko-Varga, G.: *J. Chromatogr.*, 675: (1994): 65.
- [100] Ortega, F.; Dominquez, E.; Jonsson-Pettersson, G.; Gorton, L.: *J. Biotechnol.*, 31: (1993): 289.
- [101] Cosnier, S.; Innocent, C.: *Bioelectron. Bioenerg.*, 31: (1993): 147.
- [102] Skladal, P.: *Collect Czech. Chem. Commun.*, 56: (1991): 1427.
- [103] Onnerfjord, P.; Emneus, J.; Marko-Varga, G.; Gorton, L.; Ortega, F.; Dominguez, E.: *Biosens. Bioelectron.*, 10: (1995): 607.
- [104] Navartne, A.; Lin, M.; Rechnitz, G.: *Anal. Chim. Acta.*: 237: (1990): 107.
- [105] Ruzgas, T.; Emneus, J.; Gorton, L.; Marko-Varga, G.: Unpublished results, Dept. Analytical Chemistry, Lund University, Box 124, S-221 00 Lund, Sweden.
- [106] Hall, G.F.; Best, D. J.; Turner, A.P.F.: *Anal. Chim. Acta.*, 213: (1988): 113.
- [107] Wang, J.; Lin, S., M.: *Anal. Chem.*, 60: (1988): 1545.

- [108] Campanella, L.; Beone, T.; Samartino, M.P.; Tomassetti, M.: *Analyst*, 118: **(1993)**: 979.
- [109] Campanella, L.; Su, Y.; Tomassetti, M.; Crescentini, G.; Samartino, M.P.: *Analysus*, 22: **(1994)**: 58.
- [110] Ghindilis, A.; Gavrilova, V.; Yaropolov, A.: *Biosens. Bioelectron.*, 7: **(1992)**: 127.
- [111] Yaropolov, A.; Kharybin, A.; Emneus, J.; Margo-Varga, G.; Gorton, L.: *Anal. Chim. Acta*, 308: **(1995)**: 137.
- [112] Ruzgas, T.; Emneus, J.; Marko-Varga, G.; Gorton, L.: *Anal. Chim. Acta.*, 311: **(1995)**: 245.
- [113] Dong, S.; Wang, Y.: *Electroanalysis*, 49: **(1989)**: 447A.
- [114] Zak, J.; Kuwara, T.: *J. Electroanal. Chem.*, 150: **(1983)**: 645.
- [115] Sittampalon, G.; Wilson, G., S.: *Anal. Chem.*, 55: **(1983)**: 1608.
- [116] Wang, J.; Hutchins, L. D.: *Anal. Chem.*, 51: **(1985)**: 1536.
- [117] Wang, J.; Tuzhi, P.; Golden, T.: *Anal. Chim. Acta*, 197: **(1987)**: 129.
- [118] Kaaret, T. W.; Evans, D. H.: *Anal. Chem.*, 60: **(1988)**: 657.
- [119] Wang, J.; Golden, T.: *Anal. Chem.*, 61: **(1989)**: 1397.
- [120] Wang, J.; Golden, T.; Tuzhi, P.: *Anal. Chem.*, 59: **(1987)**: 740.
- [121] Garcia, O.J.; Quintela, P.A.; Kaider, A. E.: *Anal. Chem.*, 61: **(1989)**: 679.
- [122] Chastel, O.; Kauffmann, J. M.; Christain, G. D.: *Anal. Chem.*, 61: **(1989)**: 171.
- [123] Tanaka, K.; Tamaihi, R., J.: *J. Electroanal. Chem.*, 236: **(1987)**: 305.
- [124] Uchida, I.; Ishino, A.; Matsue, T.; Itaya, K. J.: *J. Electroanal. Chem.*, 266: **(1989)**: 455.

Chapter 2

Enzyme Inhibition-based Biosensors

2.1. Mushroom Tissue-based Biosensor for Inhibitor Monitoring

2.1.1. Introduction

Much interest has evolved in replacing isolated enzymes with tissue materials as the biocatalytic entity of electrochemical sensors [1-6]. The major advantages obtained from the use of tissue materials are high stability and activity, mainly due to the presence of the enzyme in large quantities in its natural environment, and low cost. Early tissue-based electrodes consisted of placing a tissue slice on top of the working electrode [7-9], but these suffered from long response times.

A much more revolutionary approach was to incorporate the tissue loading directly into the carbon paste matrix [10], which results in the tissue becoming an integral part of the sensing element, yielding extremely short response times of the order of a few seconds. The amperometric detection of dopamine [10], hydrogen peroxide [11], oxalate [12], ethanol [13] and phenols [14] at carbon paste electrodes modified with banana, horseradish root, beet tissue, tomato seeds and mushroom tissue respectively has been well documented.

In addition to substrate detection, the tissue-based biosensors can offer effective elimination of interferences and therefore enhanced sensitivity for the analyte of interest. For example, Wang et al. [15] utilised papain in papaya tree tissue to eliminate protein interferences in the monitoring of neurotransmitters. Papain is a thiol protease which breaks down proteins by hydrolysing specific peptide bonds. The papain content allowed samples containing both neurotransmitter and albumin to be analysed without any sample pre-treatment. The electrode did not experience any protein fouling, as the albumin interferent was digested by the papain content of the biosensor. In a similar study, the ascorbic acid oxidase content of zucchini plant was used to eliminate interference from ascorbic acid and other acid metabolites in the analysis of dopamine [16].

The goal of this present study was to expand the concept of tissue biosensors towards the monitoring of important enzyme inhibitors. The use of native enzyme for the monitoring of toxic compounds through inhibition has been well documented [17-26].

These have included the inhibition of acetylcholinesterase by paraoxon [17, 18, 26], malaoxon [19], parathion [23], metrifonate [24] and fluoride [22]; the inhibition of lactate oxidase by atrazine, cadmium and chromium [20]; the inhibition of cytochrome oxidase by cyanide [21] and the inhibition of tyrosinase by carbamate pesticides [25].

In the work presented in the following sections, the rich activity of the tyrosinase content of mushroom tissue [27], was utilised as a tissue-based carbon paste biosensor for the fast and sensitive monitoring of low levels of important inhibitors. These include diethyldithiocarbamate, thiourea and benzoic acid. Such exploitation of whole-cell biosensors could lead to effective environmental monitoring based on the interaction of natural biological systems with toxic pollutants.

2.1.2. Experimental

2.1.2.1. Reagents

All solutions were prepared unless otherwise stated in deionised water prepared by passing distilled water through a Milli-Q-water purification system. Potassium dihydrogen phosphate and disodium hydrogen phosphate were supplied by Aldrich (Milwaukee, USA). The supporting electrolyte used was 0.05 M phosphate buffer, pH 7.4. The mushrooms used in this study were purchased from a local supplier and were grown on J. M. Farms Inc. (OK, USA). Catechol from Sigma (MO, USA), sodium diethyldithiocarbamate from Aldrich (Milwaukee, USA), thiourea from Fisher (USA) and benzoic acid from Baker (USA) were used without further purification.

2.1.2.2. Instrumentation

Amperometric experiments were carried out with a BAS CV27 voltammetric analyser (Bioanalytical Systems, BAS, W. Lafayette, USA), in connection with a BAS X-Y-t recorder. The carbon paste working electrode, reference electrode (Ag/ AgCl, Model RE-1, BAS), and platinum wire counter electrode joined the 10 ml electrochemical cell (Model VC-2, BAS) through holes in its PTFE cover. The flow injection system consisted of a carrier reservoir, an Alitea C-4V pump, a Rainin model 501 sample injection valve (20 μ l loop) interconnecting PTFE tubings, and a home-made large volume 20 ml wall-jet amperometric detector.

2.1.2.3. Electrode Preparation

The mushroom-based carbon paste electrode was prepared as follows. First a section of mushroom was removed using a scalpel, and was ground with a mortar and pestle. The mushroom pulp was drained of excess fluid and dried between the sheets of tissue paper. The desired amount of ground mushroom was then mixed thoroughly with 0.90 g of graphite powder Fisher (USA), with a mortar and pestle. Subsequently, 0.60 g of mineral oil, Aldrich (Milwaukee, USA) was added and hand mixed with a spatula in a weighing boat. A portion of the resulting paste was packed into the electrode cavity (3 mm diameter, 1 mm depth) of a PTFE sleeve. Electrical contact was established via a copper wire. The paste surface was smoothed on weighing paper.

2.1.2.4. Procedures

All measurements were performed at room temperature by applying the desired potential and allowing the transient current to decay prior to the amperometric monitoring. A stirring rate of 300 rpm, using an Ikameg IK250 magnetic stirrer, was employed in the batch experiments, while a carrier flow rate of 2.0 ml/ min was used in the flow injection analysis studies. Figure 2.1.1. shows a schematic of the experimental set-up for the batch and flow injection experiments along with the corresponding response profiles expected from such a system. In the batch experiments a 10 ml cell was used, the solution was stirred, and the potential applied. When the background was settled to baseline substrate was added, and after steady-state was attained, subsequent aliquots of inhibitor were added resulting in a current-time recording inhibition profile. A plot of inhibition current versus inhibitor concentration allows $I_{0.5}$ values to be calculated i.e. the concentration corresponding to 50 % inhibition.

In flow injection analysis, the substrate was injected into a flowing stream where it reached the wall-jet cell and underwent reaction. By using the same concentration of substrate and varying concentration of inhibitor, flow injection inhibition profiles were obtained. The difference in current represents the fraction of enzyme inhibited by that inhibitor at that particular concentration.

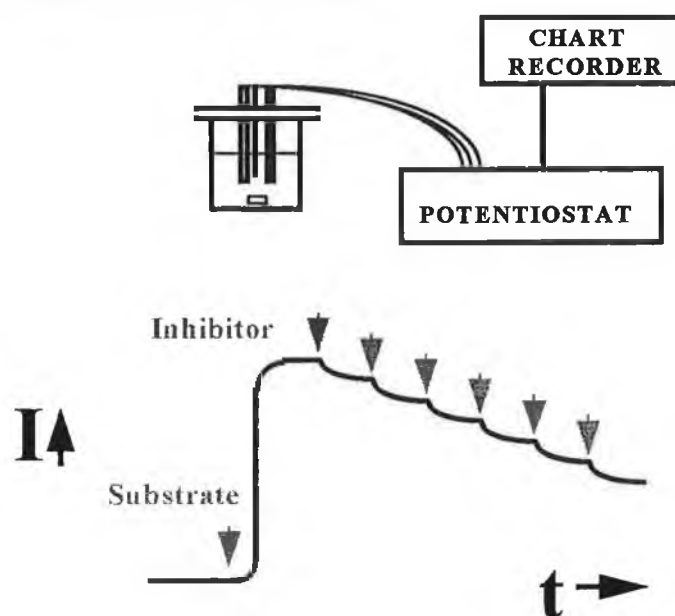
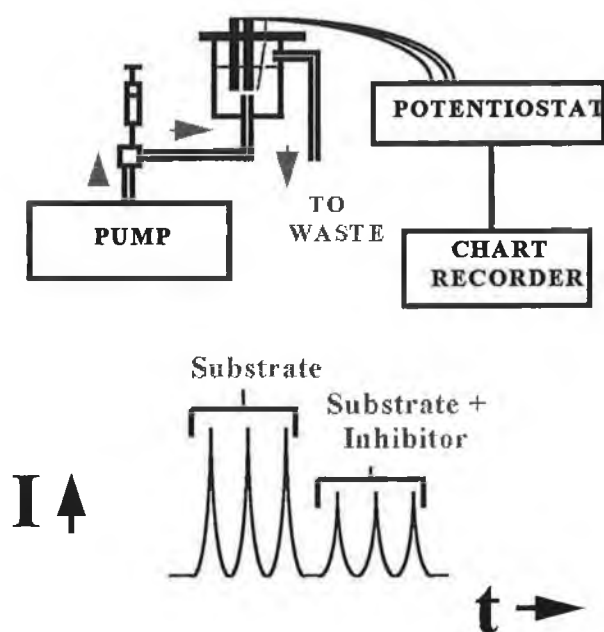
(a) BATCH ANALYSIS**(b) FIA ANALYSIS**

Figure 2.1.1. Experimental monitoring of enzyme inhibition. (a) Shows typical experimental set-up and response profile for batch experiments, and (b) shows the corresponding set-up and response profile for flow injection analysis experiments.

2.1.3. Results and Discussion

2.1.3.1. Investigation of Mushroom Tissue Loading and Activity Distribution

The preparation of the tissue biosensor had a profound effect upon inhibitor detection.

The influence of tissue loading on the biocomposite is displayed in Figure 2.1.2.

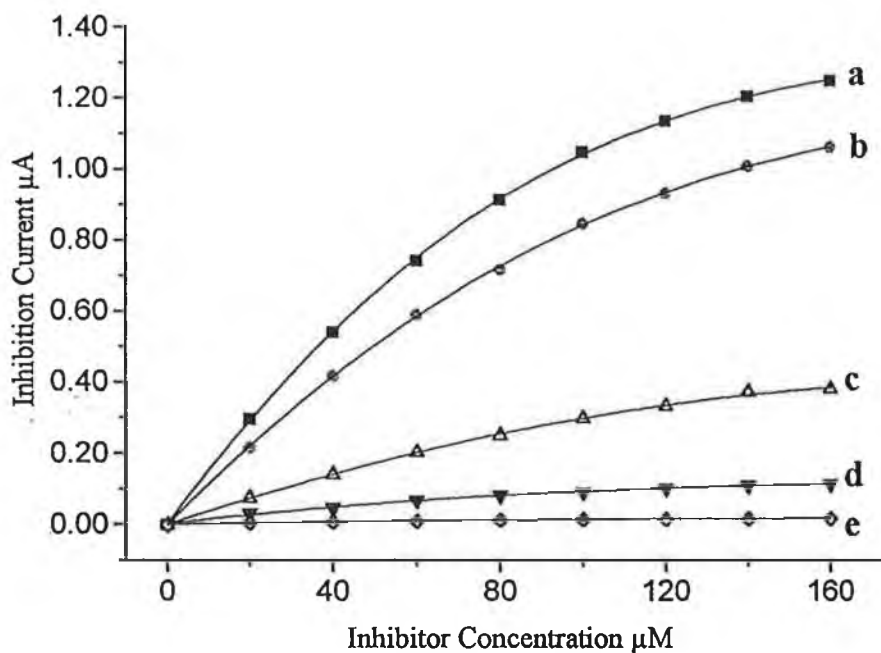


Figure 2.1.2. Effect of mushroom tissue loading on the inhibition responses of sodium diethyldithiocarbamate (a) 37.5 %; (b) 25.0 %; (c) 12.5 %; (d) 7.5 % and (e) 5.0 % mass fraction respectively. Operating potential, - 0.20 V; electrolyte solution 0.05 M phosphate buffer, pH 7.4., stirred at 300 rpm. All experiments were performed at room temperature 25 °C.

These calibration plots represent the inhibition current obtained as a function of increasing aliquots of sodium diethyldithiocarbamate. Although no notable response was observed using the 5.0 % mass fraction mushroom content (e), the sensitivity increased dramatically between 7.5 % mass fraction (d) and 25.0 % (b), and then more slowly.

By representing the substrate current response by I_{ss} and the inhibition current by I_{IN} , the relative inhibition current response as a factor of the initial substrate steady state response, $(I_{IN} / I_{ss}) * 100 \%$, obtained for sensors (a) to (d) were as follows: (a) 13.7 % to 69.4 %; (b) 22.8 % to 94.4 %; (c) 19.4 % to 93.1 % and (d) 18.2 % to 81.9% for diethyldithiocarbamate concentrations ranging from 20 to 160 μM .

A 25 % tissue loading yielded the most favourable signal to noise characteristics and was used in all the remaining experiments. Higher tissue loadings resulted in dryer pastes hence affecting mechanical stability, whilst lower tissue loadings $< 12.5 \%$ resulted in wetter pastes and perturbation of the sensor baseline, making pertinent analysis difficult to perform.

The sensitivity of the tissue biosensor was also influenced by the mushroom section used for constructing the electrode. It is well known that the distribution of tyrosinase activity in whole mushrooms is not uniform [27]. This is attributed to the various biological functions of the different sections within the mushroom system.

Figure 2.1.3. shows calibration plots for the diethyldithiocarbamate inhibitor using different tissue sections. All the tissue sections exhibited useful responses, but the lower stalk tissue, represented by section (a), displayed a higher enzyme activity than any other morphological part. This is not surprising since the lower stalk region is responsible for the production of new growth tissue, and also for the transport of nutrients and water into and out of the mushroom system. The sensitivity trend: section a $>$ section b $>$ section c $>$ section d, thus reflects the enzyme distribution patterns in a manner as similarly described by Rodriguez and Flurkey [27].

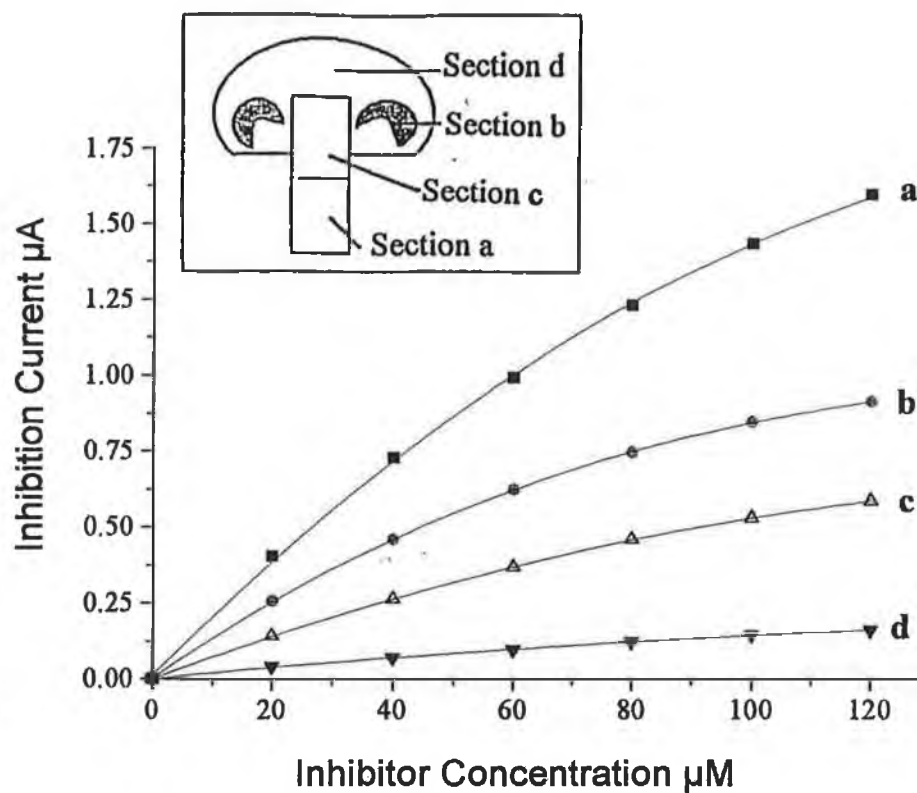


Figure 2.1.3. Investigation of the inhibition responses for diethyldithiocarbamate using different tissue sections as shown in the insert at a 25 % mass fraction tissue loading. Operating potential, -0.20 V ; electrolyte solution 0.05 M phosphate buffer, $\text{pH } 7.4$, stirred at 300 rpm and performed at room temperature.

2.1.3.2. *Batch Response Characteristics of the Mushroom Tissue Biosensor*

The perturbed biocatalytic activity of the mushroom tyrosinase in the presence of different inhibitors under a fixed level of catechol substrate was used for the amperometric detection of these toxic compounds. Figure 2.1.4(a) shows current time recordings at the mushroom based biosensor to 1×10^{-4} M additions of sodium diethyldithiocarbamate (A, i), thiourea (B, i) and benzoic acid (C, i). The relative inhibitor response i.e. $(I_{IN} \setminus I_{ss}) \times 100 \%$, for compounds A, B and C ranged from 34.7% to 98 %, 11.7 % to 47.8 % and 12.0 % to 37.4 % respectively, for inhibitor concentrations ranging from 20 to 160 μ M.

The tissue electrode responded very rapidly to the micromolar increments of inhibitor, as indicated from the decreased substrate signal. Steady state currents were achieved within approximately 12 s for benzoic acid, 15 s for thiourea and 30 s for diethyldithiocarbamate, hence requiring no incubation period. Such fast response times were also obtained by Wang and Lin [10] for the analysis of dopamine using banana tissue. These fast response times have been attributed to the large surface area of tissue containing enzyme exposed to solution. The absence of an external layer thus allows rapid transport of the inhibitor and substrate to and from the electrode surface.

Also shown in Figure 2.1.4(b) are the resulting calibration plots (I) corresponding to the batch profiles obtained. The trend in sensitivity, diethyldithiocarbamate > thiourea > benzoic acid, reflects the extent of inhibitor-enzyme interaction i.e., the degree of inhibition. These profiles can be used to estimate the coefficients of inhibition, $I_{0.5}$, which correspond to the concentration corresponding to 50 % inhibition. Values of 4.8×10^{-5} M, 5.8×10^{-5} M and 6.2×10^{-5} M were obtained for diethyldithiocarbamate, thiourea and benzoic acid respectively.

Figure 2.1.4.(b)(II) shows the corresponding calibration plots obtained at a native tyrosinase carbon paste electrode. This electrode was prepared by mixing tyrosinase enzyme with carbon paste resulting in a 3 % tyrosinase carbon paste composite. Although the response was greater than the mushroom tissue electrode, the same response profile was obtained allowing the inhibitors to be conveniently analysed. The

tissue electrode, although with a compromised signal, results in a more cost efficient electrode design which can provide the same fundamental results as that obtained by the more expensive native enzyme modified electrode.

Although it has been suggested that the inhibition of tyrosinase appears to proceed through interaction with its active copper site [28], no information is currently available pertaining to the complex mechanism of the operation of inhibitor tissue electrodes. The exact mechanism should depend on whether the immobilised cells remain intact in the carbon paste matrix or are broken down during the electrode preparation. In the former case, the mechanism would involve transport of the inhibitor into, within and from the immobilised cells. The inhibitor diffusion into and out of the cell would be facilitated by channels present in the outer cell membrane by virtue of its biological evolution.

Alternatively, if the cells are structurally broken down, the enzyme of interest is released, and inhibitor entrance into the cells is not required. The fast response of the present electrode may support the latter mechanism. Such models are analogous to those suggested for the detection of substrates at tissue electrodes [5].

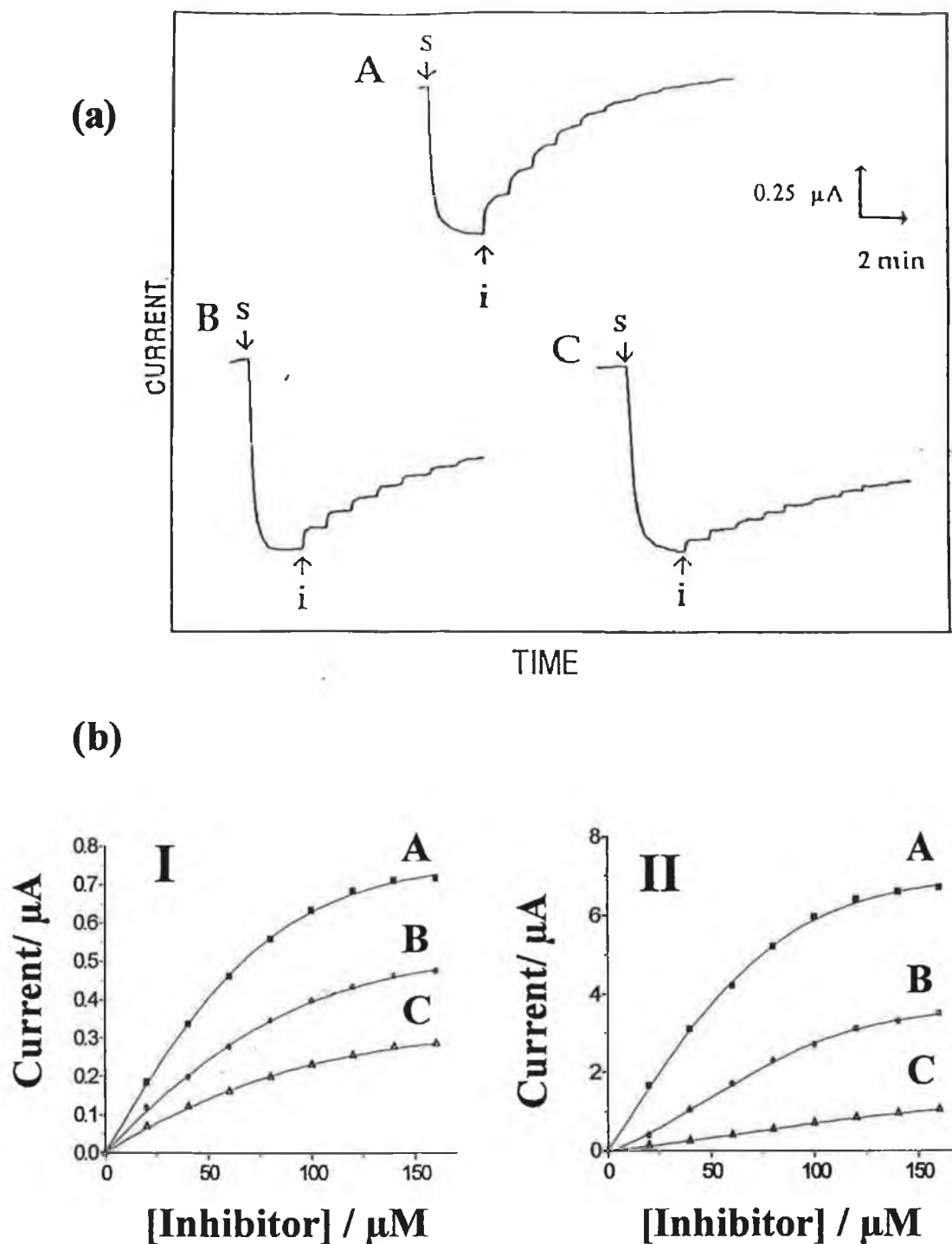


Figure 2.1.4. (a) Current-time recordings at mushroom modified carbon paste electrodes upon addition of tyrosinase substrate $1 \times 10^{-4} \text{ M}$ catechol followed by successive increments of inhibitor (i) in $2 \times 10^{-5} \text{ M}$ steps, (A) sodium diethyldithiocarbamate, (B) thiourea and (C) benzoic acid. Also shown are the corresponding calibration plots (b) for the mushroom tissue electrode 25 % mass fraction tissue loading (I) and at a 3% tyrosinase (II) carbon paste electrode. Conditions as in Figure 2.1.3. The lower stalk of the mushroom was used in these experiments.

2.1.3.3. Flow Injection Analysis Response Profile

The attractive dynamic properties of the inhibition tissue electrodes can be exploited for on-line applications, as desired for monitoring toxic compounds in flowing streams. Figure 2.1.5. displays a flow injection profile for FIA measurements of various inhibitors of mushroom tyrosinase: diethyldithiocarbamate (B); thiourea (C) and benzoic acid (D) in solutions containing catechol as substrate.

Such detection schemes rely on the decrease of the catechol peak, compared to that observed without inhibitor (A). Such well defined suppressions of the substrate response allow convenient quantification of inhibitor present. Since the slope and width of the catechol peak was not affected by the presence of these inhibitors, high injection rates of 60 samples/ hr can be realised.

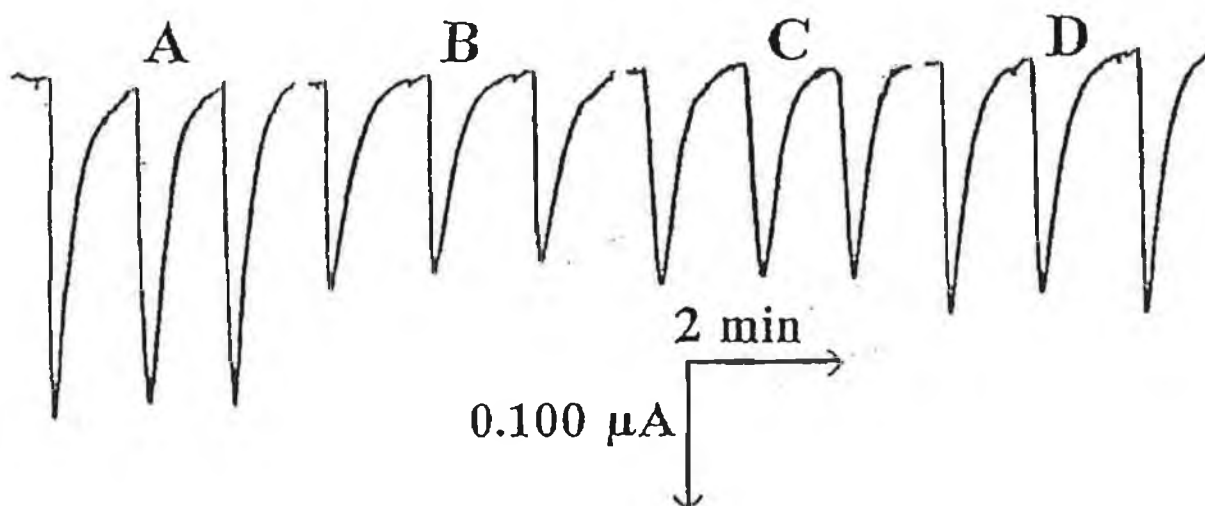


Figure 2.1.5. Flow injection peaks at a mushroom modified carbon paste electrode for 5×10^{-4} M catechol solutions with 2×10^{-4} M sodium diethyldithiocarbamate (B), thiourea (C) and benzoic acid (D), as well as without inhibitor (A). Carrier solution 0.05 M phosphate buffer pH 7.4. Applied potential - 0.20 V, flow rate 2.0 ml/min. Mushroom tissue loading 25 % mass fraction.

Similar to its batch counterpart, the tissue-based flow detector responds in a non-linear fashion to changes in the inhibitor concentration, as expected for a classical inhibition profile. For example, Figure 2.1.6.(A) shows flow injection current peaks for catechol solutions containing increasing levels of diethyldithiocarbamate, 2×10^{-4} M to 1×10^{-3} M (b to d) along with the catechol response without inhibitor (a). The peak decreases rapidly upon increasing the inhibitor at first and then more slowly. The corresponding calibration plot is also shown.

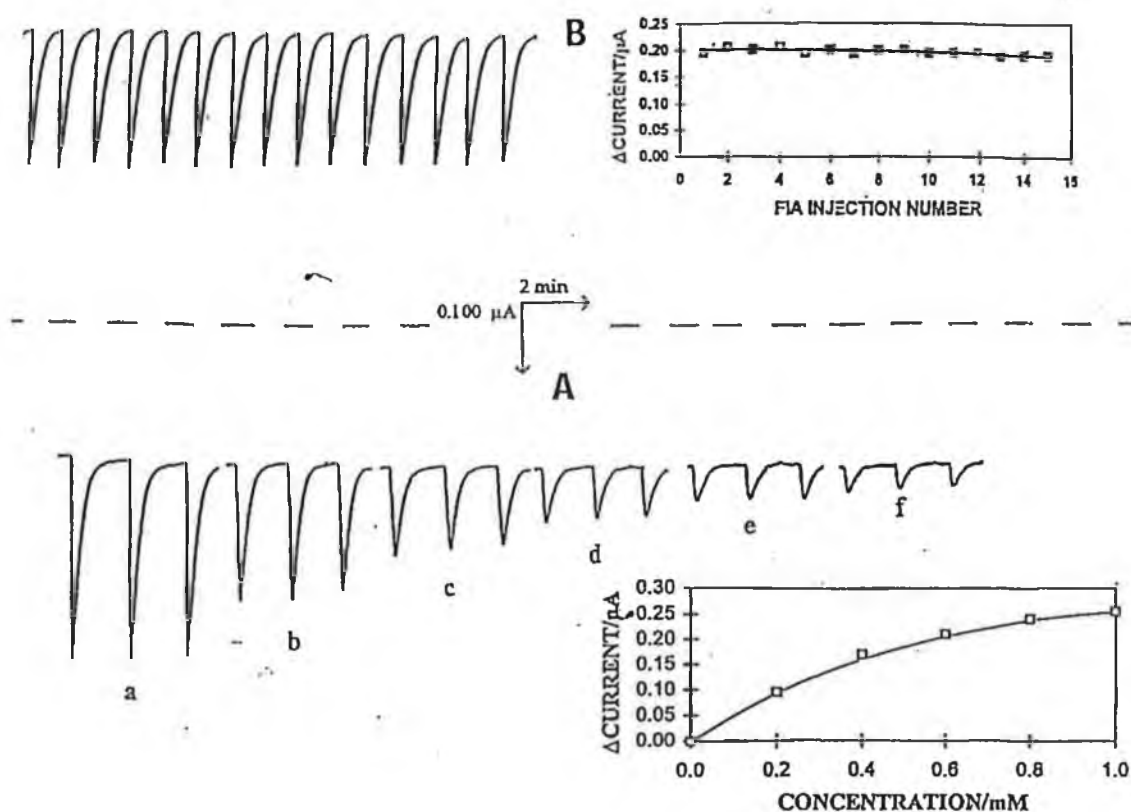


Figure 2.1.6. Flow injection calibration (A) and precision (B) data of mushroom carbon paste electrodes. In (A) 5×10^{-4} M catechol solution containing (0 to 1×10^{-3} M) sodium diethyldithiocarbamate (a-f) were used. In (B) 5×10^{-4} M catechol solution containing 2×10^{-4} M sodium diethyldithiocarbamate was used. Conditions as in Figure 2.1.5.

The precision of this flow injection system was demonstrated as shown in Figure 2.1.6. (B). The profile shows peaks for 15 repetitive injections of 2×10^{-4} M diethyldithiocarbamate containing catechol as substrate. The series yielded a mean peak current of 197 nA and an RSD of 2.4 %. Such behaviour suggests rapid dissociation of the enzyme inhibitor complex and renewal of enzyme activity.

2.1.3.4. Detection Limits and Stability Considerations

Based on a signal to noise ratio of three, detection limits of approximately 5.0×10^{-6} M were obtained for sodium diethyldithiocarbamate, whilst thiourea yielded a detection limit of 8.0×10^{-6} M and benzoic acid 1.2×10^{-5} M respectively. Such detection limits are comparable to those obtained at inhibitor biosensors based on native tyrosinase [29].

Although the electrodes yielded favourable operational characteristics as shown in the previous sections, the electrodes could not be reused on a day to day basis. It was observed that the electrode surfaces cracked whilst left overnight in phosphate buffer at 4 °C, resulting in erratic baselines. Investigation of other methods of storage will need to be explored, or alternatively the exploitation of a different electrode preparation method to improve the mechanical stability of these electrodes. The current method could be replaced with a rigid graphite epoxy material [30] within the bulk of which the mushroom tissue could be dispersed. This would result in a polishable renewable enzyme probe with enhanced mechanical stability.

Table 2.1.1. Summary of coefficients of inhibition $I_{0.5}$ and detection limits, LOD.

Compound	$I_{0.5} / 10^{-5}$ M	LOD / μ M
Sodium Diethdithiocarbamate	4.8	5.0
Thiourea	5.8	8.0
Benzoic Acid	6.2	12.0

2.1.4. Conclusion

It has been demonstrated that a tissue electrode can be employed for the rapid monitoring of micromolar levels of inhibitors. Such tissue electrodes are extremely inexpensive when compared to their native enzyme counterparts. Other pollutants inhibiting tyrosinase activity including heavy metals, pesticides or cyanide may be monitored in a similar fashion. Such biosensors hold great promise for rapid low cost toxicity testing once their mechanical stability can be improved.

The exploitation of the mushroom electrodes in organic solvents as demonstrated by Deng and Dong [31] and by Wang et al. [32] using native tyrosinase and horseradish peroxidase, could expand the scope of such inhibitor measurements to new environments. Whilst this concept is proposed for mushroom tissue electrodes, it could be expanded to other plant and animal tissue and to whole cell counterparts in general. Fundamental studies concerning the complex structure of the tissue-carbon paste composite, inhibitor transport, associated interactions and mechanical stability are needed.

2.2. Screen Printed Tyrosinase containing Electrodes for the Biosensing of Inhibitors

2.2.1. Introduction

Electrochemical biosensors hold great promise for the task of on-site environmental monitoring [33, 34]. One promising strategy is to employ enzyme electrodes for measuring various toxic compounds via the perturbation/ inhibition of the enzymes' biocatalytic activity [18].

Screen printing offers a simple and fast method for the mass production of disposable electrochemical sensors. Single use sensors have several advantages which include avoidance of contamination between samples, ease of use, portable capabilities and high reproducibility with simple inexpensive fabrication techniques. The earliest applications of screen-printed biosensors focused mainly on the determination of glucose in blood samples. However, over the years applications have expanded to include the determination of pesticides, metals and potential environmental pollutants.

Gilmartin et al. [35] developed a disposable biosensor strip consisting of a Ag/ AgCl reference electrode and a carbon electrode containing cobalt phthalocyanine as mediator coated with a layer of cellulose acetate and glucose oxidase for the amperometric determination of glucose. The monitoring of lactate was exploited by Sprules et al. [36] by screen printing a Medola blue-containing modified electrode coated with lactate dehydrogenase. Other applications have involved the use of screen printed electrodes for the monitoring of uric acid [37], ethanol [38], ethanethiol [39] and nucleic acids [40].

With environmental applications in mind, Wang et al. [41] developed a palladium-doped screen printed electrode for formaldehyde monitoring in river water samples. It was found that the screen printed electrodes required a short pre-conditioning step to electrogenerate Pd^0 which acts as the electrocatalyst in the reaction, and converts aldehyde into methanol, thus allowing the aldehyde content of river water samples in the 0.01 to 0.10 mM range to be determined. Similar studies for the monitoring of

hydrazines [42], nitrite [43], hydroquinone [44], phenols [45] and heavy metals [46] have been documented.

The use of screen printed biosensors for the monitoring of pesticides and herbicides through the inhibition of enzymatic activity has proved quite popular in recent years [47-51]. Cagnini et al. [47] developed an acetylcholinesterase based screen printed biosensor for the analysis of organophosphorous and carbamate pesticides, in a manner similar to the method of Hart and Hartley [48]. Inhibition of alkaline phosphatase was successfully exploited by Su et al. [49] for the determination of various pesticides. These electrode strip devices consisted of a ruthenised carbon working electrode, a Ag/ AgCl reference electrode and a silver counter electrode screen printed on a polyester supporting substrate.

In the work presented in this section, the characterisation and attractive performance of single-use inhibitor strips based on the screen printing of tyrosinase-containing carbon inks is described. Tyrosinase is prone to inhibition by a wide range of water pollutants [29]. Such inhibition is known to occur through interaction with the active copper site [28]. The one step preparation of tyrosinase-based screen printed strips has already been reported by Wang and Chen [45] for the analysis of phenols. The remarkable tolerance of tyrosinase to the high temperature firing conditions resulted in a greatly simplified fabrication protocol and convenient quantification of phenolic substrates. Similarly, in the following sections, the suitability of these thick-film strips for the amperometric monitoring of tyrosinase inhibitors is presented.

2.2.2. Experimental

2.2.2.1. Reagents

Chemicals were analytical grade and used as received. All solutions were prepared unless otherwise stated in deionised water prepared by passing distilled water through a Milli-Q-water purification system. Potassium dihydrogen phosphate and disodium hydrogen phosphate were supplied by Aldrich (Milwaukee, USA). The enzyme used, tyrosinase 4400 units mg^{-1} solid, was obtained from Sigma, (MO, USA), (T-7755, E.C. 1.14.18.1.). The supporting electrolyte was a 0.05 M phosphate buffer solution, pH 7.4. Catechol, 2,4-dichlorophenoxyacetic acid, 4,6-dinitro-o-cresol, warfarin, and sodium azide were obtained from Sigma (MO, USA). Sodium diethyldithiocarbamate, pentachlorophenol, sodium nitrate, cadmium and lead atomic absorption standard solutions were obtained from Aldrich (Milwaukee, USA). Benzoic acid was supplied by Baker (USA) and atrazine was supplied by Chem Service (USA). Thiourea was supplied by Fisher (USA).

2.2.2.2. Instrumentation

All voltammetric experiments were carried out using an EG & G PAR Model 264 A voltammetric analyser, in connection with a Houston Omniscrite strip-chart X-Y-t recorder. The experiments were performed at room temperature in a 10 ml electrochemical cell (BAS, Model VC-2). The working electrode strip, reference electrode (Ag/AgCl, Model RE-1, BAS) and platinum wire electrode joined the cell through holes in the Teflon cover.

2.2.2.3. Screen Printing Fabrication

A semi-automatic screen printer machine (Model TF-100, MPM Inc., Franklin, MA) was used for fabricating the working electrode strips. The modified inks were prepared by thoroughly mixing for 1 h the appropriate amount of a commercial carbon ink (Product No. C10903D14, Gwent Electronic Materials Ltd., UK) with the enzyme. Typical preparations were 0.6 % enzyme/ ink (w/w). A group of 10 electrodes were printed each time onto an alumina ceramic plate (1.33 in. x 4.00 in.) through a patterned stencil. This allowed batches of 30 electrodes to be printed by using 1 g ink mixed with 6 mg of

enzyme. Each electrode consisted of a $1.0 \times 30 \text{ mm}^2$ area. The film was cured at a temperature of 110°C for 2 h. Then a layer of insulation was screen printed onto part of the ink, leaving a defined $1.0 \times 5 \text{ mm}^2$ working electrode area.

2.2.2.4. *Procedures*

The screen printed electrodes were used without any further pre-treatment. The amperometric experiments were performed at a potential of -0.2 V , using a stirring rate of 400 rpm. The substrate addition, $5 \times 10^{-5} \text{ M}$ catechol was followed by additions of the target inhibitor, using microliter aliquots of the corresponding solutions. All measurements were performed at room temperature.

2.2.3. Results and Discussion

2.2.3.1. Investigation of Tyrosinase Enzyme Loading

Figure 2.2.1. displays the amperometric response of strips containing different tyrosinase loadings to catechol (S) followed by successive additions of diethyldithiocarbamate (I). The sensor responded very rapidly to these substrate and pesticide additions, indicating that its biocatalytic and inhibition activities were maintained despite the 2 hour curing at 110 °C. A similar observation was made by Wang and Chen [45] with biosensor strips for the monitoring of phenol.

Steady state currents were obtained in approximately one minute. Such fast responses are attributed to the absence of external membranes which may prolong response times. No incubation time was required allowing direct instantaneous monitoring of the inhibitor content, whereas strips based on acetylcholinesterase require several minutes for the signal to establish itself [52].

As shown in Figure 2.2.1. both the substrate and inhibitor responses increased upon increasing the enzyme loading in the ink. This represents the fraction of enzyme activated by substrate and inhibited by inhibitor under those conditions respectively. The resulting calibration plots indicate that the inhibitor response is nearly proportional to enzymatic activity. For example, the ratio of inhibition signal to substrate signal, (I_{IN}/I_{SS}), increased initially from 0.14 to 0.26 upon raising the enzyme loading from 0.3 % to 0.6 % w/w, and then decreased slightly to 0.24 for the 1 % loading. Indicating that maximum catalytic efficiency was obtained at mass fractions of 0.6 % and greater. For this reason a 0.6 % enzyme content was used in all further experiments.

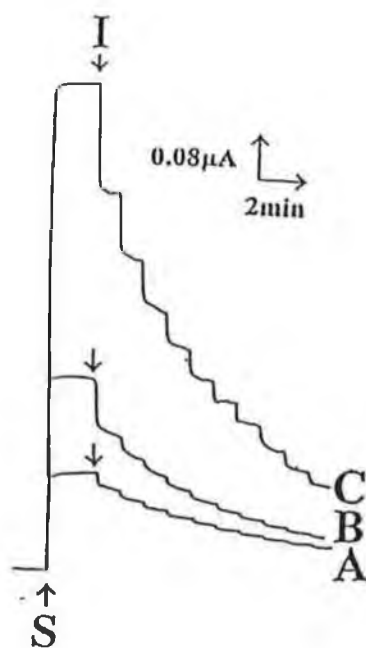
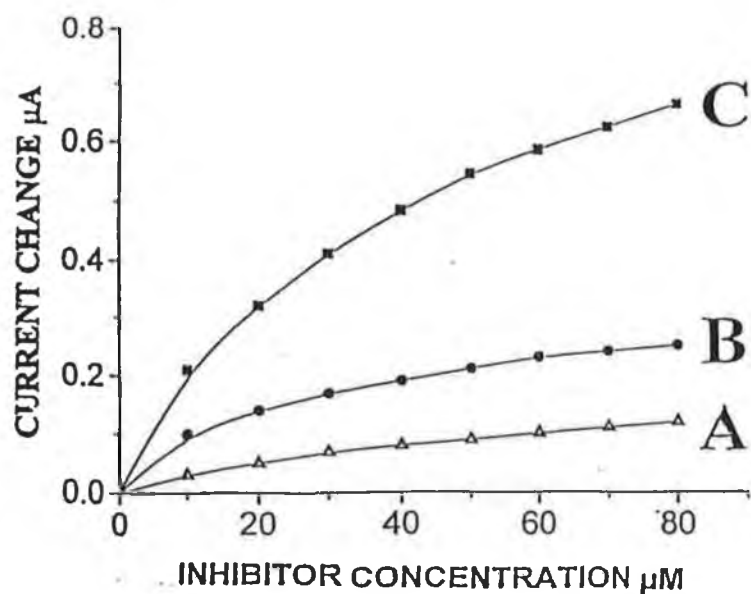


Figure 2.2.1. Enzyme loading studies at various tyrosinase screen printed electrodes. Enzyme loading : (A) 0.3 %; (B) 0.6 % and (C) 1.0 % w/w. Also shown are the respective current-time recordings. Catechol ($5 \times 10^{-5} M$) was used as substrate (S); diethyldithiocarbamate, $1 \times 10^{-5} M$ per step, was used as inhibitor (I). Applied potential $-0.2 V$; PBS $0.05 M$ pH 7.4. Stirring rate 400 rpm.

The influence of the substrate concentration upon the response of the screen printed biosensor strips is shown in Figure 2.2.2. The diethyldithiocarbamate signal nearly doubles upon raising the catechol level from 2×10^{-5} M to 5×10^{-5} M, and between 5×10^{-5} M and 1×10^{-4} M respectively. Increasing the catechol level increases the fraction of activated enzyme which can be inhibited. A substrate level of 5×10^{-5} M yielded the most favourable inhibition profile and was utilised in the remainder of the experiments.

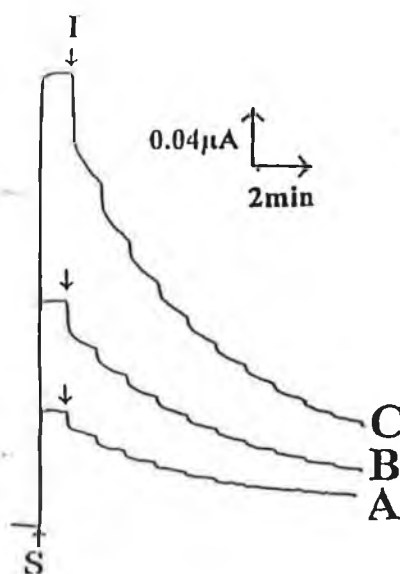
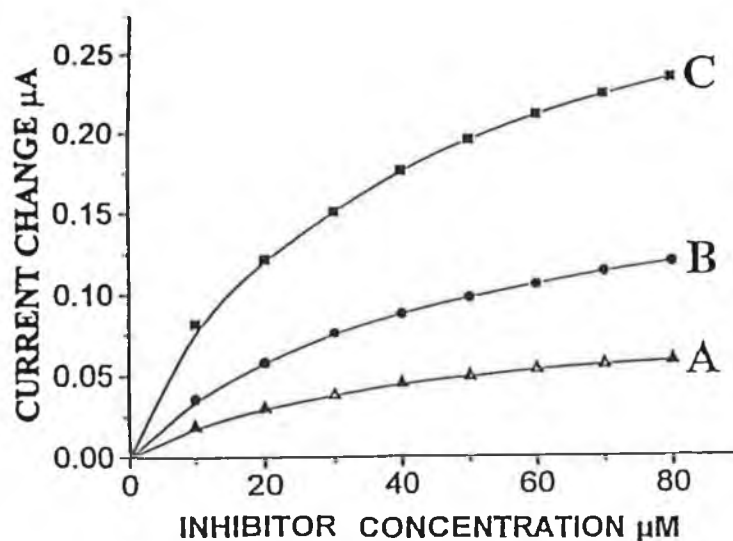


Figure 2.2.2. Effect of substrate concentration on inhibition response at the 0.6 % tyrosinase strips. Catechol concentration (A) 2×10^{-5} M; (B) 5×10^{-5} M; (C) 1×10^{-4} M. Also shown are the corresponding current-time recordings. Sodium diethyl dithiocarbamate, 10^{-5} M per step, was used as inhibitor (I). Other conditions as given in Figure 2.2.1.

2.2.3.2. *Inhibitor Screening*

Figure 2.2.3. shows the calibration plots obtained with 0.6 % w/w tyrosinase-containing strips for sub-millimolar concentrations of the pesticide diethyldithiocarbamate (A); for thiourea (B), which is the breakdown product of the latter compound; for the antifungal agent benzoic acid (C), and the herbicides 2,4 dichloroacetic acid (D) and 4,6 dinitro-*o*-cresol (E). These new strips allowed convenient quantitation of these toxic compounds and yielded characteristic inhibition profiles. The trend in sensitivity: diethyldithiocarbamate > thiourea > benzoic acid > 2,4 dichloroacetic acid > 4,6 dinitro-*o*-cresol, reflects the degree of inhibition obtained.

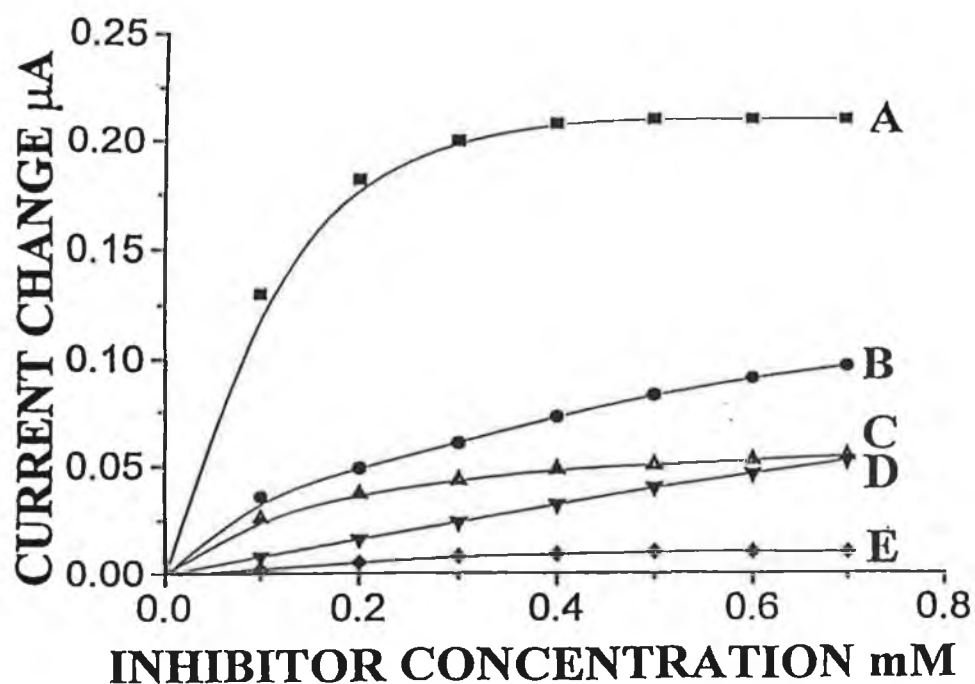


Figure 2.2.3. Calibration plots obtained for inhibition at the 0.6 % tyrosinase strip for: (A) sodium diethyldithiocarbamate; (B) thiourea; (C) benzoic acid; (D) 2,4 -dichlorophenoxyacetic acid and (E) 4,6-dinitro-*o*-cresol. Other conditions as given in Figure 2.2.1.

These profiles were used to estimate the apparent coefficients of inhibition, $I_{0.5}$, i.e. the concentration corresponding to 50 % of the inhibition signal. The $I_{0.5}$ values were estimated for only diethyldithiocarbamate, benzoic acid and 4,6-dinitro-o-cresol, as the profiles for thiourea and 2,4-dichlorophenoxyacetic acid failed to saturate within the concentration range investigated. The $I_{0.5}$ values were as follows: 9.2×10^{-5} M diethyldithiocarbamate, 1.0×10^{-4} M benzoic acid and 2.0×10^{-4} 4,6-dinitro-o-cresol respectively.

Atrazine, pentachlorophenol and warfarin were also screened at these biosensor strips, but inhibition was negligible and required concentrations of greater than 3 mM to effect an inhibition response. No responses were obtained for similar investigations involving nitrate, nitrite, fluoride, azide, lead or cadmium over the concentration range 0.1 to 10.0 ppm for each ion throughout that concentration range. The tyrosinase-free carbon ink strips used as controls, were not responsive to any of the above 14 compounds under the experimental conditions investigated.

The environmental utility of the tyrosinase-based inhibitor biosensor is illustrated in Figure 2.2.4. This shows the response for an untreated river water sample taken from the Rio Grande, New Mexico, and spiked with increasing levels of diethyldithiocarbamate in 1×10^{-5} M steps. The strip responded rapidly to these micromolar concentration increments despite the absence of added electrolyte. Similar to assays of standard samples, the response rose sharply with the inhibitor concentration at first and then more slowly, yielding a characteristic inhibition profile as expected.

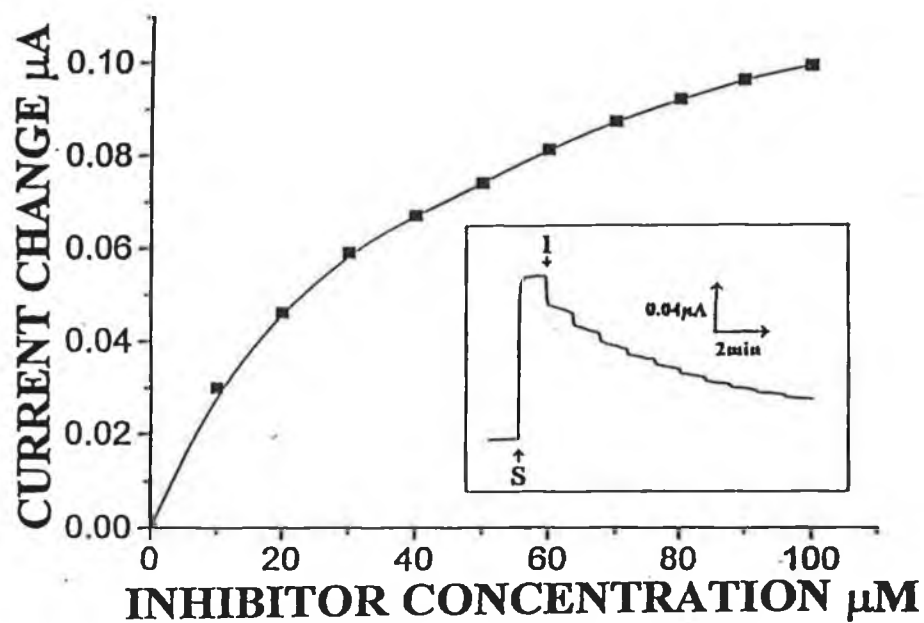


Figure 2.2.4. Calibration plot obtained using a water sample from the Rio Grande river. No supporting electrolyte was used in this experiment. The inset shows the corresponding current time recording. Catechol $5 \times 10^{-5} \text{ M}$ was used as substrate (S) sodium diethyldithiocarbamate (I), 10^{-5} M per step, was used as inhibitor.

2.2.3.3. *Detection Limits, Reproducibility and Stability Properties*

The reproducibility of sensor response and stability over a period of time is vital in the successful application of such electrodes in the marketplace. Detailed intra-assay, i.e. assessment of response variation within a batch of electrodes, and inter-assay studies, where the response of electrodes from different batches are evaluated, is of immense importance. Figure 2.2.5. shows the inhibition profiles obtained for diethyldithiocarbamate at 5 random electrodes from a 30 electrode batch. The intra-assay relative standard deviation ranged from 6.2 % for the response of 1×10^{-5} M diethyldithiocarbamate up to and not exceeding 11.8 % for inhibitor concentrations of 8×10^{-5} M. Such reproducibility requires a uniform dispersion of tyrosinase in the ink. However, the inter-assay variation between electrodes from different batches was as much as 30 %, thereby emphasising the need for separate calibration for each new batch based on the ratio of the inhibition signal to that of the substrate steady state response.

The limits of detection obtained based on a signal to noise ratio of 3 were as follows : 2.0×10^{-6} diethyldithiocarbamate; 4.0×10^{-6} thiourea; 5.0×10^{-6} M benzoic acid; 7.0×10^{-6} M 2,4-dichlorophenoxyacetic acid and 9.0×10^{-5} M 4,6-dinitro-o-cresol. Storage stability was also impressive where new strips displayed only ~ 4 % and ~ 15 % decrease in response after storage for 30 and 60 days respectively in phosphate buffer at 5 °C. Similar results were obtained by Wang and Chen [45] in their sensor strips for the analysis of phenol samples.

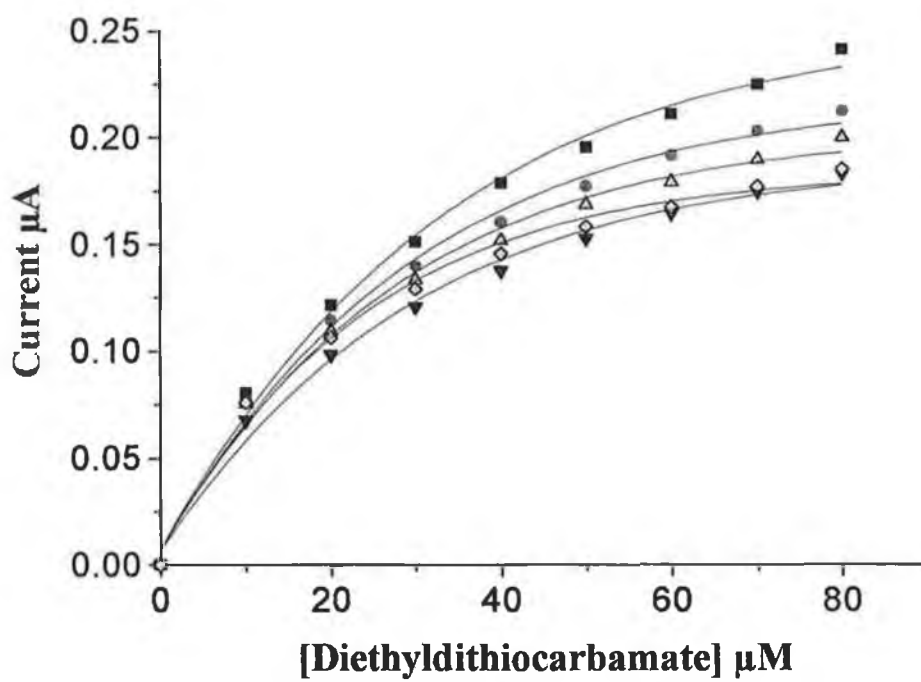


Figure 2.2.5. Calibration plots obtained for diethyldithiocarbamate at five random electrodes from a 30 electrode batch. Conditions as given in Figure 2.2.3.

2.2.4. Conclusion

The above experiments have demonstrated for the first time the utility of tyrosinase based thick film electrode strips for the monitoring of enzyme inhibitors. The new strips offer convenient quantitation of micromolar concentrations of various water pollutants and require no incubation period. A convenient one-step fabrication step was accomplished by incorporating the enzyme within the ink matrix.

As is common for enzyme inhibition processes, such detection would not be specific in complex environmental samples. Such samples would thus benefit from designing arrays of several enzyme inhibition electrodes of different properties. Further improvements in detection could be achieved through the use of metallised carbon inks or bioamplification/ recycling reaction schemes. The same strips could be useful for the on-site environmental screening of toxic pollutants.

2.3. Elucidation of Tyrosinase Inhibition and Inhibition Type

2.3.1. Introduction

Elucidation of inhibitor type is of utmost importance in environmental monitoring. Inhibition of one or more enzymes in a metabolic pathway can have detrimental effects *in vivo*. In the previous two sections, the exploitation of biosensors for the monitoring of potential enzyme inhibitors was presented. The sensors responded in an efficient and instantaneous manner to the screened analytes and yielded micromolar detection limits. However, the determination of the inhibitor type and the manner in which inhibition was achieved at the tyrosinase enzyme was not investigated.

The purpose of this section is to address these issues with a postulated approach to explain tyrosinase inhibition using diethyldithiocarbamate as a model compound. The experimental elucidation of inhibition caused by the latter compound, thiourea and benzoic acid is also demonstrated.

2.3.2. Experimental

2.3.2.1. Reagents

All solutions were prepared unless otherwise stated in deionised water prepared by passing distilled water through a Milli-Q-water purification system. Potassium dihydrogen phosphate and disodium hydrogen phosphate were supplied by Aldrich (Milwaukee, USA). The enzyme used, tyrosinase, 4400 units mg^{-1} solid was obtained from Sigma (MO, USA), (T-7755, E. C. 1.14.18.1.). The supporting electrolyte was a 0.05 M phosphate buffer solution pH 7.4. Catechol was supplied by Sigma (MO, USA), thiourea was supplied by Fisher (USA) and benzoic acid from Baker (USA) were used without further purification. Graphite powder was supplied by Fisher (USA) and mineral oil was supplied by Aldrich (Milwaukee, USA).

2.3.2.2. Instrumentation

All analyses were performed on a BAS 100B integrated, automated electrochemical workstation from Bioanalytical Systems (Stockport, UK (BAS)), connected to a three electrode 10 ml cell, containing a 3 % tyrosinase carbon paste electrode as the working electrode, platinum wire mesh counter electrode and silver/ silver chloride as the reference electrode (BAS Technicol, Stockport, UK). Solutions were stirred at 300 rpm on an Ikemeg IK50 stirring mantle.

2.3.2.3. Electrode Preparation

The carbon paste was prepared by mixing thoroughly a 70:30 composition of graphite powder and mineral oil. 97 mg of the resultant paste was mixed with 3 mg of tyrosinase enzyme to result in an electrode composite containing 3 % tyrosinase. A portion of this composite was then packed into the electrode cavity (3 mm diameter, 1 mm depth) of a PTFE sleeve. Electrical contact was established via a copper wire. The paste surface was smoothed on weighing paper.

2.3.2.4. Procedures

All experiments were performed in steady state mode. The electrodes were placed in 10 ml phosphate buffer 0.05 M pH 7.4. and were stirred at 300 rpm. A potential of - 0.2 V

was applied and the baseline allowed to stabilise. Steady state batch experiments were then performed in solutions containing both substrate and inhibitor aliquots respectively.

2.3.3. Results & Discussion

2.3.3.1. *Theoretical Treatism on Inhibition by Sodium Diethyldithiocarbamate*

As mentioned earlier in Chapter 1, tyrosinase is a bifunctional copper-containing oxidase having both catholase and cresolase activity [53]. The enzyme is a tetramer containing four atoms of copper per molecule [54], and two binding sites for aromatic compounds mainly phenolic substrates. There is also a distinctively different binding site for oxygen. The kinetics of tyrosinase catalysis have been well documented [55-58].

Figure 2.3.1(a) shows a proposed schematic of the active site of tyrosinase. The enzyme is shown in its resting state along with the two substrate binding and oxygen binding sites respectively. The mechanism of substrate catalysis at the active site is outlined in Figure 2.3.1(b). Within one enzyme turnover, two catechol molecules participate in the catalysis process resulting in the production of o-quinone products. At a biosensor surface this quinone product would then be reduced at a negative potential resulting in a signal and regeneration of the catechol substrate as shown earlier in Figure 1.5. of Chapter 1.

Sodium diethyldithiocarbamate was used as a model compound to propose the various manners in which substrate catalysis at the active site could be perturbed. Diethyldithiocarbamate belongs to the carbamate family of pesticides which accounted for over 60 % of pesticide usage world-wide in the 1950s [59]. They function through the chelation of the metal centres of enzyme active sites, thereby inhibiting enzymatic and maintaining pest control. Lacoste et al. [60] have shown that sodium diethyldithiocarbamate chelates copper stronger than any other metal which could explain its effective inhibition of tyrosinase enzyme experienced in our studies.

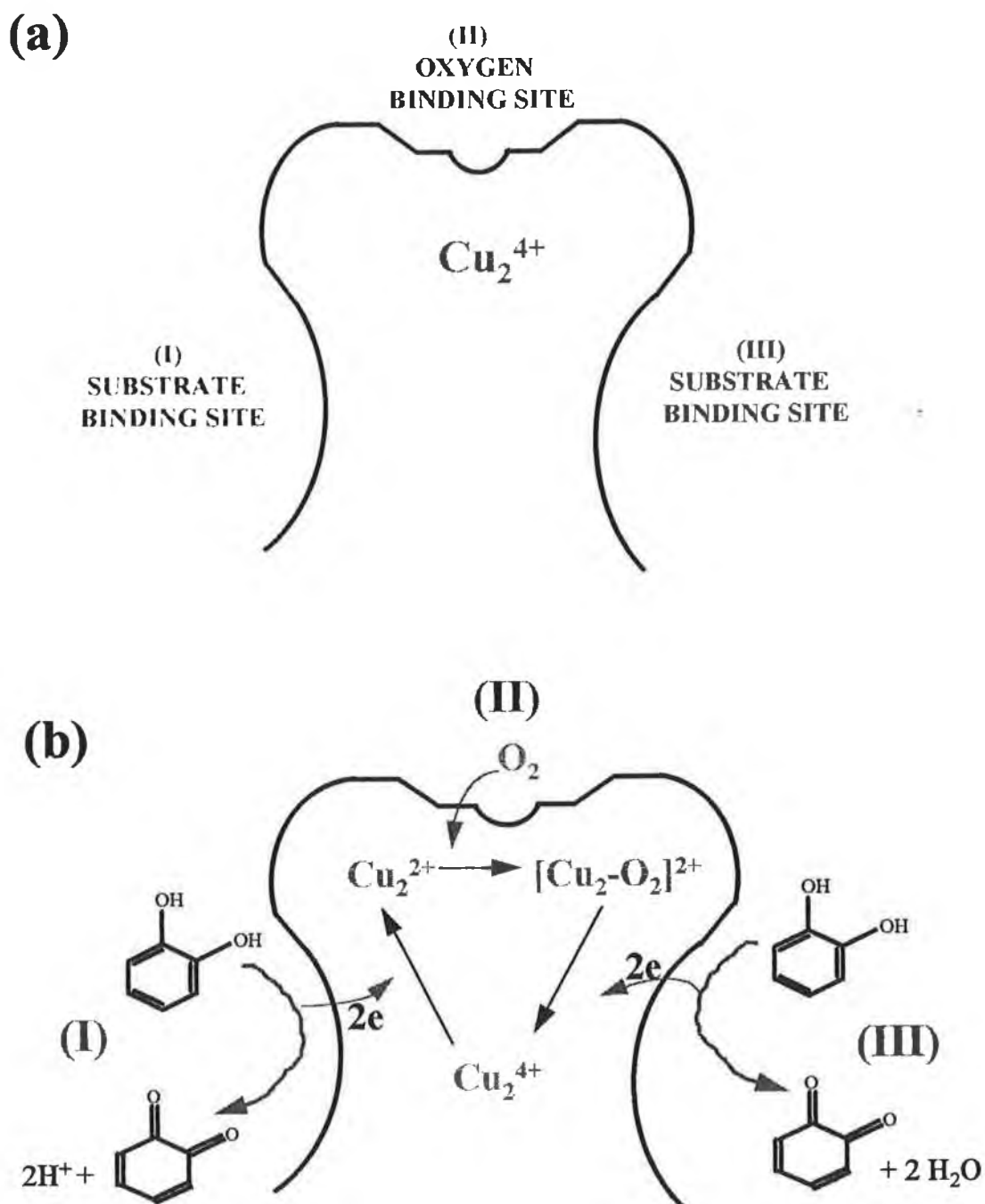


Figure 2.3.1(a) Tyrosinase active site and (b) catalysis at the active site using catechol as substrate.

Many possibilities exist for the inhibition of tyrosinase by sodium diethyldithiocarbamate. They include inhibition of the enzyme in its resting state and inhibition of the enzyme in its reduced state, amongst others. Figure 2.3.2(a) depicts chelation of the active site copper by diethyldithiocarbamate. As one can see, chelation prevents binding of the substrate and hence inhibits the enzyme. The substrate must then compete with the inhibitor for access to the active site. This scenario could also arise in stage (III) of the catalysis process shown in Figure 2.3.1(a), whereby the inhibitor may bind and inactivate the enzyme after the initial substrate (I) and oxygen binding reaction (II) respectively.

Alternatively, as shown in Figure 2.3.2(b), the inhibitor may bind after the initial substrate binding reaction, thus preventing the binding of oxygen and completion of the catalytic process. In this scenario the oxygen must compete with the inhibitor for binding to the copper active site. However since oxygen-copper binding is a lot stronger than diethyldithiocarbamate, i.e. the electronegativity of oxygen is 3.5 compared to 2.5 for sulphur, one would assume that inhibition of the enzyme at substrate binding sites (I) and (III) is more frequent, and that the inhibition process results from a competition between the substrate and inhibitor for binding to the enzyme active site, along with a less dominant competition between diethyldithiocarbamate and oxygen for the oxygen binding site.

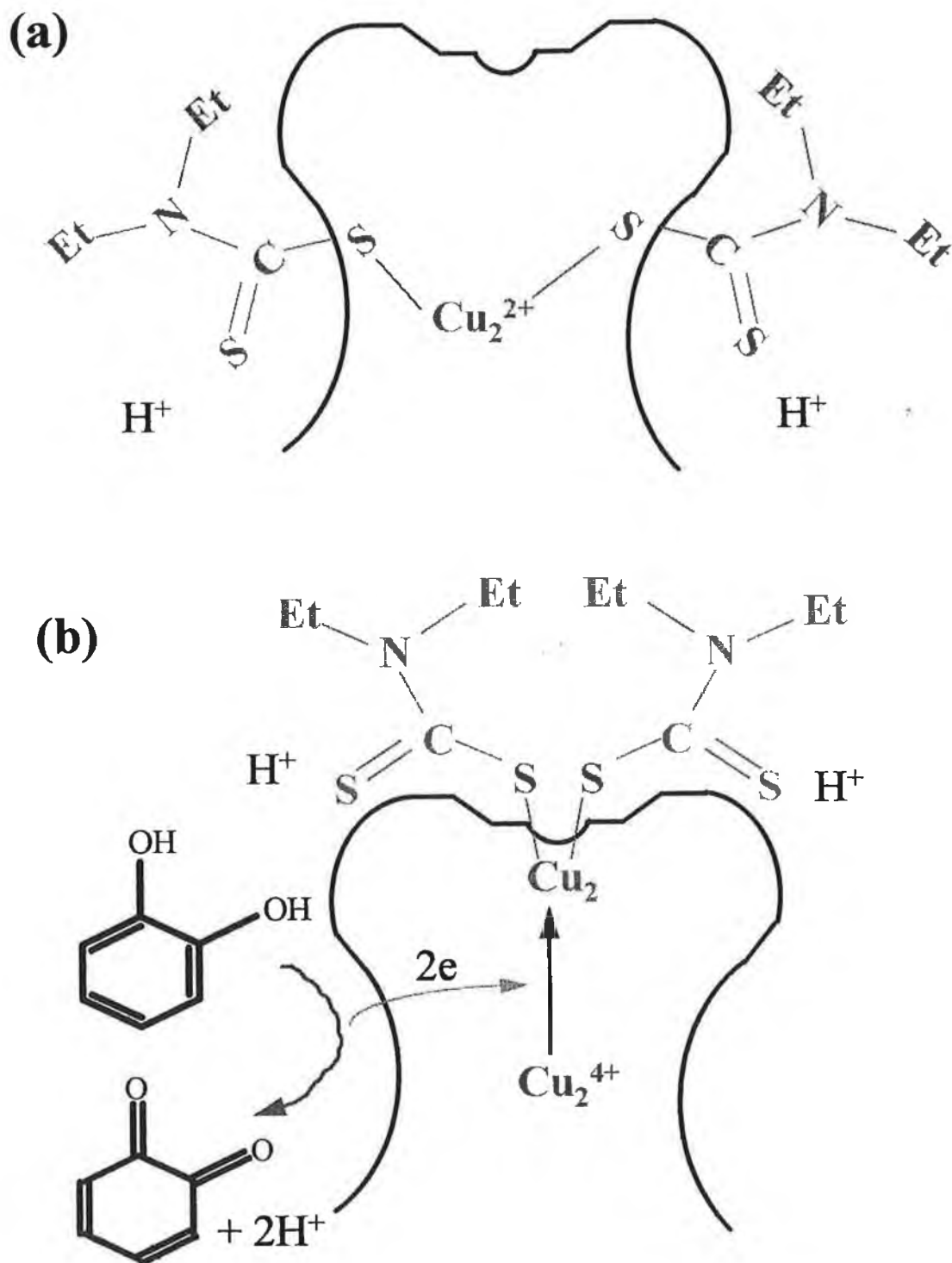


Figure 2.3.2(a) Inhibition of the enzyme in its resting state. (b) Inhibition of the enzyme in its reduced state.

It is also important to take into consideration secondary interactions between the inhibitor and the enzyme, which could present added difficulty for the substrate to remove the imposing inhibitor. Such interactions may involve hydrogen bonding interactions amongst others, between functional groups on amino acids in the active site vicinity and groups present on the inhibitor. For example, aspartic acid, glutamic acid, asparagine, glutamine, acidic amino acids and their amide residues may have a role to play.

Figure 2.3.3. shows the binding of two molecules of diethyldithiocarbamate to active site copper in its resting stage. The polypeptide chain shown to the right represents amino acid residues in close proximity to the active site centre. Shown as a dotted line is the partial charge interaction between the amino groups of the diethyldithiocarbamate molecules and the carbonyl groups of glutamine and asparagine residues respectively. Secondary interactions between the partial positive charge (δ^+) on the carbonyl carbon of the amino acid residues and the partial negative charge (δ^-) on the amine groups of diethyldithiocarbamate, make it difficult for the substrate to remove inhibitor and react with the enzyme.

2.3.3.2. *Experimental Elucidation of Inhibitor Type*

Earlier in Chapter 1, Section 1.9., the various types of enzyme inhibition and their respective classes were introduced. Generally there are two types of enzyme inhibitors: reversible and irreversible. Reversible enzyme inhibition is attributed to the non-covalent binding of inhibitor and includes: competitive, non-competitive and uncompetitive inhibition. Covalent binding of inhibitors to an enzyme's active site results in irreversible inhibition and is detrimental to human health.

Figure 2.3.4. shows the Lineweaver-Burk plots for enzyme catalysis in the presence of substrate and in the presence of substrate and inhibitor, for diethyldithiocarbamate, thiourea and benzoic acid. For thiourea and benzoic acid, the Lineweaver plots intersected at the same V_{\max} value and yielded different apparent Michaelis-Menten constants, K_m^{app} values, as expected for a competitive inhibition process.

The corresponding plot for diethyldithiocarbamate resulted in the Lineweaver-Burk plots intersecting at the same point on the baseline, suggesting a fully non-competitive process. The K_m^{app} value was unaffected by the presence of the inhibitor, but the V_{\max} values were changed as expected for non-competitive inhibition. These results are in agreement with those obtained by other researchers [25, 31, 32, 61]. Wang et al. [32] obtained reversible competitive inhibition for benzoic acid and thiourea, and reversible non-competitive inhibition for diethyldithiocarbamate. Similar results were obtained by Deng and Dong [31] for benzoic acid and thiourea.

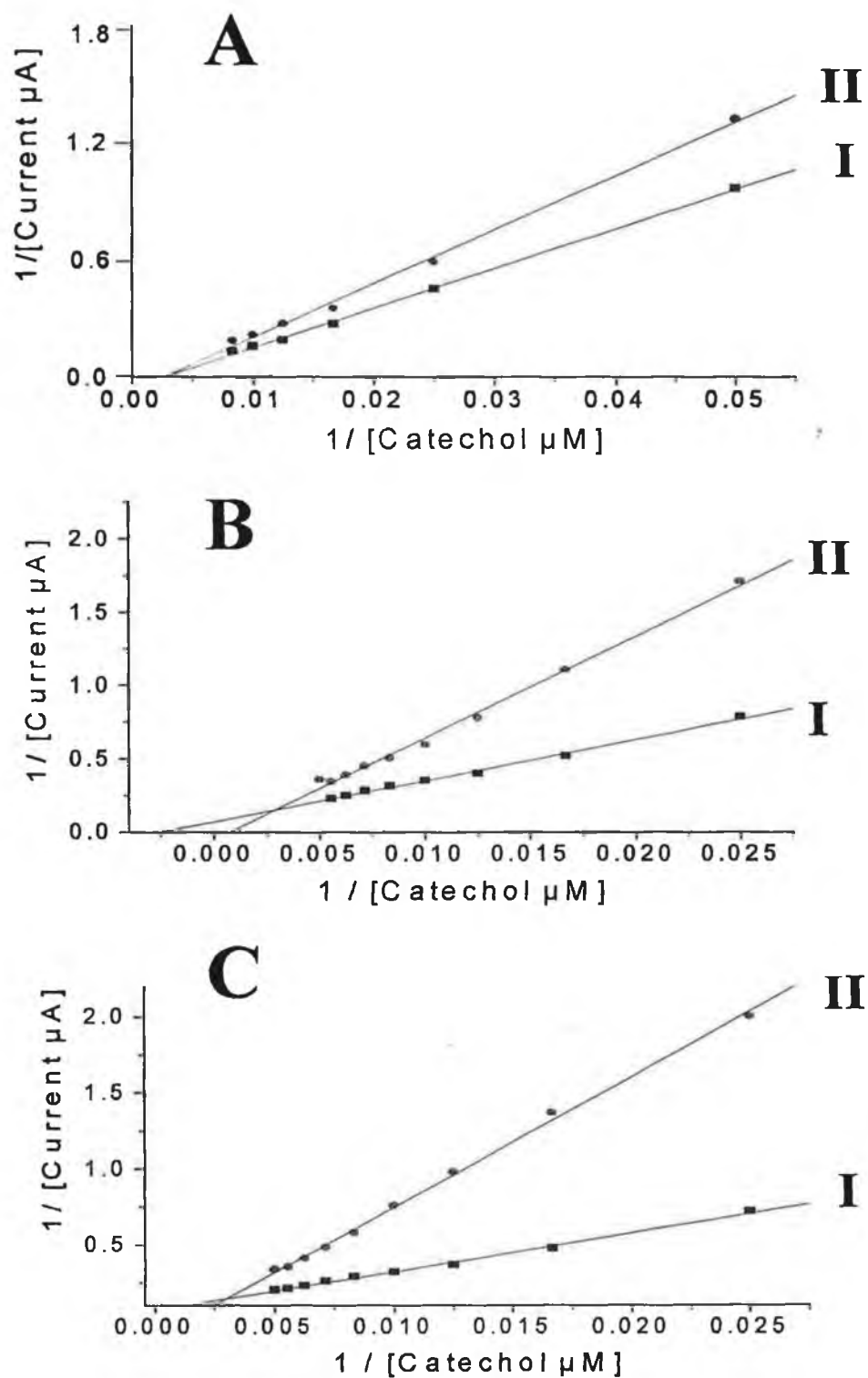


Figure 2.3.4. Lineweaver-Burk plots for catechol substrate (I) and catechol substrate additions containing 60 μM of inhibitor (II) where (A) is sodium diethyldithiocarbamate, (B) thiourea and (C) benzoic acid at a tyrosinase (3%) carbon paste electrode. Solutions were stirred at 300 rpm, phosphate buffer solution 0.05 M pH 7.4. Experiments were performed at 25 $^{\circ}\text{C}$.

An example of the substrate calibration plots obtained for a tyrosinase (3% w/w) carbon paste electrode before and after exposure to phosphate buffer solutions containing 60 μM thiourea for a duration of 30 minutes are shown in Figure 2.3.5. As one can see, the substrate profile almost returned to its original profile after the consecutive rinses following exposure to the inhibitor solution, hence emphasising the reversible competitive inhibition nature of thiourea. Table 2.3.1. summarises the results obtained earlier for inhibitor type for the various compounds investigated.

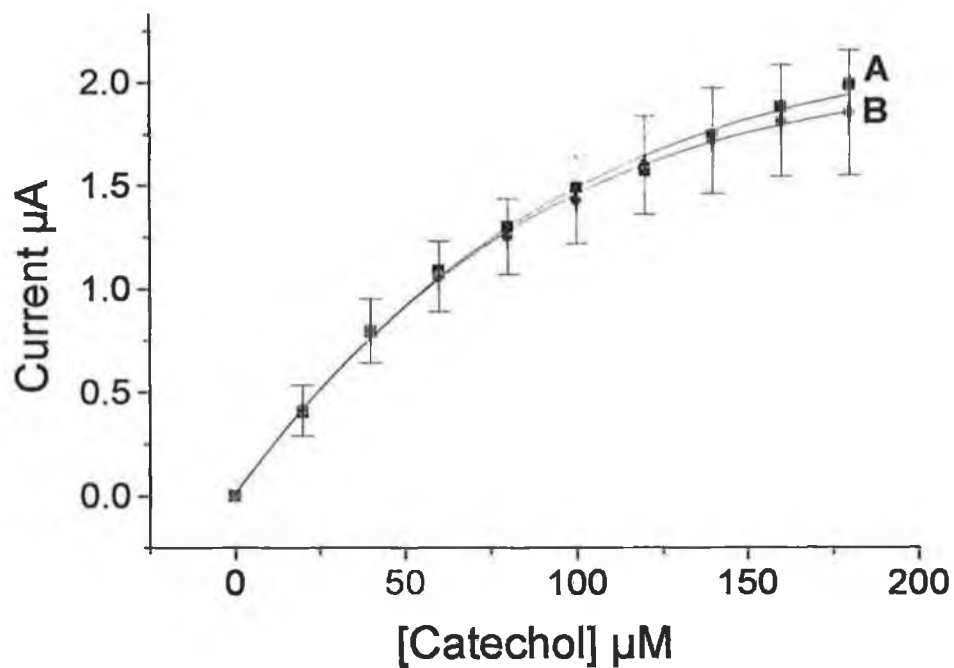
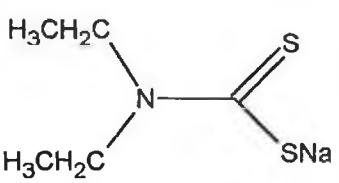
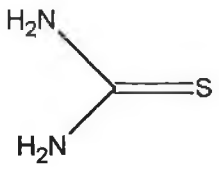
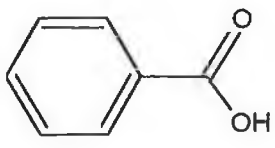


Figure 2.3.5. Substrate response profiles before (A) and after exposure (B) to solutions containing 60 μM thiourea for a duration of 30 minutes. (B) represents the average of three consecutive rinses. Solutions were stirred at 300 rpm. 0.05 M phosphate buffer, pH 7.4., applied potential - 0.2 V. Experiments performed at 25 °C.

Table 2.3.1. Summary of inhibitor type and class.

Compound	Inhibitor Type	Class
 <p>Sodium Diethyldithiocarbamate</p>	Reversible	Non-competitive
 <p>Thiourea</p>	Reversible	Competitive
 <p>Benzoic Acid</p>	Reversible	Competitive

2.3.4. Conclusion

Elucidation of inhibitor type and method of inhibition is extremely important in determining the influence of certain toxic compounds on enzymatic systems and also understanding the complexity of the inhibition process. It has been postulated that an inhibitor may inhibit the active site of tyrosinase through binding at the respective substrate bindings sites and/or alternatively binding to the oxygen binding site. Experiment studies have shown that all three inhibitor compounds resulted in reversible inhibition. Diethyldithiocarbamate was found to be a non-competitive inhibitor whilst thiourea and benzoic acid were found to be competitive inhibitors respectively.

2.4. References

- [1] Mazzei, F.; Botre, F.; Botre, C.: *Anal. Chim. Acta.*, 336: (1996): 67.
- [2] Ozsoz, M.; Erdern, A.; Kilinc, E.; Gokgunnec, L.: *Electroanalysis*, 8: (1996): 147.
- [3] Navaratne, A.; Rechnitz, G. A.: *Anal. Chim. Acta.*, 257: (1992): 59.
- [4] Rechnitz, G. A.: *Science*, 214: (1981): 287.
- [5] Arnold, M. A.; Rechnitz, G. A.: Chapter 3 of 'Biosensors: Fundamentals and Applications. Turner, A. P. F.; Karube, I.; Wilson, G., Eds.: Oxford University Press, (1987).
- [6] Wang, J.: *Electroanalysis*, 3: (1991): 255.
- [7] Rechnitz, G. A.; Arnold, M. A.; Meyerhoff, M. E.: *Nature*, 278: (1979): 466.
- [8] Arnold, M. A.; Rechnitz, G. A.: *Anal. Chem.*, 52: (1980): 1170.
- [9] Updike, S.; Treichel, I.: *Anal. Chem.*, 51: (1979): 1643.
- [10] Wang, J.; Lin, M. S.: *Anal. Chem.*, 60: (1988): 1545.
- [11] Wang, J.; Lin, M. S.: *Electroanalysis*, 1: (1989): 43.
- [12] Glazier, S. A.; Rechnitz, G. A.: *Anal. Lett.*, 22: (1989): 2929.
- [13] Ozsoz, M.; Wang, J.: *Electroanalysis*, 3: (1991): 655.
- [14] Bonakdar, M.; Vilchez, J.; Mottola, H.: *J. Electroanal. Chem.*, 266: (1989): 47.
- [15] Wang, J.; Wu, L-H.; Martinez, S.; Sanchez, J.: *Anal. Chem.*, 63: (1991): 398.
- [16] Wang, J.; Naser, N.: *Anal. Chem.*, 64: (1992): 2469.
- [17] Leon-Gonzalez, M. E.; Townshend, A.: *Anal. Chim. Acta.*, 236: (1990): 267.
- [18] Marty, J-L.; Garcia, D.; Rouillon, R.: *Tr. Anal. Chem.*, 14: (1995): 329.
- [19] Gunther, A.; Bilitewski, U.: *Anal. Chim. Acta.*, 300: (1995): 117.
- [20] Cowell, D. C.; Dowman, A. A.; Ashcroft, T.: *Biosens. Bioelectron.*, 10: (1995): 509.
- [21] Amine, A.; Alafandy, M.; Kauffmann, J-M.; Pekli, M. N.: *Anal. Chem.*, 67: (1995): 2822.
- [22] Evtugyn, G. A.; Budnikov, H. C.; Nikolskaya, E. B.: *Analyst*, 121: (1996): 1911.
- [23] Budnikov, H. C.; Evtugyn, G. A.: *Electroanalysis*, 8: (1996): 817.
- [24] Ghous, T.; Townshend, A.: *Anal. Chim. Acta.*, 332: (1996): 179.

- [25] Pita, M. T. P.; Reviejo, A. J.; Villena, F. J.; Pingarron, J. M.: *Anal. Chim. Acta.*, 340: (1997): 97.
- [26] Fennouh, S.; Casimiri, V.; Burstein, C.: *Biosens. Bioelectron.*, 12: (1997): 97.
- [27] Rodriquez, M. O.; Flurkey, W. H.: *J. Chem Educ.*, 69: (1992): 767.
- [28] Wilcox, D. E.; Porras, A. G.; Hwang, Y. T.; Lerch, K.; Winkler, M. E.; Solomon, E. I.: *J. Am. Chem. Soc.*, 107: (1985): 4015.
- [29] Besombes, J-L.; Cosnier, S.; Labbe, P.; Reverdy, G.: *Anal. Chim. Acta.*, 311: (1995): 255.
- [30] Wang, J.; Varughese, K.: *Anal. Chem.*, 62: (1990): 318.
- [31] Deng, Q.; Dong, S.: *Analyst*, 121: (1996): 1979.
- [32] Wang, J.; Dempsey, E.; Eremenko, A.; Smyth, M, R.: *Anal. Chim. Acta.*, 279: (1993): 203.
- [33] Rogers, K. R.: *Biosens. Bioelectron.*, 10: (1995): 533.
- [34] Wang, J.: *Electrochemical sensors for Environmental Monitoring: A Review of Recent Methodology*. U.S. E.P.A./5110/R45/507, Research Triangle Park Pub., NC, (1995).
- [35] Gilmartin, M. A. T.; Hart, J. P.; Patton, D. T.: *Analyst*, 120: (1995): 1973.
- [36] Sprules, S. D.; Hart, J. P.; Wring, S. A.; Pittson, R.: *Analyst*, 304: (1995): 17.
- [37] Gilmartin, M. A. T.; Hart, J. P.; Birch, B. J.: *Analyst*, 119: (1994): 243.
- [38] Park, J. K.; Yee, H. J.; Kim, S. T.: *Biosens. Bioelecron.*, 10: (1995): 587.
- [39] Napier, A.; Hart, J. P.: *Electroanalysis*, 8: (1996): 1006.
- [40] Wang, J.; Cai, X.; Tian, B.; Shiraishi, H.: *Analyst*, 121: (1996): 965.
- [41] Wang, J.; Pediero, M.; Cai, X.: *Analyst*, 120: (1995): 1969.
- [42] Wang, J.; Lu, Z.: *Electroanalysis*, 1: (1989): 517.
- [43] Neuhold, C. G.; Wang, J.; Cai, X.; Kalcher, K.: *Analyst*, 120: (1995): 2377.
- [44] McAlernon, P.; Slater, J. M.: *Anal. Proc.*, 31: (1994): 365.
- [45] Wang, J.; Chen, Q.: *Anal. Lett.*, 28: (1995): 1131.
- [46] Neuhold, C. G.; Wang, J.; Nascimento, V. b.; Kalcher, K.: *Talanta*, 42: (1995): 1791.
- [47] Cagnini, A.; Palchetti, I.; Lioni, I.; Mascini, M.; Turner, A. P. F.: *Sens. Actuators B*, 24-25: (1995): 85.
- [48] Hart, J. P.; Hartley, I. C.: *Analyst*, 119: (1994): 259.

- [49] Yu, Y.; Cagnini, A.; Mascini, M.; *Chem. Anal.*, 40; (1995): 579.
- [50] Skladal, P.; Kalab, T.: *Anal. Chim. Acta.*, 304: (1995): 361.
- [51] Skladal, P.; Kalab, T.: *Anal. Chim. Acta.*, 316: (1995): 73.
- [52] Hartley, I.; Hart, J. P.: *Anal. Proc.*, 31: (1994): 333.
- [53] Malstrom, B.; Ryden, L.: *Biological Oxidations*. Singer T. Ed., (1968), Interscience Pub.
- [54] Smith, J.; Krueger, R.: *J. Biol. Chem.*, 237: (1962): 1121.
- [55] Kertesz, D.; Brunori, M.; Zito, R.; Antonini, E.: *Biochim. Biophys. Acta.*, 250: (1971): 306.
- [56] Kertesz, D.; Rotilio, G.; Brunori, M.; Zito, R.; Antonini, E.: *Biochim. Biophys. Res. Comm.*, 49: (1972): 1208.
- [57] Keyes, M.; Semersky, F.: *Biochem. Biophys.*, 148: (1972): 256.
- [58] Garcia-Carmona, F.; Calbenes, J.; Garcia-Canoras, F.: *Biochem. Intl.*, 14; (1987): 1003.
- [59] Halley, R. J.; *The Agricultural Handbook*. (1984): Butterworths Pub.
- [60] Lacoste, R. J.; Earing, M. H.; Wiberley, S. E.: *Anal. Chem.*, 23: (1951): 871.
- [61] Stancik, L.; Macholan, L.; Scheller, F.: *Electroanalysis*, 7; (1995): 649.

Chapter 3

**Hydrocarbon Pasting Liquids for
Improved Tyrosinase-Based Carbon Paste
Phenol Biosensors**

3.1. Introduction

Phenols and substituted phenols are products of many industrial processes. In view of the high toxicity of various phenolic derivatives, reliable analytical procedures are required for their determination at low levels in various environmental matrices. Amperometric biosensors based on the enzyme tyrosinase have proved to be very useful for this task [1-5]. The enzyme tyrosinase, also known as polyphenol oxidase E.C. 1.14.18.1., is a copper-containing oxidase that catalyses the conversion of monophenols and diphenols to the corresponding quinones [6].

Reagentless devices based on the immobilisation of tyrosinase onto various carbon or platinum transducers have been developed [1]. Such devices rely on monitoring the liberation of the quinone product or consumption of the oxygen cofactor. Tyrosinase based electrodes can be used as detectors for liquid chromatography, hence providing quantitation of the individual phenolic substrates [4,5,7,8]. Such liquid chromatographic-electrochemical (LCEC) detection operation benefits from the organic phase stability of tyrosinase [9, 10]. Such activity has led also to the common use of carbon-paste transducers as hosts for the enzyme. By mixing tyrosinase, together with graphite powder and an organic pasting liquid, it is possible to obtain fast responding, versatile and renewable biosensors.

This chapter describes the evaluation of new pasting liquids for enhancing the performance of tyrosinase-based carbon paste biosensors. It is known that the exact composition of carbon paste bioelectrodes has a profound effect upon their performance [11]. Lutz et al. [12] demonstrated the influence of different additives on the sensitivity and operational stability of tyrosinase-containing carbon paste electrodes. Lindgren et al. [13] examined the effect of tyrosinase from different sources on the response of carbon paste flow detectors. Pravda et al. [4] reported on the improved stability and reproducibility associated with the use of solid paraffin-based carbon paste phenol biosensors. Marko-Varga [1] reported on the effect of various silicone and paraffin oils upon the response to tyrosinase-modified carbon paste electrodes.

In the following sections the greatly improved sensitivity of tyrosinase biosensors are illustrated in association with the use of hydrocarbon pasting liquids. The role of the hydrocarbon chain length upon the response is elucidated along with detailed comments concerning the extracting properties of the pasting liquid. The utility of the new bioelectrodes for flow injection and the chromatographic analysis of phenols is demonstrated.

3.2. Experimental

3.2.1. Reagents

Chemicals were analytical reagent grade and used as received. Tyrosinase was obtained from Sigma (MO, USA) (t-7755, E.C. 1.14.18.1., 4, 400 units mg^{-1}). Catechol, phenol, 2,4-dimethylphenol, p-cresol, o-cresol, p-chlorophenol and o-chlorophenol were supplied from Aldrich (Milwaukee, USA). The graphite powder grade # 38 was obtained from Fisher (USA). The various binders: mineral oil; silicon oil; decane; dodecane; tetradecane and hexadecane were all supplied by Aldrich (Milwaukee, USA). Acetonitrile (HPLC grade) from Fisher (USA) was used for preparing mobile phases. Potassium dihydrogen phosphate and disodium hydrogen phosphate were supplied by Aldrich (Milwaukee, USA). Deionised water was used where appropriate and was prepared by passing distilled water through a Milli-Q-water purification system. All filters and membranes were obtained from Bioanalytical Systems Inc. (W. Lafayette, USA). Nylon membranes (0.2 μm pore size, 47 mm diameter, BAS, MF 5621) were used for filtering mobile phase. Microfilters (BAS, MF 5500) and microfilter membranes (BAS, MF 5658) were used for filtering samples. Ultra high purity helium gas (Argile Welding Supply, Albuquerque, NM, USA) was used as received for degassing mobile phase and solutions.

3.2.2. Instrumentation and Procedure

Amperometric flow injection analysis and batch experiments were carried out using a BAS CV-27 Voltammograph operating at -0.05 V (vs. Ag/AgCl), in connection with a BAS X-Y recorder. A 10 ml electrochemical cell (BAS, Model VC-2) was used in the batch experiments. The working electrode, reference electrode (Ag/AgCl, Model RE-1, BAS) and platinum wire electrode joined the cell through holes in the Teflon cover. A large volume wall-jet detector was used in the FIA experiments, along with an Alitea C-4V pump operating at 1.5 ml min^{-1} . All experiments were performed at room temperature using a 0.05M phosphate buffer, pH 7.4. Chromatographic experiments were performed on a HPLC system (BAS, Model 480) in connection with a dual reciprocating pump (PM-80, BAS) and an amperometric detector (BAS, Model LC-4C) with a thin layer cell (BAS, CV-5). Injections were made through a Rheodyne valve

with a 20 μ l loop onto a C₁₈ DB reverse phase column (LC 18 DB, No.: 88773A, Supelco Inc., 5 μ m, 4.6 x 250 mm). Chromatograms were recorded on an Omniscribe strip-chart recorder (Houston Instruments). The mobile phase used composed of 25 : 75 acetonitrile : phosphate buffer (0.05 M, pH 6.5). All analyte standard solutions were prepared in the mobile phase. The mobile phase was filtered and degassed prior to use.

3.2.3. Electrode Preparation

The tyrosinase carbon paste electrodes were prepared by mixing 60 mg graphite powder with 40 mg of the corresponding pasting liquid binder; 3 mg of tyrosinase enzyme was then mixed with 97 mg carbon paste. A portion of the corresponding paste was packed into the electrode cavity (3 mm diameter, and 1 mm depth) of a PTFE sleeve. The paste surface was smoothed on weighing paper.

3.3. Results and Discussion

3.3.1. Characteristics and Performance of the Hydrocarbon Pasting Liquid Modified Biosensors

The flow injection analysis response peaks for phenol, catechol and p-chlorophenol at tyrosinase modified carbon paste electrodes based on mineral oil and dodecane pasting liquids are shown in Figure 3.1. Both detectors employed the same enzyme loading and carbon content. Yet, the dodecane based detector resulted in a significantly higher sensitivity for all three substrates where sensitivity was almost 10-fold that observed at the mineral oil composite. It is also interesting to notice the changes in response time apparent at the two electrodes, particularly the slower return to the baseline of the hydrocarbon based enzyme electrode, e.g. a response time of almost 2.5 min was observed for catechol at the dodecane modified biosensor compared to ~1.0 min at the mineral oil bioelectrode.

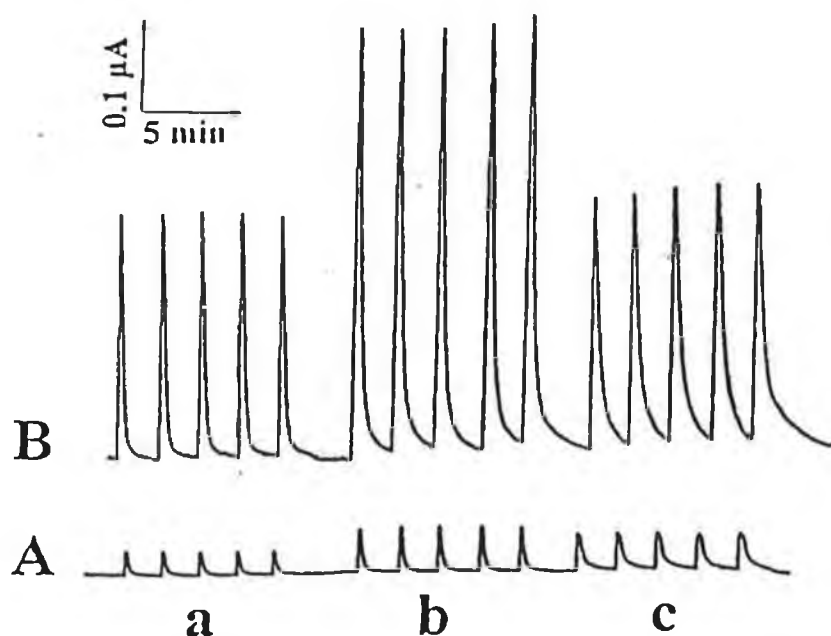


Figure 3.1. Amperometric flow injection peaks for 1×10^{-4} M phenol (a), catechol (b) and p-chlorophenol (c) using mineral oil (A) and dodecane (B) based carbon paste tyrosinase electrodes. Applied potential - 0.05 V, flow rate 1.5 ml/min, carrier solution, 0.05 M phosphate buffer, pH 7.4.

This observation prompted the investigation of various other hydrocarbons as pasting liquids for phenol biosensors. Figure 3.2 shows the dependence of the flow injection response of six different phenolic substrates upon the hydrocarbon pasting liquid. Also shown for comparison are the responses of a mineral oil-based biosensor. The response of three of these substrates: *p*-cresol (a); *p*-chlorophenol (b) and phenol (c) decreased rapidly upon increasing the chain length of the hydrocarbon pasting liquid from decane to tetradecane, followed by a plateau region for tetradecane and hexadecane similar to that of mineral oil. The other three substrates displayed a significantly smaller response, that decreases gradually upon varying the chain length from decane to tetradecane, and then plateaus out thereafter. Changes in the extracting properties of the carbon paste electrodes upon changing the length of hydrocarbon pasting liquids may be responsible for such a trend as similarly experienced by Wang et al. [14] for enhancing the sensitivity of stripping measurements for phenothiazine drugs.

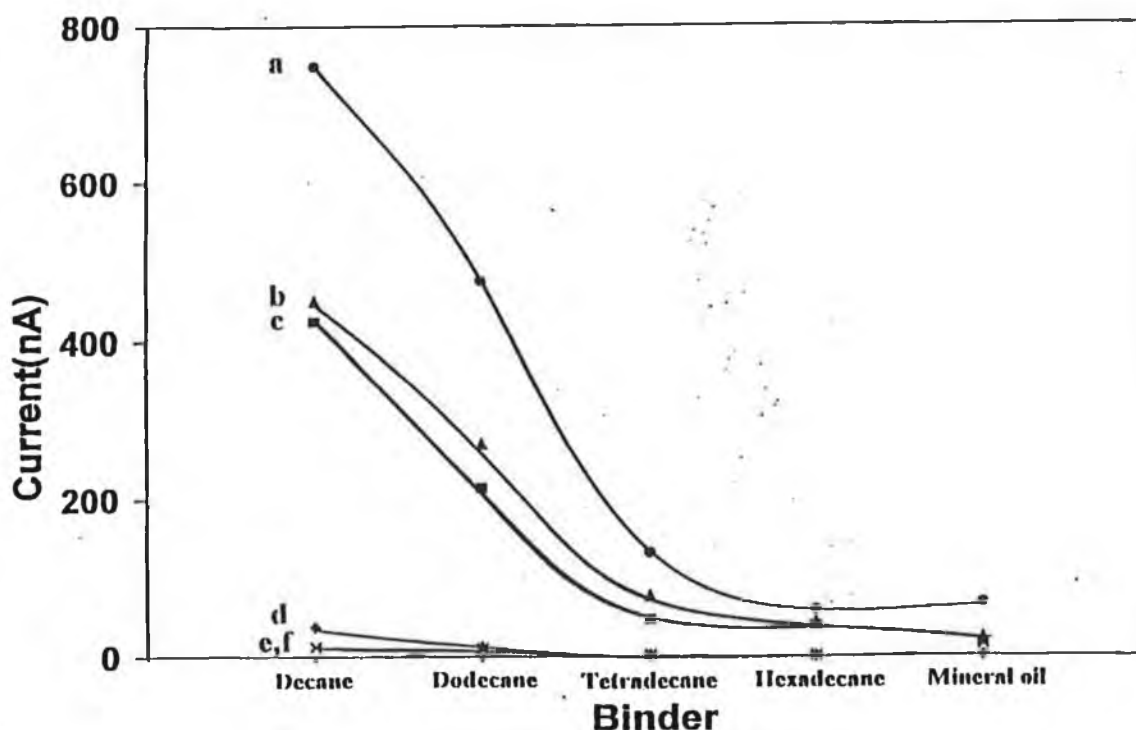


Figure 3.2. Response of carbon paste tyrosinase electrodes based on different binders to various phenolic compounds 0.1 mM (a) *p*-cresol; (b) *p*-chlorophenol; (c) phenol; (d) 2,4-dimethylphenol; (e) *o*-chlorophenol and (f) *o*-cresol. Other conditions as given in Figure 3.1.

The data of Figures 3.1 and 3.2 can be explained in terms of the extracting properties of the pasting liquid. Since carbon paste electrodes consist of a mixture of graphite and organic liquid, various organic compounds can be extracted into the paste [1, 14-16]. The partition of target analytes into the organic pasting liquid depends upon the polarity of the liquid and the structure of the analyte. Accordingly, the relatively polar phenolic compounds are extracted more readily into the shorter hydrocarbon liquids, i.e. decane and dodecane.

The penetration of phenolic substrates into the bulk of the electrodes exposes them to the enzyme present in the interior. Combining this higher apparent biocatalytic activity with the extractive accumulation of the substrates thus results in greatly enhanced sensitivity. In contrast, conventional mineral oil-containing carbon paste electrodes result in only a limited extractive preconcentration taking place and the surface rather than the bulk biocatalytic activity is responsible for most of the response. The hydrocarbon modified biosensors therefore result in highly sensitive peak responses accompanied by longer response times attributed to the extracting properties of the particular paste.

In addition to sensitivity enhancements, changing the carbon paste binder may be useful for manipulating the selectivity of the tyrosinase electrodes. Figure 3.3. compares the relative response of six phenolic compounds (normalised to phenols as 100 %) at the dodecane, mineral oil and silicon-oil based carbon paste bioelectrodes. At the silicon oil based sensor the trend in sensitivity observed was: p-chlorophenol > p-cresol > phenol > o-chlorophenol > 2,4-dimethylphenol > o-cresol. In contrast, using the mineral oil or dodecane carbon pastes results in a slightly different trend: p-cresol > p-chlorophenol > phenol > o-chlorophenol > o-cresol > 2,4-dimethylphenol.

The differences in the relative responses of these biosensors should be noticed, with the dodecane electrode suppressing the signals of the ortho compounds to approximately 10% of the phenol response, thereby enhancing the selectivity between para- and ortho-chlorophenols at biosensors of this type. In addition, the p-cresol response at the mineral

oil and dodecane carbon paste electrodes are about 3.8 and 2.2 fold larger than the phenol signal respectively

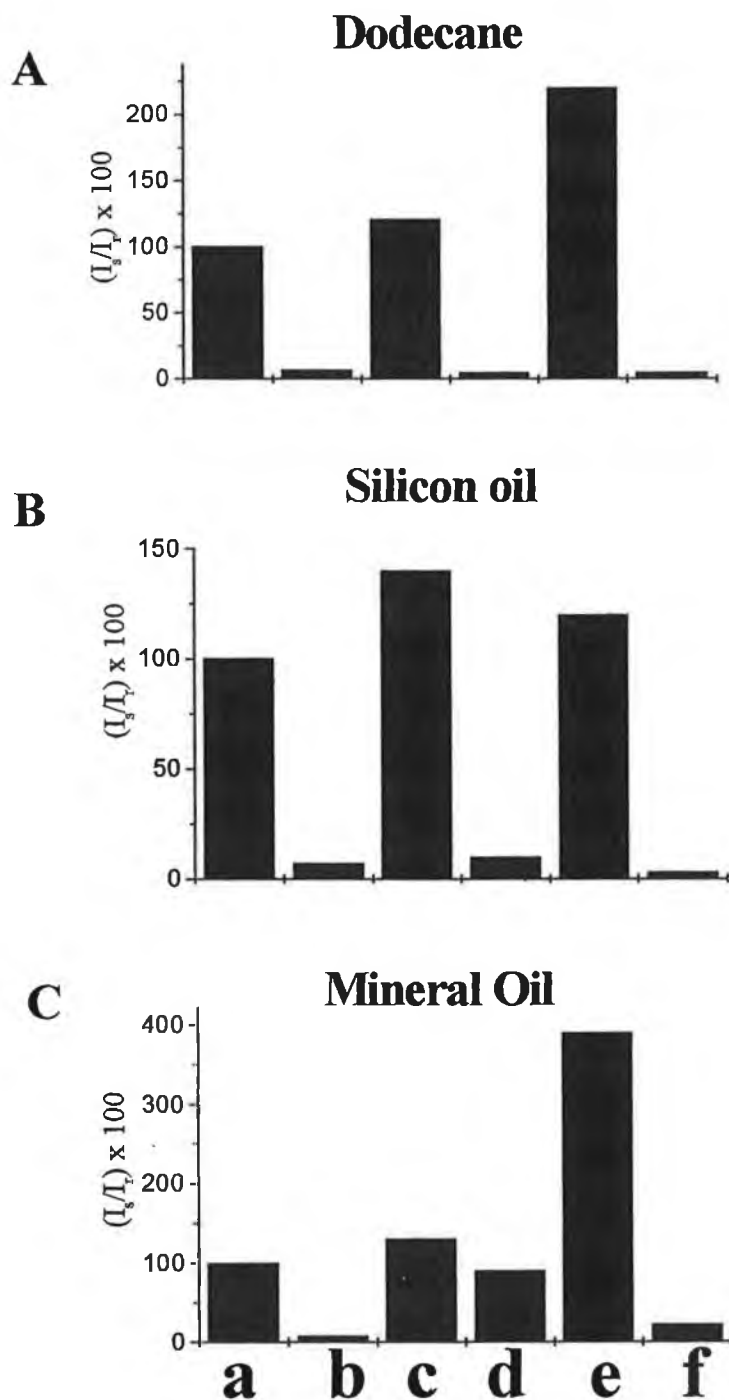


Figure 3.3. Relative response of carbon paste tyrosinase electrodes based on different binders: dodecane (A), silicon oil (B) and mineral oil (C) to different phenolic compounds: (a) phenol; (b) 2,4-dimethylphenol; (c) *p*-chlorophenol; (d) *o*-chlorophenol; (e) *p*-cresol and (f) *o*-cresol. The response was normalised in comparison to phenol taken as 100%. Concentration 0.1 mM. Other conditions as in Figure 3.1.

The different response patterns of Figure 3.3 reflect the combined effect of the biocatalytic activity of tyrosinase and the extracting properties of the pasting liquid. Changes in the oxygen (co-substrate) solubility should also be considered. Note also that in accordance to the principles of organic-phase enzymology, the tyrosinase specificity in the electrode interior may also be affected by the surrounding pasting liquid. Differences in the relative response to catechol and phenol at different silicon oil tyrosinase electrodes have been reported by Marko-Varga et al. [1] in a similar manner to the findings of this work.

3.3.2. Sensitivity, Reproducibility and Limits of Detection

Calibration profiles for p-cresol at dodecane (a), hexadecane (b) and mineral oil (c) based tyrosinase carbon paste electrodes are shown in Figure 3.4(A). As expected from Figure 3.3., the dodecane containing biosensor offered a substantially higher sensitivity than the hexadecane or mineral oil electrodes respectively. The sensitivity of the dodecane-based biosensor was about 12 fold higher than those of the hexadecane or mineral oil electrodes. Figure 3.4(B) shows the corresponding Lineweaver-Burk plots. The apparent Michealis-Menten constants, K_M^{app} , were thus estimated and found to be 133 μM for mineral oil; 168 μM for hexadecane and 245 μM for dodecane. In view of the great complexity of carbon paste enzyme electrodes, such values reflect the interplay between various factors, including the diffusional constraints of the substrate in the pasting liquid, the oxygen (co-substrate) solubility in this binder and also the specificity of the enzyme for the substrate and its behaviour in that particular matrix.

The analytical utility of the hydrocarbon based phenol biosensors were demonstrated using flow injection analysis. Figure 3.5. illustrates flow injection amperometric peaks at the dodecane-based tyrosinase carbon paste detector for increasing levels of phenol (A) and catechol (B). Well-defined peaks were observed for these low micromolar concentrations. Excellent linearity was observed with catechol displaying a curvature above 100 μM . Based on a signal to noise ratio of three, the limit of detection for catechol was found to be 6 nM, emphasising the potential of these novel biosensors for phenol monitoring in environmental samples. Even lower detection limits could be

achieved by exploiting various bioamplification, multienzyme and bioaccumulation methods.

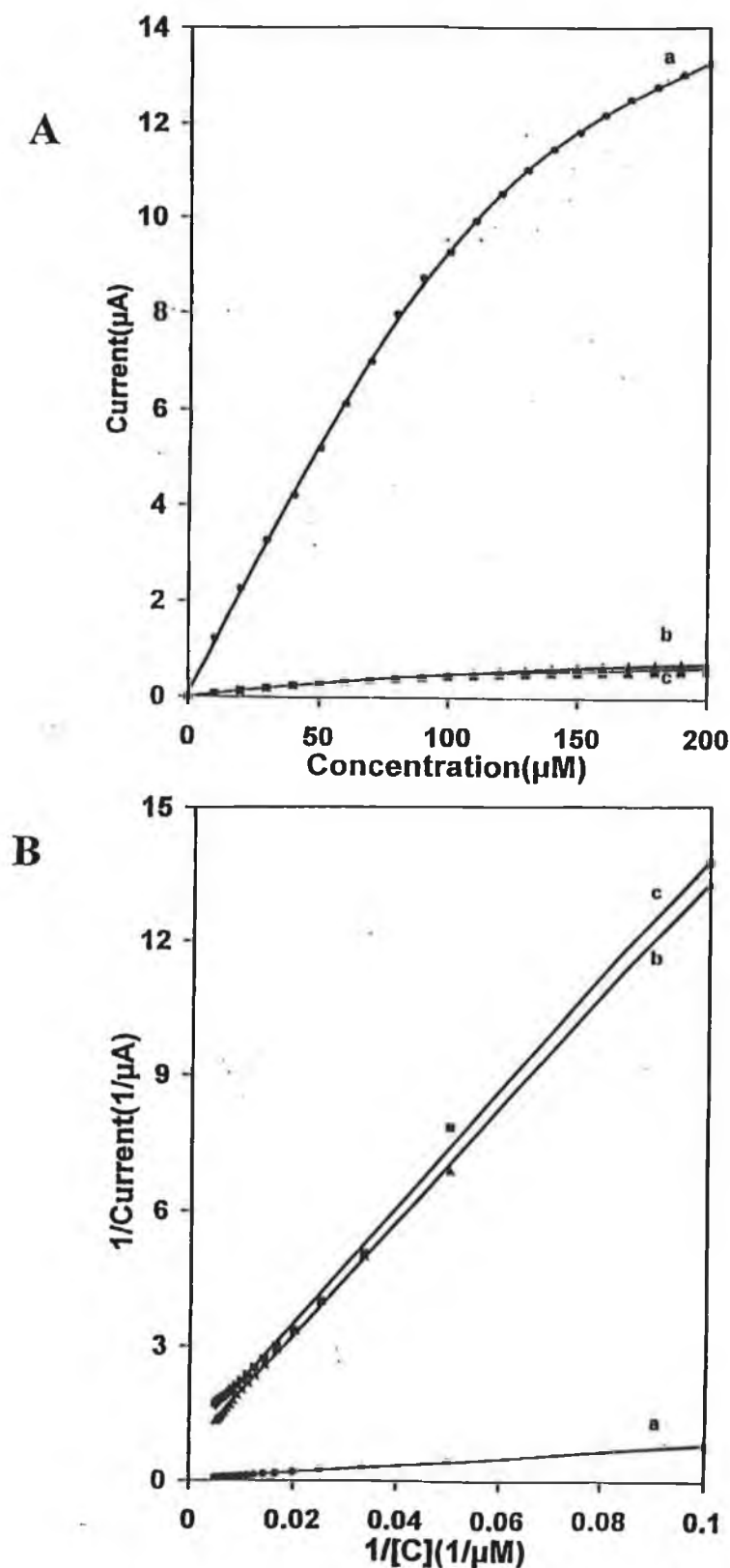
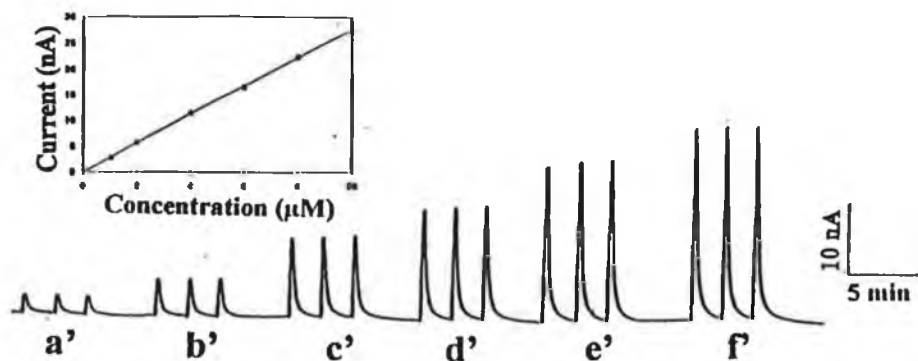


Figure 3.4. Calibration plots (A) and Lineweaver-Burk (B) plots for *p*-cresol at tyrosinase modified carbon paste electrodes with different binders: (a) dodecane, (b) hexadecane and mineral oil (c). Other conditions as in Figure 3.1.

A



B

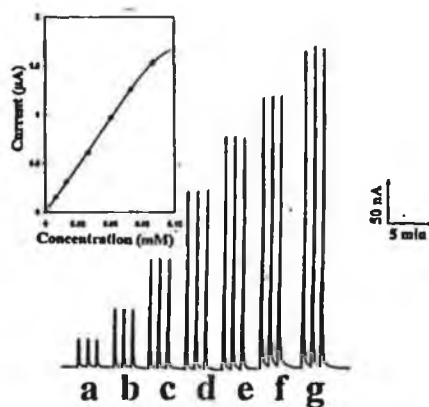


Figure 3.5. Flow-injection profiles at the dodecane-based carbon paste tyrosinase detector: (A) Response peaks for phenol solutions of increasing levels: 1 μM (a') to 10 μM (f') as shown in insert. (B) Response peaks for catechol solutions of increasing levels: 10 μM (a) to 100 μM (g) as shown in insert. Other conditions as in Figure 3.1.

The reproducibility of the dodecane modified biosensors was assessed by using 30 repetitive injections of 6 μM phenol and 60 μM catechol respectively. The results of the precision study are shown in Figure 3.6. The response remained highly stable throughout this study, yielding average currents of 17.7 nA for phenol and 214.3 nA for catechol with relative standard deviations of 3.0 % and 2.6 % respectively.

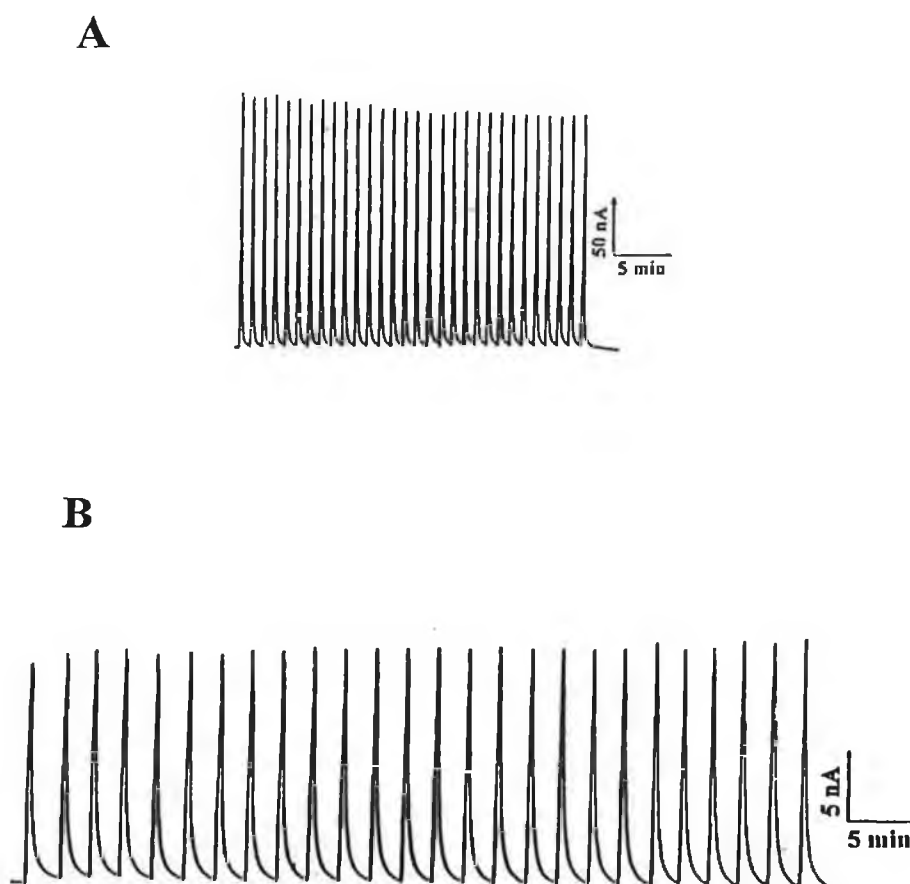


Figure 3.6. Precision studies at the dodecane modified tyrosinase biosensor for 6 μM phenol (A) and 60 μM catechol (B). Other conditions as given in Figure 3.1.

3.3.3. *Applicability to Chromatographic Analysis of Phenols*

Amperometric monitoring of phenols in chromatographic effluents is illustrated in Figure 3.7. A dual tyrosinase electrode detector based on hexadecane (bottom) and mineral oil (top) carbon pastes were used for standard (A) and river (B) water samples spiked with four phenolic compounds. Both carbon paste biosensors readily detected the respective phenols in the effluent stream. The hexadecane-based detector offered substantial enhancement of the peak current as shown by the different current-time recording scales. Attempts to use the more sensitive dodecane modified biosensor were hindered by stability problems after exposure to the acetonitrile mobile phase and could not be used in this detection mode respectively.

Although the sensitivity enhancement is important, the main advantage for such chromatographic detection is the new dimension of information provided by the dual electrode operation. Dual electrode parallel detectors commonly rely on poisoning two identical electrodes at different potentials, and monitoring the dual response ratio to evaluate the peak identity [17-20]. In the scheme used in Figure 3.7, the selectivity was improved by recording two equipotential chromatograms, and obtaining the dual response ratios based on the solvent extractability into the different pasting liquid binders. For example, while the p-methoxyphenol and phenol peaks appeared similar at the conventional mineral oil biosensor detector, differences in their extractability into the hydrocarbon paste liquid lead to a much greater phenol peak at the hexadecane based enzyme electrode. As a result distinct changes in the (hexadecane/ mineral oil) peak ratios were obtained: 1.5; 5.6; 5.1 and 6.1, for p-methoxyphenol, phenol, p-cresol and p-chlorophenol respectively.

Such trends in peak ratios reflect the relative extractability of the substrate into both pasting liquids. The peak ratios therefore offer useful information on the identification of individual analytes by virtue of the solvent extraction properties experienced at the electrode surfaces and the resultant biocatalysis under those conditions. For example the ratio of half-peak widths for p-methoxyphenol was 2.8 compared to values of only 1.5, 1.4 and 1.5 obtained for phenol, p-cresol and p-chlorophenol respectively.

The data of Figure 3.7. was used to estimate the percentage recovery for the spiked Rio Grande river water samples. Percent recoveries of 95-110 % and 89-101 % were calculated for the various phenols at the mineral oil and hexadecane-based enzyme electrodes respectively.

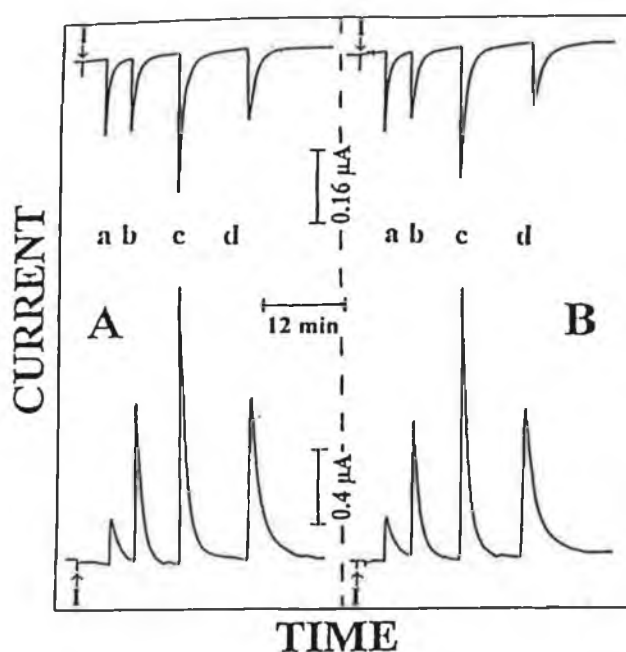


Figure 3.7. Chromatograms obtained with the hexadecane (bottom) and mineral oil (top) based modified carbon paste tyrosinase detectors for standard (A) and Rio Grande river water (B) samples spiked with 8 mM *p*-methoxyphenol, 1 mM phenol (b), 1 mM *p*-cresol (c) and 1 mM *p*-chlorophenol (d). Mobile phase: 0.05 M phosphate buffer (pH 6.5) acetonitrile (75:25); flow rate 1.0 ml/min, applied potential - 0.05 V. Electrodes were operated in parallel mode.

3.4. Conclusion

It has been demonstrated that short chain hydrocarbons offer an attractive alternative to mineral oil binders in the preparation of carbon paste tyrosinase electrodes. The new pasting liquids greatly enhance the sensitivity of the resulting phenol biosensors through the extractive accumulation of the substrates. The solvent extraction principles may also be used to influence and tune the selectivity of tyrosinase carbon paste electrodes. Similar responses could be expected for other phenolic pollutants. The hydrocarbon binders provide a favourable environment for tyrosinase and do not appear to strip the enzyme of its essential water of hydration which would have resulted in deterioration of the sensor response.

While this work sheds some insights into biocatalytic activity in the presence of different carbon paste binders, detailed studies are needed for elucidating the complex behaviour of the hydrocarbon/ graphite/ tyrosinase network. Additional improvements may be achieved by combining the new pasting liquids with various additives or enzyme stabilisers or in connection with a bioamplification technique. Also by investigating other enzyme systems, the capabilities of practical biosensors for other environmental pollutants is limitless.

3.5. References

- [1] Marko-Varga, G.; Emneus, J.; Gorton, L.; Ruzgas, T.: *Trends Anal. Chem.*, 14: (1995): 319.
- [2] Kotte, H.; Grundig, B.; Vorlop, K.; Strehlitz, B.; Stottmeister, U.: *Anal. Chem.*, 67: (1995): 65.
- [3] Wang, J.; Fang, L.; Lopez, D.: *Analyst*, 119: (1994): 455.
- [4] Pravda, M.; Petit, C.; Michotee, Y.; Kauffmann, J. M.; Vytras, K.: *J. Chromatogr.*, 47: (1996): 727.
- [5] Connor, M.; Wang, J.; Kubiak, W.; Smyth, M. R.: *Anal. Chim. Acta.*, 229: (1990): 139.
- [6] Rodriguez, M.; Flurkey, W.: *J. Chem. Educ.*, 69: (1992): 767.
- [7] Ortega, F.; Dominguez, E.; Buresdedt, E.; Emneus, J.; Gorton, L.; Marko-Varga, G.: *J. Chromatogr.*, 65: (1994): 675.
- [8] Ortega, F.; Cuevas, J.; Centenera, J.; Dominguez, E.: *J. Pharm. Biomed. Analysis* 10: (1992): 789.
- [9] Wang, J.; Lin, Y.; Chen, Q.: *Electroanalysis*, 5: (1993): 23.
- [10] Deng, Q.; Dong, S.: *Anal. Chem.*, 67: (1995): 1357.
- [11] Gorton, L.: *Electroanalysis*, 7: (1995): 23.
- [12] Lutz, M.; Burestedt, E.; Emneus, J.; Linden, H.; Gobhadi, S.; Gorton, L.; Marko-Varga, G.: *Anal. Chim. Acta.*, 8: (1995): 305.
- [13] Lindgren, A.; Ruzgas, T.; Emneus, J.; Csoregi, E.; Gorton, L.; Marko-Varga, G.: *Anal. Lett.*, 29: (1996): 1055.
- [14] Wang, J.; Deshmukh, B.; Bonakder, M.: *J. Electroanal. Chem.*, 194: (1985): 339.
- [15] Kuwana, T.; French, W.: *Anal. Chem.*, 36: (1961): 241.
- [16] Wang, J.; Freiha, B.: *Anal. Chem.*, 56: (1984): 849.
- [17] Roston, D.; Shoup, R.; Kissinger, P. T.: *Anal. Chem.*, 54: (1982): 1417A.
- [18] Zhong, M.; Zhou, J.; Lunte, S. M.; Zhao, B.; Gilando, D. M.; Kirchoff, J. R.: *Anal. Chem.*, 68: (1996): 203.
- [19] Cheng, F-C.; Lin, N-N.; Kuo, J-S.; Cheng, L-J.; Cheng, F-M.; Chia, L-F.: *Electroanalysis*, 6: (1994): 871.

- [20] Niwa, O.; Morita, M.; Solomon, B. P.; Kissinger, P.T.: *Electroanalysis*, 8: **(1996)**: 427.

Chapter 4

Sol-Gel based Sensor & Biosensor Applications

4.1. Sol-Gels

4.1.1. An Introduction to Sol-Gels

Many conventional methods of enzyme immobilisation include covalent bonding, physical adsorption or crosslinking to a suitable carrier matrix. Alternatively, enzymes can be physically entrapped and microencapsulated in polymeric matrices [1]. However, for optimum biostability and reaction efficiency, the preferred host matrix appears to be one that isolates the biomolecule, protecting it from self aggregation and microbial attack, while providing essentially the same local microenvironment as in a biological matrix.

Recent research has demonstrated that silicate glasses obtained by the sol-gel method can provide such a host matrix, and biomolecules immobilised by this method retain their functional characteristics to a large extent [2-4]. These functional glasses have been manipulated not only as host-bulk matrices, but also as membranes to maintain the host on the desired substrate transducer.

These biofunctional glasses make it possible to retain the specificity and reactivity of biological molecules in the solid state and provide morphological and structural control that is not available when the biological molecules are simply dissolved in aqueous media. Furthermore, the amorphous nature of the glassy material does not impart a geometric order to the entrapped molecules. Many of the characteristics of the liquid state are retained despite the fact that the molecule is trapped in a solid material. The process of biomolecular encapsulation is outlined in Figure 4.1.1.

The sol-gel method is a convenient way to synthesise a host matrix. The utility of sol-gel matrices as hosts for organic and organometallic dopants has been known for some time; however, it was not until 1990 that Braun et al. [2] reported the first attempts at protein encapsulation inside silica glasses. They described the preparation of biochemically active glasses with alkaline phosphatase trapped in the matrix. As one is aware, covalent attachment of proteins to a surface substrate requires that specific functionalities be

present in the biomolecule, whereas entrapment in sol-gel matrices is independent of the functionalities on the protein.

Another advantage of the sol-gel encapsulation method over covalent attachment is that physical entrapment is functionally non-invasive and preserves the integrity and directional homogeneity of the protein surface microstructure. By contrast, covalent attachment of proteins via surface modification fixes the orientation of the exposed protein and in certain cases may block substrate access to the protein active site. The success of sol-gel entrapment is largely independent of the size of the biomolecule because the matrix forms around it.

Silica biogels contain a sufficient amount of trapped interstitial water to provide an environment that is still essentially aqueous, thereby contributing to the retention of structure and reactivity of the encapsulated biomolecules. The absence of covalent interactions between the protein and the surrounding medium are of utmost importance for maintaining stability and reactivity [5].

The large sizes and high molecular weights of proteins prevent their leaching from the sol-gel matrix. Although the pore-size distribution in a monolithic glass varies, the average biomolecule is larger than any of the pores in the gel. However, many biological analytes i.e. enzyme substrates/ immunological antigens are small enough to diffuse into them. As a result, the biogel monolith provides an efficient biosensing design in which the movement of the recognition molecule is restricted, but the flow of smaller analytes through the pores of the gel is allowed.

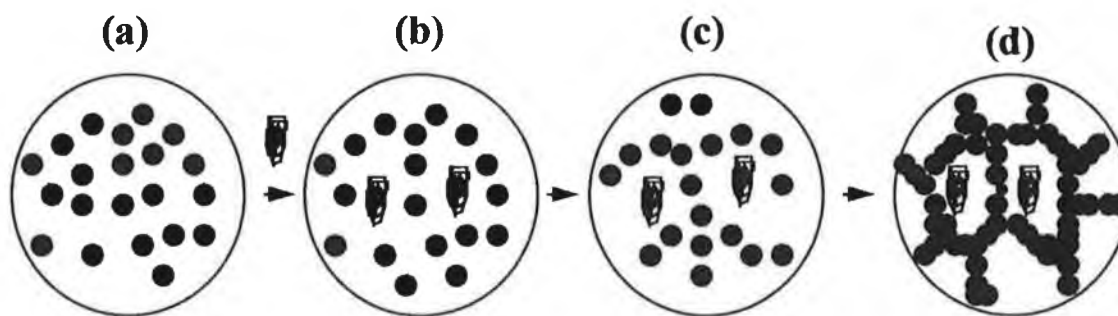


Figure 4.1.1. Protein entrapment in a silicate matrix during sol-gel polymerisation.

(a) Formation of sol particles during initial hydrolysis and polycondensation. (b) Addition of protein to the sol. (c) The growing silicate network begins to trap the dopant protein molecules. (d) The protein molecules are immobilised in the gel.

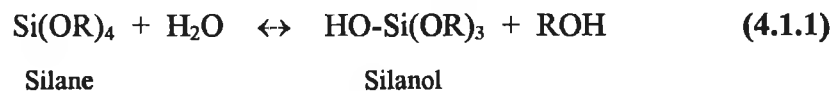
4.1.2. Sol-Gel Processing

Silicon is the most abundant element in the earth's crust [6]. Evidence of silicate hydrolysis and condensation to form polysilicate gels and particles is seen in many natural systems e.g. precious opal is composed of amorphous silica particles held together by a lower-density silica gel. The essential ingredients required to form opals are an abundant supply of readily soluble silica and a source of water flint. Our ancient ancestors recognised opal as the toughest stone available in those times, and was apparently formed from the siliceous skeletons of ancient sponges. Since the 1970s it has been recognised that soluble silica in trace amounts also plays a role in the development of mammals e.g. every 100th atom in the human body is silicon.

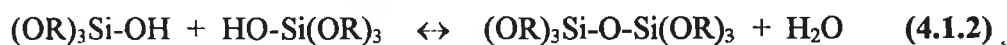
The +4 oxidation state is the only important one in the chemistry of silicon in naturally occurring systems [7], and the co-ordination number of silicon is most often four. Formation of the sol-gel network takes the following steps: (1) polymerisation of monomer to form particles; (2) growth of particles; (3) linking of particles into chains; then (4) the formation of networks that extend throughout the liquid medium, thickening it into a gel.

Silicate gels are most often synthesised by hydrolysing monomeric, tetrafunctional alkoxide precursors employing a mineral acid or base as the catalyst. At the functional group level, three reactions are generally used to describe the sol-gel process.

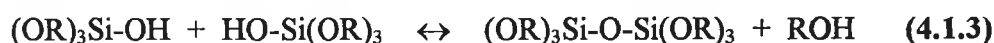
Hydrolysis



Water Condensation

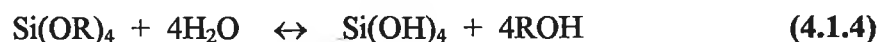


Alcohol Condensation



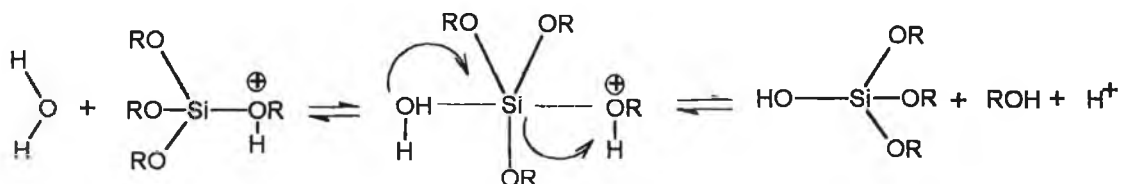
The hydrolysis reaction replaces alkoxide groups (OR) with hydroxyl groups (OH), converting the silane into silanol. Depending on the amount of water and catalyst present, hydrolysis may go to completion, or stop while the silicon is only partially hydrolysed $\text{Si(OR)}_{4-n}(\text{OH})_n$.

HCl



Subsequent condensation reactions involving silanol groups produce siloxane bonds (Si-O-Si) plus the by-product alcohol (ROH) or water. Under most conditions, condensation commences before hydrolysis is complete. Water condensation dominates the early stages of the sol-gel process, followed by a dominant alcohol condensation phase, solubilising the forming network.

In the hydrolysis reaction, the alkoxide group is protonated in a rapid first step. Electron density is withdrawn from silicon, making it more electrophilic and thus more susceptible to attack by water:



(4.1.5.)

The water molecule attacks from the rear and acquires a partial positive charge. The positive charge of the protonated alkoxide is correspondingly reduced, making alcohol a better leaving group. The transition state decays by displacement of alcohol accompanied by inversion of the silicon tetrahedron.

The condensation reactions continue on, resulting in larger silicon polymers. Formation of dimers, chains and rings are possible. Since a fully hydrolysed monomer $\text{Si}(\text{OH})_4$ is tetrafunctional ($f=4$), complex branching can occur. Hence polyfunctional units with $f > 2$ are capable of forming three dimensional structures by crosslinking linear chains or rings formed by functional units of $f = 2$.

The acid catalyst can influence both the hydrolysis or condensation rates and the structure of the condensed products. Acids serve to protonate negatively charged alkoxide groups, enhancing the reaction kinetics by producing good leaving groups.

The term 'ageing' is applied to the process of change in structure and properties after gelation. Some gels exhibit spontaneous shrinkage, called syneresis, as bond formation or attraction between particles induces contraction of the network and expulsion of liquid through the pores.

Although sol-gels form amorphous non-crystalline networks after drying, crystalline models may be formed upon heating the network. If the application requires the presence of absolutely no pores, a process called sintering will remove them, once a suitably high temperature is applied.

One can tailor-make a functional sol-gel network by use of certain precursor agents such as $R^1 Si (OR)_3$ or $R^1_2(OR)_2$; where R^1 represents the non-hydrolysable substituent. This substituent imparts specific properties to the resultant gel. For example, the silicone industry is based on poly-diorganosilanes, and many different products are possible using the various other organic substituents available [8].

4.1.2.1. Structural Evolution

The structural evolution of sol-gels, from the initial mixing of silanes and silanols in the hydrolysis stage, to complex condensation reactions, resulting in the growth of clusters that eventually collide and link together into a gel, and the period thereafter, drying and ageing, have been studied in detail using spectroscopy [9].

Nuclear magnetic resonance (NMR) spectroscopy, 1H & ^{29}Si , has been used extensively to evaluate the kinetics of the early stages of the gelation process. Infrared and Raman Spectroscopy have been used in combination with NMR to identify oligomeric species in solution and to follow the evolution of inorganic frameworks by comparisons with model compounds of known structures.

Small angle scattering investigations utilising neutrons, X-rays or visible light i.e., static light scattering or quasi-elastic light scattering have been employed to investigate the growth and topology of macromolecular networks that preceded gelation, the aggregation of colloids and the structure of porous gels.

4.1.3. Sol-Gel Film Formation - Spin Coating

The preceding section, 4.1.1., has focused on the encapsulation of enzymes in the bulk sol-gel network. However it is possible to entrap the biomolecule of interest on the transducer surface by means of a sol-gel coat. This is an attractive entrapment method, as the biomolecule is too large to leach from the sol-gel film composite, and the pores are small enough to ensure diffusion of the respective analyte through the sol-gel film and to the heart of the catalytic system, i.e. the enzyme.

Spin coating consists of four stages: deposition, spin-up, spin-off and evaporation. Firstly, an excess of liquid is dispersed on the surface during the deposition stage. The electrode is then spun at a certain rate, called the spin-up stage. In the spin-off stage, excess liquid flows to the perimeter and leaves as droplets, as shown in Figure 4.1.2. As the film thins, the rate of removal of excess liquid by spin-off slows down, because the thinner the film, the greater the resistance to flow. Also, since the concentration of non-volatile components increases, hence raising the viscosity, evaporation takes over as the primary mechanism of thinning during the fourth stage of spin coating.

An advantage of spin coating is that a film of liquid tends to become uniform in thickness during spin-off, and once uniform tends to remain so, provided that the viscosity is not shear dependent and does not vary over the surface. This tendency arises due to the balance between two main forces: a centrifugal force, which drives flow radially outward, and a viscous force (friction), which cuts radially inward. During spin-up, the centrifugal forces overwhelm the force of gravity, and the rapid thinning quickly squelches all inertial forces other than the centrifugal force.

Although the underlying physics and chemistry that govern polymer growth and gelation are essentially the same for films as bulk gels, several factors distinguish structural evolution in films. The overlap of the deposition and evaporation stages establishes a competition between evaporation, which compacts the structure, and continuing condensation reactions, which stiffen the structure thereby increasing the resistance to completion. However, in bulk systems the gelation and drying stages are normally separated.

Compared to the bulk system, aggregation, gelation and drying occur in seconds to minutes during spin coating rather than days or weeks as observed in bulk systems. The short duration of the deposition and drying stages causes films to experience less ageing, i.e. crosslinking, than bulk gels. This generally results in more compact dried structures. Fluid flow, due to draining, evaporation, or spin-off, combined with attachment of the precursor species to the surface substrate, impose a shear-stress within the film during deposition. After gelation, continued shrinkage due to drying and further condensation

reactions creates a tensile stress within the film. Bulk gels are not constrained in any dimension. However, it does suffice to note that films, for a particular sol-gel precursor, will usually crack on drying if they exceed a critical thickness.

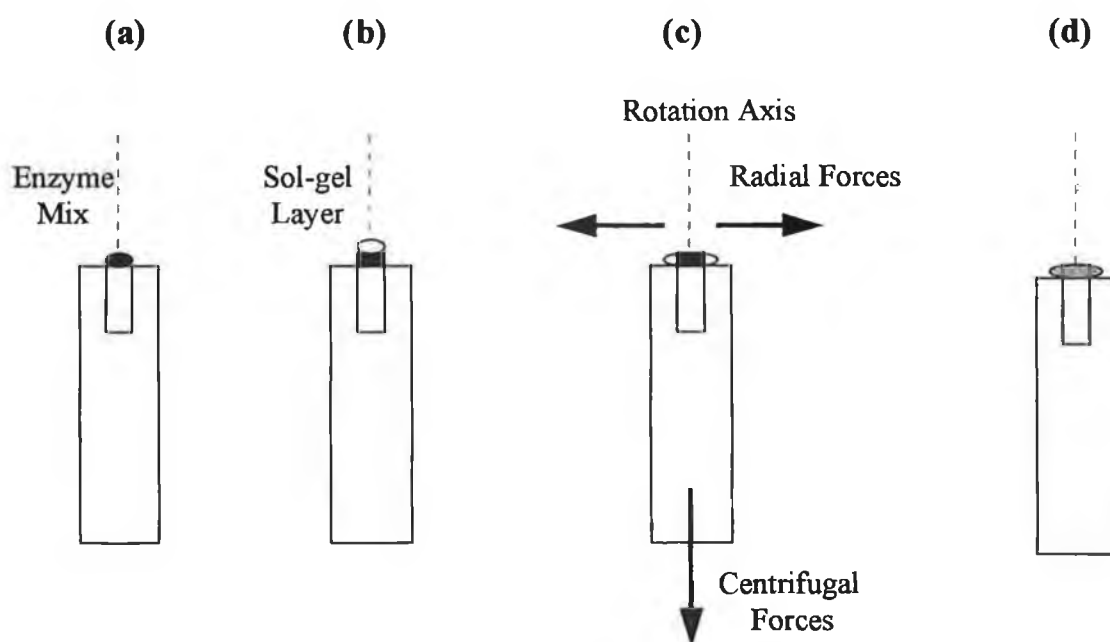


Figure 4.1.2. Spin coating process: (a) Enzyme mix on surface; (b) Deposition; (c) Spin-up and spin-off and (d) Evaporation and resultant film formation.

4.1.4. Universal Sol-Gel Applications

Applications for sol-gel processing derive from the various special shapes obtained directly from the gel state, e.g. monoliths, films, fibers and monosized powders, combined with compositional and microstructural control and low processing temperatures. The sol-gel method is exothermic and occurs readily at room temperature. As a result of the high surface areas and small pore sizes experienced in such gel systems,

the crystallisation and phase separation characteristic of glass manufacturing is avoided resulting in a plethora of new materials made available to the technologist.

4.1.4.1. Thin Films and Coatings

Films and coatings represent the earliest commercial application of sol-gel technology [10]. Thin films (normally $< 1 \mu\text{m}$ in thickness) formed by dipping or spinning use little in the way of raw materials and may be processed quickly without cracking, overcoming most of the disadvantages of bulk sol-gel processing. In addition, large substrates can be accommodated and it is possible to uniformly coat both sides of planar and axially symmetric substrates such as pipes, tubes, rods and fibers, not easily handled by more conventional coating processes. The earliest applications for sol-gel films were in optical coatings, as reviewed by Schroeder [10]. Since then many new uses for sol-gel films have appeared in electronic, protective, membrane and sensor applications.

4.1.4.1.1. Optical Coatings

Optical coatings alter the reflectance, transmission or adsorption of the substrate. IROX[®] coated architectural glass is the best example of the current state of the art which is commonly used in the glass of skyscrapers [11]. SiO_2 controls the reflectivity and the palladium content, due to its intrinsic properties, provides the desired absorption. In this manner buildings appear uniformly reflective, whilst light transmission is controlled in accordance with sun exposure to minimise cooling costs.

4.1.4.1.2. Protective Films

Protective films impart corrosion or abrasion resistance, promote adhesion, increase strength or provide passivation properties [12]. Such applications have included the use of a flexible metal-mirror developed for terrestrial and low earth orbit solar applications. In these applications sol-gel films perform several protective functions: (a) the planarisation layer prevents corrosion of the Fe-Ag galvanic couple; (b) planarizing the stainless steel substrate significantly improves the specularity of satellite mirrors and (c) the overlayer prevents corrosion and abrasion of the underlying silver reflective surface. Organically modified silicate films are being used as antiscratch coatings on acrylic and

polycarbonate windows and lenses, and as the protective coatings to protect medieval glass from corrosion.

4.1.4.2. Monoliths

Monoliths are defined as bulk gels (smallest dimension ≥ 1 mm) cast to shape and processed without cracking. Monolithic gels are of potential interest because complex shapes may be formed at room temperature and consolidated at rather high temperatures without melting. The principle applications for monolithic gels are optical ones: fiber optic preforms, lenses and other optical components, graded refractive index glasses and transparent foams used in superinsulation [13].

4.1.4.3. Powders, Grains, Spheres & Fibers

Powders are the starting point for most polycrystalline ceramic processing schemes. Ceramic powders and grains are also used as catalysts, pigments, abrasives and fillers, and they are employed in electro-optical and magnetic devices [14]. Potential advantages of sol-gel powders over conventional powders (often physical mixtures of minerals and chemicals), are controlled size and shape, molecular scale homogeneity and enhanced reactivity. Sol-gel methods have also been used to prepare continuous refractivity, polycrystalline fibers that exhibit high strength and stiffness in addition to chemical durability [15].

4.1.4.4. Composites

Composites combine different types of materials to obtain synergistic properties unattainable by one material alone. Mixed organic-inorganic and ceramic-metal composites are also possible. High performance ceramic-ceramic composites such as SiC-reinforced alumina are candidate materials for turbine blades as well as highly efficient ceramic diesel engines. Epoxysilanes have been exploited for scratch-resistant materials. Thermoplastic and photocurable ligands such as methacryl, vinyl, or alkyl groups combined with a variety of polymerizable monomers have been utilised for coatings, adhesive films and bulk materials respectively [16].

4.1.4.5. Porous Gels & Membranes

High surface areas and small pore sizes characteristic of sol-gels are properties unattainable by conventional ceramic processing methods. These unique properties may be exploited in applications such as filtration, separations, catalysis and chromatography. One such application involves the microfiltration of water, wine and beverages and also the ultrafiltration of milk [17].

4.1.5. Biosensor Applications of Sol-Gel Systems

4.1.5.1. Optical Methods

4.1.5.1.1. Dissolved Oxygen Biosensor

Biorecognition of dissolved oxygen is possible with haemoglobin and myoglobin, using optical based enzyme sol-gel systems [18]. Haemoglobin (Hb) and myoglobin (Mb) are two haem proteins that reversibly bind atmospheric oxygen. The high affinity of these proteins for oxygen, coupled with the changes in visible absorption spectra that occur when oxygen is bound, provides an opportunity to develop an oxygen sensor based on these proteins.

Measuring the prominent differences in absorption maxima of the deoxy and oxy forms of the proteins in the 430 nm region is a convenient way to quantify oxygen interactions. By monitoring the rate of absorbance changes of the 436 nm transition for the deoxy form, a linear relationship can be established between the optical response of the enzyme and the concentration of dissolved oxygen. Since myoglobin also binds carbon monoxide, the myoglobin biogel can also be used as a sensor for carbon monoxide, by taking advantage of the distinct changes in the absorption spectrum for that interaction at another particular wavelength.

4.1.5.1.2. Nitric Oxide Biosensor

This is based on the enzyme manganese myoglobin (MnMb). At trace levels, nitric oxide is involved in a variety of biological functions including muscle relaxation, platelet inhibition, neurotransmission and immune regulation. Although the Fe-containing types of haemoglobin and myoglobin can bind nitric oxide, under aerobic conditions the reaction is non-specific, and competitive oxygen adduct formation also takes place. To avoid interference from atmospheric oxygen, manganese-containing myoglobin is chosen because of its proven specificity for nitric oxide [19]. The important diagnostic feature of this novel optical sensor is its ability to bind specifically to nitric oxide in an aerobic environment and to detect it at levels similar to those found under physiological conditions [20].

4.1.5.1.3. Glucose Biosensor

Monitoring blood glucose levels is important in many clinical applications. Biosensors for glucose use the enzyme glucose oxidase (GO_x), which catalyses the oxidation of β -D-glucose to yield gluconic acid and hydrogen peroxide. Yamanaka et al [21], developed a glucose sensor based on biogel methodology, which contained glucose oxidase immobilised in combination with horseradish peroxidase (HRP), and suitable quinoneimine dye precursors in a sol-gel system. The dye precursors 4-aminoantipyrene and p-hydroxybenzene sulfonate formed a quinoneimine dye with an absorption maxima at 510 nm. When the sensor was exposed to glucose, the glucose oxidase component catalysed the generation of hydrogen peroxide that in turn triggered the HRP-catalysed formation of dye from its precursors. The rate of formation of coloured dye was directly proportional to glucose oxidase reactivity and to the concentration of glucose in the sample.

4.1.5.2. *Electrochemical Methods*

The dielectric nature of silicate glasses allows the flow of charge only to the ionic impurity carriers, and the conductivities are thus very low. The lack of electronic conduction in silica glass means that electrochemical methods must rely on electron transport mediators for signal transduction.

Sanchez et al. [22] have demonstrated the generation of catalytic currents in the presence of glucose by using immobilised GO_x with hydroxymethylferrocene as the mediator. Pankratov et al. [23] presented an excellent report on sol-gel derived renewable surface biosensors, incorporating an organically modified silica backbone with percolating carbon powder to provide electrical conductivity. The silica backbone provides rigidity, and the organically modified surface ensures minimal surface contamination. Similar work was performed earlier by Narang et al. [24].

Park et al. [25-27] presented a selection of enzyme modified glassy carbon surfaces. One consisted of a glucose biosensor similar to the bulk sol-gel sensors of Pankratov et al. [23] and Narang et al. [24] except in this case a multilayered glucose osmium redox polymer with sol-gel film coat was applied [25]. This work also included an inhibition based amperometric biosensor for the detection of low levels of cyanide [26], where potential interferents sodium azide, potassium thiocyanide and thiourea gave no response.

4.1.6. Experimental Overview

As one has seen, sol-gels have been used extensively in a wide spectrum of applications. They are easy to prepare, the reactions are exothermic and occur at room temperature. They can be shaped into any size or form, and can be tailor-made for specific applications.

In the following sections, two examples of sol-gel methodology for use in electrochemical sensor applications are demonstrated. The first section represents the exploitation of bulk sol-gel in a carbon composite electrode as an electrochemical detector for the chromatographic analysis of catecholamines, whereas the next section represents an example of a horseradish peroxidase based biosensor for the analysis of phenols.

4.2. Sol-Gel Carbon Composite Electrode as an Amperometric Detector for Liquid Chromatography of Catecholamines

4.2.1. Introduction

In this particular application the use of bulk sol-gel for constructing a sol-gel modified carbon paste composite electrode for use as a liquid chromatography electrochemical detector (LCEC) for various catecholamines is described. Although the work demonstrated within is purely a pharmaceutical application, the sensors can be easily utilised in any environmental monitoring mode.

Catecholamines (CA) play an important role in higher animals as neurotransmitters between nerve cells. Their over and under production in disease states result in the breakdown of the homeostasis of the body e.g. epinephrine is used to treat shock and cardiac arrest, to control and prevent local haemorrhages, to explore the retina, to treat some glaucomas and bronchial asthma and to inhibit womb contractions. Thus, the determination of catecholamines in various samples is required for the diagnosis of their related diseases such as pheochromocytoma, neuroblastoma, idiopathic oedema and hypertension.

One of the major breakthroughs in probing the brain chemistry of catecholamines was achieved by Adams in 1976 [28]. Adams introduced *in vivo* voltammetry whereby a miniaturised carbon paste voltammetric electrode could be implanted in the brain and oxidation currents from catecholamines could be observed. Following this work, Ponchon et al [29] investigated the use of electrodes made of other carbon based materials for detecting catecholamines. They encased a carbon fiber in a glass micropipette and created an electrode that was small enough to be implanted into brain tissue, and in combination with differential pulse voltammetry, could detect catechol and indole-based catecholamines.

Although the work of Adams and others showed that voltammetric measurements *in vivo* were possible, selectivity and sensitivity needed to be improved because other oxidisable molecules, notably ascorbic acid, obscured the current response. Two breakthroughs in

selectivity were achieved with the use of Nafion coating [30], an anionic polymer that reduced interference from ascorbic acid and acid metabolites, and with electrochemical pre-treatment [31] which shifted the oxidation potentials of interferences.

Since then a whole plethora of electrochemical and analytical techniques for the monitoring of catecholamines evolved. Some have included the application of various immobilised crown ether platinum modified electrodes as potentiometric and amperometric detectors for flow injection analysis of catecholamines [32]. The diffusion and reaction characteristics of catecholamines using electroactive polymer films has also been documented [33].

The recycling and amplification characteristics of a biosensor reactor based on tyrosinase and L-ascorbic acid has also been exploited [34, 35]. The production of o-quinone compounds from the oxidation of catecholamines by tyrosinase are chemically reconverted to the original substrate compound by L-ascorbic acid resulting in an enhanced current output. The use of microelectrodes has also proved quite popular where detection limits in the femtomole and subfemtomole region have been realised [36-43]. Techniques involving capillary electrophoresis with electrochemical detection [44-46], capillary electrophoresis with luminescence detection [47], capillary electrophoresis with mass spectroscopy [48], reverse phase high performance liquid chromatography with spectroscopic detection [49-52], titrimetry [53], fluorimetry [54, 55] and spectroscopy [56-58] are widely used for the analysis and characterisation of these compounds.

Much interest has evolved throughout the years in the use of electrochemical detection in liquid chromatography as a sensitive and selective tool for the determination of a wide variety of electroactive compounds [59, 60]. The large selection of working electrode materials has been responsible for the success of LCEC. Such materials include glassy carbon, gold, platinum, carbon paste and modified electrodes of the latter origin to mention but a few. Choice of electrode depends mainly on the redox behaviour of the target analytes and the background current, and associated noise characteristics, at the

operating potential of interest. Other considerations include the potential window, mechanical properties, electrical conductivity and cost.

Carbon-based electrodes have typically served as working electrodes for the detection of oxidisable species in the anodic region. A variety of carbon electrode materials have been developed for LCEC, with glassy carbon and carbon paste being most popular. Yet, the development of new and improved electrode materials remains a very important need in LCEC [60].

In the work presented here, the performance characteristics of a wall-jet amperometric detector was evaluated using a sol-gel carbon composite. The use of LCEC for the monitoring of catecholamines has been well documented [61-73]. However, sol-gel carbon composites represent a new class of carbon-based electrodes, that are composed of graphite powder homogeneously dispersed in modified silica ceramics [74]. Recent electroanalytical applications of these carbon ceramic electrodes include amperometric biosensing [23, 75] and gas phase monitoring [76]. As desired for LCEC, such sol-gel derived carbon electrodes display favourable electron-transfer kinetics and a wide potential window, are physically rigid, have a renewable surface, and are amenable to chemical or biological modification. Such attractive features are combined with the versatility of sol-gel processes [77].

Sol-gel carbon materials thus appear to be a viable alternative to other carbon based working electrodes used in LCEC. The opportunities accrued from the development of LCEC detectors based on sol-gel carbon composite electrodes are explored in the following sections.

4.2.2. Experimental

4.2.2.1. Reagents

All solutions were prepared unless otherwise stated in deionised water prepared by passing distilled water through a Milli-Q-water purification system. Catechol, epinephrine, norepinephrine and dopamine, were purchased from Sigma (MO, USA). Methyltrimethoxysilane was purchased from Fluka (Germany), absolute alcohol analytical grade 200 proof, Quantum Chemistry Company, (TX, USA) and graphite powder, grade # 38, Fisher Scientific were used for the preparation of the sol-gel carbon composite electrodes. Chloroacetic acid from Aldrich (Milwaukee, USA) and ethylenediaminetetraacetic acid (EDTA) disodium salt from Fisher Scientific (USA), were used for the preparation of the mobile phase. Nylon membranes (0.2 μm pore size, 47 mm diameter, MF 5621) were used for filtering the mobile phase. Micro filters (MF 5500) and microfilter membranes (MF 5658) were used for filtering the samples. All were obtained from Bioanalytical Systems (BAS) Inc., (W. Lafayette, USA). Ultrahigh purity helium gas (Agile Welding Supply, Albuquerque, USA), was used as received for degassing the mobile phase and solutions.

4.2.2.2. High Performance Liquid Chromatography

All experiments were performed on a reverse phase high performance liquid chromatography system (BAS Model 480) in connection with a dual reciprocating pump (BAS, PM-80) and an amperometric detector (BAS Model LC-4C) along with a homemade wall-jet electrode configuration, as shown in Figure 4.2.1. Injections were made through a Rheodyne valve with 20 μl loop onto a C₁₈ column (ODS-3, BAS, Model MF 6213, 3 μm , 3.2 x 100 mm). Chromatograms were recorded on an Omniscrite strip-chart dual pen recorder (Houston Instruments). The sol-gel carbon working electrode, the Ag/AgCl (Re-1, BAS), reference electrode and the platinum wire counter electrode were joined through the holes in the Teflon cover of the wall-jet cell.

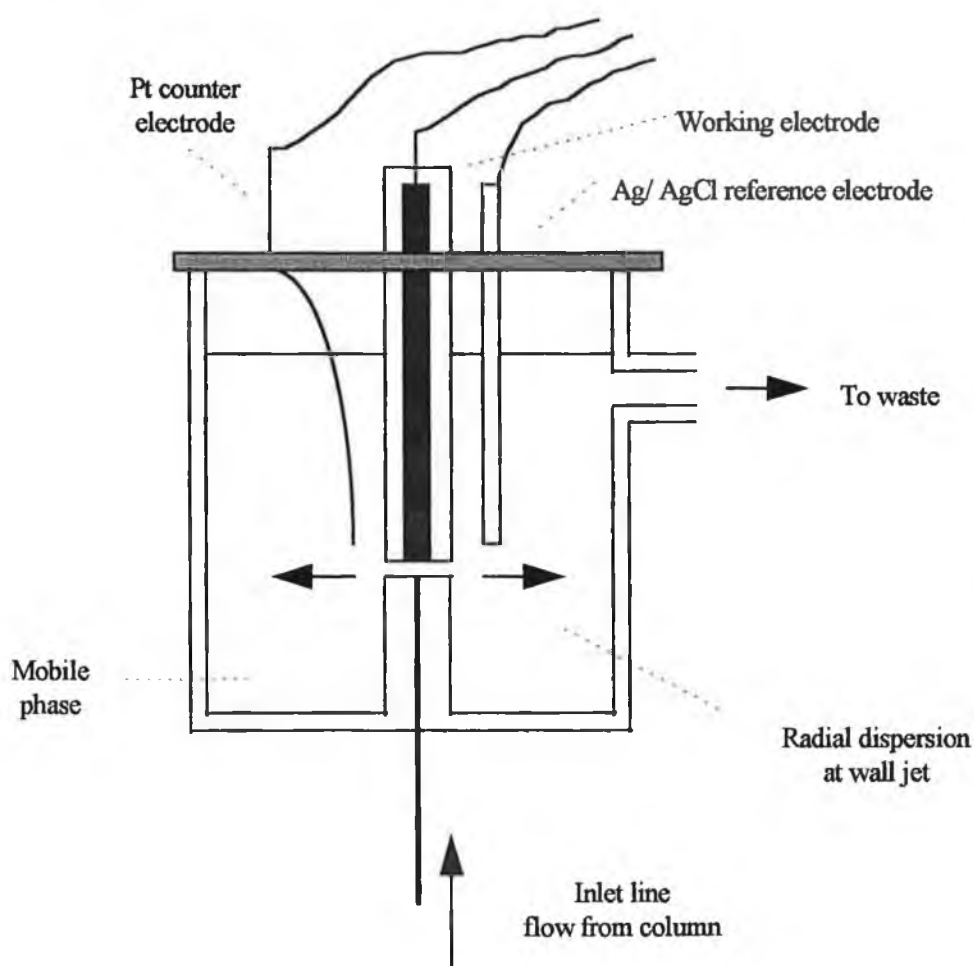


Figure 4.2.1. Schematic of Wall-Jet Detector

4.2.2.3. Electrode Preparation

Sol-gel derived carbon electrodes were prepared by mixing 500 μl methyltrimethoxysilane, 750 μl ethanol and 50 μl 11 M hydrochloric acid, sonicating the mixture for 1 min and adding 2.0 g of graphite powder. This mixture was then further sonicated, mixed thoroughly and filled into the cavities of 3 mm (i.d.) glass tubes. These composites were dried under ambient conditions for 24 h. Similar procedures were used for making more porous sol-gel electrodes, except for the fact that the initial mixture (before addition of graphite) was sonicated for the longer times of 15 and 30 min. The sol-gel carbon electrodes were polished after drying on a 400 grade emery paper and polished again on weighing paper. The resultant electrode surfaces were shiny and

smooth. Carbon-paste electrodes were prepared by thoroughly mixing graphite powder and mineral oil in the ratio of 70:30. This mixture was filled into the cavities of 3 mm i.d. glass tubes. The connections were made by inserting a copper wire through the other end of the capillary in both sol-gel and carbon paste electrodes.

4.2.2.4. Procedures

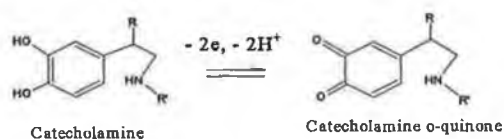
All the measurements were carried out under ambient conditions. Amperometric measurements were carried out after applying the appropriate potential to the electrode and allowing the transient signal to reach steady-state value. The mobile phase used was 0.1 M chloroacetic acid solution containing 0.2 g of disodium ethylenediaminetetraacetic acid (EDTA) adjusted to pH 3.5 with phosphoric acid. All mobile phase and standard solution samples were filtered and degassed prior to use.

4.2.3. Results and Discussion

4.2.3.1. Mechanism of Catecholamine Oxidation

Catecholamines have shown to be unstable in alkaline solutions [40, 43, 78], where they tend to decompose quite rapidly. Irreversible electrochemistry is also observed in solutions of high pH as shown in Figure 4.2.2. In acidic solutions this cyclisation 1,4-Michael addition reaction is prohibited resulting in reversible electrochemistry [40, 43]. The mechanism involves a 2 electron oxidation resulting in the formation of catecholamine o-quinones. For this reason a mobile phase of pH 3.5 0.1 M chloroacetic acid containing ethylenediaminetetraacetic acid was used as reported similarly elsewhere [38, 65, 69, 72].

(a). Reversible Electrochemistry - Acidic pHs



(b). Irreversible Electrochemistry - Alkaline pHs.

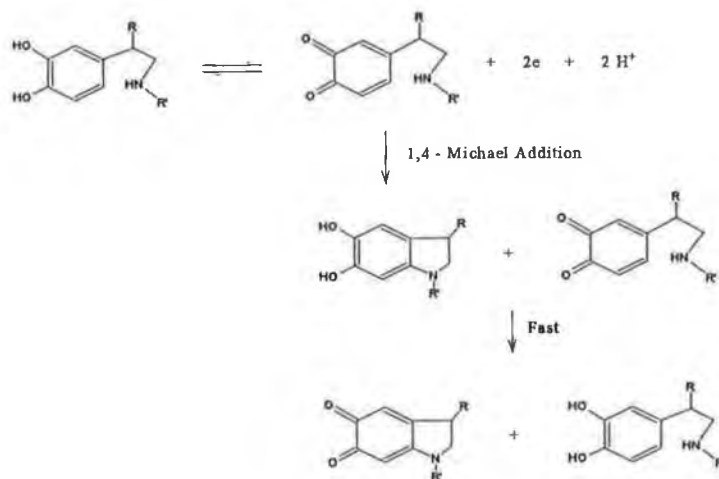


Figure 4.2.2. Reaction scheme for the electrochemical oxidation of catecholamines. (a) Represents reversible electrochemistry in acidic solutions and (b) represents irreversible electrochemistry in alkaline solutions. For each of the catecholamines, R and R' are respectively as follows: dopamine H, H; norepinephrine, OH, H and epinephrine OH, CH₃.

4.2.3.2. Choice of Sol-Gel Porositie 's

The sol-gel process involves a low-temperature production of ceramic materials through the hydrolysis and polycondensation of alkoxides [77]. By incorporating graphite powder in the initial sol-gel mixture, it is possible to obtain black rigid xerogels with percolating graphite powder in the silica backbone [74]. The preparation conditions can be controlled to manipulate the physical characteristics, particularly the microporosity of the resultant electrodes [79]. Due to the carbon character of these sol-gel derived electrodes their performance is compared with that of common carbon-paste based detectors.

For example, Figure 4.2.3. compares chromatograms for a mixture of 0.1 mM norepinephrine, epinephrine, dopamine and catechol, obtained with a conventional carbon-paste electrode and using sol-gel carbon composite surfaces of different porosities. The well defined peaks and low noise level of the non porous sol-gel composite compare favourably with those of the carbon-paste detector, (compare B and A). In contrast, the porous composite electrodes display a large noise level and drifting baseline, and overall an inferior performance, associated with the penetration of mobile phase into the electrode interior. All subsequent work was thus carried out using the non porous sol-gel carbon composite detector.

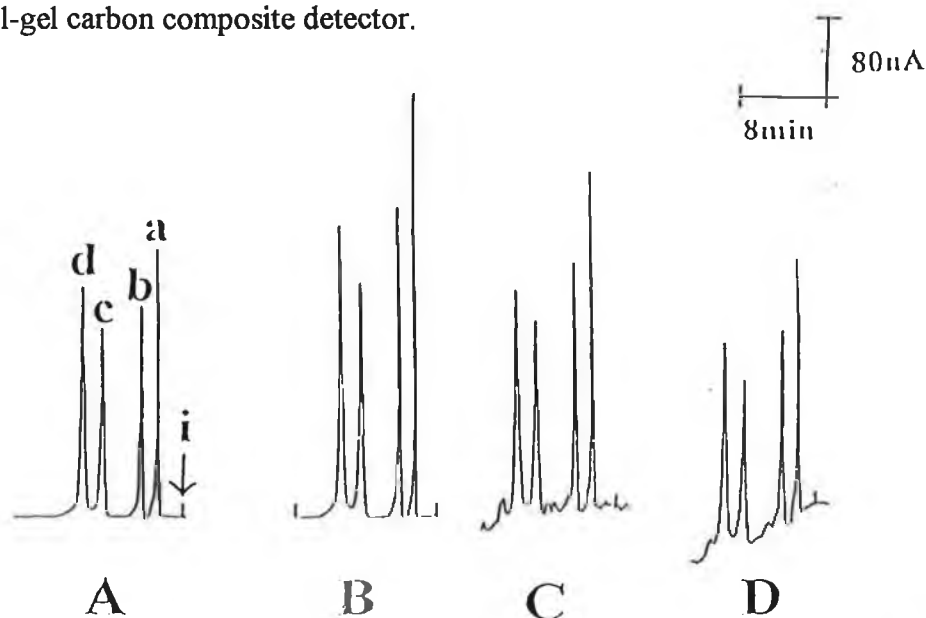


Figure 4.2.3. Chromatograms of 100 μM norepinephrine, (a), 100 μM epinephrine (b), 100 μM dopamine (c), and 100 μM catechol (d), at a carbon-paste electrode (A) or sol-gel carbon composite electrodes with 1 min (B), 15 min (C), or 30 min (D), sonication times. Applied potential: 0.75 V; flow rate: 0.5 ml min⁻¹; mobile phase: 0.15 M chloroacetic acid with 0.2g disodium EDTA.

4.2.3.3. Hydrodynamic Voltammetry

Hydrodynamic voltammograms (HV) provide useful electrochemical information concerning half-wave potentials and reversibility [80]. The shape of the HV has an influence on selectivity, the steeper the hydrodynamic wave, the better the selectivity. For a reversible oxidation [81] the equation for the HV is:

$$E = E_{1/2} + (RT/nF)[\ln (i/(i_{\max} - i))] \quad (4.2.1)$$

where E is the potential in V; $E_{1/2}$ is the half wave potential in V; R is the Universal gas constant, $8.314 \text{ J mol}^{-1} \text{ K}^{-1}$; T is the temperature in K; n is the number of electrons; F is Faradays constant, $96\,480 \text{ C mol}^{-1}$; i is the current in A and i_{lim} is the anodic limiting current.

However, $\ln (i/(i_{\max} - i))$ versus E plots for catecholamines deviate substantially from linearity, and hence do not yield pertinent information concerning the reversibility of the system [82, 83]. This is attributed to the presence of quasi-reversible reactions and possible overlapping of electron waves. Another way to interpret the data is to quote the difference in potential (ΔE) between $i = 0.05i_{\text{lim}}$ and $i = 0.95i_{\text{lim}}$, and for a two electron reaction, equation 4.2.1. predicts a ΔE of 75.6 mV.

The hydrodynamic voltammograms for norepinephrine, epinephrine, dopamine and catechol are shown in Figure 4.2.4. The ΔE values obtained for the sol-gel composite systems range from $62.5 \pm 2.8 \text{ mV}$ to $79.6 \pm 3.8 \text{ mV}$ as shown in Table 4.2.1., and from 54.0 ± 1.5 to 70.3 ± 3.1 for the carbon paste composites.

Table 4.2.2. shows the corresponding half-wave potentials, $E_{1/2}$, for the various neurotransmitters at the working electrode surfaces. The $E_{1/2}$ values for epinephrine, $534.9 \pm 4.2 \text{ mV}$ and dopamine $444.1 \pm 3.2 \text{ mV}$ at the sol-gel composite electrode are in well agreement with values of 510 mV and 470 mV obtained by Aoki et al using microelectrode arrays [80].

Table 4.2.1. ΔE values from hydrodynamic voltammograms

Compound	$\Delta E/$ mV Sol-gel Composite	$\Delta E/$ mV Carbon Paste Composite
Norepinephrine	73.7 ± 3.8	70.3 ± 3.1
Epinephrine	79.6 ± 3.8	64.3 ± 1.6
Dopamine	62.5 ± 2.8	70.2 ± 2.7
Catechol	75.3 ± 2.9	54.0 ± 1.5

Table 4.2.2. $E_{1/2}$ values from hydrodynamic voltammograms

Compound	$E_{1/2}/$ mV Sol-gel Composite	$E_{1/2}/$ mV Carbon Paste Composite
Norepinephrine	533.8 ± 4.2	636.7 ± 3.9
Epinephrine	534.9 ± 4.2	580.8 ± 1.8
Dopamine	444.1 ± 3.2	569.4 ± 3.1
Catechol	496.5 ± 3.1	543.4 ± 1.7

As can be seen from Figure 4.2.4., the sol-gel composite electrodes display well-defined hydrodynamic waves for all four compounds. The anodic wave starts at + 0.25 V and rises rapidly. A limiting current plateau is reached at potentials greater than + 0.65 V for dopamine and + 0.70 V for epinephrine, norepinephrine and catechol.

The sol-gel composite detector offers a substantial decrease in the potential of the voltammetric wave for all four compounds when compared with the carbon paste surface as shown by the data in Table 4.2.2. Also there is a considerable increase in the current response observed at the sol-gel composite. In view of the use of the same graphite powder as the carbon paste composite, the more favourable redox behaviour observed at

the sol-gel detector may be attributed to a catalytic action by the silicon oxide component. Enhanced electron-transfer kinetics by metal-oxide surface catalysts has been used previously to lower the operating potential of LCEC detectors [84]. Based on the data obtained in Figure 4.2.4, an applied potential of + 0.75 V was used throughout this study.

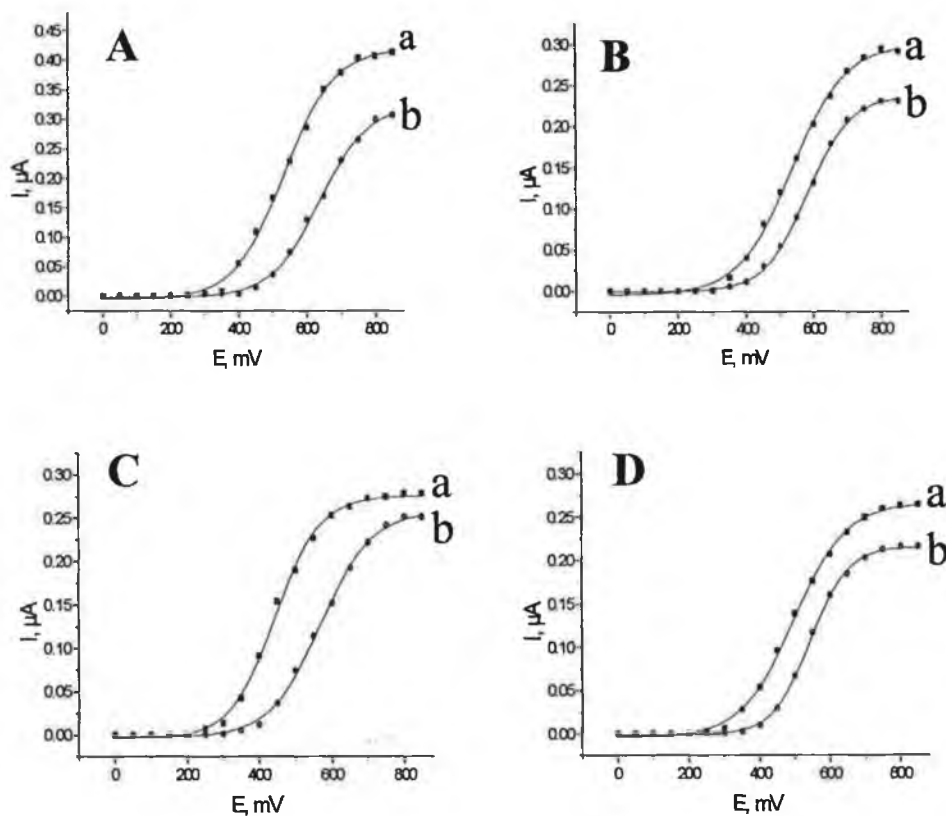


Figure 4.2.4. Hydrodynamic voltammograms of 100 μM norepinehrine (A), 100 μM epinephrine (B), 100 μM dopamine (C) and 100 μM catechol (D), at sol-gel carbon composite electrodes with 1 min hydrolysis (a) and a carbon-paste electrode composite (b) in HPLC detection. Other conditions as in Figure 4.2.3. Boltzman sigmoidal plots were fitted to the experimental data.

4.2.3.4. Operational Characteristics and Performance of the LCEC

The dependence of the chromatographic peak currents upon the flow rate is shown in Figure 4.2.5. The peak heights increase linearly with the flow rate at first, between 0.1 and 0.3 ml min⁻¹, and then more slowly up to 0.5 ml min⁻¹. The sensor response then decreases after 0.5 ml min⁻¹ up to 0.8 ml min⁻¹.

The amperometric signal is therefore related to the instantaneous flow rate and the concentration of electroactive species at the detector. In the case of a wall-jet cell [85], the peak current is given by:

$$I_p = 1.38 nFC_{\max}D^{2/3}\nu^{-5/2}a^{1/2}V^{3/4}r^{3/4} \quad (4.2.2)$$

where I_p is the peak current; n is the number of electrons; F is Faraday's constant; C_{\max} is the concentration at the peak of the solute profile in the cell; D is the diffusion constant; ν is the kinematic viscosity; a is the diameter of the inlet flow line, see Figure 4.2.1.; V is the volume flow rate, and r is the radius of the working electrode.

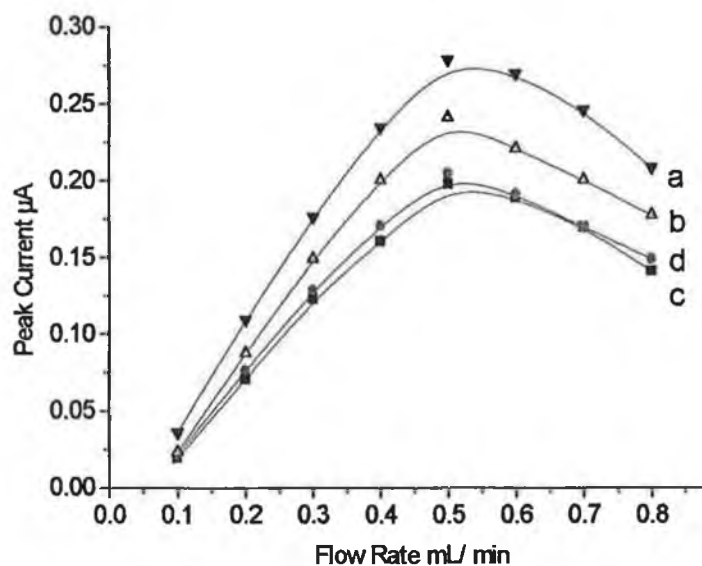


Figure 4.2.5. Effect of flow rate on the amperometric peak current in the HPLC detection of 100 μ M norepinephrine (a), 100 μ M epinephrine (b), 100 μ M dopamine (c) and 100 μ M catechol (d) at a sol-gel carbon composite electrode. Other conditions as in Figure 4.2.3.

Equation 4.2.2. predicts that the peak current is related to the volume flow rate to the power of $3/4$. A plot of the log of peak current versus the log of flow rate for catechol from 0.5 ml min^{-1} to 0.8 ml min^{-1} , yielded a gradient of 0.70 which is in close agreement with the theoretical value of 0.75 [85].

The oxidation efficiency of the catecholamines decreased as the flow rate increase beyond 0.5 ml min^{-1} because of the decrease in residence time of the electroactive species at the working electrode surface [86]. A flow rate of 0.5 ml min^{-1} was chosen as optimum for all further studies.

The sensitivity and linearity of the response were evaluated using the average of 11 successive injections of mixtures containing increasing concentrations of various catecholamines (from 5 to $100 \mu\text{M}$) as shown in Figure 4.2.6. The current response increased linearly upon increasing the concentration of these compounds. The slopes of these calibration plots correspond to sensitivities of 3.84 ± 0.05 (norepinephrine), 2.95 ± 0.04 (epinephrine), 2.43 ± 0.04 (dopamine) and 2.62 ± 0.03 (catechol) $\text{nA } \mu\text{M}^{-1}$, with correlation coefficients of 0.999 for all four plots.

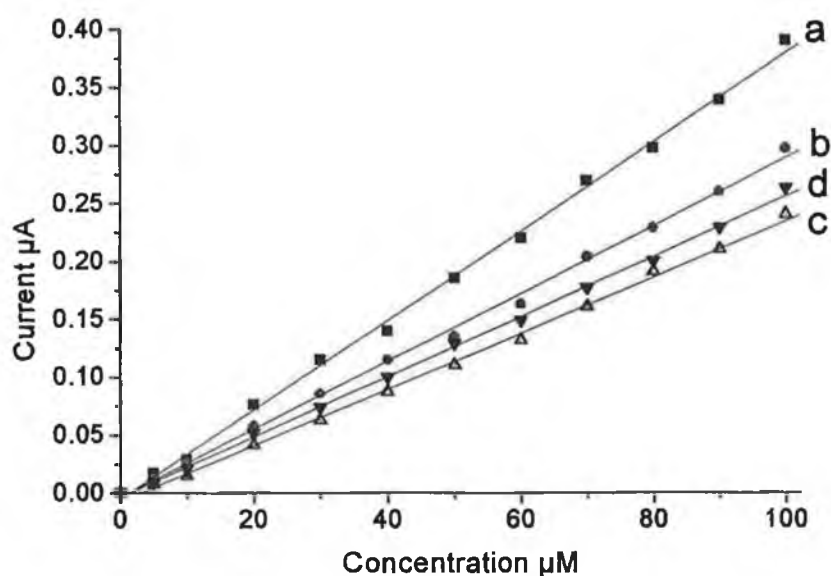


Figure 4.2.6. Calibration plots of norepinephrine (a), epinephrine (b), dopamine (c) and catechol (d), at a sol-gel carbon composite electrode for the successive additions of the analytes in HPLC detection. Other conditions as given in Figure 4.2.3.

An example of chromatograms obtained for 20 μM to 100 μM catecholamine mixtures is shown in Figure 4.2.7. Excellent efficiency factors of ~ 1.0 were obtained for all four compounds and selectivity, i.e. peak separation, was achievable to almost baseline resolution. Retention times of 2.0 min, 3.4 min, 7.0 min and 8.7 min were obtained for norepinephrine, epinephrine, dopamine and catechol respectively, allowing repetitive samples to be run every 10 minutes, with a sampling capacity of 6 mixtures per hour.

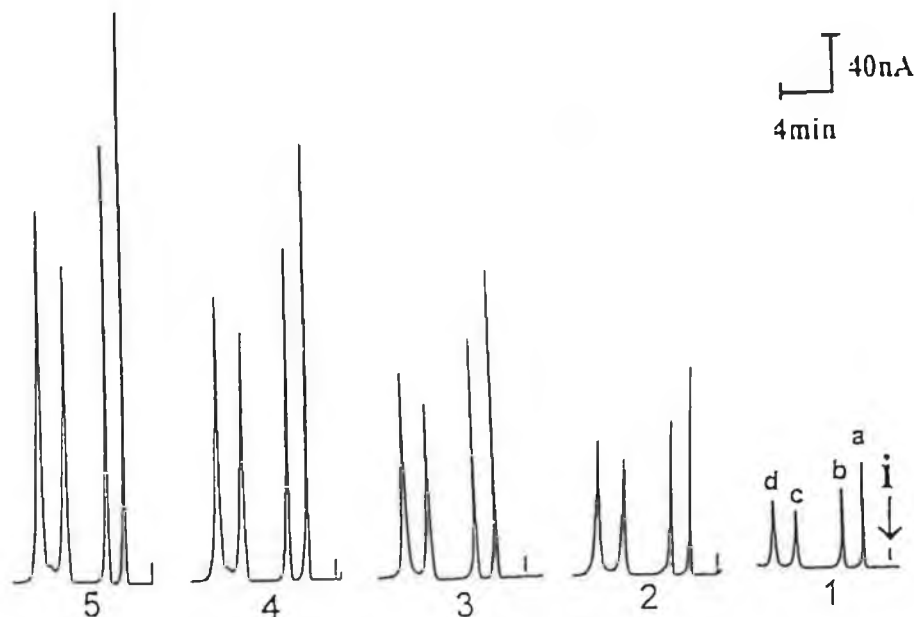


Figure 4.2.7. Chromatograms for norepinephrine (a), epinephrine (b), dopamine (c) and catechol (d), at a sol-gel carbon composite electrode for the successive additions of the analytes in HPLC detection. 1-5 represents the concentrations of 20 - 100 μM , respectively. Other conditions as given in Figure 4.2.3.

4.2.3.5. Detection Limits and Reproducibility

An injection of a 0.5 μM mixture of the catecholamines was used to estimate the minimum detectable quantities at a signal to noise ratio of three. From the data obtained in Figure 4.2.8.(a), the detection limits were extrapolated based on a signal-to-noise ratio of three. They were found to be 25 nM (norepinephrine), 32 nM (epinephrine), 50 nM (dopamine) and 25 nM (catechol). Such levels correspond to 85, 110, 170 and 55 pg, respectively, based on an injection volume of 20 μl .

Such extremely low detection limits are attributed to the composite character of the sol-gel derived carbon surface. These detection limits are quite impressive compared to detection limits at the 10^{-7} M level obtained through

capillary electrophoresis with mass spectroscopy and luminescence detection [47, 48]; detection limits of 10^{-6} M using crown ether modified electrodes [32]; detection limits of 10^{-7} for a multicylinder microelectrode system [37], and detection limits of 250 pg for a platinum working electrode in a wall-jet configuration [65].

The reproducibility of the electrodes was assessed from a series of 20 successive injections of a mixture containing 100 μ M of the various catecholamines during an unbroken 200 min period, conditions as given in Figure 4.2.3. The mean peak currents were found to be 405 nA epinephrine, 288 nA epinephrine, 218 nA dopamine and 256 nA catechol with relative standard deviations of 2.6 %, 3.1 %, 3.2 % and 3.7 % respectively, which are well acceptable in the realms of analytical chemistry.

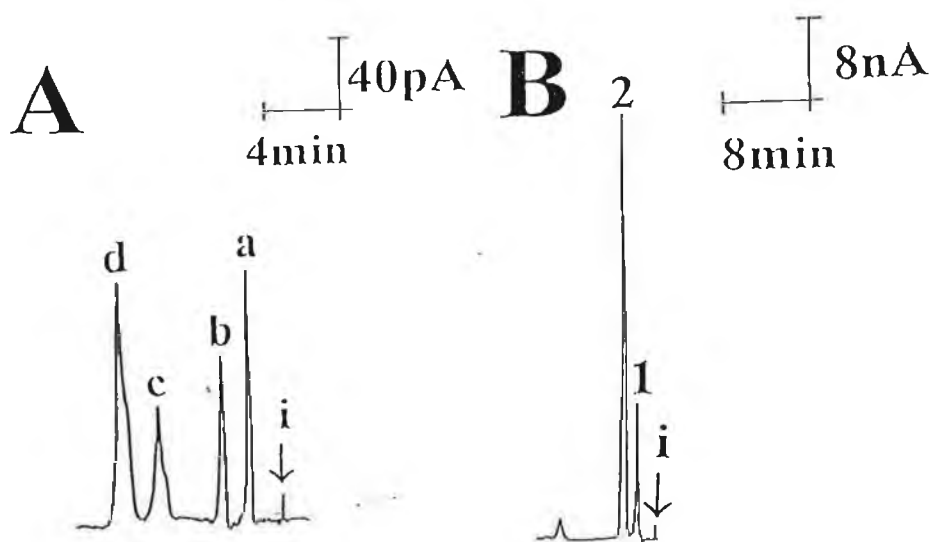


Figure 4.2.8. Chromatograms for submicromolar (0.5μ M) concentrations of catecholamines (A) and a urine sample diluted (1:50) in mobile phase (B) at a sol-gel composite electrode. (a) - (d) represent norepinephrine, epinephrine, dopamine and catechol respectively, whilst 1 and 2 represent ascorbic acid and uric acid. Other conditions as given in Figure 4.2.3.

As mentioned earlier in Section 4.2.1., the problems with the initial ground breaking work in probing brain chemistry by Adams [28], were mainly due to the oxidation of acids presence in biological fluids. Figure 4.2.8.(b) shows the response of the sol-gel composite electrode to a 1:50 dilution of a human urine sample. The sample displayed clearly defined peaks at retention times of 2.0 min and 3.5 min respectively.

These retention times corresponded to ascorbic acid and uric acid present in the urine, thus obscuring the possibility of identifying norepinephrine or epinephrine if they were present in the sample, which have corresponding retention times of 2.0 min and 3.4 min as shown earlier.

Therefore treatment of the electrodes with Nafion films to reduce interference from ascorbic acid and acid metabolites and also sample pre-treatment as described by others [62, 78] will be required if these sol-gel composites are to be used routinely in clinical analysis.

4.2.4. Conclusion

The experiments performed in the previous sections clearly indicate that sol-gel carbon composites can provide versatile, easy to prepare, renewable LCEC detectors, possessing high sensitivity, selectivity and stability. While such features are presented in connection with a wall-jet detector, other detector configurations could benefit from the attractive properties of sol-gel carbon composites. The shape and form of the sol-gel derived electrodes can be controlled to suit the specific application. Application of this detector for monitoring other electroactive compounds in chromatographic effluents appears promising. Enzyme-based detectors (e.g. for phenols, amino acids or carbohydrates) could benefit from the attractive, low-temperature encapsulation of biocomponents within sol-gel networks. Doping of the sol-gel carbon composite with an electrocatalyst (e.g. dispersed metal particles) could offer additional detection advantages.

4.3. Development of a Sol-Gel based Amperometric Biosensor for the Analysis of Phenolics

4.3.1. Introduction

The analysis of phenols is of immense importance in environmental monitoring. The concentration of these compounds in natural waters may vary to some degree, but on the whole they are usually present at the $\mu\text{g/L}$ level [87-90]. The detrimental effect of phenols on human health requires a stringent mandate for the analysis and quantitation of such compounds.

Many detailed methods of analysis exist for the monitoring of these compounds, including gas chromatography with flame ionisation detection [91, 92] and gas chromatography with mass spectroscopy detection [93-98] for more detailed studies. However, these techniques are highly demanding, requiring skilled operators for the numerous troubleshooting problems which may arise. Biosensors based on the marriage of a biological entity with a suitable transducer offer an alternative route. Technical expertise is less demanding, the analysis can be performed in nearly real time i.e., the response times are in the order of several seconds. They are inexpensive, robust, easy to prepare and are capable of being mass produced economically using currently available technology.

The use of the polyphenol oxidase enzyme tyrosinase for the measurement of phenols has been well documented [99-103]. It oxidises phenols to quinone products, which are then reduced at a working electrode surface giving rise to an electrical signal. In this particular study the use of a horseradish peroxidase (HRP)/osmium polymer/sol-gel based amperometric biosensor for the analysis of phenols is presented.

Several methods exist for the construction of horseradish peroxidase biosensors. These can be characterised into the following distinctions: (a) electrode surfaces modified with either adsorbed or covalently linked peroxidase; (b) electrodes modified with a redox or electron conducting polymer, into which peroxidase molecules are physically or

chemically attached, and (c) bulk modified composite electrodes where peroxidase molecules are homogeneously incorporated into the bulk electrode.

The most popular covalent linkage method used has been based on the use of carbodiimide [104, 105], although glutaraldehyde has also proved popular [106]. Peroxidase has also been incorporated into electropolymerised polypyrrole [107] and o-phenylenediamine [108]. Bulk modified composite electrodes have also been widely used, examples include epoxy [109, 110], silicon [111, 112] and paraffin oil [113, 114] composites respectively. Peroxidase tissue rich modified carbon paste electrodes based on asparagus [115], tobacco callus tissue [116], horseradish root [117] and kohlrain skin [118] have also been well studied.

In the model presented in this study the osmium polymer $[\text{Os}(\text{bpy})_2(\text{PVP})_{10}\text{Cl}]\text{Cl}$ functions as a non-diffusional mediator, electrostatically bound to HRP through interaction of the positive osmium centres with negatively charged amino acid residues of HRP. This “molecular wiring” process results in direct electron transfer between the HRP $\text{Fe}^{3+/2+}$ centres and the electrode due to the presence of the stable $\text{Os}^{2+/3+}$ redox couple, which permits rapid electron self-exchange. The length and flexibility of the osmium polymer allows it to fold along the protein chains of the enzyme resulting in extremely effective molecular wiring. The use of such polymers in glucose oxidase biosensors has been well documented [119-121].

Much interest has evolved in recent years on the use of sol-gel glasses as biosensor encapsulation matrices and membrane layers [21-27]. Sol-gels are produced from the acid or base hydrolysis of silane monomers. This process is followed by water and alcohol condensations, linking chains and forming extensive networks resulting in the formation of a gel. The synthetic process occurs at room temperature, the starting materials are inexpensive, the gels can be shaped into any shape or size and can be tailor-made to contain pores of a required diameter. This engineering of pore size is extremely important as the resultant pores in a sol-gel layer can be made sufficiently large enough to allow diffusion of the analyte to the enzyme-electrode redox surface, and yet be sufficiently small enough to prevent leaching of the enzyme.

Due to the lack of electronic conduction, electrochemical methods must rely on an electron transport mediator for signal transduction. In this work, horseradish peroxidase functions as the redox enzyme, the osmium polymer functions as the mediator and the sol-gel functions as a membrane layer.

The principle of direct and mediated electron transfer of peroxidases has been dealt with in detail by Ruzgas et al. [122]. Operational characteristics of an osmium-polymer mediated horseradish peroxidase biosensor in the absence of phenols has been demonstrated by Iwuoha et al. [123]. The principle of operation of this biosensor is that the oxyferryl horseradish peroxidase compound, produced by the reaction of H_2O_2 and HRP in its ferric peroxidase resting state, catalyses the one electron oxidation of phenol. The osmium polymer redox species acts as an electron donor for the reduction of the hydroxyferryl HRP compound, regenerating the enzyme, whilst the osmium polymer is regenerated through reduction at the electrode surface (Figure 4.3.1).

This work outlines the electrochemical behaviour of this biosensor to both hydrogen peroxide and cumene hydroperoxide substrates in aqueous and organic solvents. The performance of this biosensor for the screening of a selection of phenols is also demonstrated.

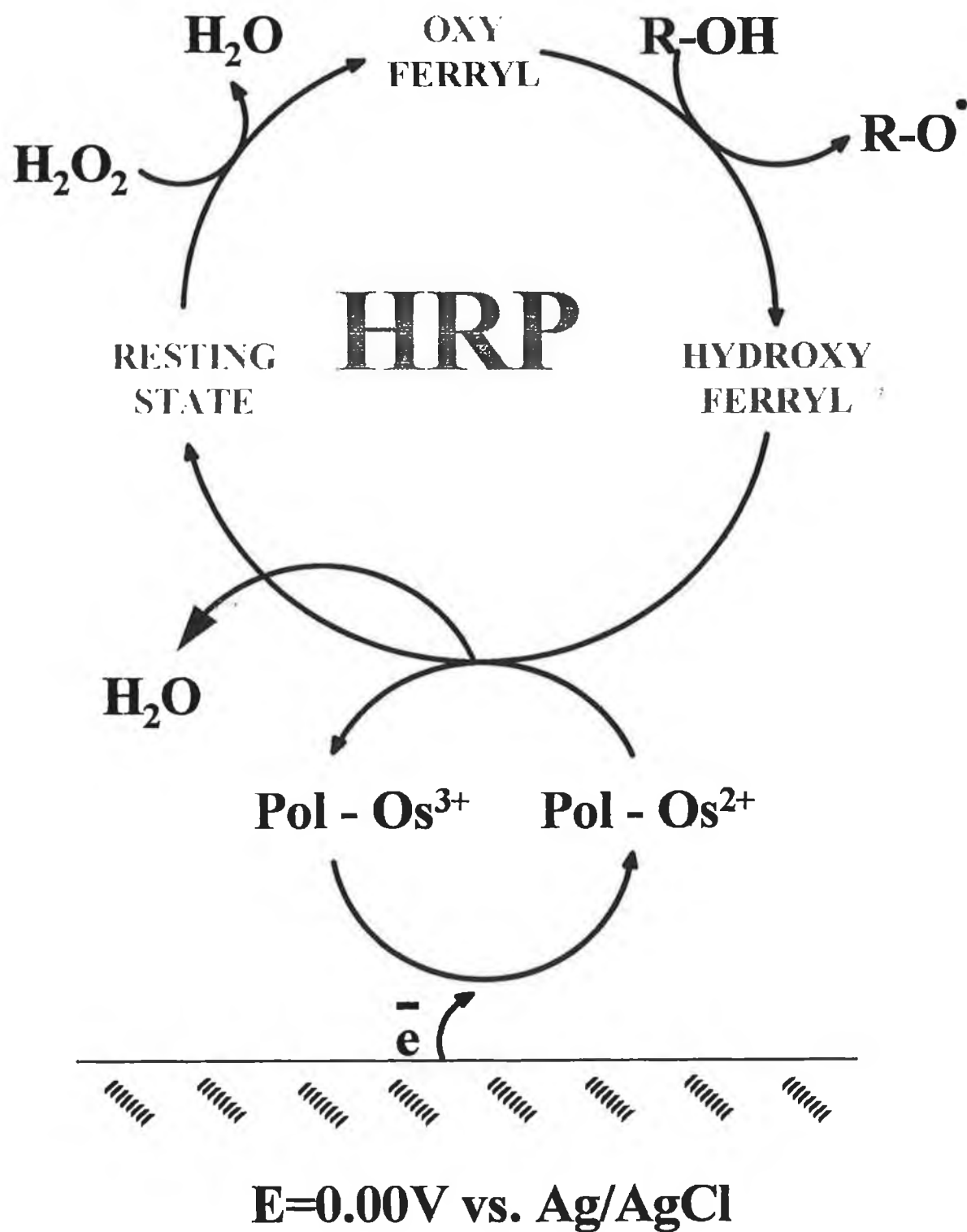


Figure 4.3.1. Substrate and phenol catalysis at the horseradish peroxidase/osmium polymer/sol-gel based electrode.

4.3.2. Experimental

4.3.2.1. Reagents

Pentachlorophenol, m-aminophenol, o-aminophenol, p-aminophenol, m-chlorophenol, o-chlorophenol, p-chlorophenol, o-cresol, p-cresol, 2,6-dimethoxyphenol, 1-naphthol, 2-naphthol and L-tyrosine were all supplied by Sigma (MO, USA). Potassium dihydrogen phosphate and disodium hydrogen phosphate were supplied by Aldrich (Milwaukee, USA). HPLC grade acetonitrile, obtained from Lab-Scan (Dublin, Ireland), was used to dissolve all phenolic compounds. 0.05 M tetraethylammonium p-toulenesulphonate, obtained from Aldrich (Milwaukee, USA), was used as electrolyte in the organic phase analyses. Analytical grade argon Air-Products Plc (UK) was used to degas all samples. Horseradish peroxidase, EC. 1.11.1.7., 727 U/mg, was supplied by Fluka Biochemika (Buchs, Switzerland). Sol-gel layers were prepared from methyltriethoxysilane (Aldrich, Milwaukee, USA). Osmium polymer, see Figure 4.3.2., was synthesised according to the method of Forster et al [124]. Buehler (IL, USA) alumina micropolish and polishing pads were used for electrode polishing. All solutions were prepared in deionised water prepared by passing distilled water through a Milli-Q-water purification system. Hydrogen peroxide and cumene hydroperoxide were obtained from Sigma (MO, USA).

4.3.2.2. Instrumentation

All analyses were performed on a computer operated BAS100B electrochemical analyser, connected to a three electrode 10 ml cell, containing glassy carbon as the working electrode, platinum counter electrode and silver/silver chloride as the reference electrode. A Heto (Denmark) thermostatically controlled waterbath was used to maintain the experimental temperature at 25 °C. A home-made Ikameg Reo spin coater and a Steinal HL 1800E heated gun were used to prepare the electrodes.

4.3.2.3. *Sol-Gel and Electrode Preparation*

The sol-gel was prepared by mixing 500 μl methyltriethoxysilane with 750 μl deionised water and 50 μl 0.1 M HCl, in a 10 ml glass reaction vessel. This was stirred at 300 rpm for one hour, and left for 24 hr before use. The glassy carbon electrodes were polished prior to use using 1.0 μm , 0.3 μm and 0.05 μm grade alumina, rinsed thoroughly with deionised water and allowed to dry. The glassy carbon electrodes were then mounted in the spin coater and a 3 μl (50:50) mixture of 1% osmium polymer in methanol and horseradish peroxidase (2 mg/ 0.1 ml) was deposited on the electrode surface. The electrodes were spun at a rate of 400 rpm for a duration of 1 hr under low heat. Then a 3 μl coat of the methyltriethoxysilane derived sol-gel was applied to the modified surface, and left to spin under the same conditions for another hour. The electrodes were then stored for 12 hours at room temperature in a closed vessel in darkness.

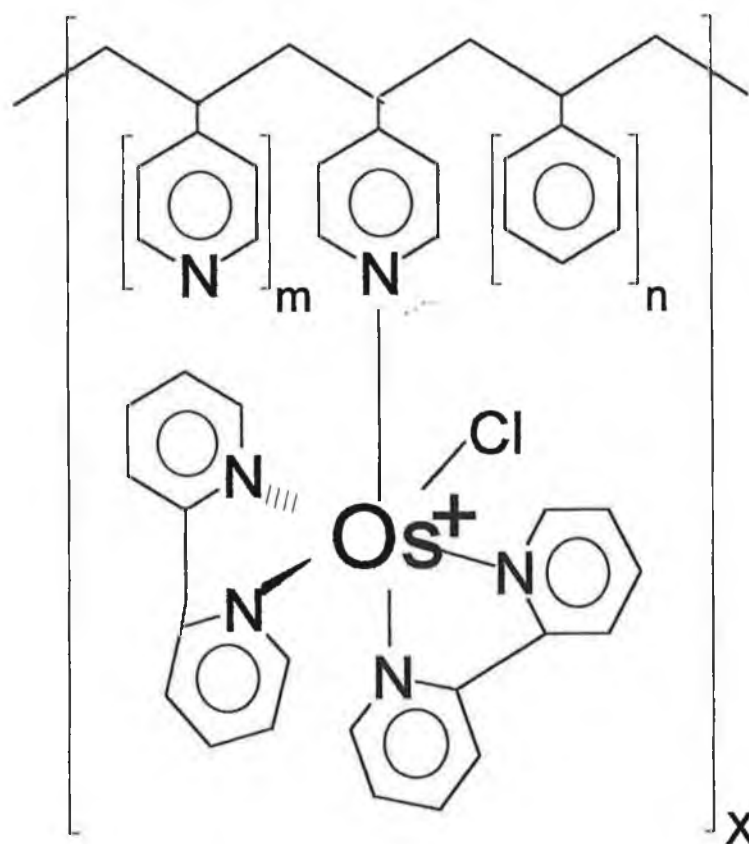


Figure 4.3.2. Schematic of osmium bipyridyl polyvinylpyridine redox polymer

4.3.2.4. *Procedures*

For the aqueous phase analyses, 10 ml 0.01 M phosphate buffer, pH 7.4. was used. For the organic phase analyses, acetonitrile made 0.05 M in tetraethylammonium p-toluenesulfonate, was used as the electrolyte. Hydrogen peroxide and cumene hydroperoxide were used as substrates respectively. All samples were degassed for a period of 15 minutes prior to analysis and kept under an argon atmosphere for the duration of the experiment. All experiments were carried out at a thermostatically controlled temperature of 25 °C.

4.3.3. Results & Discussion

4.3.3.1. Electrochemical Behaviour of the Biosensor

Focusing firstly on the kinetic performance of this biosensor, the hydrodynamic CV's for the GCE/OsHRP/Sol-gel composite are displayed in Figure 4.3.3(a). Scans from 2 mV/s to 200 mV/s were performed. It can be seen that electron transfer is better in the 80% : 20% acetonitrile : H₂O than the corresponding phosphate buffer one. Using a Randles-Sevcik plot [125], the diffusion coefficients were evaluated for both systems:

$$I_p = 2.69 \times 10^5 n^{3/2} D_e^{1/2} C_m v^{1/2} \quad (4.3.1)$$

where I_p is the peak current in amperes; n is the number of electrons; D_e is the diffusion coefficient in $\text{cm}^2 \text{s}^{-1}$; C_m is the concentration in mol cm^{-3} and v is the scan rate in V s^{-1} . Substituting the appropriate terms it was found for the phosphate buffer system that $D_e(\text{aq}) = 0.69 \times 10^{-10} \text{ cm}^2 \text{ s}^{-1}$, and the corresponding diffusion coefficient in 80% : 20% acetonitrile : H₂O yielded a $D_e(\text{org}) = 3.19 \times 10^{-10} \text{ cm}^2 \text{ s}^{-1}$. The current was proportional to $v^{1/2}$ as shown in Figure 4.3.3(b), implying that the electroreduction current of the biosensor composite is a diffusion controlled current [126]. Although electron transfer was faster in the organic phase, solvent resistivities, solvation of substrate and analyte, and also diffusion and partitioning through the sol-gel coating, will have a part to play in responses observed when the substrate and analyte are used..

Since the osmium polymer was cast as an electrostatic enzyme polymer film one would have expected the peak current to have varied linearly with scan rate as discussed in Section 5.3.3. However, since the osmium polymer is extremely complex, where the osmium centres are found along lengthly polyvinylpyridine chains, see Figure 4.3.2., the non-diffusional mediator displayed the same characteristics as a mediator in solution. There is also the possibility of repulsion of the osmium-enzyme layer from the electrode surface under certain conditions, which may very well explain the observed electrochemistry of the biosensor in aqueous solutions as seen in Figure 4.3.3.(a)(i).

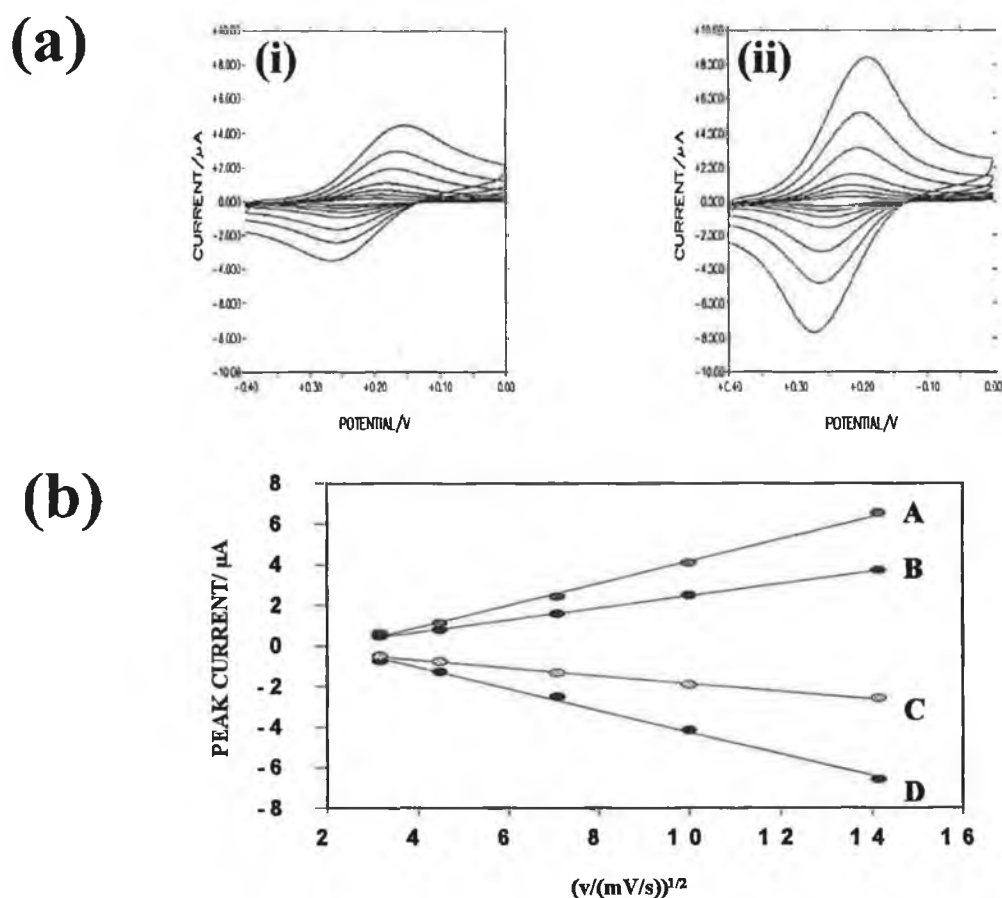


Figure 4.3.3. (a) Hydrodynamic CVs of a GCE/OsHRP/Sol-gel composite in (i) phosphate buffer solution, 0.01 M, pH 7.4., and (ii) 80% : 20% acetonitrile : H_2O . Cathodic current (+ve), anodic current (-ve). Scan rates are 2, 5, 10, 20, 50, 100 and 200 mV/s. (b) Randle Sevcik Plots for the cathodic organic (A) and aqueous (B) peak currents, and the corresponding anodic aqueous (C) and organic (D) peak currents.

According to studies by Pankratov et al. [23], when tetramethoxysilane sol-gel monomers are used as precursors, the resultant sol-gel membrane network is highly hydrophilic and water easily penetrates through the layer. When it was attempted to use tetramethoxysilane in this study, the resultant gel layer cracked and peeled after curing, making it inappropriate for this application. Methyltriethoxysilane was used instead, resulting in a hydrophobically modified membrane network.

4.3.3.2. *Biosensor Catalytic Response*

An example of the electrocatalysis of hydrogen peroxide at the biosensor is shown in Figure 4.3.4(A). The scan (I) represents the diffusional current of the biosensor GCE/OsHRP/Sol-gel composite in the absence of substrate, whilst scan (II) represents the catalytic current when the substrate hydrogen peroxide was added. The electrocatalytic peak reduction current occurred at + 178 mV vs. Ag/ AgCl reaching a plateau thereafter. In order to obtain a high electrocatalytic response, and at the same time minimise the electroreduction of interferents, the operating potential in steady state modes was maintained at 0 mV vs. Ag/ AgCl.

Figure 4.3.4(B-D) shows comparative substrate catalytic currents for H₂O₂ in 80%: 20% acetonitrile: H₂O, B, and for cumene hydroperoxide in phosphate buffer C, and 80%: 20% acetonitrile: H₂O D, respectively. The kinetically controlled current values (I_K) for H₂O₂ show greater sensor responses in phosphate buffer than acetonitrile, due to the more facile diffusion of H₂O₂ in aqueous buffer. The lower catalytic current observed in acetonitrile can be attributed to the solvation of the sol-gel's hydrophobic membrane's outer surface and inner lining of silica pores by acetonitrile, hence making it more difficult for the hydrogen peroxide to diffuse through.

The I_K values for cumene hydroperoxide in phosphate buffer and 80% : 20% acetonitrile : H₂O differ slightly. However, the I_K value for cumene hydroperoxide in the buffer system is greater than that in acetonitrile. One might have expected the trend in this case to be the reverse. However, one can explain the poorer response in acetonitrile as follows. The acetonitrile probably solvates the cumene hydroperoxide greater than it solvates the sol-gel membrane layer. Since one is dealing with a partitioning effect whereby the substrate must diffuse through a liquid organic phase, and then a 'solid' sol-gel layer, its affinity for the liquid phase is obviously greater than that for the 'solid' sol-gel layer. The response times are also in agreement with this experimental observation, i.e. for H₂O₂ in phosphate buffer a response time of 14.2 s was obtained, compared to a response time of 15 s in acetonitrile. Similarly, for cumene hydroperoxide in phosphate

buffer a response time of 15.7 s was obtained whereas a response time of 14.5 s was obtained in acetonitrile.

There is also a noticeable shift to higher catalytic potentials as a result of the iR drop in organic solvents. For example, for the H_2O_2 substrate system, the optimal cathodic peak potential in phosphate buffer was +178 mV, followed by a shift of +27 mV to an $E_{p,c}$ of +205 mV in 80% acetonitrile. Similarly, for the cumene hydroperoxide substrate system, the $E_{p,c}$ in phosphate buffer was +178 mV, followed by a shift of +40 mV to +218 mV in 80% : 20% acetonitrile: H_2O . The higher resistivity of the organic phase is responsible for this trend.

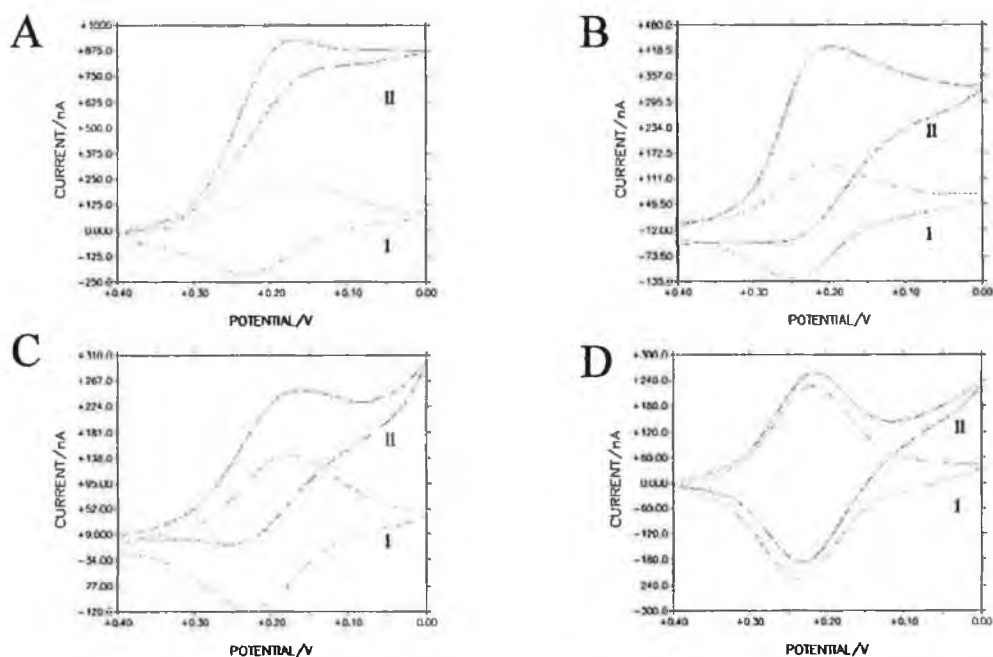


Figure 4.3.4. Cyclic Voltammograms in the presence (II) and absence (I), of substrate: 1 mM hydrogen peroxide in (A) & (B); 5 mM cumene hydroperoxide in (C) & (D), at a GCE/OsHRP/Sol-gel composite, in the following media: phosphate buffer solution 0.01 M, pH 7.4., for (A) & (C); and 80:20 acetonitrile: H_2O for (B) & (D), containing tetraethylammonium *p*-toulenesulphonate 0.05 M, as electrolyte. A scan rate of 2 mV/s was used in (A) & (B), and a scan rate of 1 mV/s was used in (C) & (D). All experiments were performed at 25°C.

As mentioned before, I_K is the kinetically controlled current or catalytic current, and is controlled by the enzyme kinetics at the steady state. The polarographic wave in the absence of substrate depends on diffusion at the electrode surface and is represented by I_D . Therefore, the catalytic efficiency, C_{eff} , of a biosensor is determined as the ratio of the peak current controlled by the enzyme catalytic reduction of the substrate to that controlled by diffusion due to the osmium polymer at the electrode surface, i.e.

$$C_{eff} = (I_K / I_D) \quad (4.3.2)$$

After evaluating the C_{eff} values for both substrates, it has been established that the C_{eff} for H_2O_2 in both aqueous and organic systems is greater than that of cumene hydroperoxide, i.e. C_{eff} (aq) 3.9 (H_2O_2) vs. 1.7 (cumene hydroperoxide), and C_{eff} (org) 2.9 (H_2O_2) vs. 1.1 (cumene hydroperoxide) respectively. This trend is not surprising as acetonitrile can strip the enzyme of essential water of hydration hence resulting in decreased sensor performance.

Analysis of the Tafel regions on the kinetically controlled current, I_K of the CVs of the substrate were carried out to ascertain the number of electrons transferred at the electrode according to the equation:

$$\log I = \log I_0 + (\alpha n F / 2.3 RT) E \quad (4.3.3)$$

where I is the catalytic current, A; I_0 is the exchange current, A; α is the transfer coefficient; n is the number of electrons transferred at the electrode, and is 2 for horseradish peroxidase; E is the potential, V; R is the Universal gas constant, 8.314 J mol⁻¹ K⁻¹ and T is the temperature in K.

In these studies, Tafel slopes of 116 mV/ decade and 102 mV/ decade were obtained for hydrogen peroxide and cumene hydroperoxide in phosphate buffer respectively, which are in good agreement with the theoretical value of 118 mV/ decade for a two electron transfer process, as expected with horseradish peroxidase [122, 123]. Figure 4.3.5. shows the Tafel plots for the electrocatalysis of 1 mM H_2O_2 at the biosensor in

phosphate buffer. The insert shows the extended electrocatalysis region from which the plots were taken.

However, for hydrogen peroxide and cumene hydroperoxide in acetonitrile, Tafel slopes of only 61 and 81 mV/ decade were obtained. It is quite possible that the resistivity of the acetonitrile has a role to play resulting in a large Ohmic iR drop. Hence, by decreasing the acetonitrile content or alternatively increasing the electrolyte concentration, these slopes could approach the theoretically expected one.

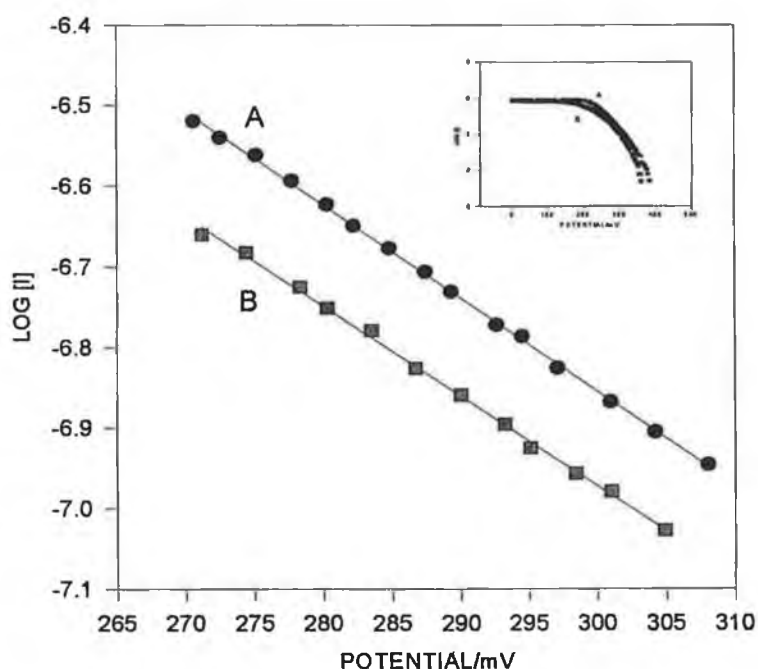


Figure 4.3.5. Tafel plots for the electrocatalysis of 1 mM H₂O₂ at a glassy carbon electrode modified with osmium polymer-horseradish peroxidase sol-gel composite, in phosphate buffer, 0.01M, pH 7.4. (A) cathodic current (B) anodic current. Inset shows extended catalytic region. Other conditions as in Figure 4.3.4.

4.3.3.3. Steady State Amperometry

I_K/I_D values are usually evaluated from cyclic voltammetry experiments. One can also evaluate a similar catalytic efficiency from steady-state current time recordings [127]. This takes the form of Michaelis-Menten kinetics:

$$I = [S][I_{\max}]([S] + K'_M)^{-1} \quad (4.3.4)$$

where I is the current in amperes; $[S]$ is the concentration of substrate in mol cm^{-3} ; I_{\max} is the maximum current in amperes, i.e. the current at which enzyme activity is saturated by substrate; K'_M is the apparent Michaelis-Menten constant, and is a measure of substrate-enzyme binding. This equation can also be represented as follows:

$$I = [S](nFAk_{\text{cat}}\tau[\text{HRP}])([S] + K'_M)^{-1} \quad (4.3.5)$$

where k_{cat} is the rate of catalysis, s^{-1} ; F is Faraday's constant; n is the number of electrons involved; τ is the thickness of the enzyme layer, cm , and $[\text{HRP}]$ is the concentration of enzyme, mol cm^{-3} . The term $k_{\text{cat}}\tau[\text{HRP}]$ defines the maximum response of the biosensor realisable at saturating concentrations of substrate. By replacing $k_{\text{cat}}\tau[\text{HRP}]$ with k'_{cat} , the apparent rate of catalysis, $\text{mol cm}^{-2} \text{s}^{-1}$, we get:

$$I = [S](nFAk'_{\text{cat}})([S] + K'_M)^{-1} \quad (4.3.6)$$

Since this equation resembles equation (4.3.4), it suffices that

$$I_{\max} = nFAk'_{\text{cat}} \quad (4.3.7)$$

The k'_{cat} / K'_M values, known as the substrate specificity factor or catalytic efficiency, are indicators of the biosensor's electrocatalytic reaction and are an indication of sensor performance. The higher this value, the better the sensor performance [128]. For this biosensor it was found that for H_2O_2 the k'_{cat} / K'_M values were greater than that for cumene hydroperoxide and hence in agreement with the earlier observed catalytic efficiencies.

4.3.3.4. *Temperature Optimisation*

A temperature study to determine the optimum temperature of performance was established using H₂O₂ as substrate in phosphate buffer. The well known relationship between reaction rate and temperature is represented by the Arrhenius equation [129], which implies that reactions go faster at higher temperatures:

$$k = A e^{-E_a/RT} \quad (4.3.8)$$

where k is the rate of reaction, s⁻¹; A is called the pre-exponential term; E_a is the energy of activation, KJ mol⁻¹; R is the universal gas constant, 8.314 J mol⁻¹ K⁻¹, and T is the temperature in K. By taking natural logarithms of both sides, the following relationship is obtained:

$$\ln k = \ln A - (E_a/RT) \quad (4.3.9)$$

The catalytic efficiencies were plot against the temperature in Kelvin as shown in the insert of Figure 4.3.6, and the activation energy was evaluated from a plot of $\ln k$ the reaction rate versus $1/T$. The activation energy was evaluated from the slope of the line and was found to be $E_a = 24.1$ KJ mol⁻¹, suggesting that on exceeding temperatures of 308 K, the transition state of the enzymatic reaction is destabilised, resulting in protein unfolding and denaturation.

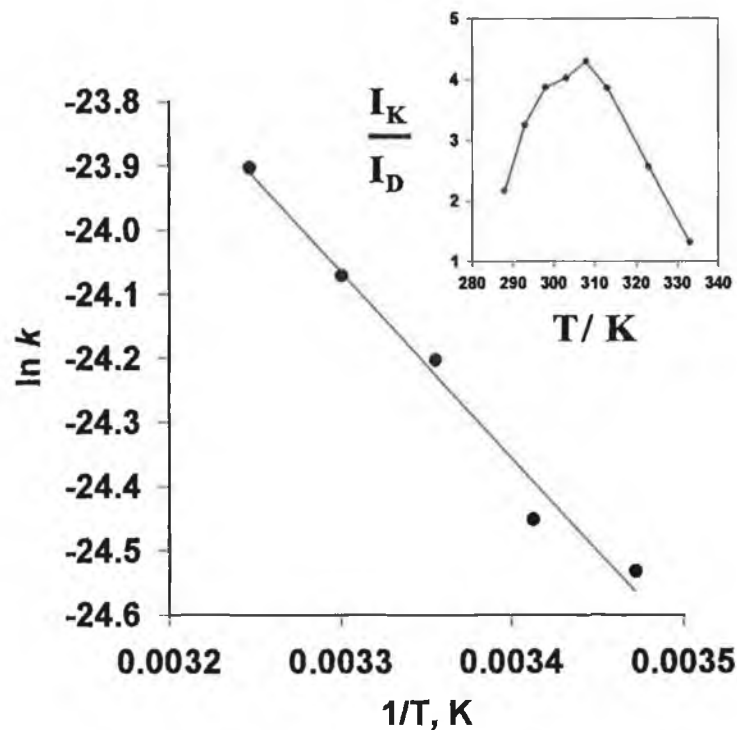


Figure 4.3.6. Temperature study for energy of activation evaluation and optimum temperature assessment.

The same trend was observed on repeating this study. There was little variation between reaction rate at 298 K and 303 K, so a temperature of 298 K was used throughout the experiment. Although the optimum temperature was found to lie at 308 K, a sharp decline in reaction rate was observed at temperatures exceeding this.

4.3.3.5. Screening of Phenols

Using the information obtained from the preliminary assessment of sensor performance, screening of phenolic compounds was then evaluated. An example of the catalysis mechanism was shown earlier in Figure 4.3.1. Addition of hydrogen peroxide to HRP in the resting state results in the formation of an oxy ferryl compound which is reduced by the one-electron oxidation of a phenolic compound. The hydroxy ferryl peroxidase is then reduced through the osmium polymer mediator, regenerating the enzyme. The osmium polymer itself being regenerated by reduction at the electrode.

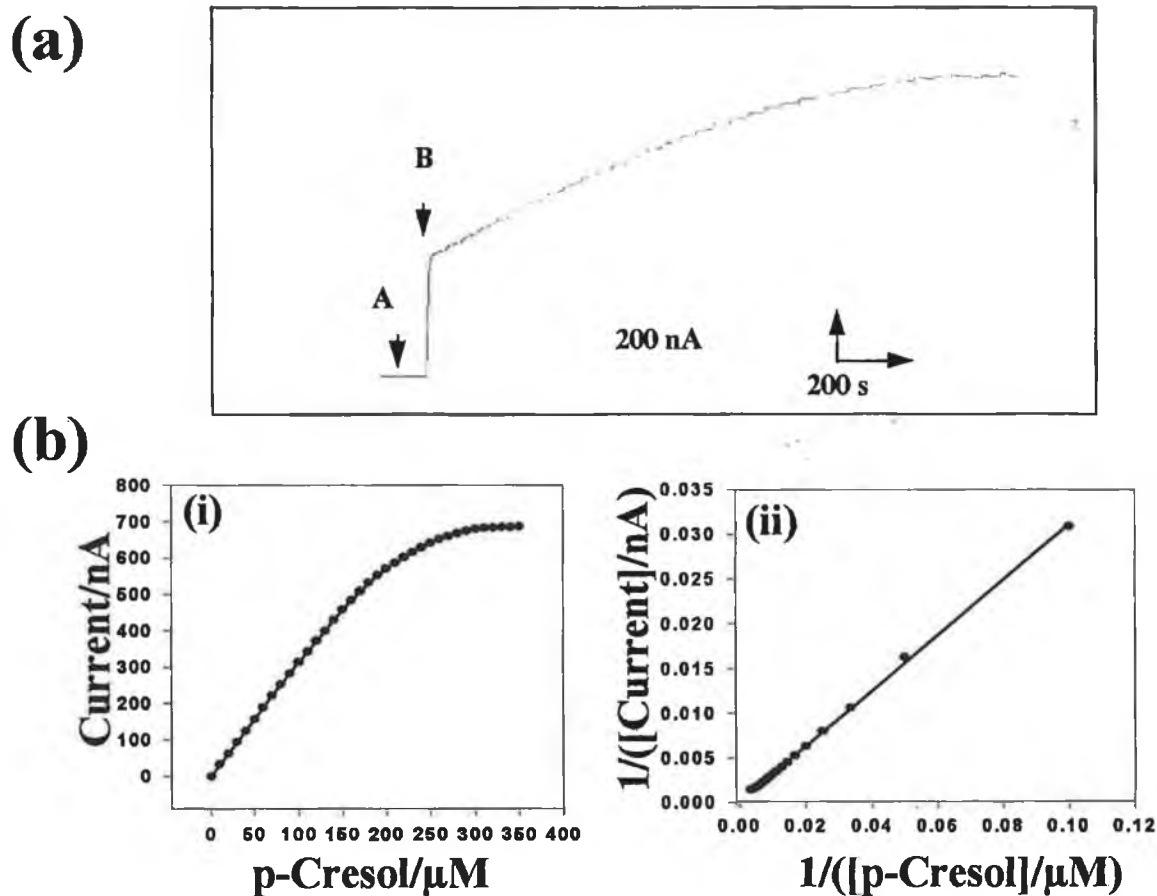


Figure 4.3.7. (a) Batch analysis profile for *p*-cresol. 1 mM H_2O_2 was used as substrate (A), followed by successive additions (B) of 10 μM *p*-cresol until saturation. Solution was stirred at 300 rpm and performed in 10 ml 0.01 M pH 7.4. phosphate buffer. (b) Michaelis-Menten (i) and Lineweaver-Burk plots (ii) for *p*-cresol.

An example of the batch analysis current-time recording obtained for *p*-cresol using H_2O_2 as substrate in phosphate buffer is shown in Figure 4.3.7(a), along with the corresponding Michaelis-Menten plots and Lineweaver-Burk plots respectively Figure 4.3.7(b)(i & ii). These results were obtained at a working potential of 0 V vs. Ag/AgCl.

Control experiments (results not shown) using only (a) bare glassy carbon; (b) glassy carbon coated with sol-gel; (c) glassy carbon coated with enzyme and sol-gel, and (d) glassy carbon coated with osmium-polymer and sol-gel, gave no interfering response at this potential when screened in the presence and absence of substrate and phenolic compounds respectively.

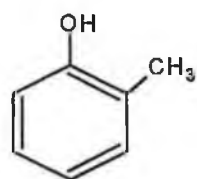
Thirteen phenolic compounds were screened: *m*-aminophenol; *o*-aminophenol; *p*-aminophenol; *m*-chlorophenol; *o*-chlorophenol; *p*-chlorophenol; *o*-cresol; *p*-cresol; 2,6-dimethoxyphenol; pentachlorophenol; 1-naphthol; 2-naphthol and L-tyrosine. Of these thirteen compounds only eight gave a response: *o*-aminophenol, *m*-chlorophenol, *o*-cresol, pentachlorophenol and L-tyrosine failed to yield any noticeable signal even after excessive additions of these compounds.

In order to explain this trend the properties of each individual compound must be addressed to establish suitable reasoning. In the case of pentachlorophenol, there are two possibilities: (a) the electron withdrawing affect of the chlorine groups may make it difficult to form the free radical and/or (b) the compound may have difficulty passing through the sol-gel membrane. It is most likely that (a) is the case here, as high positive potentials need to be applied to oxidise pentachlorophenol at a bare glassy carbon electrode. In the case of L-tyrosine, this compound may have difficulty in diffusing through the sol-gel layer due to the hindrance effect of the aliphatic chain present on the compound preventing it from reaching the enzyme and reacting.

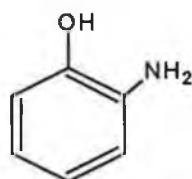
With both *o*-cresol and *o*-aminophenol an important trend was observed. Both methyl and amino groups are electron donating, and in this study it was found that electron donating groups in the ortho-position resulted in no response. On the other hand,

electron withdrawing groups in the meta-position also resulted in no response, as was the case with m-chlorophenol. These observations are summarised in Figure 4.3.8.

Electron donating groups in the ortho-position result in no response

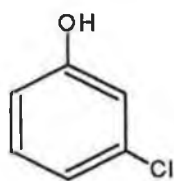


o-cresol



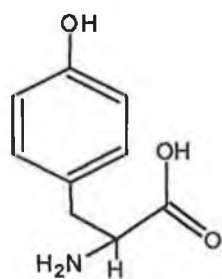
o-aminophenol

Electron withdrawing groups in meta-position result in no response



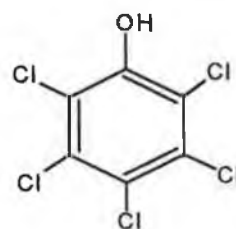
m-chlorophenol

Partitioning or Specificity



L-tyrosine

Formation of Free Radical unfavourable



Pentachlorophenol

Figure 4.3.8. Summary of compounds yielding no response at the biosensor composite

For compounds yielding a response the following response trend was obtained: 2-naphthol > m-aminophenol > p-aminophenol \cong p-cresol > p-chlorophenol > o-chlorophenol > 1-naphthol > 2,6-dimethoxyphenol. The biosensor was more than six times more sensitive to 2-naphthol than 1-naphthol as summarised in the response factor column of Table 4.3.1. This trend in response has been found to be unique to this study and is probably attributed to partitioning across the sol-gel membrane, hence deviating from theoretical trends as predicted from the Hammett functions for phenols by Jinno and Kawaski [130]. Response times for m-aminophenol, p-aminophenol, o-chlorophenol, p-chlorophenol, 1-naphthol, 2-naphthol and 2,6-dimethoxyphenol, the corresponding catalytic efficiencies and detection limits for these compounds and p-cresol are shown in Table 4.3.1.

Table 4.3.1. Kinetic Data for the biocomposite GCE/OsHRP/Sol-gel in 0.01 M pH 7.4. PBS.

Compound	Response Time/ s	$10^6 k_{cat} / K_M$	LOD μM	Response Factor
m-aminophenol	12.5	303	0.15	9.9
p- aminophenol	13.5	240	0.65	8.6
o- chlorophenol	11.0	44	1.48	3.7
p- chlorophenol	12.0	60	1.29	6.2
p- cresol	18.5	87	0.93	8.7
1- naphthol	27.0	24	1.16	1.6
2- naphthol	29.0	283	0.32	10.6
2,6- dimethoxyphenol	12.0	58	1.21	1.0

Cumene hydroperoxide was also used as substrate in this study. However, poor responses were obtained for all phenols making it difficult to assess or correlate their performance to the corresponding H_2O_2 model. Steric hindrance or poor enzyme-substrate fit of cumene hydroperoxide could be responsible for the observations made. Alternatively the cumene product of the enzyme reaction may have diffusional problems, hence blocking the active site of the enzyme for phenol catalysis.

4.3.3.6. *Organic Phase Analysis*

No responses were obtained for all phenols in both substrate models for the 80% : 20% acetonitrile: H₂O system. One would initially assume that loss of essential water of hydration and active site water in the organic system has resulted in protein folding and enzyme inactivation. However, this was not the case, as was shown earlier in Figure 4.3.4. where substrate response profiles for both H₂O₂ and cumene hydroperoxide in 80% : 20% acetonitrile : H₂O were obtained. The reasoning behind this lack in response was a solvation and partitioning effect similar in some regards to the separation chemistry of solid-phase extraction.

The phenolic compounds were probably heavily solvated by the acetonitrile, retarding their partitioning through the sol-gel membrane. This hypothesis was proved by lowering the acetonitrile content by 10% decrements. No signals were observed for any of the 8 compounds listed in Table 4.3.1, at concentrations of 70%, 60%, 50% or 40% acetonitrile. However, slight responses were observed at 30% : 70% acetonitrile : H₂O, and much improved responses at 20% : 80% acetonitrile: H₂O. An example of the current-time recording obtained for p-aminophenol in 20% : 80% acetonitrile : H₂O is shown in Figure 4.3.9.

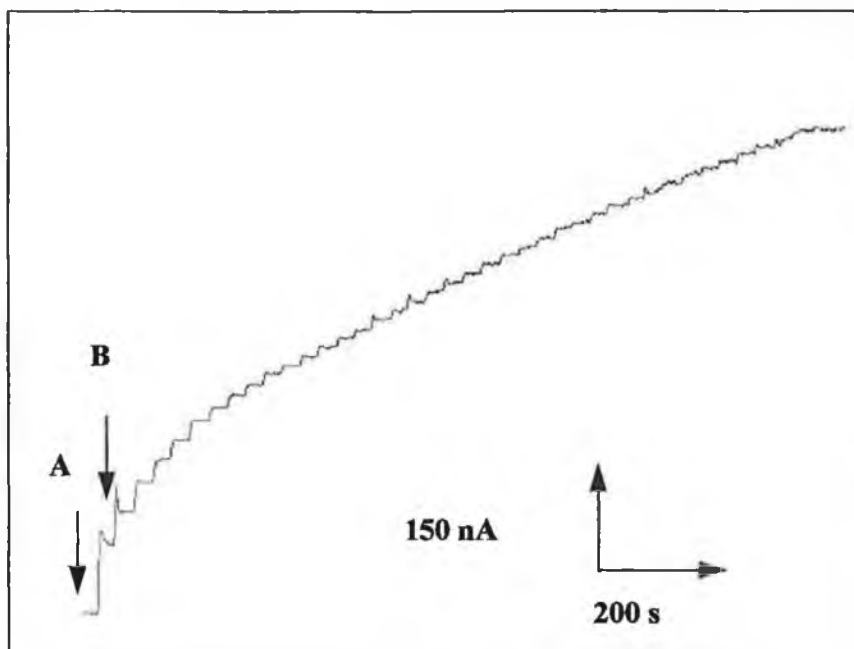


Figure 4.3.9. Batch analysis current-time recording for p-aminophenol in 20% : 80% acetonitrile : H₂O. 1 mM H₂O₂ was used as substrate (A), followed by successive additions (B), of 10 μ M p-aminophenol. Other conditions as given in Figure 4.3.7.

4.3.3.7. Storage and stability

The GCE/OsHRP/Sol-gel biocomposite yielded a lifetime of 4 days when stored in a dry dark container at room temperature. Activity decreased to 50% on the third day, and to 10% of the original response on the fourth day. A lifetime of 6 days was observed when the electrode was stored dry in a refrigerator at 4 °C. However, a similar decay in activity was observed resulting in no response on the seventh day. The stability of the electrode could possibly be improved through crosslinking with glutaraldehyde and /or encapsulation within a lipid vesicle system which would simulate biological membrane conditions possibly resulting in enhanced lifetimes.

4.3.4. Conclusion

This study has demonstrated the ability of a novel GCE/OsHRP/Sol-gel biosensor to analyse a range of phenolic compounds. Detection limits within the micromolar region were obtained and response times were established within 11 to 29 s for all compounds.

It was established that compounds with electron donating substituents in the ortho-position and electron withdrawing substituents in the meta-position yielded no response for the group of phenols investigated. More detailed studies encompassing a wider range of phenols and the corresponding responses would need to be performed before this biosensor could be exploited in future studies of environmental importance.

The stability of the electrodes may also be improved by incorporating the horseradish peroxidase and osmium polymer complex into a suitable sol-gel matrix. This sol-gel encapsulation process has the ability to stabilise enzymes by allowing freedom of rotation in a fluidic pore environment similar to physiological conditions. The activity of the enzyme would thus be preserved and might prolong the lifetime and also result in lower limits of detection.

This encapsulation process would also make the sensor favourable for organic phase analysis. As mentioned with the sol-gel layer in this study, the phenols had difficulty in diffusing through the sol-gel pores at concentrations of acetonitrile greater than 20% with no responses obtained at concentrations of 40% acetonitrile or higher. Encapsulation would overcome this problem by increasing the surface area of the enzyme exposed to solution and could result in responses at higher acetonitrile concentrations.

4.4. References

- [1] Guillbault, G. G.: Analytical Uses of Immobilised Enzymes. Mercel Dekker, New York, (1984).
- [2] Braun, S.; Rappoport, S.; Zusman, R.; Avmir, D.; Oholenghi, M.: Mater. Lett., 10: (1990): 1.
- [3] Ellerby, L. M.; Nishida, C. R.; Nishida, F.; Yamanaka, S. A.; Dunn, B.; Valentine, J. S.; Zink, J. I.: Science, 255: (1992): 1113.
- [4] Wu, S.; Ellerby, L. M.; Cohan, J. S.; Dunn, B.; El-Sayad, M.; Valentine, J. S.; Zink, J. I.: Chem. Mater., 5: (1993): 115.
- [5] Dill, K. A.; Biochemistry, 29: (1990): 7133.
- [6] Ller, R. K.: The Chemistry of Silica. Wiley, New York, (1979).
- [7] Baes, C. F.; Mesmer, R. E.: The Hydrolysis of Cations. Wiley, New York, (1976).
- [8] Anderson, R.; Arkles, B.; Larson, C. L.; Petrarch Systems Silanes and Siloxanes. Petrarch Systems Pub., (1987).
- [9] Sen, P. N.; Thorpe, M. F.: Phys. Rev., B15: (1977): 4030.
- [10] Schroeder, H.; Chapter 5, Physics of Thin Films, ed. Hass, G. Academic Press, New York, (1969).
- [11] Dislich, H.; Hussmann, E.: Thin Solid Films, 77, (1981), 129.
- [12] Pantano, C.G.; Brow, R. K.; Carmen, L. K.: Sol-gel Technology for Thin Films, Preforms, Electronics and Speciality Shapes. Ed. Klein, L. C. Noyes C. F. Pubs., Park Ridge, N.J., (1988).
- [13] Lannutti, J. J.; Clark, D. E.: Ceramics International, 11: (1985): 91.
- [14] Barringer, E.; Jubb, N.; Fegley, B.; Pober, R. L.; Brown, H. K.: Ultrastructure Processing of Glasses, Ceramics and Composites. Eds., Hench, L. L. & Ulrich, D. R. Wiley, New York, (1984).
- [15] Mahler, W.; Bechtold, M. F.: Nature, 285: (1980): 27.
- [16] Brinkler, C. J.; Clark, D. E.; Ulrich, D. R.: Better Ceramics through Chemistry. Elsevier, New York, (1984).
- [17] Gillot, J.; Brinkman, G.; Garcera, D.: New Ceramics filter Media for Cross Flow Microfiltration and Ultrapurification. S.C.T. Ceramic Membranes, Tubes, France, (1986).

- [18] Chung, K. E.; Lan, E. H.; Davidson, M. S.; Dunn, B. S.; Valentine, J. S.; Zink, J. I.: *Anal. Chem.*, 67: (1995): 1505.
- [19] Bull, C.; Fisher, R. G.; Hoffmann, B. M.: *Biochem. Biophys. Res. Commun.*, 59: (1974): 140.
- [20] Lan, E. H.; Chung, K. E.; Dunn, B. S.; Valentine, J. S.; Zink, J. L.: University of California, Los Angeles, unpublished results.
- [21] Yamanaka, S. A.; Nishida, F.; Ellerby, L. M.; Nishida, C. R.; Dunn, B.; Valentine, J.S.; Zink, J. I.: *Chem. Mater.*, 4: (1992): 495.
- [22] Sanchez, C.; Audebert, P.; Demaile, C.: *Chem. Mater.*, 5: (1993): 911.
- [23] Pankratov, I.; Lev, O.: *J. Electroanal. Chem.*, 393: (1995): 35.
- [24] Narang, U.; Prasad, P.N.; Bright, F. V.; Ramanathan, R.; Kumar, N. D.; Malhotra, B. D.; Kamalasanan, M. N.; Chandra, S.: *Anal. Chem.*, 66: (1994): 3139.
- [25] Park, T. M.; Iwuoha, E. I.; Smyth, M. R.; MacCraith, B. D.: *Anal. Comm.*, 33: (1996): 271.
- [26] Park, T. M.; Iwuoha, E. I.; Smyth, M. R.; *Electroanalysis*, 9: (1997): 14.
- [27] Park, T. M.; Iwuoha, E. I.; Smyth, M. R.; Freaney, R.; McShane, A. J.: *Talanta*, 44: (1997): 973.
- [28] Adams, R. N.: *Anal. Chem.*, 48: (1976): 1128A.
- [29] Ponchon, J. L.; Cespuoglio, R.; Gonon, F.; Jouvét, M.; Pujol, J. F.: *Anal. Chem.*, 51: (1979): 1483.
- [30] Gerhardt, G. A.; Oke, A.F.; Nagy, G.; Moghaddam, B.; Adams, R. N.: *Brain Res.*, 290: (1984): 390.
- [31] Gonon, F.; Fombarlet, C.; Boda, M.: *Anal. Chem.*, 53: (1981): 1386.
- [32] Lunsford, S. K.; Ma, Y-L; Galal, A.; Striley, C.; Zimmer, H.; Mark, H. B.: *Electroanalysis*, 7: (1995): 420.
- [33] Lyons, M. E. G.; Greer, J. C.; Fitzgerald, C. A.; Bannon, T.; Barlett, P. N.: *Analyst*, 121: (1996): 715.
- [34] Hasebe, Y.; Takamori, K.; Uchiyama, S.: *Anal. Chim. Acta.*, 282: (1993): 363.
- [35] Uchiyama, S.; Itoi, N.; Hasebe, Y.: *Electroanalysis*, 7: (1995): 731.
- [36] Schroeder, T. J.; Jankowki, J. A.; Kawagoe, K. T.; Wightman, R. M.; Lefrou, C.; Amatore, C.: *Anal. Chem.*, 64: (1992): 3077.

- [37] Peng, W.; Wang, E.: *Anal. Chim. Acta.*, 281: **(1993)**: 663.
- [38] Tabei, H.; Takahashi, M.; Hoshino, S.; Niwa, O.; Horiuchi, T.: *Anal. Chem.*, 66: **(1994)**: 3500.
- [39] Chen, T. K.; Luo, G.; Ewing, A. G.: *Anal. Chem.*, 66: **(1994)**: 3031.
- [40] Ciolkowski, E. L.; Maness, K. M.; Cahill, P. S.; Wightman, R. M.; Evans, D. H.; Fosset, B.; Amatore, C.: *Anal. Chem.*, 66: **(1994)**: 3611.
- [41] Pihel, K.P.; Schroeder, T. J.; Wightman, R. M.: *Anal. Chem.*, 66: **(1994)**: 4532.
- [42] Cahill, P. S.; Walker, Q. D.; Finnegen, J. M.; Mickelson, G. E.; Travis, E. r.; Wightman, R. M.: *Anal. Chem.*, 68: **(1996)**: 3180.
- [43] Tait, R. j.; Finnin, B. C.; Reed, B. L.; Bond, A. M: *Anal. Chim. Acta.*, 324: **(1996)**: 1.
- [44] Slater, J. M.; Watt, E. J.: *Analyst*, 119: **(1994)**: 2303.
- [45] Zhong, M.; Lunte, S. M.: *Anal. Chem.*, 68: **(1996)**: 2488.
- [46] Zhong, M.; Zhou, J.; Lunte, S. M.; Zhao, B.; Giolando, D. M.; Kirchhoff, J. R.: *Anal. Chem.*, 68: **(1996)**: 203.
- [47] Zhu, R.; Kok, W. T.: *Anal. Chem.*, 69: **(1997)**: 4010.
- [48] Chang, S. Y.; Yeung, E. S.: *Anal. Chem.*, 69: **(1997)**: 2251.
- [49] Papadoyannis, I.; Arzoglou, p.; Asvesta, S.; Grammatopoulos, D.; Lazaridis, A.: *Anal. Lett.*, 22: **(1989)**: 545.
- [50] Higashidate, S.; Imai, K.: *Analyst*, 117: **(1992)**: 1863.
- [51] Camanas, R. M. V.; Mallols, J. M. S.; Lapasio, J. R. T.; Ramos, G. R.: *Analyst*, 120: **(1995)**: 1767.
- [52] Nohta, H.; Yukizawa, T.; Ohkura, Y.; Yoshimura, M.; Ishida, J.; Yamaguchi, M.: *Anal. Chim. Acta.*, 344: **(1997)**: 233.
- [53] Salem, F. B.: *Anal. Lett.*, 26: **(1993)**: 1959.
- [54] Nohta, H.; Lee, M-k.; Ohkura, Y.: *Anal. Chim. Acta.*, 267: **(1992)**: 137.
- [55] Salem, F. B.: *Anal. Lett.*, 26: **(1993)**: 281.
- [56] Rudewicz, P.; Straub, K. M.: *Anal. Chem.*, 58: **(1986)**: 2928.
- [57] Camanas, R. M. V.; Mallols, J. M. S.; Alfonso, E. F. S.; Ramos, G. R.: *Anal. Lett.*; 25: **(1992)**: 1425.
- [58] Hirabayashi, A.; Sakairi, M.; Koizumi, H.: *Anal. Chem.*, 67: **(1995)**: 2878.
- [59] Patony, G., Ed. *HPLC Detection*. VCH, NY, **(1992)**.

- [60] Lunte, C., in Kissinger and Heineman (Eds.). Laboratory Techniques in Electroanalytical Chemistry, 2nd Edition. MerceL Dekker, NY, (1996).
- [61] Brunt, B. O.; Westerink, B. H. C.; Doornbos, D. A.: Anal. Chem., 52: (1980): 203.
- [62] McClintock, S. A.; Purdy, W. C.; Young, S. N.: Anal. Chim. Acta., 166: (1984): 171.
- [63] Gunasingham, H.; Tay, B. T.; Ang, K. P.: Anal. Chem., 59: (1987): 262.
- [64] Hong, C. S.; Bush, B.; Seegal, R. F.; Broshc, K. O.: Anal. Lett., 20: (1987): 435.
- [65] Owens, D. S.; Johnson, C. M.; Sturrock, P. E.; Jaramillo, A.: Anal. Chim. Acta., 197: (1987): 249.
- [66] Masters, C. F.; Markey, S. P.; Mefford, I. N.; Duncan, M. W.: Anal. Chem., 60: (1988): 2131.
- [67] Aoki, A.; Matsue, T.; Uchida, I.: Anal. Chem., 62: (1990): 2206.
- [68] Cooper, B. R.; Jankowski, J. A.; Leszczyszyn, D. J.; Wightman, R. M.; Jorgenson, J. W.: Anal. Chem., 64: (1992): 691.
- [69] Galal, A.; Atta, N. F.; Rubinson, J. F.; Zimmer, H.; Mark, H. B.: Anal. Lett., 26: (1993): 1361.
- [70] Cheng, F-C.; Lin, N-N.; Kao, J-S.; Cheng, L-J.; Chang, F-M.; Chia, L-G.: Electroanalysis, 6: (1994): 871.
- [71] Msimanga, H. Z.; Sturrock, P. E.: Electroanalysis, 7: (1995): 967.
- [72] Niwa, O.; Morita, M.; Soloman, B. P.; Kissinger, P. T.: Electroanalysis, 8: (1996): 427.
- [73] Hsieh, S.; Jorgenson, J. W.: Anal. Chem., 69: (1997): 3907.
- [74] Tsionsky, M.; Gun, G.; Glezer, V.; Lev, O.: Anal. Chem., 66: (1994): 1747.
- [75] Wang, J.; Pamidi, P. V. A.; Park, D. S.: Anal. Chem., 68: (1996): 2705.
- [76] Jun, J.; Tsionsky, M.; Rabinovich, I.; Golan, Y.; Rubenstein, I.; Lev, O.: J. Electroanal. Chem., 395: (1995): 57.
- [77] Dave, B.; Dunn, B.; Valentine, J. S.; Zink, J.: Anal. Chem., 66: (1994): 1120A.
- [78] Tsuchiya, H.; Koike, T.; Hayashi, T.: Anal. Chim. Acta., 218: (1989): 119.

- [79] Lev, O.; Tsionsky, M.; Rabinovich, L.; Glezer, V.; Sangarth, S.; Pankratov, I.; Gun, J.: *Anal. Chem.*, 67: (1995): 22A.
- [80] Aoki, A.; Matsue, J.; Uchida, I.: *Anal. Chem.*, 64: (1992): 44.
- [81] Van-Zee, J.; Newman, J.: *J. Electrochem. Soc.*, 124: (1977): 706.
- [82] Hawley, M. D.; Tatawawada, S. V.; Piekarski, S.; Adams, R. N.: *J. Am. Chem. Soc.*, 89: (1967): 447.
- [83] Sterson, A. W.; McCreedy, R.; Feinberg, B.; Adams, R. N.: *J. Electroanal. Chem.*, 46: (1973): 313.
- [84] Wang, J.; Freiha, B.: *Anal. Chem.*, 56: (1984): 2266.
- [85] Gunasingham, H.; Tay, B. T.; Ang, K. P.: *Anal. Chim. Acta.*, 176: (1985): 143.
- [86] Fleet, B.; Little, C. J.: *J. Chromatogr. Sci.*, 12: (1974): 747.
- [87] Crompton, T. R.: *Determination of Organic Substances in Water*. John Wiley & Sons; New York, (1985).
- [88] Health, A. G.: *Water Pollution and Fish Physiology*. CRC Press: Boca Raton, (1987).
- [89] Greenburg, A. E.; Trussell, R. R.; Clesceri, L. S.: *Standard Methods for the Examination of Water and Wastewater*. WPCF Pub., (1985).
- [90] Ewing, G. W.: *Environmental Analysis*. Academic Press Pub. NY, (1977).
- [91] Hawthorne, S. B.; Yang, Y.; Miller, D. J.: *Anal. Chem.*, 66: (1994): 1912.
- [92] Costarramone, N.; Hazourli, S.; Bonnecuze, G.; Astruc, M.: *Environ-Technol.*, 15(3): (1994): 199.
- [93] Angelino, S.; Gennaro, M. C.: *Anal. Chim. Acta.*, 346: (1997): 61.
- [94] Heberer, T.; Stan, H. J.: *Anal. Chim. Acta.*, 341: (1997): 21.
- [95] Poerschmann, J.; Zhang, Z.; Kopinke, F.D.; Pawliszyn, T.: *Anal. Chem.*, 69: (1997): 597.
- [96] Kontsas, H.; Rosenburg, C.; Pfaffli, P.; Jappinen, P.: *Analyst*, 120: (1995): 1745.
- [97] Fingler, S.; Tzalcevic, B.; Frobe, Z.; Drevenker, V.: *Analyst*, 119: (1994): 1135.
- [98] Bechholz, K. D.; Pawliszyn, J.: *Anal. Chem.*, 66: (1994): 160.
- [99] Pravda, M.; Petit, C.; Michotte, Y.; Kauffmann, J. M.; Vytras, K.: *J. Chromatogr.*, 727: (1996): 47.

- [100] Connor, M.; Wang, J.; Kubcik, W.; Smyth, M. R.: *Anal. Chim. Acta.*, 229: (1990): 139.
- [101] Ortega, F.; Dominguez, E.; Burestedt, E.; Emneus, J.; Gorton, L.; Marko-Varga.: *J. Chromatogr.*, 675: (1994): 65.
- [102] Ortega, F.; Cuevas, J.; Centenera.; Dominguez, E.: *J. Pharm. Biomed. Analysis.*, 10: (1992): 789.
- [103] Wang, J.; Lu, F.; Kane, S. A.; Choi, Y. K.; Smyth, M. R.; Rogers, K.: *Electroanalysis*, 9: (1997): 14.
- [104] Kulys, J.; Schmid, R. D.: *Bioelectrochem. Bioenerg.*, 24: (1990): 305.
- [105] Kulys, J.; Bilitewski, U.; Schmid, R. D.: *Bioelectrochem. Bioenerg.*, 26: (1991): 277.
- [106] Tatsuma, T.; Okawa, Y.; Watanabe, T.: *Anal. Chem.*, 61: (1989): 2352.
- [107] Tatsuma, T.; Gondaira, M.; Watanabe, T.: *Anal. Chem.*, 64: (1992): 1183.
- [108] Deng, Q.; Dong, S.: *J. Electroanal. Chem.*, 377: (1994): 191.
- [109] Wollenberger, U.; Wang, J.; Ozsoz, M.; Gonzalez-Romero, E; Scheller, F.: *Bioelectrochem. Bioenerg.*, 26: (1991): 287.
- [110] Zulfikar, X.; Hibbert, D. B.; Alexander, P. W.: *Electroanalysis*, 7: (1995): 722.
- [111] Gorton, L.; Csoregi, E.; Dominguez, E.; Emneus, J.; Jonsson-Pettersson, G.; Marko-Varga, G.; Persson, B.: *Anal. Chim., Acta.*, 250: (1991): 203.
- [112] Gorton, L.; Jonsson-Pettersson, G.; Csoregi, E.; Johansson, K.; Dominguez, E.; Marko-Varga, G.: *Analyst*, 117: (1992): 1235.
- [113] Popescu, I. C.; Zetterberg, G.; Gorton, L.: *Biosensors Bioelectro.*, 10: (1995): 443.
- [114] Domenguez-Sanchez, P.; Miranda-Ordieres, A. J.; Costa-Garcia, A.; Tunon-Blanco, P.: *Electroanalysis*, 3: (1991): 281.
- [115] Oungpipat, W.; Alexander, P. W.; Southwell-Keely, P.: *Anal. Chim. Acta.*, 309: (1995): 35.
- [116] Navaratne, A.; Rechnitz, G. A.; *Anal. Chim. Acta.*, 257: (1992): 59.
- [117] Wang, J.; Lin, M. S.: *Electroanalysis*, 1: (1989): 43.
- [118] Chen, L.; Lin, M. S.; Hara, M.; Rechnitz, G. A.: *Anal. Lett.*, 24: (1991): 1.
- [119] Pravda, M.; Adeyoju, O; Iwuoha, E. I.; Vos, J. G.; Smyth, M. R.; Vytras, K.: *Electroanalysis*, 7: (1995): 619.

- [120] Iwuoha, E. I.; Smyth, M. R.; Vos, J. G.: *Electroanalysis*, 6: (1994): 982.
- [121] Rohde, E.; Dempsey, E.; Smyth, M. R.; Vos, J. G.; Emons, H.: *Anal. Chim. Acta.*, 278: (1993): 5.
- [122] Ruzgas, T.; Csoregi, E.; Emneus, J.; Gorton, L.; Marko-Varga, G.: *Anal. Chim. Acta.*, 330: (1996): 123.
- [123] Iwuoha, E. I.; Leister, I.; Miland, E.; Smyth, M. R.; Fagan C.: *Anal. Chem.*, 69: (1997): 1674.
- [124] Forster, R.J.; Vos, J.G.: *Macromolecules*, 23: (1990): 4372.
- [125] Brett, O. & Brett, C.: *Electrochemistry, Principles, Methods and Applications*. (1993), Oxford University Press.
- [126] Nicholson, R., S.; Shain, I.: *Anal. Chem.*, 36: (1964): 706.
- [127] Adeyoku, O.; Iwuoha, E. I.; Smyth, M. R.: *Anal. Chim. Acta.*, 305: (1995): 57.
- [128] Iwuoha, E. I.; Smyth, M. R.; Lyons, M. E. G.: *J. Electroanal. Chem.*, 390: (1995): 35.
- [129] Matthews, C. K.; van Holde, K. E.: *Biochemistry*; Benjamins/ Cumins Pub., Inc. (1990).
- [130] Jinno, K.; Kawasaki, K.: *Chromatographia*, 18: (1984): 90.

Chapter 5

Electrochemical Reactivities of Cytochrome

P450_{cam} Immobilised in a

Methyltriethoxysilane Sol-Gel

and its

Environmental Application

5.1. Introduction

Cytochromes P450 are important enzymes for a wide range of organisms. The vast array of biological reactions catalysed by cytochromes is paralleled by the large number of isozymic forms isolated and evaluated from different sources [1,2]. These distinct cytochrome P450 systems are not uniquely defined by their chemical reactivities, but rather by their relative preference for various substrates. The relative preference demonstrated by a given cytochrome P450 for a particular substrate reflects not only differences in chemical intermediates, but also differences in active site topology which allows for more efficient juxtaposition of substrate with a common oxidising intermediate.

They constitute a ubiquitous family of haem-dependent monooxygenases, which along with their redox components catalyse a two electron reduction of oxygen to produce an active iron-oxygen species and a single molecule of water. This iron-oxygen complex is active in hydroxylation, epoxidation and heteroatom dealkylation, and is responsible for the metabolism of drugs, the processing of steroid hormones, carcinogen activation, the detoxification and solubilisation of lipophilic xenobiotics and various other roles in peripheral catabolic pathways [3-6].

Cytochrome P450_{cam} has been genetically engineered [7] from the soil bacterium, *Pseudomonas putida*, and expressed in plasmids incorporated into *Escherichiae coli*. It is responsible for the regiospecific hydroxylation of the monoterpene camphor to form 5-exohydroxycamphor, and has the ability to hydroxylate several other substrates, as demonstrated by Iwuoha et al [8].

However, it is extremely difficult to observe the electrochemistry of this enzyme on unmodified electrode surfaces as shown by Kazlauskaite et al [9] and Bianco and Haladjian [10], due to repulsive and thus unfavourable surface interactions [11]. This problem can be overcome by incorporating the enzymes into biomembranes that isolate the enzyme from surface contact but yet facilitate rapid electron exchange with the underlying electrode surface. For example, electron transfer to haem iron in liquid-

crystal myoglobin lipid films was enhanced up to 1000-fold compared with rates at bare electrodes in protein solutions [12-13].

This electrode design can be achieved by incorporating the cytochromes P450 into vesicle dispersions of the synthetic lipid material didodecyldimethylammonium bromide (DDAB). The latter material forms stable lamellar crystal films at 25 °C which can be used as hosts for the enzyme allowing immobilisation onto the electrode surface and rapid electron transfer into and out of the film, simulating *in vivo* catalytic metabolism [14-16].

Despite the added advantages of such a system, Iwuoha et al. [8] have shown the P450_{cam}-DDAB electrodes to be unstable under hydrodynamic conditions. This has been attributed to the partial desorption of the lipid crystal layer from the surface of the electrode. In an effort to stabilise the P450_{cam} - DDAB biosensor, the work presented in this chapter involves the encapsulation of P450_{cam}-DDAB crystals into a methyltriethoxysilane (MTEOS) sol-gel layer.

Much interest has evolved in recent years in the use of sol-gels for the immobilisation and entrapment of enzymes at electrode surfaces [17-20]. Sol-gels are formed through the acid or base hydrolysis of the silane monomer followed by rapid condensation reactions, resulting in the formation of high density silica gels. These silica gels can be tailor-made for specific applications depending on choice of parent monomer and dopant molecules. Sol-gels of various pore-sizes can be constructed, and the gel can be cast into any shape or form. The reactions are non-violent, occur at room temperature, and the raw materials are relatively inexpensive.

The enzymes are encapsulated by the sol-gel network resulting in a fluidic environment similar to that of biological membranes. The pore sizes are sufficiently large enough to allow substrate/ product diffusion into and out of the sol-gel network whilst still being adequately small enough to prevent leaching of the enzyme into solution.

The electrochemical behaviour of this cytochrome-P450_{cam}-DDAB-sol-gel encapsulated biosensor is evaluated in this chapter. The behaviour of the biosensor in both aqueous and organic media is demonstrated along with the relevant kinetic data pertaining to the system. The catalytic response of this biosensor to camphor and adamantanone substrates and the polyaromatic hydrocarbon pyrene is presented and discussed.

The potential mutagenic and carcinogenic [21-23] effects of polyaromatic hydrocarbons have warranted their extensive analysis by a wide range of analytical techniques and methodologies. Gas chromatography with mass spectroscopy [24-26], high performance liquid chromatography [27], fluorimetry [28] and cyclodextrin modified capillary electrophoresis have all been utilised [29]. The possibility of using this cytochrome-P450_{cam}-DDAB-sol-gel encapsulated biosensor as an alternative method for the analysis of PAHs is critically assessed.

5.2. Experimental

5.2.1. Reagents

Cytochrome P450_{cam} (M_r 46 500) was prepared by genetic engineering [7] with subsequent purification as a 50 μ M solution. The enzyme was stored in the freezer at - 80 °C when not in use. Didodecyldimethylammonium bromide (DDAB) was obtained from Fluka (Germany) and stored at 5 °C. A 10 mM vesicle dispersion of DDAB was prepared by sonicating for 8 hours a 4.6 mg sample of the compound in 1 ml of water. Camphor, adamantanone, glutaraldehyde and methyltriethoxysilane were obtained from Aldrich (Gillingham, UK). Analytical standard pyrene (99.9 % purity) was obtained from Forbairt (Dublin, Ireland). HPLC grade acetonitrile and hydrochloric acid were obtained from Lab Scan (Dublin, Ireland). Absolute alcohol analytical grade was obtained from James Burrough Ltd (Essex, UK). 1 mM tetraethylammonium p-toulenesulphonate, obtained from Aldrich (Milwaukee, USA), was used as electrolyte in the organic phase studies. Analytical grade argon (Air-Products Plc, UK) was used to degas all samples. Buehler (IL, USA) alumina micropolish and polishing pads were used for electrode polishing. All solutions were prepared in deionised water obtained by passing distilled water through a Milli-Q-water purification system, unless otherwise stated. 0.05 M phosphate buffer (pH 7.5), containing 0.01 M potassium chloride, Fluka (Germany), was prepared from AnalaR grade anhydrous disodium hydrogenorthophosphate, and AnalaR grade potassium dihydrogenphosphate dihydrate from Merck (Poole, Dorset). The anhydrous salt was dried for 3 h at 110 °C and cooled in a dessicator before it was used for buffer preparation. Cobalt sepulchrate, which was the electron transfer mediator in the steady state experiments [30], was obtained from Aldrich (Milwaukee, USA). Bovine serum albumin was obtained from Sigma (MO, USA).

5.2.2. Instrumentation

All analyses were performed on a BAS 100B integrated, automated electrochemical workstation from BioAnalytical Systems (BAS, Stockport, UK), connected to a three electrode 10 ml cell, containing glassy carbon (GCE) as the working electrode (0.071 cm² Metrohm, Herisau, Switzerland), platinum wire mesh counter electrode and

silver/silver chloride as the reference electrode (BAS Technicol, Stockport, UK). A Heto (Denmark) thermostatically controlled waterbath was used to maintain the experimental temperature at 25 °C. A home-made spin coater and a Steinal HL 1800E heated gun were used to prepare the electrodes. Amperograms and voltammograms were recorded with a computer interfaced to the BAS 100B electrochemical workstation. For the steady state experiments, an analytical rotator (Model ASRE 416) and ASR speed control unit were utilised from the Pine Instrument Company (Pennsylvania, USA).

5.2.3. *Sol-gel and Electrode Preparation*

5.2.3.1. Sol-gel preparation

The sol-gel was prepared by mixing 500 μl methyltriethoxysilane (MTEOS) with 750 μl deionised water and 50 μl 0.1 M HCl in a 10 ml glass reaction vessel. This was stirred at 300 rpm for one hour, and left for 24 hr before use. The glassy carbon electrodes were polished prior to use using 1.0 μm , 0.3 μm and 0.05 μm grade alumina, rinsed thoroughly with deionised water and allowed to dry.

5.2.3.2. GCE/[P450_{cam} + DDAB + Sol-gel] biosensor preparation

The electrode composite was prepared as follows. 50 μl of the 10 mM aqueous vesicle dispersion of DDAB was mixed with 2 mg bovine serum albumin (BSA) to form solution A. 50 μl of 38 $\mu\text{g ml}^{-1}$ P450_{cam} was added to solution A to form the enzyme synthetic membrane complex, called solution B. 130 μl glutaraldehyde was added and mixed thoroughly with the sol-gel. Then 3 μl of solution B was mixed with 2 μl of the MTEOS sol-gel containing 2.5% glutaraldehyde on a 0.071 cm^2 GCE.

The electrodes were cast by both passive deposition and spin coating. For the passive deposition electrodes, the cast layer was deposited onto the electrode surface and allowed to dry for 1 hr under the low heat of a heated gun. For the spin coated electrodes the enzyme film was placed on the electrode surface and the electrodes were spun at a rate of 400 rpm for a duration of 1 hr under low heat. The deposition and spin

coating processes resulted in the formation of P450_{cam}-DDAB liquid crystals encapsulated within a sol-gel network layer.

The electrodes were then stored for 12 hours at room temperature in a closed vessel in darkness. The final composition of the biosensor on the electrode was 0.08 mg cm⁻² P450_{cam}, 15 nmol DDAB, 0.05mg BSA and 1.0% glutaraldehyde. For simplicity purposes the GCE/[P450_{cam} + DDAB + Sol-gel] biosensor will be referred to as the GCE-[P450_{cam}/DDAB/SG] biosensor in the remainder of this text.

5.2.4. Procedure

For the aqueous phase analyses, 0.05 M phosphate buffer (pH 7.5) containing 0.01 M potassium chloride was prepared from anhydrous disodium hydrogenorthophosphate and potassium dihydrogenphosphate dihydrate. For the organic phase analyses, acetonitrile made 1 mM in tetraethylammonium p-toluenesulfonate, was used as the electrolyte. All solutions were degassed for a period of 20 minutes prior to analysis and kept under an argon atmosphere for the duration of the experiment. All experiments were carried out at a thermostatically controlled temperature of 25 °C. Voltammograms were recorded in the presence and absence of 3 mM camphor (ethanolic solution) at a potential sweep rate of 500 mV/s from an initial potential, $E_i = + 100$ mV to a switch potential, $E_\lambda = - 650$ mV.

5.2.5. Steady State Amperometry

For these measurements the enzyme electrode was polarised at -800 mV vs. Ag/AgCl and experiments were performed under a thermostated temperature of 25 °C. The electrolyte was 10 ml of 0.05 M phosphate buffer containing 0.01 M KCl solution, and 50 μM cobalt sepulchrates as the electron mediator. The experiments were performed under anaerobic conditions and the background current was allowed to decay to steady state, followed by 0.1 mM successive additions of camphor and pyrene, to the cell solution which was stirred continuously at 500 rpm.

5.3. Results and Discussion

5.3.1. Properties of Cytochrome $P450_{cam}$

It has been shown through the analysis of X-ray crystal structures for free enzyme, camphor bound enzyme and inhibitor complexed forms of cytochrome $P450_{cam}$, that no significant conformational changes occur when camphor binds at the enzyme active site [31, 32]. The major structural difference which distinguishes the substrate-free enzyme from the camphor bound form of cytochrome $P450_{cam}$ results from the camphor induced expulsion of six water molecules from the enzyme's active site. In the absence of substrate, the enzyme possesses a low spin six-coordinate aquo-ligated ferric haem which, upon camphor addition, becomes high spin five coordinate with the 5-carbon of camphor situated 2-3 Å above the iron center poised for hydrogen abstraction by the putative $[FeO]^{3+}$ intermediate. This change from low spin to high spin haem is accompanied by a change in reduction potential facilitating electron transfer [33].

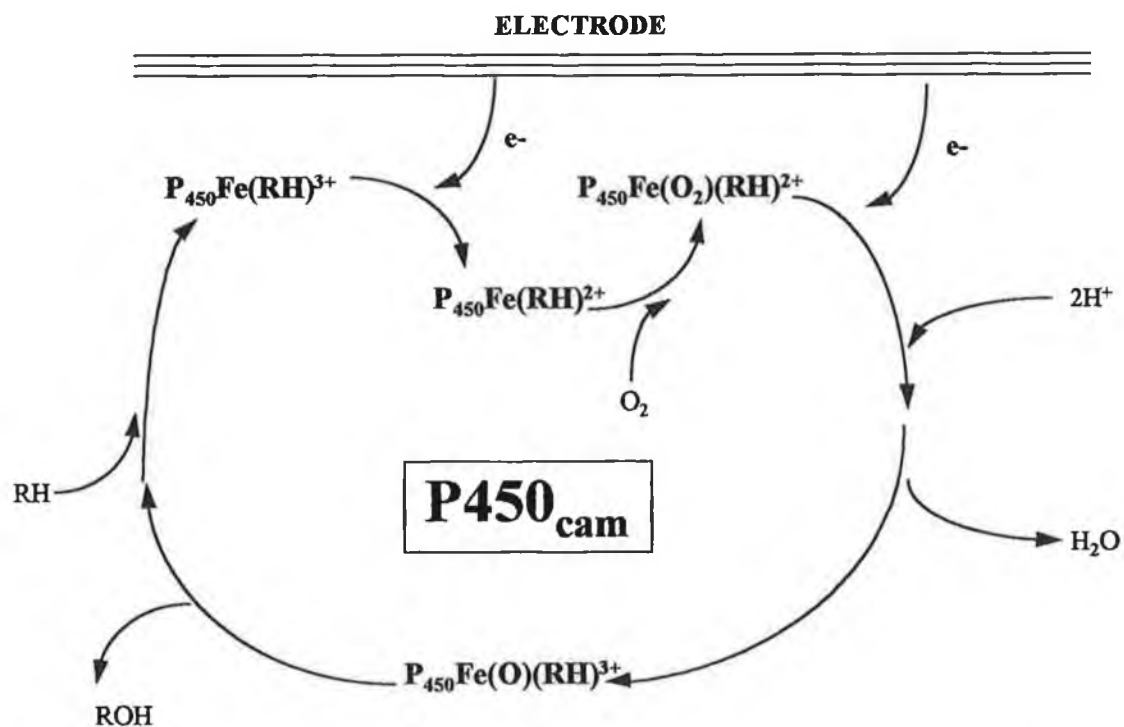


Figure 5.1. Suggested electrocatalytic mechanism for cytochrome $P450_{cam}$ (From Iwuoha et al. [8]).

The reduction of cytochrome P450_{cam} is followed by binding of molecular oxygen to produce dioxy-ferrous cytochrome P450_{cam}, followed by a second electron transfer which results in the net two electron reduction of molecular oxygen with subsequent O-O bond scission and monooxygenation of camphor to produce 5-exo-hydroxycamphor as the sole product [34], as shown in Figure 5.1. Whilst bound at the active site, the camphor molecule is in van der Waals' contact with several protein residues, including valine 295, valine 247, leucine 244 and phenylalanine 87. There is also a unique hydrogen bond formed between the carbonyl moiety of camphor and tyrosine 96, as shown in Figure 5.2. The role of this hydrogen bond in substrate binding and spin state equilibria is of utmost importance in dictating the regioselectivity of hydroxylation. It is also of importance to note that the cluster of water molecules ligated to the haem iron do not hydrogen bond to tyrosine 96, hence facilitating the rapid expulsion of the water molecules from the haem pocket upon substrate binding.

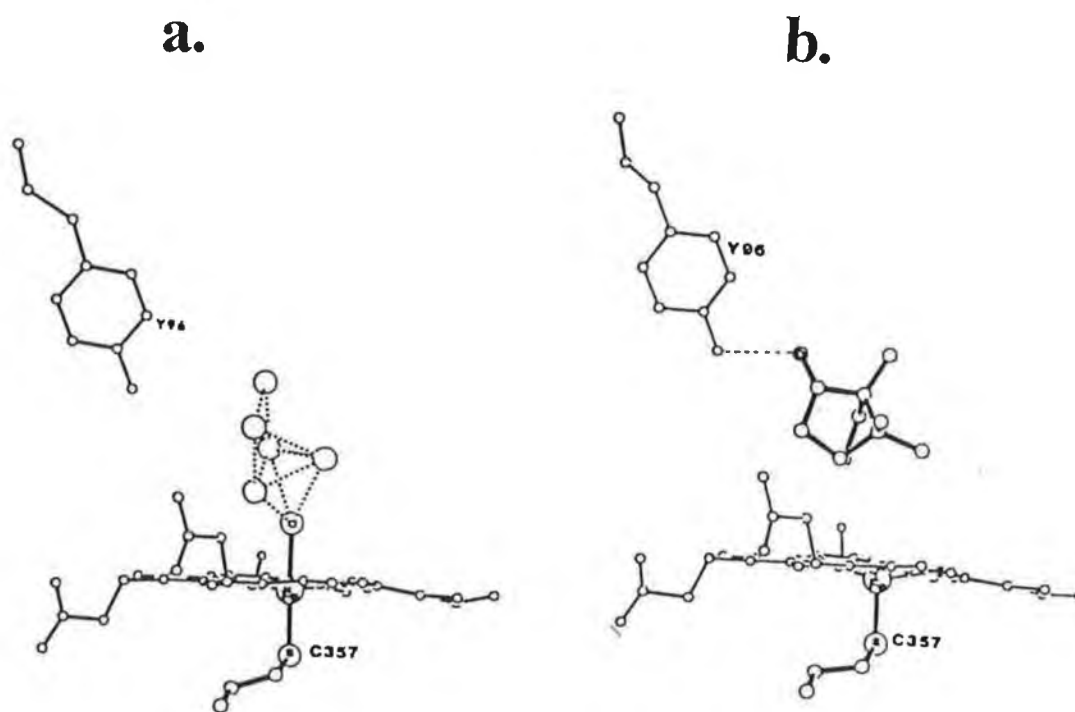


Figure 5.2. Active site structure of cytochrome P450_{cam}. (a) Represents an edge on view of the heme pocket in the absence of camphor, showing the presence of a cluster of water molecules. (b) Represents, the same perspective in the presence of camphor.

Cytochrome P450_{cam} also demonstrates a K⁺ ion dependence for its spin state equilibria, where increasing concentrations of potassium result in a higher fraction of high spin form for a given substrate concentration [35]. The structural basis for this K⁺ dependence is known to involve a specific K⁺ binding site. The cation sits at the end of a short helical segment formed by residues 90-96. The tyrosine 96 carbonyl oxygen flips from the helical axis toward the cation to form a metal ligand. This distortion allows for the Tyr96-camphor interaction, and is the reason why 0.01M KCl was incorporated in the experimental regime of this work, hence ensuring maximum high spin configuration.

5.3.2. Electrode Characterisation

Three different preparations of cytochrome P450_{cam} were investigated for their catalytic performance. This involved using 38 μ M P450_{cam}, 28 μ M P450_{cam} and 38 μ M native P450 enzyme, and preparing the biosensors as outlined in Section 5.2.3.2. The maximum catalytic currents, I_{max} , obtainable for each electrode were 5.6 μ A, 4.6 μ A and 4.4 μ A respectively. It is not surprising that the genetically engineered P450_{cam} gave greater I_{max} values due to its higher specificity for the camphor substrate.

The 38 μ M cytochrome P450_{cam} stock solution was used in the preparation of the GCE-[P450_{cam}/DDAB/SG] biosensors in the remainder of these studies. Two electrode preparation methods were investigated, the first being that of spin coating and the second method being simple deposition. In the spin coating method, the enzyme-lipid sol-gel mix was deposited on a home-made spin coater and the resultant enzyme layer was formed through the combined action of centrifugal and radial forces. However, electrodes prepared by this method tended to crack as the film dried. This was attributed to shear stress due to the complexity of the enzyme lipid crystal vesicle system forming whilst encapsulated within a sol-gel network.

It was therefore decided to use a simple deposition method to allow the enzyme lipid crystals to self-assemble naturally within the sol-gel network, resulting in more intact enzyme layers on the electrode surface. The electrodes prepared by simple deposition also yielded higher responses than those prepared by spin-coating, suggesting that some

of the cytochrome P450 enzyme may be damaged by the centrifugal and radial forces in retrospect of lipid crystal vesicle formation within the sol-gel network.

5.3.3. Cyclic Voltammetry of the GCE-[P450_{cam}/DDAB/SG] biosensor

As discussed by other authors [12-16], the incorporation of cytochrome P450_{cam} into lipid crystal vesicles results in rapid electron hopping into and out of the lipid film to and from the electrode surface, without the enzyme coming into contact with the surface and hence avoiding unnecessary repulsive interactions [9-10]. Since the enzyme lipid sol-gel network is cast on the electrode surface, one would expect [36] a linear variation of peak currents with scan rate according to equation 5.1.:

$$I_p = v [n^2 F^2 \Gamma_T / 4RT] \quad (5.1)$$

where I_p is the peak current observed in A; v is the scan rate in mV/s; n is the number of electrons involved in the system; F is Faraday's constant, $96\,480\text{ C mol}^{-1}$; Γ_T , mol cm^{-3} is the total amount of electro-active material on the electrode surface; R is the universal gas constant, $8.314\text{ J mol}^{-1}\text{ K}^{-1}$ and T is the temperature in K.

Figure 5.3.(b) shows plots of peak cathodic (A) and anodic (B) currents versus scan rate for the GCE-[P450_{cam}/DDAB/SG] biosensor in both phosphate buffer solution(I) and 90% acetonitrile solution (II). A linear correlation between peak currents and scan rate was obtained as expected. Figure 5.3.(a) shows cyclic voltammograms of various scan rates up to 200 mV/s. The voltammograms have clearly defined cathodic and anodic peaks, representing the presence of only one redox species. Since the experiments were performed in oxygen-free solutions, these peaks can be attributed to the haem $\text{Fe}^{3+/2+}$ redox centre in cytochrome-P450_{cam}. The voltammograms had nearly symmetrical shapes which is characteristic of electrochemistry in a thin film [37] suggesting that all the active Cyt P450 Fe^{3+} is reduced to P450 Fe^{2+} on the forward scan, and Cyt P450 Fe^{2+} is oxidised to P450 Fe^{3+} on the reverse scan.

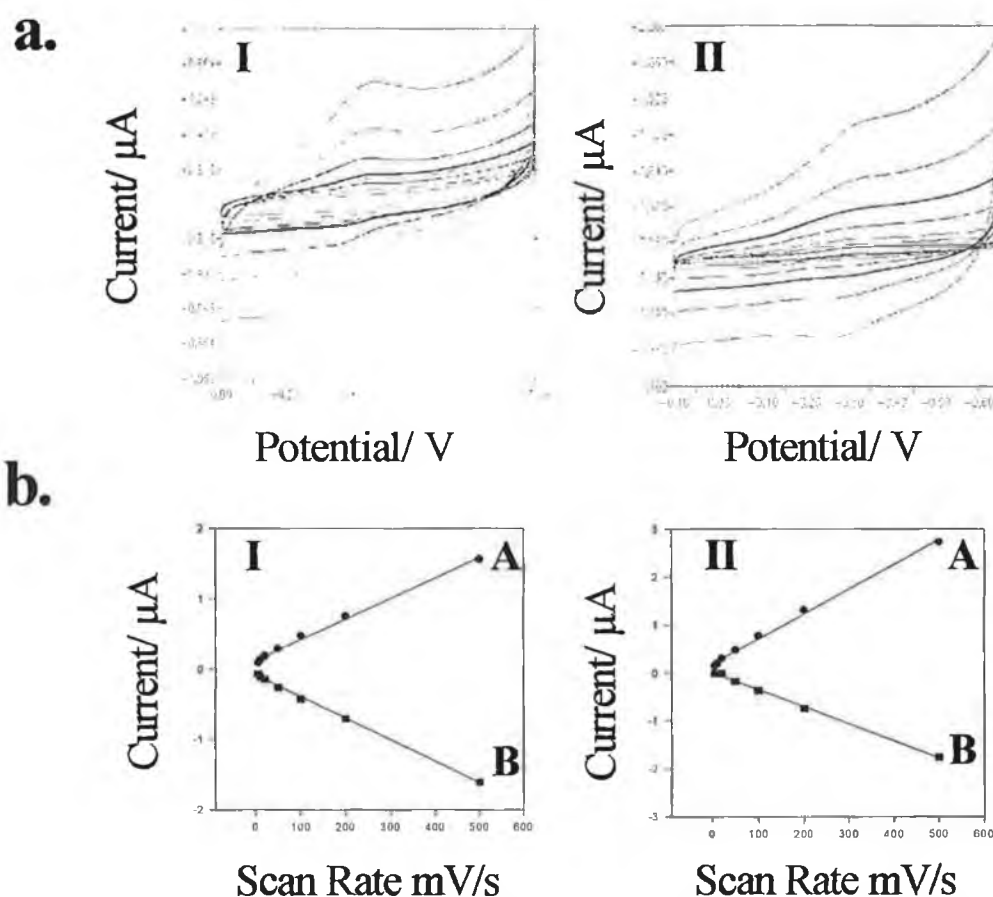


Figure 5.3. (a) Cyclic voltammograms of the GCE-[P450_{cam}/DDAB/SG] biosensor from 2 mV/s to 200 mV/s in (I) 0.05M phosphate buffer and (II) 90% acetonitrile. (b) Represents the corresponding current versus scan rate plots up to 500 mV/s. (A) cathodic current, (B) anodic currents. Experiments were performed at 25 °C, and scanned from + 0.10 V to - 0.60 V. All solutions were degassed and maintained under an argon atmosphere.

Information pertaining to the reversibility of an electrochemical process can be obtained from the ΔE_p and $I_{p,a}$ and $I_{p,c}$ values of a redox species [38, 39]. An $I_{p,a}/I_{p,c}$ value of 1.0 shows that the electron transfer reaction at the electrode is reversible. A ΔE_p value of less than 65 mV is indicative of a surface bound electroactive substance undergoing fast reversible electron transfer reactions at the electrode surface [37]. For the phosphate buffer system an $E_{p,c}$ value of - 408 mV was obtained, Tables 5.1. and 5.2. of page 183, followed by an $E_{p,a}$ value of

-304 mV, and a ΔE_p value of -104 mV. A value of 1.03 was obtained for $I_{p,a}/I_{p,c}$. The relatively high value of ΔE_p of -104 mV can be attributed to the complexity of the enzyme/ lipid/ sol-gel system. Zhang et al. [40] obtained similar results for a phosphatidylphospholipidcholine dimyristoyl encapsulated P450_{cam} system. The higher ΔE_p values were attributed to protein-lipid interactions and possible lipid-dependent electrical double layer effects on the electrode potential. The presence of a complex sol-gel network may also have a role to play in these phenomena.

For the 90% acetonitrile water system an $I_{p,a}/I_{p,c}$ value of 0.64 was obtained with higher peak cathodic currents than the corresponding anodic ones. The $I_{p,c}$ values for the acetonitrile system were also higher than the phosphate buffer system, suggesting an efficient reduction process and electron transfer from Cyt-P450Fe³⁺ to Cyt-P450Fe²⁺. However, for the acetonitrile system, the reverse reaction is not as efficient; this could be due to removal of water molecules from the active site centre [41] hence causing perturbation of the haem orbitals and therefore affecting the Cyt-P450Fe²⁺ to Cyt-P450Fe³⁺ oxidation reaction.

For this organic phase system an $E_{p,c}$ value of - 331.7 mV and an $E_{p,a}$ value of - 269.6 mV was obtained, and a resultant ΔE_p value of - 62.1 mV is representative of a reversible system for a thin layer film on an electrode surface [37]. Both the $E_{p,c}$ and $E_{p,a}$ values for the organic system were shifted to lower reduction and oxidation potentials respectively, compared to the phosphate buffer phase. This could be attributed to a fluidic effect [42] caused by the acetonitrile on the lipid encapsulated sol-gel system. It is possible that under aqueous conditions, the enzyme/lipid/sol-gel network is extremely rigid resulting in large ΔE_p values of - 104 mV. However, in the presence of acetonitrile, the lipid layers are solubilised somewhat within the sol-gel network, resulting in a fluidic effect more representative of a biological membrane observable at lower operating potentials and yielding a more ideal ΔE_p of - 62.1 mV. These results are summarised in Table 5.1. and 5.2., along with values of ΔE_p and E_m obtained by other researchers.

Table 5.1. Peak cathodic and peak anodic potentials, and peak separation ΔE_p .

Electrode	$E_{p,c}$	$E_{p,a}$	$\Delta E_p = (E_{p,c} + E_{p,a})$
GCE-[P450 _{cam} /DDAB/SG] in buffer	-408	-304	-104
GCE-[P450 _{cam} /DDAB/SG] in 90% ACN*	-331.7	-269.6	-62.1
GCE-[P450 _{cam} /DDAB] in buffer [8]	-278	-242	-36

* ACN=acetonitrile

Table 5.2. Comparison of ΔE_p and E_m values

Electrode	$\Delta E_p = (E_{p,c} - E_{p,a})$	$E_m = 1/2(E_{p,c} - E_{p,a})$
GCE-[P450 _{cam} /DDAB/SG] in buffer	-104	-356
GCE-[P450 _{cam} /DDAB/SG] in 90% ACN*	-62.1	-301
GCE-[P450 _{cam} /DMPC] in buffer [40]**	-113	-53
GCE-[P450 _{cam} /DDAB] in buffer [40]	6	47
GCE-[P450 _{cam} /DDAB] in buffer [8]	-36	-260

* ACN=acetonitrile, ** DMPC = phosphatidylphospholipid choline dimyristoyl

5.3.4. Electrochemical Catalysis of the GCE-[P450_{cam}/DDAB/SG] biosensor

As mentioned earlier, the enzyme possesses a low spin six-coordinate aquo-liganded ferric haem which, upon camphor addition, becomes a high spin five coordinate with the 5-carbon of camphor facilitating hydroxylation by the putative $[\text{FeO}]^{3+}$ intermediate. This change from low spin to high spin haem is accompanied by a change in reduction potential facilitating electron transfer [33]. Figure 5.4. shows the catalytic and non-catalytic responses of the GCE-[P450_{cam}/DDAB/SG] biosensor in both aerobic and anaerobic conditions in phosphate buffer for both camphor and pyrene respectively. Also note the insert in Figure 5.4.(a); this represents the response obtained under anaerobic conditions to 3mM camphor when a GCE-[P450_{cam}-SG] biosensor was used. In this GCE-[P450_{cam}-SG] biosensor, no DDAB, glutaraldehyde or bovine serum albumin was used in the electrode preparation. The response is only in the order of a few hundred nA when compared to several μA obtained when the lipid crystal vesicle system is employed.

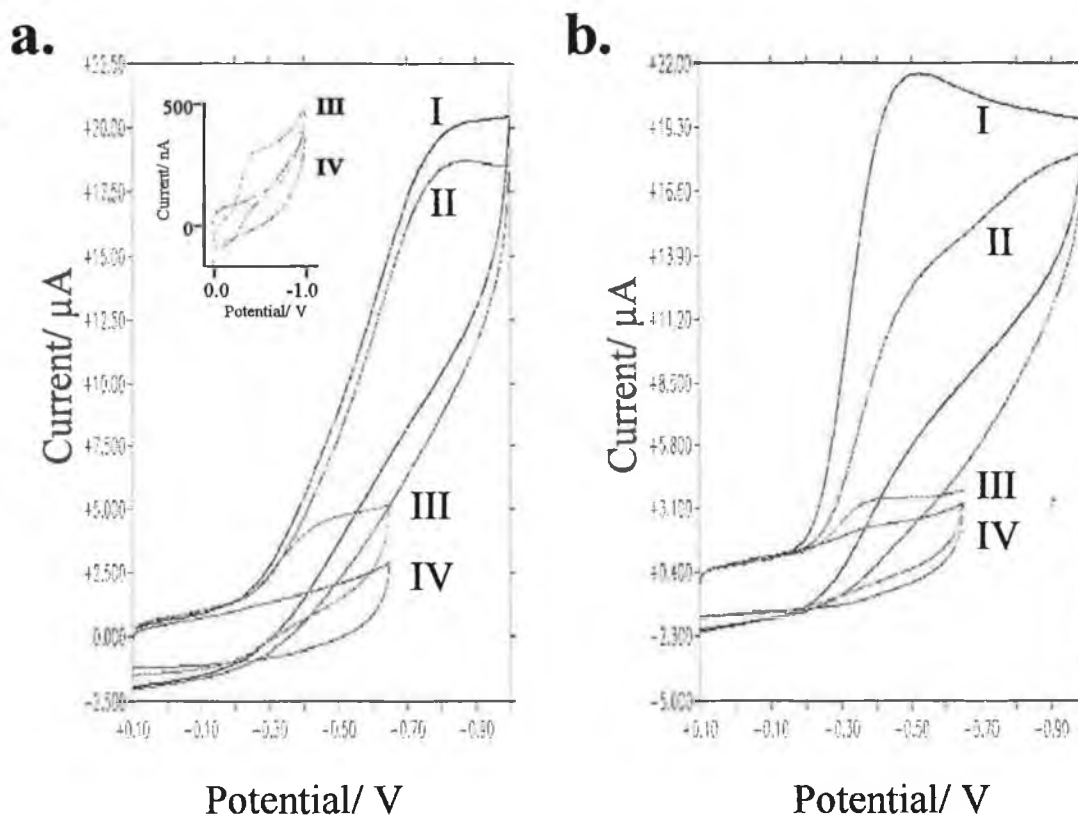


Figure 5.4. Cyclic voltammograms for camphor (a) and pyrene (b) in phosphate buffer solution at a GCE-[P450_{cam}-DDAB-SG] biosensor. Voltammograms (I) and (II) were performed in aerobic solutions and represent the presence and absence of camphor/pyrene respectively. Voltammograms (III) and (IV) were performed in anaerobic solution in the presence and absence of camphor/pyrene respectively. All experiments were performed using a scan rate of 500 mV/s and a temperature of 25 °C. The inset of Figure 5.4.(a) represents the response to camphor at a GCE-[P450_{cam}-SG] biosensor.

Scans (I) and (II) of Figure 5.4.(a) show clearly defined cathodic peaks, which represents the rapid coupling of a fast electron transfer reaction at the electrode surface with oxygen binding to give Cyt P450Fe²⁺-O₂. Irreversible electrochemistry was observed in aerobic solutions both in the presence and absence of camphor. This suggests that one is observing the binding of oxygen to the haem redox centre, where all the Cyt P450Fe²⁺ produced during the cathodic scan is used up in a fast follow up reaction, making it

unavailable for reoxidation during the anodic scan. The presence of camphor increases the rate of this process as shown by the increase in the voltammetric current, resulting in the hydroxylation of camphor to 5-exohydroxycamphor.

The cyclic voltammograms obtained in the presence of camphor under anaerobic conditions, allow the hydroxylation process to be observed more clearly, and represent the coupling of the fast reversible electrochemistry of the haem $\text{Fe}^{3+/2+}$ to the hydroxylation of camphor, with the ethanolic solution in which the camphor was prepared providing enough oxygen for the hydroxylation to occur. The hydroxylation of camphor and pyrene are illustrated in Figure 5.5.

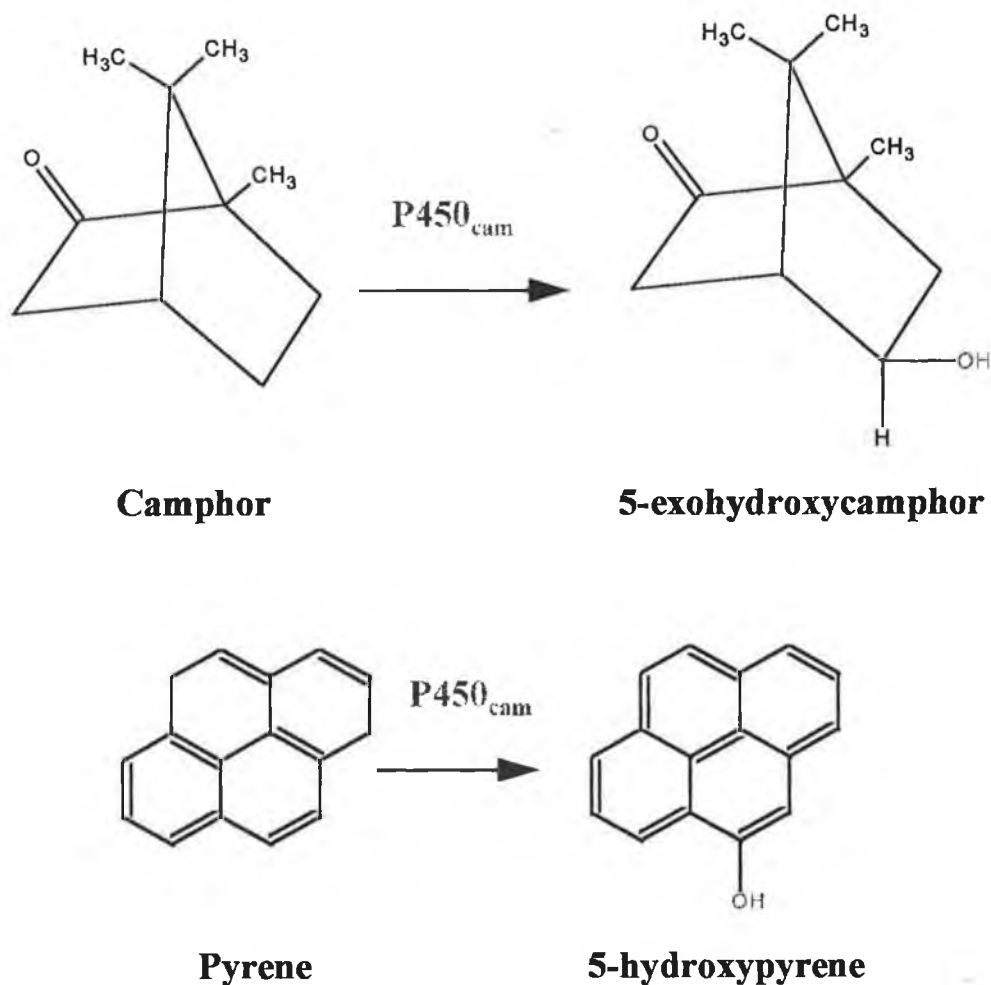


Figure 5.5. Stereospecific hydroxylation of camphor and pyrene.

Under anaerobic conditions, in the absence of camphor in phosphate buffer media, the $E_{p,c}$ value was - 408 mV followed by a shift of + 22.6 mV upon camphor binding to an $E_{p,c}$ value of - 385.4 mV. In acetonitrile, the respective values were - 331.7 mV in the absence of camphor, with a shift of - 58.6 mV in the presence of camphor to an $E_{p,c}$ value of - 390.3 mV. These observed shifts are in agreement with the transformation of the low spin haem centre to a high spin six coordinate, observed upon substrate binding [33].

A similar trend was observed for 3 mM pyrene, as shown in Figure 5.4(b), with an $E_{p,c}$ value of - 395 mV in phosphate buffer, and also yielding an $E_{p,c}$ value of - 351.5 mV in acetonitrile, corresponding to shifts of + 13 mV and - 20.5 mV respectively. These negative shifts observed in acetonitrile could be attributed to the abstraction of water molecules from the active site centre as observed by Iwuoha et al. [41] in other enzyme systems.

In aerobic phosphate buffer solutions, in both the absence and presence of camphor, the cathodic peaks were shifted to more negative potentials. The same trend was observed in the absence of pyrene and to a much lesser extent when pyrene was present. These results disagree with those obtained by Zhang et al. [40] and Iwuoha et al. [8] who observed positive shifts in cathodic potentials in aerobic solutions. However, in the presence of sol-gel, the silicon-oxide component has the ability to bind oxygen resulting in a negative shift in redox potentials as observed here and in earlier work [43].

5.3.5. Temperature Optimisation

In the presence of substrate, the kinetically controlled current or catalytic current (I_K) is controlled by the enzyme kinetics. The electrochemistry in the absence of substrate depends on diffusion to the electrode surface and is represented by I_D . Therefore, the catalytic efficiency of a biosensor, C_{eff} , is determined by the ratio of the peak catalytic current to that of the peak diffusion current:

$$C_{eff} = (I_K / I_D) \quad (5.2)$$

By monitoring the catalytic efficiencies as a function of temperature one can determine the optimum temperature of the system. As shown in Figure 5.6., the optimum temperature was found to be 318 K. The catalytic efficiencies increased firstly up to 293 K, (data not shown), and then plateaued out up to ~ 303 K. The activity then increased exponentially reaching a peak temperature of 318 K, and decreased thereafter. For convenience purposes a temperature of 298 K was chosen for experimental conditions.

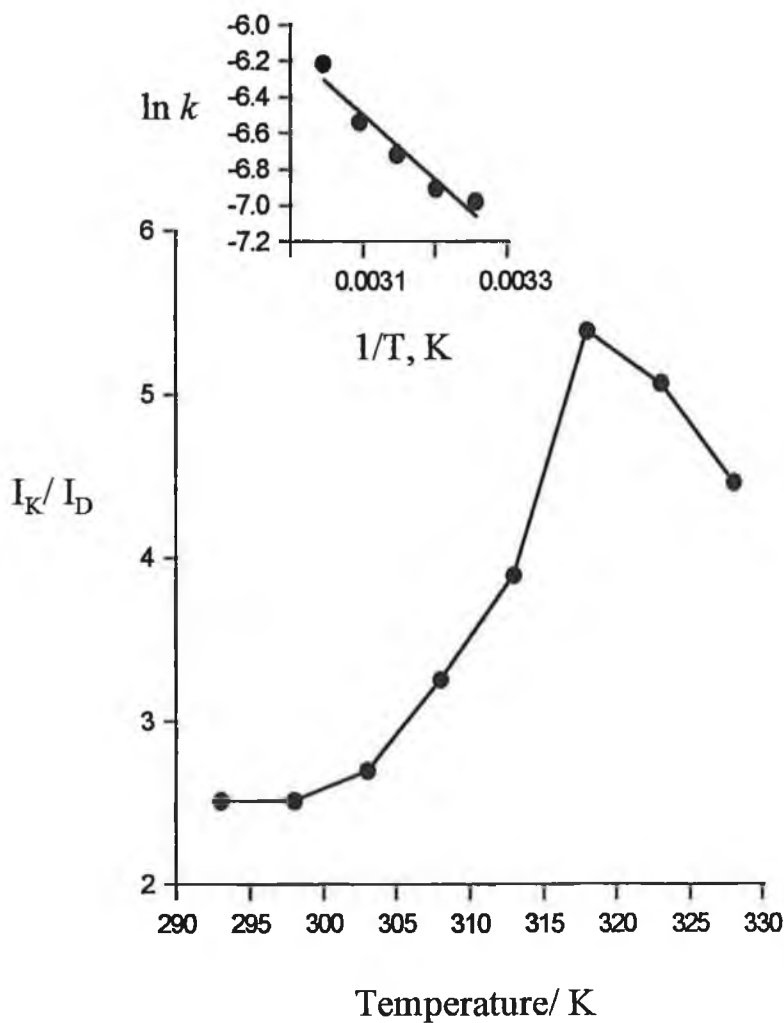


Figure 5.6. Evaluation of optimum temperature conditions.

The catalytic current obtained at each temperature evaluation represents the maximum catalytic current obtainable under those conditions. One can therefore relate the catalytic current to the rate of catalysis through the following equation:

$$I_K = nFAk \quad (5.3)$$

where n is the number of electrons involved in the process; F is Faraday's constant, 96480 C mol^{-1} ; A is the electrode area 0.071 cm^2 , and k is the rate constant of reaction, s^{-1} . The well known relationship between reaction rate and temperature is presented by the Arrhenius equation, which implies that reactions go faster at higher temperatures [42]:

$$k = A e^{-E_a/RT} \quad (5.4)$$

where A is called the preexponential term; E_a is the energy of activation, KJ mol^{-1} ; R is the universal gas constant, $8.314 \text{ J mol}^{-1} \text{ K}^{-1}$, and T is the temperature in K . By taking the natural logarithms of both sides, the following relationship is obtained:

$$\ln k = \ln A - (E_a / RT) \quad (5.5)$$

By plotting the natural logarithm of the rate constant $\ln k$ against the inverse in temperature, $1/T$, the activation energy can be evaluated from the slope as shown by the insert in Figure 5.6., and was found to be $E_a = -29.7 \text{ KJ mol}^{-1}$. This suggests that on exceeding temperatures of $318 \text{ }^\circ\text{C}$, the transition state of the enzymatic reaction is destabilised, resulting in protein unfolding and denaturation and hence a decrease in sensor response.

5.3.6. Organic Phase Studies

These experiments were performed using 3 mM camphor and the catalytic efficiency (I_K/I_D) was evaluated at a scan rate of 500 mV/s in various acetonitrile:water media ranging from 100% to 40% acetonitrile respectively. A plot of the catalytic efficiencies versus the acetonitrile content is shown in Figure 5.7. As can be seen the catalytic efficiency is poor in 100% acetonitrile, and increases as the acetonitrile content decreases and then

plateaus after 90% to 40% acetonitrile. This suggests that in the presence of 100 % acetonitrile, the enzyme could be stripped of its essential water of hydration hence affecting its performance. However, on lowering the acetonitrile content, the activity increases as shown for the 90% acetonitrile evaluation. Iwuoha et al. [41] reported similar results for glucose oxidase in acetonitrile. However, no results were obtained in 100% acetonitrile, but activity increased markedly when a 95% and 90% acetonitrile content was used, indicating that a small amount of water is necessary for enzymic activity in the organic phase.

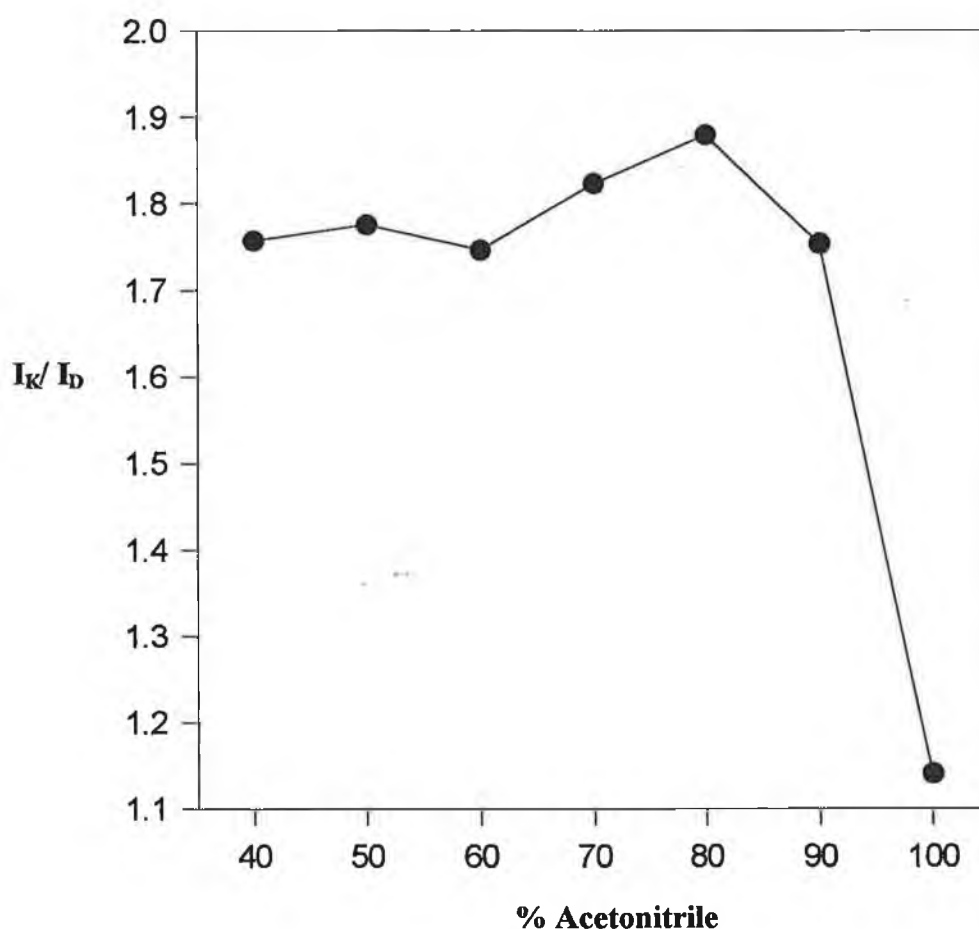


Figure 5.7. Plot of catalytic efficiencies versus acetonitrile percentage. Experiments were performed in anaerobic solution, 500 mV/s, 25°C.

5.3.7. Steady State Amperometry

I_K/I_D values are usually evaluated from cyclic voltammetry experiments. One can also evaluate a similar catalytic efficiency from steady state current time recordings [44]. This takes the form of Michaelis-Menten kinetics:

$$I = [S][I_{\max}]/([S] + K'_M)^{-1} \quad (5.6)$$

where I is the current in Amperes; $[S]$ is the concentration of substrate in mol cm^{-3} ; I_{\max} is the maximum current in Amperes, i.e. the current at which enzyme activity is saturated by substrate; K'_M is the apparent Michaelis-Menten constant, and is a measure of substrate-enzyme binding. This equation can also be represented as follows:

$$I = [S](nFAk_{\text{cat}}\tau[\text{P450}_{\text{cam}}])/([S] + K'_M)^{-1} \quad (5.7)$$

where k_{cat} is the rate of catalysis, s^{-1} ; F is Faraday's constant, $96\,480 \text{ C mol}^{-1}$; n is the number of electrons involved; τ is the thickness of the enzyme layer, cm , and $[\text{P450}_{\text{cam}}]$ is the concentration of enzyme, mol cm^{-3} . The term $k_{\text{cat}}\tau[\text{P450}_{\text{cam}}]$ defines the maximum response of the biosensor realizable at saturating concentrations of substrate. By replacing $k_{\text{cat}}\tau[\text{P450}_{\text{cam}}]$ with k'_{cat} , the apparent rate of catalysis, $\text{mol cm}^{-2} \text{ s}^{-1}$, we get:

$$I = [S](nFAk'_{\text{cat}})/([S] + K'_M)^{-1} \quad (5.8)$$

Since this equation resembles equation (5.6), it suffices that

$$I_{\max} = nFAk \quad (5.9)$$

The k'_{cat}/K'_M values, known as the substrate specificity factor or catalytic efficiency, are indicators of the biosensor's electrocatalytic reaction and are an indication of sensor performance [45].

Figure 5.8. shows the calibration plots obtained for substrates camphor and adamantanone, and the polyaromatic hydrocarbon, pyrene, in phosphate buffer media. These experiments were performed in normal batch mode as the signals obtained with rotating disk electrode mode were extremely noisy. The electrodes were also found to be unstable when steady state experiments were performed in acetonitrile media. Upon examination of the electrodes after exposure to 80%: 20% acetonitrile: water media for more than 30 minutes it was found that the enzyme films were partially dissolved and peeling from the electrode surface, hence making the electrodes unsuitable for batch analysis in organic media.

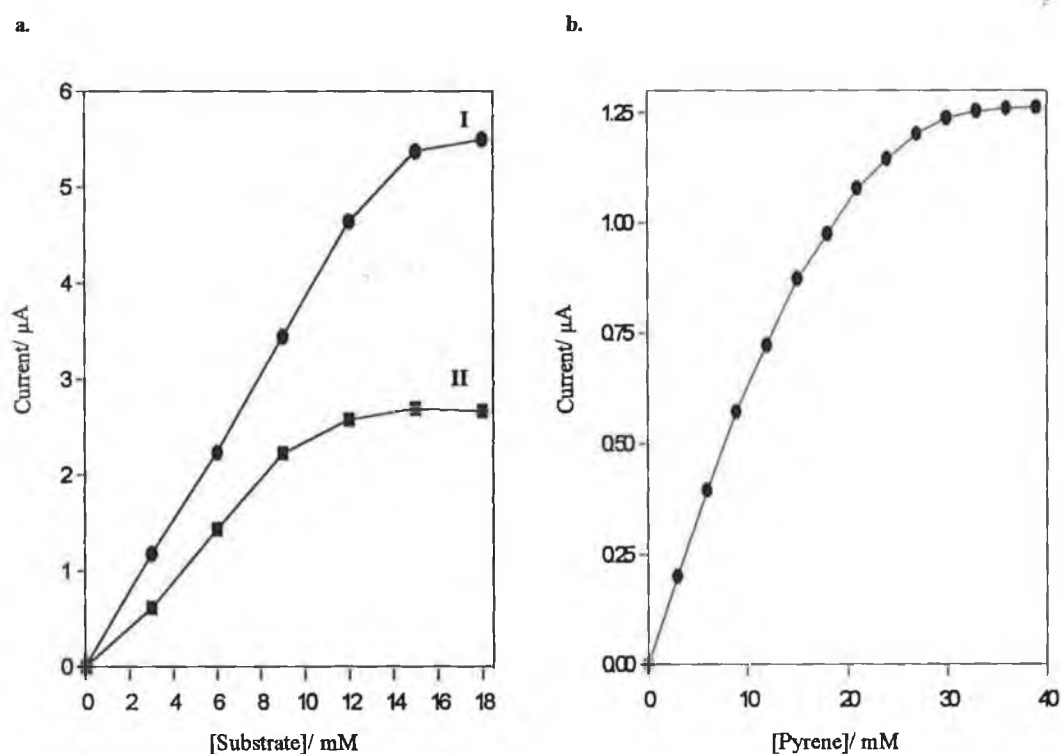


Figure 5.8. Calibration plots from steady state data. (a) Represents camphor (I) and adamantanone (II). (b) Represents pyrene. Experiments were performed in 0.05M phosphate buffer, applied potential - 800 mV vs Ag/AgCl, 10 ml cell stirred at 400 rpm, at 25°C.

The presence of the sol-gel encapsulation method did not show an improved enhancement in stability as postulated by Iwuoha et al. [8] in an earlier study. As mentioned earlier it has been shown by various researchers [12-16] that P450 cytochromes are stabilised when incorporated into lipid crystal vesicle systems. Furthermore it has been well documented that the use of sol-gels also stabilises enzymes [17-20], creating a gel-like environment in which the enzyme has freedom of rotation similar to that within a biological system.

Therefore the instability experienced in this study and the earlier work performed by Iwuoha et al [8] is more likely related to the extreme reduction potentials (-800mV vs. Ag/AgCl) under which the steady state experiments are performed. Cytochromes have been shown by Manjaoui et al. [46] to be progressively damaged when submitted to repetitive scanning and especially to reducing potentials in steady state even when protected in lipid crystal vesicle systems.

Table 5.3. shows the kinetic data obtained for the biosensor in phosphate buffer media. The I_{\max} value is related to the turnover rate constant of the sensor (equation 5.9), and can be used as an index of sensor sensitivity. It is therefore clear that the biosensor is more sensitive to camphor, followed by adamantanone and pyrene respectively. The apparent rate of catalysis k_{cat} for camphor is twice that of adamantanone and more than four times that of pyrene. This is not surprising since the stereospecific methylene hydroxylation of camphor is the first step in the compounds catabolism as the sole source of carbon in bacterial systems [7]. The catalytic efficiency of the biosensor for camphor was almost twice that of adamantanone and six times that of the polyaromatic hydrocarbon, pyrene. It is also interesting to note that this biosensor yielded a two fold increase in I_{\max} for camphor when compared to a similar system without sol-gel [8].

Table 5. 3. Kinetic data from steady state data

Analyte	$I_{\max} / \mu\text{A}$	$k_{\text{cat}} / \text{nmol cm}^{-3} \text{s}^{-1}$	$k_{\text{cat}} / K_{\text{M}} \text{cm s}^{-1}$
Camphor	5.51	0.41	5.7
Adamantanone	2.66	0.20	3.5
Pyrene	1.26	0.09	0.9

5.3.8. Electrode Lifetime

The electrode lifetime was evaluated by using a freshly prepared GCE-[P450_{cam}/DDAB/SG] biosensor and storing it at 4 °C in an air-tight container. The current response ($I_K - I_D$) was evaluated using cyclic voltammetry at 500 mV/s, with 3 mM camphor under anaerobic conditions. Figure 5.9. shows the electrode lifetime over a ten week period. The first 3 weeks yielded a reproducible signal, with a deviation of only 0.3 % for the second week and 0.8 % for the third week respectively. From the fourth week onwards, the electrode response deteriorated progressively stabilising out after 8 weeks to a response one fifth of the original signal.

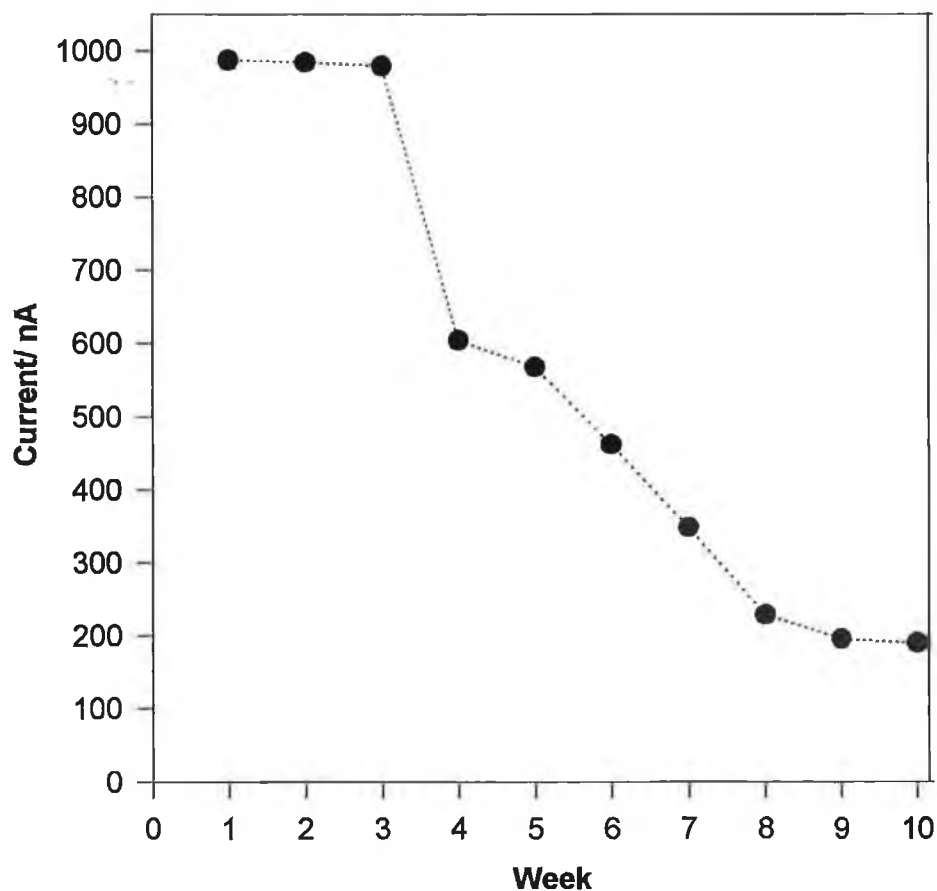


Figure 5.9. Plot of electrode response versus week number.

5.4. Conclusions

It has been demonstrated that the combination of a GCE-[P450_{cam}/DDAB/SG] biosensor for the monitoring of camphor and adamantanone substrates and the polyaromatic hydrocarbon pyrene is achievable. The ability of the biosensor to hydroxylate the pyrene hydrocarbon has important implications for the environmental monitoring of such substances.

Careful examination of the experimental regime will be required if these preliminary experimental results are to be improved for the construction of a GCE-[P450_{cam}/DDAB/SG] biosensor for the routine monitoring of polyaromatic hydrocarbons. The electrode has a lifetime of over 10 weeks, with only a 0.8 % deviation in response after the third week. The biosensor yielded a two fold increase in response to camphor when compared to systems without sol-gel [8]. However, instability after prolonged exposure to organic solutions and also when exposed to extreme reduction potentials presents a challenge in the utilization of these sensors.

Re-evaluation of sensor design is therefore required and examination of experimental conditions under steady state is necessary, in order to improve the stability problem apparent in this system. Once achieved, this sensor could present a promising alternative to current methods of analysis for PAHs. Detailed statistical studies for the sensor could be obtained along with limits of detection, linear ranges and catalytic efficiencies providing important comparative data for the potential replacement of currently used routine methods of analysis.

5.5. References

- [1] Black, S. D.; Coon, M. J.: *Adv. Enzymol. Relat. Areas Mol. Biol.*, 60: (1987): 48.
- [2] Atkins, W. M.; Sligar, S. G.: *J. Biol. Chem.*, 263: (1988): 8842.
- [3] Conney, A. H.: *Pharmacol. Rev.*, 19: (1967): 317.
- [4] Lu, A. Y. H.; Levin, W.: *Biochim. Biophys. Acta.*, 344: (1974): 205.
- [5] Nebert, D. W.: *Mol. Cell. Biochem.*, 27: (1979): 27.
- [6] White, R. E.; Coon, M. J.: *Annu. Rev. Biochem.*, 49: (1980): 315.
- [7] Unger, B. P.; Gunsalus, I. C.; Sligar, S. G.: *J. Biol. Chem.*, 261: (1986): 1158.
- [8] Iwuoha, E. I.; Joseph, S.; Zhang, Z.; Smyth, M. R.; Fuhr, U.; Ortiz de Montellano, P. R.: *J. Pharm. Biomed. Anal.*: (1998): in press.
- [9] Kazlauskaitė, J.; Westlake, A. C. G.; Wong, L-L.; Hill, H. A. O.: *J. Chem. Soc. Chem. Commun.*, (1996): 2189.
- [10] Bianco, P.; Haladjian, J.: *J. Electroanal. Chem.*, 367: (1994): 79.
- [11] Bianco, P.; Haladjian, J.: *Electroanalysis*, 7: (1995): 442.
- [12] Rusling, J. F.; Nassar, A-E. F.: *J. Am. Chem. Soc.*, 115: (1993): 11891.
- [13] Nassar, A-E. F.; Narikiyo, Y.; Sagara, T.; Nakashima, N.; Rusling, J. F.: *J. Chem. Soc., Faraday Trans.*, 91: (1995): 1725.
- [14] Bianco, P.; Haladjian, J.: *Electrochim. Acta.*, 39: (1994): 911.
- [15] Hanzlik, J.; Bianco, P.; Haladjian, J.: *J. Electroanal. Chem.*, 380: (1995): 287.
- [16] Tominaga, M.; Yanagimoto, J.; Nassar, A-E. F.; Rusling, J. F.; Nakashima, N.: *Chem. Lett.*, (1996): 523.
- [17] Yamanaka, S. A.; Nishida, F.; Ellerby, L. M.; Nishida, C. R.; Dunn, B.; Valentine, J. S.; Zink, J. I.: *Chem. Mater.*, 4: (1992): 495.
- [18] Sanchez, C.; Audebert, P.; Demaile, C.: *Chem. Mater.*, 5: (1993): 911.
- [19] Pankratov, I.; Lev, O.: *J. Electroanal. Chem.*, 393: (1995): 35.
- [20] Narang, U.; Prasad, P. N.; Bright, F. V.; Ramanathan, R.; Kumar, N. D.; Malhotra, B. D.; Kamalasanan, M. N.; Chandra, S.: *Anal. Chem.*, 66: (1994): 3139.
- [21] Bjorseth, A., Ed.: *Handbook of Polycyclic Aromatic Hydrocarbons*. Marcel Dekker Pub., N.Y., (1983).
- [22] Holgate, S. T.: *Asthma and Outdoor Pollution*. HMSO, London, (1995).

- [23] Pope, C. A.; Dockerty, D. W.; Schwartz, J.: *J. Inhal. Toxicol.*, 7: (1995): 1.
- [24] Simonsick, W. J.; Ronald, A. H.: *Anal. Chem.*, 56: (1984): 2749.
- [25] Hankin, S. M.; John, P.; Simpson, A. W.; Smith, G. P.: *Anal. Chem.*, 68: (1996): 3238.
- [26] Okumura, T.; Nishikawa, Y.: *Anal. Chim. Acta.*, 325: (1996): 175.
- [27] Nielsen, T.: *Anal. Chem.*, 55: (1983): 286.
- [28] Tucker, S. A.; Bates, H. C.; Amszi, V. L.; Acree, W. E.; Lee, H.; Di-Raddo P.; Harvey, R. G.; Fetzer, J. C.; Dyker, G.: *Anal. Chim. Acta.*, 278: (1993): 269.
- [29] Brown, R. S.; Luong, J. H. T.; Szolar, O. H. J.; Halasz, A.; Hawari, J.: *Anal. Chem.* 58: (1996): 287.
- [30] Faulkner, K. M.; Shet, M. S.; Fisher, C. W.; Estabrook, R. W.: *Proc. Natl. Acad. Sci. U.S.A.*, 92: (1995): 7705.
- [31] Poulos, T. L.; Finzel, B. C.; Howard, A. J.: *Biochem.*, 25: (1986): 5314.
- [32] Poulos, T. L.; Howard, A. J.: *Biochem.*, 26: (1987): 8165.
- [33] Sligar, S. G.; Gunsalus, I. C.: *Proc. Natl. Acad. Sci. U.S.A.*, 73: (1976): 1078.
- [34] Gelb, M. H.; Heimbrook, D. C.; Malkonene, P.; Sligar, S. G.: *Biochem.*, 21: (1982): 370.
- [35] Peterson, J. A.: *Arch. Biochem. Biophys.*, 144: (1971): 678.
- [36] Aoki, K.; Tokada, K.; Matsuda, H.: *J. Electroanal. Chem.*, 146: (1984): 417.
- [37] Murray, R. W.: *Electroanal. Chem.*, 13: (1984): 191.
- [38] Nicholson, R. S.; Shain, I.: *Anal. Chem.*, 36, (1996), 706.
- [39] Greet, R.; Peat, R.; Peter, L. M.; Pletcher, D.; Robinson, J.; (Southampton Electrochemistry Group), *Instrumental Methods in Electrochemistry*. Ellis Horwood, London, (1990), pp. 178-228.
- [40] Zhang, Z.; Nassar, A-E, F.; Lu, Z.; Schenkman, J. B.; Rusling, J. F.: *J. Chem. Soc. Faraday Trans.*, 93: (1997): 1769.
- [41] Iwuoha, E. I.; Smyth, M. R.; Lyons, M. E. G.: *Biosens. Bioelec.*, 12: (1997): 53.
- [42] Mattews, C. K.; van Holde, K. E.: *Biochemistry*, Benjamins/ Cumins Pub. Inc., (1990).
- [43] Pamidi, P. V. A.; Parrado, C.; Kane, S. A.; Wang, J.; Smyth, M. R.; Pingarron, J.: *Talanta*, 44: (1997): 1929.

- [44] Adeyoju, O.; Iwuoha, E. I.; Smyth, M. R.: *Anal. Chim. Acta.*, 305: **(1995)**: 57.
- [45] Iwuoha, E. I.; Smyth, M. R.; Lyons, M. E. G.: *J. Electroanal. Chem.*, 390: **(1995)**: 35.
- [46] Manjaoui, A.; Haladjian, J.; Bianco, P.: *Electrochim. Acta.*, 35: **(1990)**: 177.

Chapter 6

**Summary, Future Trends
and Conclusions**

Sol-gel technology has proven to be extremely useful for its applications in sensor manufacturing. The convenient monitoring of neurotransmitters was achieved using a novel sol-gel carbon composite electrode. The electrodes offered a method of analysis which was as good as, if not better than, several currently available and routinely used analytical methods, for the monitoring of neurotransmitters. This sol-gel carbon composite could easily be utilised in future work concerning environmental analysis, and can be conveniently doped with biocatalytic materials in the interests of biosensor design. Also covered in Chapter 4, was the use of sol-gel as a membrane layer for the detection of phenolics, based on the use of an electrostatic horseradish peroxidase osmium polymer network. Interesting trends were developed whereby only certain phenols yielded responses. The combined action of the sol-gel modified biosensor and also the catalytic entity resulted in partial selectivity for particular phenolics. Although the long term stability only extended over a few days, the response trend observed may find convenient applications in the design of biosensor arrays. The sensor stability may also be improved by encapsulating the horseradish peroxidase osmium polymer complex within a sol-gel network, rather than using the sol-gel as a membrane layer as was the case in this work.

The operational characteristics and sensor performance of genetically engineered cytochrome P450_{cam} was covered in Chapter 5. It had been postulated that the incorporation of the cytochrome lipid vesicle system into a sol-gel network would have improved sensor stability under steady state mode. Although incorporation within a sol-gel has a well known reputation for increasing the stability of enzymes by creating a fluidic environment similar to that of biological systems, it did not improve the stability of the biosensor system in this application. Instead it was suggested and also proven by other researchers that the stability of the cytochrome P450_{cam} biosensors was more a factor of the experimental method, i.e. prolonged exposure to reducing potentials, rather than the sol-gel method of sensor preparation. The biosensor functioned satisfactorily when operated in amperometric sweep mode, being exposed to reducing potentials only for a short period of time. The operational characteristics of this sensor may be improved by carefully examining and improving the experimental method. A fully functional P450_{cam} based biosensor will therefore find convenient applications in the monitoring of polyaromatic hydrocarbons as shown in the preliminary work of this thesis.

6.2. Conclusion

As one is aware there is a considerable divide between sensors developed at the academic level and their convenient applications in the industrial or real life environment. What may be acceptable for the purposes of academic research may not be tolerated in industrial circles without fundamental improvement in sensor design and independent analytical evaluation and validation of the said operation of certain biosensor devices.

It is therefore obvious that the performance characteristics of such electrodes described in this thesis will need to be improved. Many suggestions have been made and include the necessity of longer stability studies ideally over a six month period, under different storage conditions, temperatures and various ranges of humidity. This would allow the behaviour of such electrodes in various environments to be established. Detailed intra-assay and inter-assay electrode variations will need to be developed, which will allow a detailed statistical history to be constructed, of which any given electrode, from any batch would be characteristic of. This would allow the construction of a suitable quality assurance and quality control model for each sensor design. Effects of interferences, and the evaluation of false positives and false negatives would also be included in this work. Investigation of various methods of improving sensor operational and mechanical stability would be of prime importance.

The work performed throughout this thesis represents the tip of the iceberg. There is a wealth of research which could be performed based on the findings therein. The assurance of water quality with regards to inhibitor content and toxic phenol concentrations, will obviously result in more detailed studies on these electrodes, especially in the area of quantitative analysis and the construction of enzyme arrays of pattern recognition, allowing relatively novel methods of analysis to be performed routinely in the analytical environmental monitoring laboratory.

Publications and Presentations

Publications

1. *'Mushroom Tissue-based Biosensor for Inhibitor Monitoring'*
Joseph Wang, Stephen Kane, Jie Liu, Malcolm R. Smyth & Kim Rogers
Food Technol., Biotechnol., 34 (1) 51-55 (1996).
2. *'Screen-Printed Tyrosinase containing Electrodes for the Biosensing of Enzyme Inhibitors'*
Joseph Wang, Valberes Nascimento, Stephen Kane, Kim Rogers, Malcolm R Smyth, Lucio Angnes.
Talanta, 43, 1903-1907, (1996).
3. *'Sol-gel Carbon Composite Electrode as an Amperometric Detector for Liquid Chromatography'*
Prasad Pamidi, Concepcion Parrado, Stephen Kane, Joseph Wang, Malcolm R., Smyth & Jose Pingarron.
Talanta, 44, 1929-1934, (1997).
4. *'Hydrocarbon Pasting Liquids for Improved Tyrosinase-Based Carbon-Paste Phenol Biosensors'*
Joseph Wang, Fang Lu, Stephen Kane, Yong-Kook Choi, Malcolm R. Smyth & Kim Rogers.
Electroanalysis, 9, No. 14, 1102-1106, (1997).
5. *'Development of a Sol-gel Based Amperometric Biosensor for the Analysis of Phenols'*
Stephen Kane, Emmanuel Iwuoha, Malcolm R. Smyth.
Analyst, submitted for publication, (1998).
6. *'Development of a Sol-gel Encapsulated Cytochrome P-450 Biosensor for Environmental Monitoring'*
Stephen Kane, Emmanuel Iwuoha, Malcolm R. Smyth.
In preparation, (1998).

Presentations

1. September 1997
Title of Lecture: 'Biosensors of Pharmaceutical & Environmental Importance'
1st Analytical Science Network Conference of Ireland. Cork, Ireland.
2. December 1997
Title of Lecture: 'Development of a Sol-gel based Amperometric Biosensor for the Analysis of Phenols'
2nd Inco Copernicus Biosensor Conference. Athens, Greece.

Posters

1. March 1998
Poster Title : 'Development of a Sol-gel based Amperometric Biosensor for the Analysis of Phenols'
Eirelec Conference. Howth, Ireland.
2. May 1998
Poster Title : 'Some Novel Amperometric Enzyme-based Biosensors for Environmental Monitoring'
Aiseac Conference. Coimbra, Portugal.